Development of a re-mountable timber car park

DESIGNING OF A CAR PARK FLOOR AND RE-MOUNTABLE JOINTS

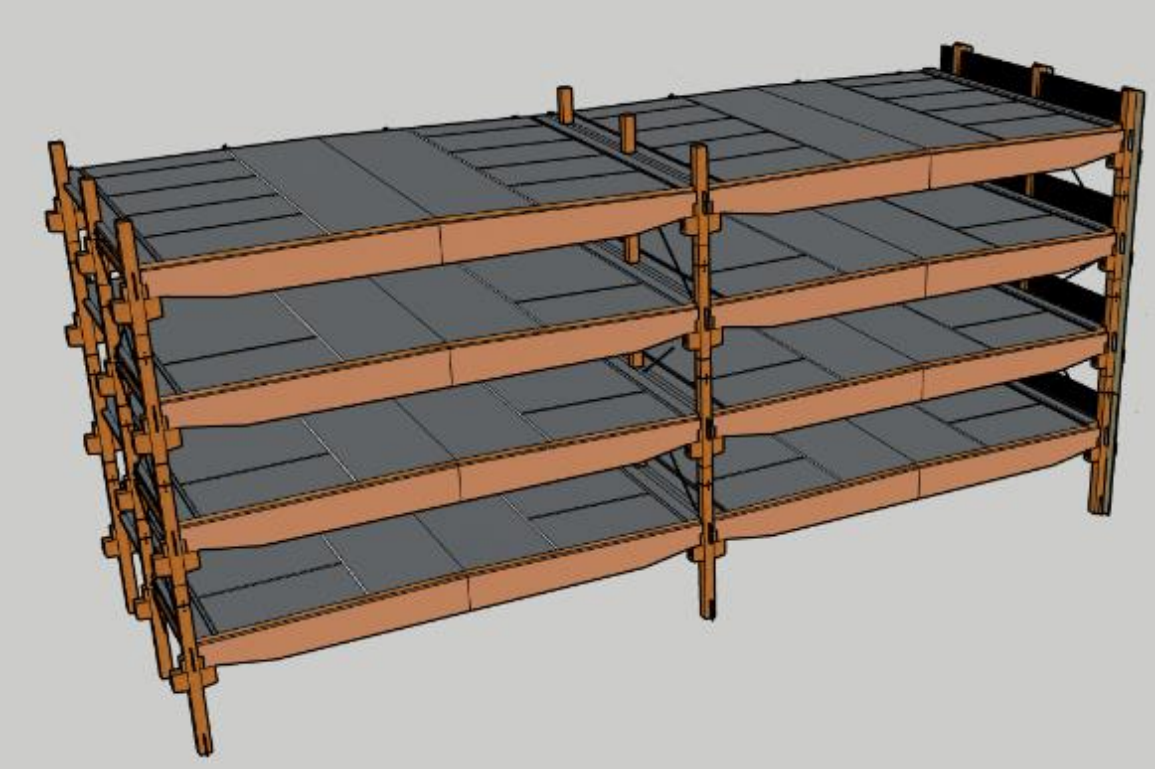

I.T. Pronk

TU Delft

Ballast Nedam
Park & Connect

Development of a re-mountable timber car park

By

Ivo Pronk

To obtain the degree of Master of Science
at the Delft University of Technology,
to be defended publicly on October 25, 2023 at 13:15

Student number:	4593022	
Thesis committee:	Prof. dr. ir. J.W.G. van de Kuilen	TU Delft, Chairman
	Drs. W.F. Gard,	TU Delft
	Dr. ir. G.J.P. Ravenshorst,	TU Delft
	Prof. dr. ir. P.C. Louter	TU Delft
	Ir. H.G.E. Damen	Ballast Nedam Park&Connect
	Ing. W. van der Heide	Ballast Nedam Park&Connect

Preface

This report represents the final step of my Master's in Structural Engineering at the Delft University of Technology. During the previous years in my Master's and Bachelor's, I became interested in structural design, especially in timber. Also, the indicated necessary environmental challenges the building industry has to make motivates me to help in this process. After doing my Bachelor's Thesis about a timber wildlife crossing, I also wanted to design a timber structure for my Master's Thesis. Both aspects come together in the design of the re-mountable timber car park.

I would like to thank Ballast Nedam Park & Connect for allowing me to investigate this topic for my Master's Thesis. Especially thanks to my two supervisors. First, Jeroen Damen for the weekly meetings to discuss the research progress and increase my knowledge in structural design. Next, Wim van de Heide for creating a broader view to look at challenges and to help contact other companies.

In addition, I would like to thank my TU Delft supervisors Jan-Willem van de Kuilen, Geert Ravenshorst, Wolfgang Gard, and Christian Louter, for their guidance during my Master's Thesis. The critical view and experience in the structural design of timber elements helped me improve the research completeness and quality.

Finally, thanks to my parents, girlfriend, sisters, friends and housemates for supporting me during this research and creating the possibility to relax. Doing my Master's Thesis at the same time as my girlfriend and housemate was beneficial to be able to talk about the necessary steps involved in a Master's Thesis process and to discuss the challenges faced during the thesis.

Ivo Pronk
October 2023

Executive summary

Nowadays, the people on Earth have a complex challenge to save the world from environmental problems, for example, the depletion of resources and global warming. In the Netherlands, specifically the nitrogen emission reduction. All industries, including the construction industry, must act on this challenge. A way to tackle these environmental problems is by designing biobased and re-mountable. Biobased to reduce emissions and use renewable resources. Re-mountability decreases the request for raw materials by reducing the number of actions required for re-mounting the structure at the same functional level and increasing the functional service life.

A car park is a simple structure that can face a lower functional service life than a technical service life due to changes in demand. That makes designing it as a re-mountable car park can create a high potential benefit.
Combining the re-mountable character with timber has never been done before.
The reason behind this is the open character of the car park to ensure natural ventilation. The term natural ventilation indicates one of the problems. Moisture can get in through the facade, creating a risk for deterioration of the natural and hygroscopic timber elements. In addition, the fire behaviour of a timber structure creates a different design process than steel and concrete due to its combustible character.
With the guidance of Ballast Nedam Park & Connect, already making re-mountable car parks of steel and concrete, an open timber re-mountable car park is investigated in this research. Next, to the challenge of re-mountability, optimising the floor height is beneficial to create a higher profit in two ways: a smaller ramp gives a more efficient floor area, and more levels are possible for a certain total height. The combination of both goals results in the following main research question:

What is the most suitable design for a timber re-mountable car park, including global structure and details based on structural performance and feasibility?

The starting point for answering this question is investigating the reference timber car parks to determine their structural layout, strengths, weaknesses, and challenges for making them re-mountable. Afterwards, the reference floor systems are investigated. First, the existing floor systems based on literature and reference car parks are determined, and new floor systems are generated. Assessing all the floor systems with a focus on structural performance and feasibility using the gained knowledge of their strengths and weaknesses results in the following four floor designs:

- Floor design 1: CLT floor
- Floor design 2: Closed CLT plus glulam rib floor
- Floor design 3: Complete prefabricated closed CLT plus glulam rib floor with a concrete top layer
- Floor design 4: Prefab concrete floor

By preliminary designing those floor systems on moisture resistance, structural performance and fire resistance, background information is gathered for the multi-criteria assessment to make a final decision for the most suitable floor system. Concluding that a glulam beam plus CLT floor, shown in Figure 1, is the most suitable design and the answer to one of the two objectives of this research. Figure 2 shows the results of the multi-criteria analysis, indicating the main benefit is the favourable total height and weight.
Next, the ways of moisture exposure and measures to prevent direct exposure are investigated. It shows that a combination of a partly open façade, column wood protection panels and a Triflex coating on the top surface of each floor cover all timber elements. Triflex is more suitable than mastic asphalt and concrete due to its low self-weight, high feasibility and re-mountable potential.

In case of fire, flashover is hard to prevent despite the open facade due to the combustion of timber increasing the fire growth and firepower compared to a steel and concrete car park fire. However, the serviceability limit state governs the floor structural design due to timber's lower stiffness than steel and concrete. Therefore, applying a conservative fire resistance of 90 minutes only slightly increases the column cross-section.

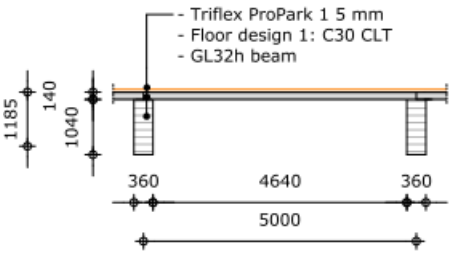

Figure 1: Cross-section CLT floor system with glulam beams

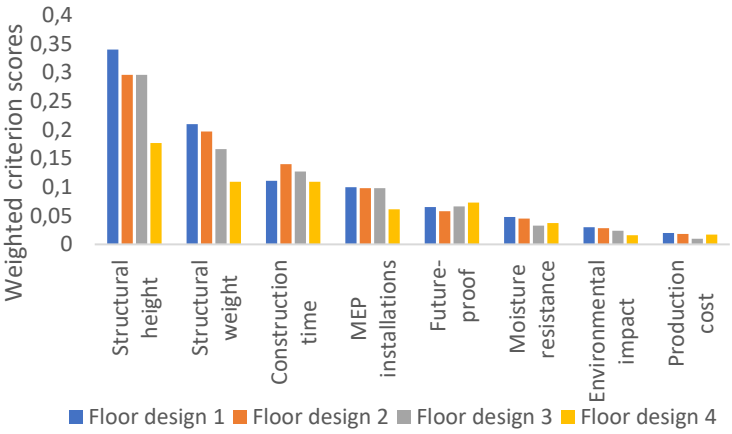

Figure 2: Main criterion scores floor alternatives

The second part of this research focuses on designing the chosen load-bearing system re-mountable and, based on the lessons learned, optimizing the number of manual actions to create higher feasibility. Four types of joints are possible in a timber structure: bolts, dowels, screws, and carpentry joints. Screws and carpentry joints can become stuck in the timber elements due to the timber's dimensional instability. In addition, screws create irreversible damage each time it is demounted. The bolt and dowel do not face those problems. However, a dowel cannot take up tensile forces from wind, which is possible in a bolted connection. Therefore, bolts are the most suitable type of connection to create a re-mountable timber structure. See Figures 3 and 4. The connection of Figure 5 does not need tensile capacity, so it uses a corbel instead of bolts to limit the manual actions.

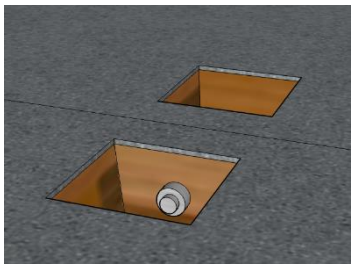

Figure 3: Top view bolted floor-to-floor connection

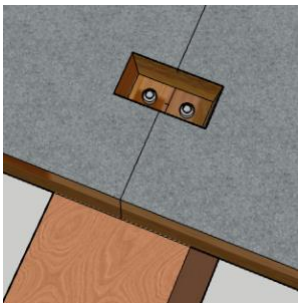

Figure 4: Top view bolted floor-to-beam connection

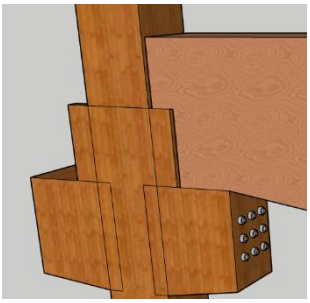

Figure 5: Column-beam console connection

This research concludes that combining spruce timber as a biobased material with a re-mountable car park design is possible. The floor system should be CLT elements with a span of 5 meters and glulam beams spanning 16 meters. Next, a partly open facade, wood protection panel, and a floor Triflex coating combined with connections made by bolts or a corbel create a timber load-bearing system of an open timber car park satisfying all structural performance and durability requirements. Next, the system can be demounted and re-mounted without decreasing the functional level of the load-bearing structure and the necessity of applying new raw materials.

Further research is recommended to develop software for the fire behaviour in an open timber car park and to test the Triflex coating performance more accurately. For Ballast Nedam Park & Connect, cost optimization is valuable. Finally, policymakers should stimulate the requests for re-mountable timber car parks, increasing the knowledge and experience to create a more optimized design.

Contents

List of Figures

List of Tables

List of Abbreviations

BNPC	**Ballast Nedam Park & Connect**
BCI	**Building circularity index**
CLT	**Cross-laminated timber**
ECI	**Element circularity index**
GLT	**Glued laminated timber**
HAZ	**Heat-affected zone**
LCA	**Life cycle assessment**
LVL	**Laminated veneer lumber**
MCA	**Multi-criteria analysis**
MCI	**Material circularity index**
MC%	**Moisture content percentage**
MEP	**Mechanical electrical plumbing**
PCI	**Product circularity index**
PMMA	**Polymethylmethacrylaat**
UC	**Unity check**
W/C	**water-to-cement ratio**

List of symbols

Greek symbols

α	Taper	rad
β_0	One-dimensional charring rate	mm/min
β_n	Notional charring rate	mm/min
γ_g	Partial safety factor self-weight	
γ_q	Partial safety factor variable load	
γ_m	Partial material factor	
$\gamma_{m,fi}$	Partial material factor fire	
Δh	Height increase taper	mm
ρ_k	Characteristic density	kg/m^3
ρ_{mean}	Mean density	kg/m^3
$\sigma_{m,y,d}$	Design value bending stress around y-axis	N/mm^2
$\sigma_{m,\alpha,d}$	Design value bending stress taper	N/mm^2
σ_t	Tensile diaphragm stress	N/mm^2
τ_{ed}	Design shear stress	N/mm^2
ψ_0	Combination value factor variable action	
ψ_1	Frequent value factor variable action	
ψ_2	Quasi-permanent value factor variable action	

Latin symbols

A_{req}	Required area	mm^2
b_{eff}	Effective width	mm
$c_{pe,1}$	Pressure coefficient areas up to 1 m^2	
$c_{pe,10}$	Pressure coefficient areas larger than 10 m^2	
d_{char}	Charring depth	mm
d_{ef}	Effective charring depth	mm
e	Eccentricity	mm
E	Young's Modulus	N/mm^2
EI	Bending stiffness	Nmm^2
f	Frequency	Hz
F_{beam}	Support force beam	kN
F_c	Diaphragm compression force	kN
$f_{d,fi}$	Design resistance fire situation	N/mm^2
$F_{h,edge}$	Compression force elevated corbel edge	kN
$f_{m,k}$	Characteristic bending strength	N/mm^2
$f_{m,d}$	Design bending strength	N/mm^2
F_t	Diaphragm tension force	kN
$f_{v,k}$	Characteristic shear strength	N/mm^2
$f_{v,d}$	Design shear strength	N/mm^2
f_{20}	20% fractile strength at room temperature	N/mm^2
G_k	Characteristic total self-weight	kN or kN/m or kN/m^2
h_{eff}	Effective height	mm
I	Moment of inertia	mm^4
k_{def}	Creep factor	
k_{fi}	Slip modulus fire situation	
k_h	Height factor	
k_{mod}	Modification factor	
$k_{mod,fi}$	Modification factor fire situation	

$K_{m,\alpha}$	Taper bending stress reduction factor	
K_0	Exposure time factor charring	
M_{ed}	Design bending moment	kNm
$M_{rd,430}$	Bolt design bending moment resistance height 430	kNm
$M_{rd,330}$	Bolt design bending moment resistance height 330	kNm
$M_{rd,230}$	Bolt design bending moment resistance height 230	kNm
q_f	Variable line load from car park load	kN/m
q_g	Line load permanent action	kN/m
q_k	Characteristic surface load car park floor	kN/m^2
Q_k	Characteristic point load car park floor	kN
Q_{prelim}	Transportation weight preliminary module design	kN
q_q	Line load variable action	kN/m
q_{ULS}	Design ultimate limit state load	kN/m
q_{SLS}	Design serviceability limit state load	kN/m
$Q_{sol,2}$	Transport weight global layout optimization solution 2	kN
Q_{wind}	Wind force	kN
$S_{d,fi}$	Design stiffness in fire situation	N/mm^2
S_{20}	20% fractile stiffness at room temperature	N/mm^2
u	Deflection	mm
u_{inst}	Instantaneous deflection	mm
u_{fin}	Final deflection	mm
V_{ed}	Design shear load	kN
w_{max}	Maximum crack width concrete	mm

I Research set-up

Chapter 1 Introduction

This first chapter explains the reason for carrying out this research. First, the problem statement is given in paragraph 1.1. Next, paragraph 1.2 provides the resulting research goal based on the problem statement. Finally, paragraph 1.3 gives the research questions to reach this goal.

1.1: Problem statement

At this moment, the world has important environmental problems to solve, like global warming, pollution, depletion of resources, and so on. Goals are formulated to try to overcome these problems. In the Netherlands, the goals are to use 50% fewer primary raw materials in 2030 and to be completely circular in 2050 (Rijksoverheid, n.d.). Nowadays, most of the constructions are built for one functional or economic lifetime (Chapter 3), which is not the right thing to do from an environmental point of view. Namely, about 50% of all the raw materials in the Netherlands are used in the construction industry (Schut et al., 2015). Resulting in 40% of the total waste in the Netherlands (van Dam & van den Oever, 2019). Circularity and the corresponding re-mountability of structures in the building industry give the materials or elements a second life and partially solve the stated environmental problems. Designing for re-mountability will increase the functional lifetime of the materials or elements. If the technical service life becomes governing instead of the functional service life, there is a reduced need for new raw materials.

The research is going about a re-mountable car park made of timber.
A car park is a relatively simple structure. In addition, if the demand for extra parking lots reduces or the car park is not needed anymore because it was intended for temporary use. Then, re-mountability allows for improving the efficiency of this structure. Therefore, a re-mountable car park made of timber probably has a high potential to be profitable because of the favourable properties of timber concerning the environment, prefabrication level, and self-weight. However, the limited experience and knowledge in designing timber construction re-mountable is a challenging combination. Especially in open structures like car parks, there is limited experience and knowledge in using timber. Namely, due to environmental influences, timber's characteristics make it a more complicated material than traditional steel and concrete.
Deterioration is one of the crucial moisture aspects. For example, fungi will reduce the structural performance of timber. Next, the hygroscopic character of timber creates more swelling and shrinkage compared to steel and concrete, which corresponding strains can also create damage in, for example, a joint. So, choosing the right timber species combined with appropriate protection measures is crucial for preventing deterioration and limiting swelling and shrinkage to satisfy the required technical service life. (van der Lught, 2021).
Fire resistance is also an important aspect. Because timber is a combustible material, it will be affected by the fire in terms of loss of structural properties and the charring process, but it also contributes to the fire.

There are a few examples of timber car parks in Europe, but none of these references is re-mountable, indicating the knowledge gap investigated in this research. These timber car parks are made with other materials like the ones in Studen, Switzerland and Antwerp, Belgium (Pieters, 2019;

Zaugg, 2018), or complete timber car parks, like those Malmö and Bad Aibling (B&O Holzparkhaus, Bad Aibling, n.d.; Rosholm, 2021). The references show that there is a recent development in open timber structures. Nevertheless, that is still on a relatively global level with a less scientific background because minimal scientific papers are available corresponding to open timber car parks. Furthermore, the timber car parks are not yet re-mountable. Re-mountable car parks are only made in steel and concrete, such as the ModuPark of Ballast Nedam Park & Connect (from now on: BNPC).

Therefore, this research will design a re-mountable timber car park. With only focusing on designing a car park module of four adjacent grid areas, see the grey area in Figures 1-1 and 1-2. This four grid module covers all governing load configurations on the load-bearing structure. So, a complete load-bearing design is known after this research. For example, an edge column is indicated by column 1 in the figures. Next, a column in the middle of the four grids is indicated by column 2 in the figures. The investigated grey part can be extended in the vertical and horizontal directions of Figures 1-1 and 1-2, meaning the whole car park structure is known by designing this module except for the ramp grid with a different area.
In addition, a car park with four floor levels will be assumed because this is the most applied design by BNPC. Four levels mean ground level plus four extra parking levels.

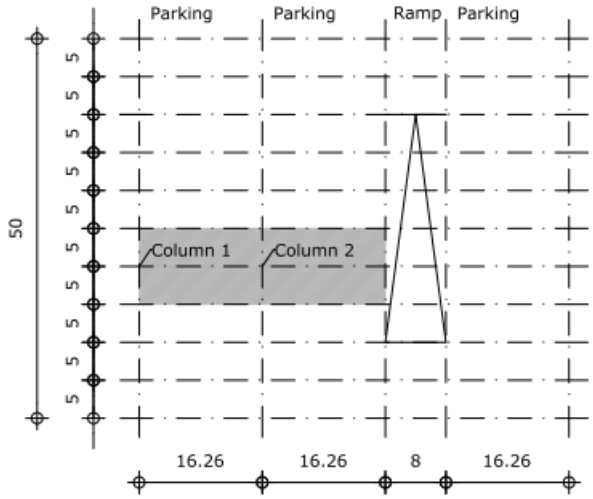

Figure 1-1: Grid lines with investigated module car park in grey in m

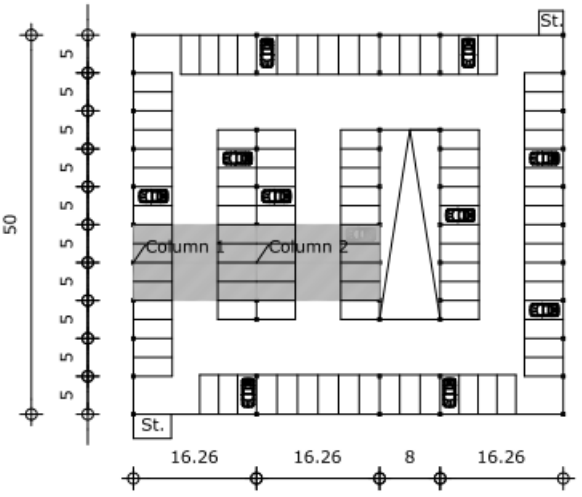

Figure 1-2: Example car park layout with investigated module in grey in m (st=stairwell)

The most crucial car park details are the floor system and re-mountable joints. The joint must be easily dismounted to ensure a good performance of the car park. However, it must be designed and erected precisely to ensure the joint will not be affected by weather influences. These two aspects can conflict with each other. For the floor, the limitation of the floor height and durability in terms of material use and degradation are the most important aspects. Water comes into the car park by grooves of the wheels or directly by rain. In winter, de-icing salt can come together with water inside the car park. Resulting in a wet floor with acids and driving cars over it. This mixture of events can lead to increased degradation if not considered during the design (Gillon, 2002). A normally used car park floor of concrete can resist those impacts.
Nevertheless, using a thick or heavy floor is not a good solution from an economic and environmental point of view. The most efficient for a car park is a floor system that is thin and lightweight. The thinner the floor, the more parking layers can be constructed for the same height, and the shorter the ramp length. In addition, the lighter the floor, the smaller load-bearing elements plus foundation are required. This research tries to find the optimal type of floor, which is also re-mountable.

Concluding, this research helps to fill this scientific gap about open re-mountable car parks. As expressed by the following problem statement:

Problem statement: The application of timber in an open re-mountable car park has not yet been fully developed, therefore not ready to use in practice. That means the current re-mountable car parks, only made of steel and concrete, are not suitable for the future in which environmental issues are crucial.

1.2: Research goals

The previous paragraph states which problem should be solved in this report. That problem is translated into a goal for this research. Below is the goal expressed.

To design a re-mountable car park made of timber, focusing on the structural performance and feasibility of the car park module and important details like the floor system and the re-mountable connections.

1.3: Research question

Answering research questions is the best tool to achieve this goal. In this paragraph, the research questions will be discussed.

1.3.1: Main research question

The main research question tries to find an answer to solve the problem statement and reach the goal.
Below is the main research question formulated.

What is the most suitable design for a timber re-mountable car park, including global structure and details based on structural performance and feasibility?

1.3.2: Sub-research questions

It is necessary to divide the main research question into sub-research questions because it could not be answered directly. The sub-research guides to answer the main research question.
These sub-research questions are linked to all phases of the report, as stated in paragraph 2.2

- ***How are the current structures of re-mountable and non-remountable timber car parks made?***
- ***What are the constructive requirements corresponding to an open re-mountable car park made of timber?***
- ***What measures can be taken against the performance-affecting aspects of timber at a global and detailed level to ensure an appropriate technical lifetime and resistance?***
- ***What is the potential of a combination of materials in the floor system?***
- ***Which type of long-span floor system is most suitable in the open timber re-mountable car park?***
- ***Which type of global load-bearing structure fits the best within the structural performance and feasibility boundary conditions?***
- ***What are the most feasible types of re-mountable connections in the car park module?***

Chapter 2 Research approach

Chapter 2 provides the research approach. Paragraph 2.1 gives the scope of this research. Subsequently, the methodology of this research is provided in paragraph 2.2. The methodology explains the main parts and coherence of this report. This methodology is visualized and summarized in paragraph 2.3.

2.1: Scope

As the paragraph problem definition shows, this research topic is broad. In addition, it is also a topic on which less research is done. That means much time is needed to investigate all the car park's design details. Within the prescribed time of this Master Thesis, it is impossible to investigate the whole problem of a re-mountable timber car park and to make a complete design. Therefore, it is essential to define the scope of the research. The indicated topics below are not included in this report and are possible valuable ideas for further research indicated in the recommendations of Chapter 12.

- As mentioned in the problem statement, only the grey part of the car park shown in Figures 1-1 and 1-2 will be designed in this research. This module can be expanded in the longitudinal and the transverse direction without creating new structure parts. The global element layout and grid area are different for the ramp grid, so this research will not investigate the ramp grid.

- As mentioned in Chapter 1, environmental issues are the motivation to start the research in a timber car park. The reason for using timber and the background will be discussed in Chapter 3. However, a complete life cycle assessment (LCA) will not be made in this research. Performing a complete LCA next to the designs is impossible within the prescribed time, and the LCA is not directly linked to the research goal. Nevertheless, parts of the life cycle assessment will certainly be included, for example, in the assessments of the alternatives.
  For the same reason, this research does not calculate the circularity potential.

- The re-mountable timber car park design is intended for application in the Netherlands. Therefore, only the Dutch design requirements and regulations will be used.

- In this report, a car park above the ground will be discussed. Designing an underground car park will result in different requirements and regulations, leading to a completely different design.

- This research will not focus on the design of the foundation because this is not directly linked to the car park module. In addition, designing a re-mountable foundation is a possible new topic for complete research. Also, ground mechanics topics like settlements will not be discussed because this is a different type of mechanic than necessary to design the timber car park structure.

- The global façade design will be discussed in Chapter 5, affecting the performance of the timber in terms of fire and moisture. Nevertheless, several layouts exist for facades but do not influence the structural design. So, the detailed façade design will not be part of this research.

- Finally, boundary conditions are indicated in the final design to create a background for the reasoning of the final re-mountable connection type. However, this research does not apply an assessment study comparing alternative connection types due to time limitations.

2.2: Methodology

The stated research questions of paragraph 1.3 will be answered in this report. To answer those questions, information and knowledge are required. The methodology used in this report will be discussed in this paragraph to gain this information, and knowledge is given below. It consists of four main parts: the research set-up, the study phase, the design phase, and the results phase.

I) Research set-up

This first phase formulates the basis of the research. It defines the problem statement of this research, then the research goal and research questions. Followed by the methodology of this research. Chapter 1 and 2 covers those topics.

II) Study phase

The study phase is presented in Chapters 3,4,5 and 6.

- Chapter 3 focuses on the circularity and re-mountability principle. So, it shows the background of these principles and how they can be applied in this research. This chapter also introduces the design principles of fire and moisture resistance.
- In Chapter 4, the already-built timber car parks are presented and analysed. This analysis will answer the following four questions: How is the car park designed? What are the advantages and disadvantages in terms of re-mountability? What are the lessons to learn from the design? And what are the intelligent ideas of the design? The answers to these questions provide the key points in a car park design, which are valuable for the subsequent phases of this research. Also, the limiting factors concerning re-mountability will be indicated.
- Chapter 5 presents the starting points, requirements, and performance-affecting aspects necessary for designing and assessing the floor systems. The requirements for a car park, considering safety, loads, dimensions, material characteristics, and strength limits, are strictly noted in codes and guidelines. In addition, there are also two critical performance-affecting aspects of using timber, namely moisture and fire resistance. There will be a specific consideration in this chapter on how to deal with them in the design phase.
- Next, Chapter 6 lists the possible configurations of timber floor systems to be able to design the load-bearing structure in the next phase. These configurations are determined from the literature and the references of Chapter 4. Then, the floor alternatives will be analysed. This analysis uses the same questions as for analysing the reference car parks. So, the goal is to determine the floor alternatives' design, weaknesses, and strengths. Finally, based on the analysis of the floor systems and the requirements, it is possible to determine which floor systems have the highest potential for the re-mountable timber car park. So, this chapter results in a list of potential alternatives.

Summarized, the end product of this part is a list of potential floor systems and a program of requirements in combination with the information about the two design principles.
The information required in this phase will primarily be gathered through literature research like papers and online articles. Next to literature research, interviews with supervisors from BNPC give valuable information for this phase.

III) Design phase

Third, the design phase includes Chapters 7,8,9 and 10.

- In Chapter 7, a preliminary load-bearing system design, including a beam and floor system, will be made for the resulting alternatives of Chapter 6. This preliminary design includes structural performance, fire resistance, and moisture resistance.

- In Chapter 8, a multi-criteria analysis will be done to determine which alternative, including the beam type and floor system, belongs to the most suitable floor system. This multi-criteria analysis is based on the information gathered in Chapter 7 and the study phase, focusing on the aspects of re-mountability and structural performance covered in the research goal. To make sure the complete set of information is available for the assessment, pitching the design to employees of BNPC gives extra information. Especially on feasibility and cost, in which experience is important. The first part of Chapter 8 determines the criteria. Afterwards, the alternatives are assessed on those criteria. Finally, it is possible to determine the most suitable floor system.
- Chapter 9 gives the final design for the most suitable floor system determined in Chapter 8 including the global floor system layout and the most suitable layout of the installations based on the lessons learned (Chapter 4) and requirements (Chapter 5).
- Then, Chapter 10 covers the final design of the details for the most suitable floor system, like re-mountable connections and element cross-sectional areas, using the information gathered in all previous chapters. Chapter 10 finishes the final floor design with the car park module's mounting and demounting sequence.

Summarized, the end product of this phase is a thoroughly designed timber car park module, including connection designs and a mounting and demounting sequence.
As mentioned earlier, the remaining floor designs of Chapter 6 will be used in the preliminary design phase of Chapter 7. Next, the lessons learned from the reference car park analysis of Chapter 4 are valuable to consider in the preliminary design of Chapter 7 and the final design phase of Chapters 9 and 10. Formulas from Eurocode combined with Excel and FEM software are used in both design phases. The required information for the multi-criteria analysis can be taken from the study phase, the designs made in Chapter 7, and by pitching the designs to BNPC employees.

IV) Result phase

This last phase consists of Chapters 11 and 12.

- Chapter 11 discusses this research's methodology, assumptions, and outcomes.
- Finally, Chapter 12 provides the conclusion by answering the main- and sub-research questions. In addition, it presents the recommendations for further research.

This phase will be made using the information gathered during the research in the previous three phases. Finally, SketchUp will be used to model the concluding final design.

Figure 2-1 shows a summary of the above methodology.

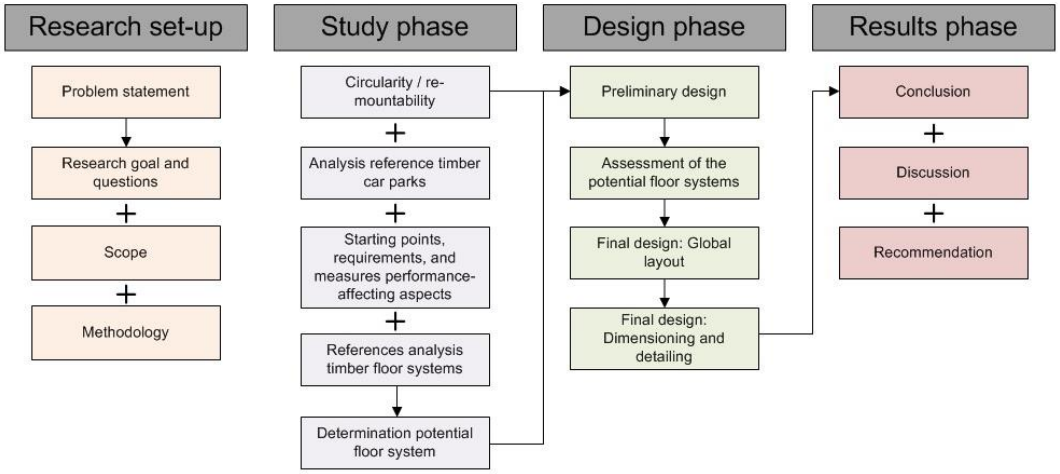

Figure 2-1: Summary of the methodology

II Theoretical analysis

Chapter 3 Sustainability and durability background

This chapter focuses on how to apply circularity and re-mountability in a timber car park. First, paragraph 3.1 explains the concepts. Paragraph 3.2 shows different alternatives to quantify circularity. Then, paragraph 3.3 presents the application of circularity in combination with the use of timber in a car park. Finally, paragraph 3.4 discusses the performance-affecting aspects of timber.

3.1: Basics of circularity and re-mountability

As mentioned in the problem statement (paragraph 1.1), the building industry should take some action against environmental problems. The most crucial measure to prevent further problems is applying the circularity principle, especially re-mountability. Nevertheless, what are circularity and re-mountability exactly, and why is this used in the timber car park design? This paragraph will give a background about these aspects, what they mean, and what they stand for.

There are three approaches in a circular economy: a design for longevity, a design for disassembly, and a design for reuse. Design for longevity means improving the lifetime of a material or product. Design for disassembly is creating more awareness of the demolition phase to use materials again. Finally, design for reuse means designing a structure to make the reuse of components or materials possible (Cambier et al., 2019). Reuse is the second highest step on the "Ladder of Lansink". This ladder provides the possible options to deal with waste. Prevention is the best, and landfilling is the worst option (“Framework Circulair Bouwen Versie 1.0,” 2019).
Moreover, it is important to design for simplicity in a circular construction so the construction can quickly be erected and demounted. Simplicity improves the quality of the system substantially. These four design considerations are essential to developing a re-mountable car park in this research. Design for longevity will be applied in choosing the appropriate protection measures. The re-mountability aspect of the research covers the design for disassembly and the design for reuse aspects. Finally, design for simplicity will be considered by designing the elements smartly to limit the number of connections, elements, and especially the number of different elements, ensuring a fast and reduced risky erection process.

Ensuring a long lifetime of the structural elements is an important aspect. Because if the materials have a longer technical lifetime than the functional or economic ones, then applying circularity in the design achieves the highest benefits. In conclusion, multiple applications can be made with the same material. This result creates less material use, preventing the depletion of resources, and it limits the amount of waste. Both aspects create high sustainability, favourable for the environment.

Next, knowing the different service life of the elements makes it clear how to design, connect and use these components. For example, the component with the shortest lifetime should be well-accessible for repair or to replace (Brancart et al., 2017).
Figure 3-1 shows the layering principle of Brand, which covers this topic. This principle includes six components: stuff, space plan, services, skin, structure, and site. Arranged from a short expected lifetime of stuff to an eternal life of the site. Those components will certainly be linked at several points and strongly influence each other. So, the mutual relationship and influence of the various

components on each other should be known. (*Principes Bij Circulair Detailleren*, 2020)
This principle of Brand should be applied in this research because it shows the importance of knowing all the components linked to each other and their mutual influence. So, it is a valuable principle to consider in the final design phase in Chapters 9 and 10, but also for the concluding (de)mounting sequence.

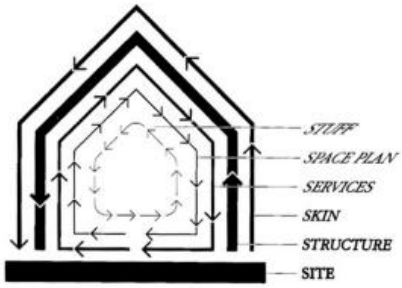

Figure 3-1: Layering principle Brand (Brand, 1995)

Circularity is a broad concept because there are different ways to reuse materials. The most optimal type of circularity is to keep the product at its highest value. So, use it the same way or even with a higher value (Zhao et al., 2022). Downcycling makes the product less functional than it was, so the product will never meet the earlier performance. Unwanted increasing amounts of elements or materials are necessary to reach the initial performance. The three goals below summarize the circularity principle.

- Material sources: Prevent depletion of sources
- Environment: Improve the quality of the living environment or keep it at the same level.
- Present value: Keep the product at least at the same level of quality and functionality.

Re-mountability is an example of circularity, which keeps the elements at the same level. This concept means that elements can be dismounted and re-mounted with the same quality as first without environmental influencing processes required during the re-mounting phase. Therefore, the carbon footprint does not increase during this re-mounting process. The second-use phase requires as limited as possible new raw materials and actions to erect with corresponding harmful sustainable aspects like emissions, energy use, and waste. For this reason, the design's goal is to make it re-mountable, creating a highly sustainable design.

3.2: Measuring methods circularity

There are methods for assigning a circularity value to a product. The BCI method consists of four main indices, as shown in Figure 3-2. These are the Material Circularity Index (MCI, Product Circularity Index (PCI), Element Circularity Index (ECI), and Building Circularity Index (BCI). They have a value between zero and one, meaning they go from completely linear to circular. ("Meetmethode Circulair Vastgoed - Building Circularity Index Versie 1.0," 2022; *Uitgebreide Toelichting BCI Gebouw*, n.d.)

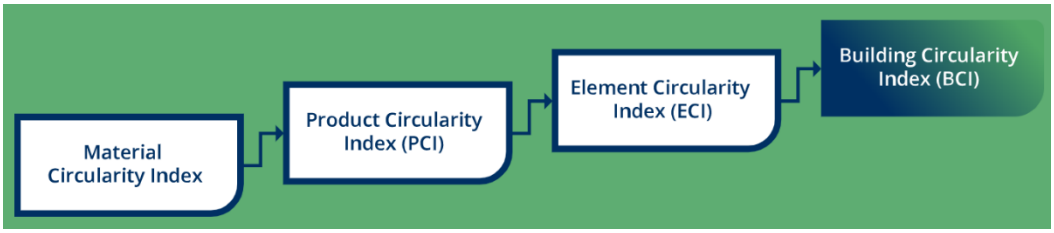

Figure 3-2: Steps BCI circularity measuring system (*Uitgebreide Toelichting BCI Gebouw*, n.d.)

Another example is the method of Platform CB'23 ("Leidraad Meten van Circulariteit Version 3.0," 2022). This method is in development, so it is not ready to use in this research. Furthermore, "Het Nieuwe Normaal 0.3" (*Het Nieuwe Normaal van 0.2 Bijna Naar 0.3*, 2022) is only a norm, including the main aspects of circular constructions. In conclusion, the BCI method is the most suitable method, but it is outside the scope of this research. So, it is a valuable topic for further research.

3.3: Circularity potential of a timber in car park

The problem statement and paragraph 3.1 state why a timber re-mountable car park should be designed. Nevertheless, what makes a car park suitable as a re-mountable structure? Moreover, what is the benefit of using timber? This paragraph tries to find answers to these questions.

An example of a re-mountable car park developed by BNPC several years ago is the ModuPark concept. Figure 3-3 shows an example of the ModuPark.
Until now, several ModuPark car parks have been realized in the Netherlands, and some of them are already re-mounted. An example is the temporary car park of Zaandam that is now in Almelo.

Figure 3-3: ModuPark car park TU Delft P-sports (*Parkeergarage TU Delft P-Sports*, n.d.)

Biobased material such as timber can also function as a load-bearing material and has fewer disadvantages in circularity and sustainability. Using timber as a load-bearing material is still a small market compared to conventional materials (Hildebrandt et al., 2017). Nevertheless, timber has advantages that conventional materials do not have. The greenhouse gas CO2 is captured in timber, which means a timber building stores CO2 (van Dam & van den Oever, 2019). On the other hand, in the production of concrete and steel, there is CO2 emission (Fennell et al., 2022). In summary, a building made of timber can be CO2 neutral, while in a steel or concrete building, CO2 is emitted into the environment. Timber is also a renewable material, which is a good solution against the depletion of resources mentioned in this chapter. These aspects are the main important advantages compared to conventional concrete and steel. Next to these, timber also has the following advantages: low density, relatively strong, and possibility for prefabrication. (Ahmed & Arocho, 2021)

For re-mountable structures, those last four additional advantages are very important. When the density is low, the weight will be low if the dimensions are limited. Low weight means quicker and less costly transport, requiring less heavy foundations. The smaller foundation is favourable because foundations are the only part of a construction that cannot be designed re-mountable nowadays. Achieving a material-optimal lightweight structure makes the design extra profitable in terms of environmental impact and costs. Prefabrication means less construction time, but it also gives a higher potential to use the elements in a re-mountable construction. Finally, timber has favourable strength properties when it is taken care of the direction in which the load acts on the timber element because timber is an anisotropic material.

This paragraph shows that timber has a high potential as a material for re-mountable structures, and a car park is a suitable type of building to make re-mountable. Therefore, using timber in a re-mountable car park has the potential to be profitable.

3.4: Introduction performance-affecting aspects of timber

As mentioned in the problem definition, there are two main performance-affecting aspects of using timber. These are durability and fire. Both aspects will be introduced shortly in this paragraph.

ISO 15686 (ISO 15686-1, 2000) describes durability as “The capability of a building or its parts to perform its required function over a specified period of time under the influence of the agents anticipated in service”. In general, it is about its resistance to attacks. Because wood is a natural material, it faces more types of attacks than synthetical materials. There are two types of wood degradation mechanisms: abiotic degradation and biological degradation (Reinprecht, 2016a, 2016b).

Each timber species' natural resistance to degradation is expressed in a durability class. Ranging from very durably species in class 1 to perishable species in class 5. These classes are linked to the five use classes to determine if the natural durability of a species is sufficient for a particular use. An essential aspect of the durability class is that it only refers to the tree's heartwood. Due to the living character of the sapwood, there are nutrients available. Therefore, organisms that cause the degradation of the wood can live and grow in the sapwood (Ermakov & Stepanova, 2020; Taylor et al., 2002), which raises the need to determine the living conditions of those degradation mechanisms. For fungi, the living conditions are a 20% to 60% moisture content, temperature between 20˚C and 30˚C, free oxygen available, and pH-value between 5 and 6. For insects, it is a moisture content of 20% to 60% and a temperature between 20˚C and 30˚C.
Therefore, it is necessary to carefully determine the timber species in this research according to their durability class and prevent the presence of the living conditions of biological degradation organisms.

There are three types of protection measures: structural, chemical, and modifying (Reinprecht, 2016a, 2016b). The major structural protection measure is to avoid sharp corners of timber because it results in a higher possibility for accumulation of dust and moisture. These circumstances create a favourable environment for the indicated degradation mechanisms. In addition, maintenance of the measures is also essential to ensure good protection during the whole service life.

The next moisture design issue is the increased swelling and shrinkage due to timber’s hygroscopic character, lowering the timber elements’ structural performance (Ermakov & Stepanova, 2020). It creates moisture-induced strains leading to, for example, cracks of coatings or elements becoming stuck. Finally, a higher moisture content gives a higher service class and reduces the strength and stiffness by factors k_{mod} and k_{def} (NEN-EN 1995-1-1+C1+A1, 2011). Therefore, the possible changes and ultimate moisture content value should be considered and minimized during the design phases.

Special attention for fire is required by using timber because it is a combustible material. The combustibility means timber elements will burn and contribute to the fire. From 300 °C, the charring process of the timber starts. So, the cross-sectional dimensions will be irreversibly reduced from this temperature because the charring layer can no longer contribute to strength and stiffness. However, this process is well predictable. In addition, strength and elasticity properties also reduce for elevated temperatures. This process starts from lower temperatures than the charring process. Timber elements can be classified by their fire resistance in combination with the necessary wall or floor protection function. Additional protection measures like non-combustible claddings or sprinklers can possibly limit the unfavourable effect of timber in a fire situation. (Buchanan, 2000)

Summarizing the fire resistance design in this research. It should be investigated what measures can be applied to limit the fire growth. Subsequently, it is necessary to check the corresponding fire resistance of the timber elements.

Chapter 4 References timber car parks

After presenting the background of this research in Chapter 3, the knowledge from reference projects should be gained to optimal design and assess the re-mountable timber car park. This chapter analyses five reference car parks. The overview of the car park designs with characteristics is provided in Appendix A. Paragraph 4.1 compares the floor designs used in the references. Next, the weaknesses and strengths per car park are indicated in paragraph 4.2. Finally, Paragraph 4.3 concludes the overall lessons learned from the car parks.

All included references are not designed to be re-mountable. So, in terms of re-mountability, no ideas can be found. However, knowledge about the connections that should be avoided in this research or how to improve them to be re-mountable can still be gathered.
In addition, for this research's design of the timber floor system. The benefits and the disadvantages of the used reference floor systems are valuable to be investigated, just like for the global layout of the references.

4.1: Comparison of the reference car park floor systems

The design parameters influencing the floor height are grid size, beam height, and floor system design. Table 4-1 shows these aspects per car park. The final column of Table 4-1 presents the resulting floor height if all height information is present. This resulting floor height is calculated by the beam height plus the floor plate height.

From Table 4-1, it can be concluded that there are a few different grid sizes used. In the transverse direction, they are all divisible by 2.5 meters due to the parking lot size (paragraph 5.1). The most used length of 16 meters in the longitudinal direction is also related to the car park layout requirements (paragraph 5.1). Studen is the only car park not accessible by the public, which probably explains the limited span of 15 meters due to a possible smaller driveway.

Next, all timber beams are made of glued laminated timber (GLT) or a laminated veneer lumber (LVL) variant called Baubuche. Based on the information in Appendix A, all car parks except for the Sege Park in Malmö have timber beams in the parking lot direction. By designing the beams in this way, the resulting span of the floor system is smaller. However, the size of the timber beam in this orientation will be larger than in a perpendicular way due to the parking lots. From Table 4-1, the references' beam heights are between 600 and 960 mm. The largest beam height corresponds most logically to the largest grid. Nevertheless, based on Table 4-1, it cannot be concluded if this correlation is always the case because there are also parameters influencing, like the type of timber beam used and the weight of the floor system. Nevertheless, the advantageous structural performance of BauBuche compared to glulam can also be concluded from Table 4-1.

Three types of floor systems are used: a CLT plus mastic asphalt floor, a complete concrete floor, and a prefab concrete floor plus cast in-situ compression layer. Concrete is presumably used due to its favourable structural and moisture resistance features. On the other hand, CLT is a lightweight material, which makes it favourable for the execution and dimensioning of the load-bearing structure and foundation. Mastic asphalt creates the required water-resistant layer on top of the timber floor. The references show that about 60 mm of mastic asphalt is sufficient. However, these car parks are not re-mountable, so the erection of a non-prefabricated mastic asphalt layer on-site plus low re-mountability potential is not a problem.

The resulting floor height is in the range of 700 to 1100 mm. From Table 4-1, the beam height contributes most to the resulting height.

Table 4-1: Comparison floor systems references

References	Grid	Main load-bearing beam	Floor system	Resulting floor height
Park & Ride Antwerpen	7.5 m x 16.26 m	GLT: 360 mm x 1400 mm	Prefab concrete deck plus compression layer: ≈400 mm	≈1800 mm
Car Park Studen	5.1 m x 15 m	GLT: 200 mm x 960 mm	CLT panel: 140 mm Mastic asphalt: 55 mm	1100 mm
Sege Park Malmö	5 m x 7.5 m	GLT: unknown height	CLT panel: unknown height Mastic asphalt: 60 mm	Unknown
Car Park Bad Aibling	2.6 m x 16.0 m	GLT & Baubuche: 240 mm x 680-840 mm, 240 mm x 600-760 mm	CLT: 100 mm Mastic asphalt: 70 mm	700 to 900 mm
Car Park Pollmeier and TUMWood	2.5 m x 16.5 m	240 mm x 600 mm Baubuche beam	Prefab concrete: 130 mm	730 mm

4.2: Assessment of the reference timber car parks

As mentioned in the introduction of this chapter, there are five references, namely the Park&Ride Antwerp Belgium, car park Studen Switzerland, Sege Park Malmö, car park Bad Aibling Germany, and car park design Pollmeier and TUMWood. This paragraph presents the strengths and weaknesses of each car park. Appendix A.1 to A.5 presents the design analysis of these five car parks.

Park&Ride Antwerp Belgium

The first car park is located in Antwerp, Belgium. It combines concrete and timber. See Figures 4-1 and 4-2. (*Oosterweel Verbinding: Hout En Beton Op Park & Ride [Powerpoint-Slides]*, n.d.; *Park+Ride Antwerp / HUB* , n.d.; Pieters, 2019)

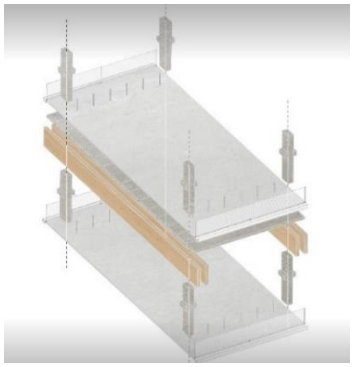

Figure 4-1: load-bearing system Park&Ride Antwerp (*Park+Ride Antwerp / HUB* , n.d.)

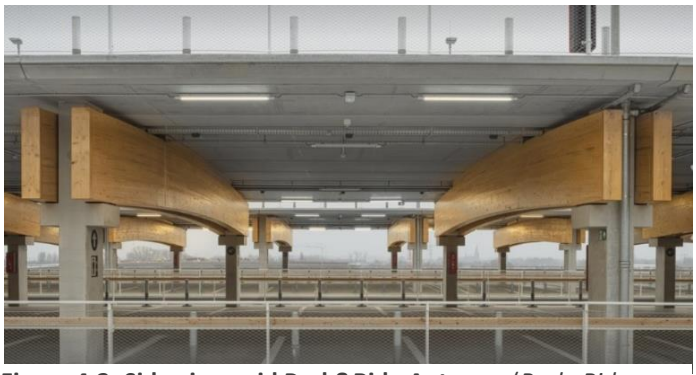

Figure 4-2: Side view grid Park&Ride Antwerp (*Park+Ride Antwerp / HUB* , n.d.)

Weaknesses:

Due to the large self-weight of the concrete floor, the timber beams must have large dimensions. Therefore, the storey height becomes large. This type of floor system creates inefficient timber usage because timber structures focus on a lightweight design.

Next, two separate timber beams near one column create unfavourable extra handlings. In addition, the steel elements between the timber beams are difficult to execute and maintain due to the limited accessibility based on the experience of the BNPC supervisors.

The cast in-situ concrete screed creates a fixed connection of the floor elements, which reduces the re-mountability of the floor system, like the monolithic concrete connections between the concrete column parts.

Strengths:
The curvature in the timber can easily ensure sufficient water drainage if considering the timber beam's creep. Concrete's high self-weight increases vibrational resistance.

Car park Studen Switzerland
The second car park, shown in Figure 4-3, is the timber plus steel car park in Studen, Switzerland. (Zaugg, 2018)

Figure 4-3: Car park Studen Switzerland (Zaugg, 2018)

Weaknesses:
Table 4-1 shows that the floor height is significant compared to the other references. On the other hand, the grid size is also the largest of all references.

The columns of the load-bearing structure have a V-form. This design limits the available space for parking lots see Figures A-8 and A-9. So, it reduces the car park efficiency.

Five CLT panels must be used for each floor grid. This amount of panels creates a large number of handling. Next, CLT has a limited fire behaviour compared to other timber elements and concrete due to the glued layered design. Layers CLT can fall off, after which the charring rate increases. A mastic asphalt layer for moisture and fire resistance is only on the top side of the floor. So, the CLT panel's bottom surface is unprotected from fire and moisture.
The mentioned mastic asphalt probably has a limited re-mountability potential due to the high temperatures during erection, so there is a high chance of merging multiple materials. In addition, erection on-site results in an increased number of actions on site, so a low prefabrication level, as indicated by the BNPC supervisors.
Also, the carpentry joints reduce the re-mountability level because of the dimensional instability of timber. The elements can get stuck together, creating a non-remountable joint, as indicated by the BNPC supervisors.

Based on sustainability, it is not the most favourable solution to apply steel elements in the whole façade as moisture protection. Because steel production is not environmentally friendly and moisture protection is necessary.

Strengths:
Due to the large grid size, fewer elements should be used, so a low number of handling is required. Next, this structure uses only one size of timber beams and columns, which makes the design more flexible and the execution easier due to the lower amount of risks stated by the BNPC supervisors.

The V-form of the pillars reduces the span of the longitudinal joists. Next, it creates a larger contact area, lowering the column's stress. Moreover, it increases the dispersion of horizontal forces. The resulting connections are easy to construct based on the experience of the BNPC supervisors, which is favourable from a feasibility point of view and interesting for the design.

Third, the bending moment distribution in the joists is optimized by designing the connection between two joists close to the pillar. Approximately at the position of zero bending moments for a continuous joist. This connection is beneficial for optimizing the dimensions of the connection.

Fourth, the timber columns are protected against moisture by concrete or aluminium close to the floor on each level, as shown in Figures A-8 and A-9. These protection measures are beneficial because water on the floor surface can flow toward the columns, making them wet.

Sege Park Malmö Sweden

The third design is the timber car park Sege Park in Malmö, Sweden. Figures 4-4 and 4-5 show this car park. (*Gjutasfalt i P-Huset Sege Park* , 2021; *Nu Sätts Trästommen På Plats i Sege Park* , 2021; Plaschke, 2021; Rosholm, 2021)

Figure 4-4: Sege Park Malmö (*Sweden's Largest Multi-Storey Solid Wood Car Park* , 2022)

Figure 4-5: Load-bearing system Sege Park Malmö (Rosholm, 2021)

Weaknesses:

Based on Table 4-1, the grid is relatively small, which results in a large number of columns. These columns are located between the parking lot and the driving lane. The first aspect is not favourable for material efficiency, and the parking efficiency is reduced due to the columns' hindrance factor on the parking lots' location. In addition, multiple different grid sizes and connections resulted in higher complexity of the design and execution phase indicated by the BNPC supervisors, which is not favourable for the feasibility of the car park.

As stated for the car park in Studen, the CLT in the floor has an increased charring rate due to the possibility of panels that fall off in combination with the fire spread via the complete timber bottom side of the floor panels.

From a structural and feasibility point of view, the slotted-in steel plate connection in the façade is less favourable than the console type of connection. The loads on the column are higher because of the lever arm between the column's end and the column's centre. Next, timber behaves more favourably in normal force instead of bending due to the layup with the timber fibres.

As already mentioned for the car park Studen, an investigation is required into the re-mountability and the level of prefabrication for the mastic asphalt layer. In addition, applying screws in the beam-to-column connection reduces the re-mountability. They can get stuck in the timber and create irreversible damage.

Strengths:

The columns span 3,5 levels, which makes the execution process faster compared to the design with columns per level. Only stability measures should be taken to assure stability during execution. However, the supervisors of BNPC indicated that this is not a problem.

Timber cover boards on the façade column protect them against moisture. Those boards are non-load bearing and placed on the outside face of the façade, so they can be easily replaced. Combining

that with a biobased material makes it a sustainable measure. Protection is beneficial due to the favourable reduction in the required use class of the columns. So, less strict design factors should be used in that case.

The vertical load transferred by the consoles for the inside columns is a favourable way of load distribution. On-site, the beam can easily be placed on the consoles. During the erection of the connection, the crane can already move to the next span, as stated by the BNPC supervisors. This results in an efficient construction process. In addition, the console's connection can be made in the factory.

Car park Bad Aibling Germany

The fourth reference car park, visualized in Figures 4-6 and 4-7, is in Bad Aibling, Germany. (*B&O Wooden Multi-Storey Car Park, Bad Aibling*, n.d.)

Figure 4-6: Car park Bad Aibling (*B&O Wooden Multi-Storey Car Park, Bad Aibling*, n.d.)

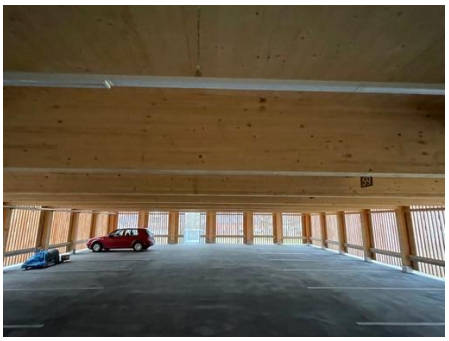

Figure 4-7: Inside view second level car park Bad Aibling

Weaknesses:

Using a column every 2.5 meters results in a relatively small grid compared to the 5 meters x 16 meters grid used by BNPC, so more timber for the columns is necessary. However, it can save some material in the floor system, as concluded from Table 4-1. Next, the limited grid result also in a higher number of elements and connections, which is less favourable from a feasibility point of view.

The maximum floor height is about 700 to 900 mm, which is not the most optimal floor system, as concluded from Table 4-1. Using a GL24h strength class results in no optimized dimensions of the roof beam.

Stability walls inside the car park block the lines of sight. These walls are unwanted because of social safety.

As already mentioned for the car park in Studen, the re-mountability potential and the level prefabrication of the mastic asphalt layer are probably unfavourable. Next, the use of a carpentry joint reduces the re-mountability level.
Also, the limited fire resistance of the CLT, as indicated for the car park in Studen, is important for this car park.

As indicated by the BNPC supervisors, using fewer different sizes per element in the car park reduces the execution risks and improves design flexibility. This statement is not the case for this car park, with different beam sizes and materials.

Strengths:

The timber columns are protected from direct rainfall by timber panels. These panels are a good solution from a feasibility and sustainability point of view, as indicated for Sege Park.
In addition, all vulnerable timber parts are covered for protection against moisture, like the edges of

the floor and the top of the columns. So, all timber elements can be assigned to a favourable use class with favourable design factors.

Tapered beams in this design ensure a sufficient slope for water drainage. Using these beams is a simple way to ensure this slope, which is important for a timber floor system.
Next, the first and the last timber beam is designed to be smaller, possibly due to the lower load on this beam. So, the material use is optimized.

Car park design Pollmeier and TUMWood
The final timber car park is only a concept made by Pollmeier and TUMWood. See Figure 4-8. (*Development of Construction System for Multi-Storey Car Parks in BauBuche*, n.d.)

Figure 4-8: Render concept car park of Pollmeier and TUMWood (*Development of Construction System for Multi-Storey Car Parks in BauBuche*, n.d.)

Weaknesses:
The design uses a column every 2.5 meters in the transverse direction. So, more beams and connections should be installed compared to a grid of 5 meters in width, which BNPC mostly uses. This small grid can result from the relatively large self-weight of the concrete floor, which is not optimal for a lightweight timber structure. This high weight also affects the dimensions of the columns and foundation negatively.

Three concrete elements are required for a 2.5-meter by 16.5-meter grid, which requires many crane movements per grid. In addition, multiple actions are required to connect the two posts. Therefore, the construction time increases, as indicated by the BNPC supervisors. This joint is also not re-mountable due to the secureness of the mortar.

There are multiple non-biobased materials used in the design. Only a third of the materials used are renewable. This amount is low for a timber car park.

Strengths:
Based on Table 4-1, it can be concluded that the resulting floor height is most optimal.
Due to the large concrete self-weight, the vibrational resistance is less important than the lightweight timber floor elements. Furthermore, it uses a BauBuche beam instead of glulam.

There is high flexibility in the arrangement of the grids. It is relatively easy to extend the existing car park vertically and horizontally, which is important from a circularity point of view. Also, using one size for the posts and beams benefits the execution. For example, there are fewer risks in the execution process, as indicated by the BNPC supervisors. Next, it makes the design more flexible.

The fire resistance of the floor design is favourable because the concrete slab extends the grid. Therefore, it creates a complete fire barrier between the levels and the grids. There are also no cavities in the timber elements through which the fire can spread.

Finally, the applied cambered beams are a relatively simple measure to ensure sufficient water drainage if considering the creep behaviour.

4.3: Lessons learned from the timber car park references

Below, the lessons learned from the five analyzed car parks are listed based on the discussion of the floor systems (paragraph 4.1) and the determined weaknesses and strengths of the references (paragraph 4.2).

- Maximizing the element size is favourable for the erection. Based on Table 4-1, the largest grid is about 5 meters by 16 meters. In this way, the number of beams, columns, and connections can be limited, which is beneficial for feasibility and the possible number of parking. In addition, due to the limited available information, it is impossible to give a clear conclusion on the effect of the grid size on the resulting floor height based on Table 4-1.

- From Table 4-1, limiting the beam height benefits the total floor height. In addition, a lower floor height results in a shorter ramp. Moreover, shorter ramps can be designed steeper, as stated in Figure 36 of NEN 2443 (NEN 2443, 2013). So, limiting the height is beneficial for ramp design and parking efficiency because a smaller ramp increases the possible number of parking lots. Next, it probably results in more levels for the same total height. So, more parking lots are possible, meaning a higher profit.

- An optimized floor in weight is essential to further improve the structural efficiency, like the beams discussed above. However, it should be noted that heavy materials, like mastic asphalt and concrete, are favourable in terms of vibrational, fire, and moisture resistance. Based on the references, a floor with CLT plus mastic asphalt is the most favourable one, with the annotation that the prefabrication level and fire resistance should be sufficient.

- The floor elements should have a high prefabrication level to improve the feasibility.

- A fixed connection between two load-bearing element parts, like a concrete screed, should be prevented to get a re-mountable structure. In addition, connection types that are hindered by the dimensional instability of timber, like screws and carpentry joints, negatively influence the re-mountability level.

- Mastic asphalt is used in all car parks with a timber floor system to protect the timber against moisture. The references of Antwerp and Pollmeier use concrete for the floor system, which faces less degradation, as indicated in paragraph 3.4. However, the re-mountability level of this system is most probably very low.

- The most favourable type of connection between the beam and column is placing the beam on the column and securing it afterwards, as used in the Sege park and or in the car park of Studen. So, the construction time is optimized because the crane can go earlier to the next element, which is beneficial from a feasibility point of view.

- From a feasibility point of view, using one size of a certain element in the whole car park is efficient, as used in the concept of Pollmeier. In addition, it creates high flexibility in design. However, it is important to investigate the dilemma between the one-size principle and the material-optimized design to avoid oversizing. This dilemma also holds for applying a column over multiple levels as done in Malmö or over one level like the other references.

- Protecting the columns in the façade with timber cover boards, like the Sege Park Malmö or the car park in Aibling, is a sustainable and feasible solution for the re-mountable car park.

- Only stability from columns or steel bracings will be used in the design phase because the use of walls is an undesirable stability method due to blocking the lines of sight for social safety.

- Cambered or tapered timber beams, applied in all references with timber beams, are an interesting and simple measure to ensure sufficient water run-off.

- The performance of CLT floor systems needs an investigation into their resistance.

Chapter 5 Starting points, requirements, and design principles

The following step in being able to design and assess the re-mountable car park is knowing the starting points, requirements, and design principles. Paragraph 5.1 provides the starting points for the design. Then, the requirements will be provided in paragraph 5.2. In addition, the two main design principles, fire and moisture resistance, will be discussed in respectively paragraphs 5.3 and 5.4.

5.1: Starting points for the design phase

The starting points are based on the practical experience of BNPC and NEN 2443 (NEN 2443, 2013).

It will be assumed that the rural area of Zandvoort is the location for the car park. The highest wind loads are present in the coastal area, but this is a very small part of the Netherlands, which is not an often-used location for a car park above the ground. So, the assumed combination of wind zone 1 with rural area gives the heaviest wind loads possible on the structure. Due to the proximity to the sea, the salt percentage in the air is high. (NEN-EN 1991-1-4+A1+C2/NB+C1, 2020)

Below are the starting points for the car park design and layout listed.

- The car park will be accessible to the public and intensively used.
- The parking lots will be located with a 90 degrees angle on both sides of the driving lane to get the most efficient area usage. If the corresponding grid dimensions become impossible to design, 70 degrees parking is the second option.
- A width of 2.5 meters will be used for the parking lots, corresponding to a public and intensively used car park. Resulting in a parking lot area of about 13.5 m^2 for 70 and 90 degrees parking.
- As stated in the problem statement (paragraph 1.1), one module of four floor areas will be designed, as shown in Figure 5-1.
- The resulting distance in the longitudinal direction, shown in Figure 5-1, is 16.26 meters for 90 degrees parking and 14.74 meters for 70 degrees parking in combination with a 2.5 meters wide parking lot. These widths span from column surface to column surface. The distance between the columns in the width direction is not specified in the code, so it is a design variable.

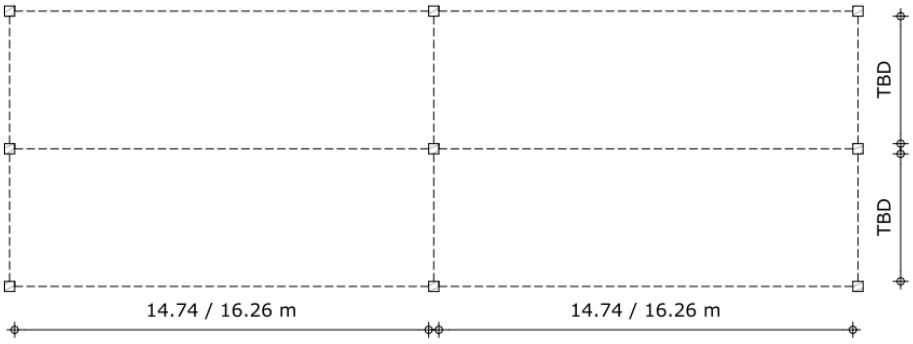

Figure 5-1: Dimensions investigated car park module

- The minimal free height is 2.2 meters.
- The installations below the floor have a maximum height of 300 mm, as indicated by BNPC.
- The car park will be suitable for cars, but not heavy vehicles. So, the limit for the car's weight will be 25 kN. (NEN-EN 1990+A1+A1/C2/NB, 2019)
- For the installations below the floor, like Figure 5-2, a self-weight of 0.25 kN/m2 will be assumed based on the experience of BNPC.

5.2: Main requirements for the design phase

The main requirements are provided in this paragraph and the remaining in Appendix B.1. Below, the Eurocodes with corresponding requirements are stated.

The national annex of Eurocode 1990 provides the following general requirements for a constructive design. (NEN-EN 1990+A1+A1/C2/NB, 2019)

- A car park belongs to design class 3, resulting in a design service life of 50 years.
- Based on the stated maximum weight of 25 kN. The design belongs to load type category F.
- Car parks belong to the CC2 consequence class.
- The deflection limit is 0.003 times the length for the frequent load combination and 0.004 times the length for the characteristic load combination.

There are no requirements based on the vibrations in car parks. The minimum required frequency in a residential building is 8 Hz (NEN-EN 1995-1-1+C1+A1, 2011). Including the maximum frequency of humans based on jumping of 5 Hz (NEN-EN 1990+A1+A1/C2/NB, 2019). This excitation is not present in a car park, so a reduced frequency is possible. A minimum vertical vibration frequency for bridges is 5 Hz (NEN-EN 1990+A1+A1/C2, 2019). In addition, a long-span timber floor system looks like a bridge, so a limit of 5 Hz will be applied in this research.

Eurocode 1991 provides the configuration of the loads corresponding to a car park. The National Annex present the loads that should be used in the Netherlands. These loads are listed below.

- The point load should be divided into two surface loads, presented in Figure 5-2. These rectangle surfaces have a length of 100 mm, indicated by parameter “a” in Figure 5-2 (NEN-EN 1991-1-1+C1+C11, 2019).

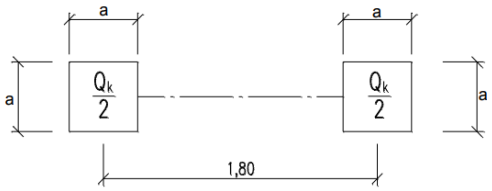

Figure 5-2: Car park point load configuration (NEN-EN 1991-1-1+C1+C11, 2019)

- Based on the required category F and the maximum weight of 25 kN. The loads on the car park floor will be q_k= 2 kN/m^2 and Q_k= 10 kN. (NEN-EN 1991-1-1+C1+C11/NB, 2019)

In case of a fire, Eurocode 1991-1-2 provides the following two requirements for the loads during a fire. (NEN-EN 1991-1-2+C3, 2019)

- Loads that are very likely to act during a fire should be considered.
- Exceptional load should not be taken into account simultaneously with fire load.

In the National Annex of the Eurocode 1991-1-4, the requirements for the wind load calculations for the Netherlands are given. The wind loads depend on the height of the car park and the location, as mentioned in the starting points. These values are given in Appendix B.1.

From the use of timber, the deflection requirement is the most important.

- The maximum deflection for a beam on two supports is L/150 to L/300 (NEN-EN 1995-1-1+C1+A1, 2011). This deflection consists of two parts, namely instant deflection and creep. This limit is less strict than the one from the National Annex of Eurocode 1990. So, the National Annex requirement will be assumed.

Nowadays, it is also important to investigate the regulations of cars with other types of fuels due to their increasing number. Specific requirements for those types of cars are not yet available. Research is going on to investigate if extra requirements are necessary and what those requirements are. Research shows that the risk of starting a fire is approximately similar to conventional cars, but the fire behaviour differs. The fire development will take longer but with a higher peak in firepower, which results in a greater chance of a travelling car fire. There is also a possibility of re-ignition due to the residual energy in the battery. Next, an electric car fire emits more toxic gasses into the air. Nevertheless, the major problem is the lack of knowledge and experience in efficiently extinguishing these types of cars, like the example of the study by Terlouw (Terlouw, 2019). Finally, identifying the type of car and corresponding extinguishing measures is problematic due to the amount of smoke. Grouping cars per type of fuel can be an efficient solution (de Witte & van der Graaf, 2021; Hilster et al., 2020; Rosmuller et al., 2021; van de Leur, 2015)

5.3: Fire resistance design of the car park

Fire can cause a lot of damage in car parks, like the car park fire in Alkmaar. See Figures 5-3 and 5-4. In addition, the mentioned innovation in electric or other non-conventional fuel cars in paragraph 5.2 increases the risk and consequences of a fire.

Figure 5-3: Car park fire Alkmaar (Hessels & Ebus, 2020)

Figure 5-4: Electric car in car park fire Alkmaar (Hessels & Ebus, 2020)

Sub-paragraph 5.3.1 gives the requirements and states how to deal with this performance-affecting topic in the design phase. Possible measures to improve fire resistance are given in 5.3.2.

5.3.1: Fire requirements and characteristics

Timber is a combustible material, so it is important to design it smartly and correctly. On the other hand, timber behaves predictably during a fire, making it easier to design for a fire situation. (Introduction to Timber & Fire, n.d.)

A car park consists of two types of fire compartments, the stairwells and all parking levels together. First, the requirements for a car park fire will be shown. The Dutch building decree (*Bouwbesluit 2012*, 2011) states that for a car park, the following regulations are required:

- Fire resistance means no collapse of construction due to fire in a building part not located in this structure. So, a fire in the parking levels should not lead to a collapse of the stairwells and vice versa. Fire resistance of 90 minutes must be used for a car park with a top floor level higher than 5 meters above ground level.
- If the fire load in the compartment is smaller than 500 MJ/m^2, the fire resistance can be lowered by 30 minutes, as mentioned in 2.10.6.
- Table 2.66 of the building decree states the fire classes of Table B-17 for a remaining use function.

A complete timber car park requires a fire resistance of 90 minutes with no reduction. Namely, a 25 mm thick timber floor element already has a fire load of 333 MJ/m^2 plus a beam of 220mm x 70mm 205 MJ/m^2 (NEN 6090, 2017). Combining both elements results already in 500 MJ/m^2, and the sizes are small compared to the ones used in the reference car parks.

The main parameter of the fire behaviour in a car park is the layout of the façade. It can be designed open or closed. The requirements for an open car park are given in Appendix B.1.
In open structures, the weather will influence the smoke and heat expansion. It results in a more rapid expansion of fire due to high wind speeds, but it also has positive effects on the temperature due to the natural ventilation that creates extraction of smoke and heat. Flashover is, in this case, mostly not possible. (de Witte & van der Graaf, 2021; van de Leur, 2015; van Herpen, 2014). In the case of a closed façade car park, the heat development is faster, and the smoke can spread through the whole compartment. An unfavourable flashover scenario will be reached more easily.(Rosmuller et al., 2021) Because a flashover results in a larger fire, it gives more damage. This phenomenon should be prevented to limit the disadvantage of a fire. In addition, dividing the parking garage into small compartments is also not favourable due to the block of view lines negatively for social safety, and it hinders the attack of the fire brigade. (NEN 6069+A1+C1, 2019; van de Leur, 2015)

An open façade will be applied in this research. No flashover results in a fire that stays locally. However, this fire can still move from car to car, called a travelling fire, which is a local fire moving through the car park (de Witte & van der Graaf, 2021; Hamerlinck et al., 2011; Rosmuller et al., 2021; van de Leur, 2015). Due to the combustion of the timber elements in the car park, there is a second way of transporting the fire next to the spread from car to car. Therefore, a local fire cannot be ensured based on the experience of Nieman. No literature about this topic exists, and no software is available to check this statement. For this research, this assumption is assumed to be correct. Nevertheless, for upcoming timber car parks, it is a valuable topic of further research to develop a test or a model for determining the effect of the timber on the presence of a local fire.
Nieman indicated two options to help achieve a local fire: applying a sprinkler or protecting all timber elements with a non-combustible material. In 5.3.2, the measures will be analysed.

5.3.2: Measures for fire resistance design

Sprinkler

The application of a sprinkler system is shown in Figure 5-5 and is also used in the reference car park of Malmö (Appendix A.3). A sprinkler aims to achieve a local fire by limiting the fire's growth. If designed according to the regulations (NEN-EN 12845+A1, 2019) and in a standard car park situation, the fire limits most probably to only one car. Literature states this is probably also true for cars with non-conventional fuel. (de Witte & van der Graaf, 2021).
However, the performance of a sprinkler in a timber car park has not yet been investigated. Further research is necessary to determine if a sprinkler can ensure a local fire. Applying a sprinkler gives some disadvantages, like the required inspection and maintenance to satisfy the performance during the complete technical lifetime of the car park. In addition, the corresponding installations increase the number of elements on-site and can increase the minimum floor height.

Figure 5-5: Sprinkler system below the ceiling (Martinez, n.d.)

Cover non-combustible material

Covering the timber elements with a non-combustible material prevents the spread of a fire. So, the car park becomes comparable to non-combustible using steel or concrete.

There are two main types of covers, namely gypsum boards (Buchanan, 2000; "European Technical Assessment ETA-20/0893," 2020) or a fire-resistant coating (Lucherini et al., 2019). However, both measures have not yet been investigated combined with a timber car park.

Gypsum board, see Figure 5-6, acts as a non-combustible material which delays ignition of the timber surface (Buchanan, 2000). However, gypsum degrades when it is in contact with moisture, which is possible in this application due to the open façade. This exposure can lead to the falling of the elements from the ceiling, which is unacceptable to occur. (Maundrill et al., 2023)

Intumescent coating, shown in Figures 5-7 to 5-9, can delay the surface ignition and the start of the charring process. Next, it also lowers the charring rate. (Lucherini et al., 2019). Applying it on the bottom surface of the floor has the highest potential to prevent wearing off by the wheels of the cars and conflict with the moisture resistance measure. However, it is an expensive measure, requires good surface preparation and maintenance (Amir et al., 2016), and in moist circumstances, the ingredients can leach out (Puri & Khanna, 2017).

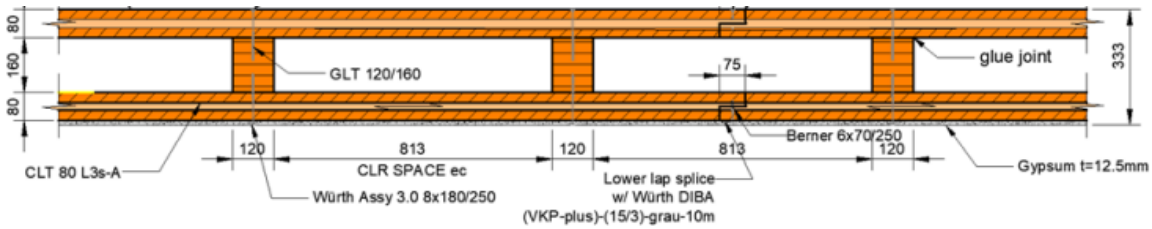

Figure 5-6: Application gypsum board ("European Technical Assessment ETA-20/0893," 2020)

Figure 5-7: Coated test sample (Lucherini et al., 2019)

Figure 5-8: Flaming of uncoating test sample (Lucherini et al., 2019)

Figure 5-9: Flaming coated test sample (Lucherini et al., 2019)

In conclusion, no clear evidence exists that the given measures ensure the fire stays local. Moreover, the measures have all negative aspects like costs and performance in wet circumstances.

Therefore, this research will assume a flashover situation with a fire resistance requirement of 90 minutes. The compartment size in which the flashover will occur is the complete parking area of the car park. However, the maximum size and duration of the fire depends on the design of the car park.

For example, in the reference project of Pollmeier (Appendix A.5), the concrete limits fire propagation through adjacent timber elements. Furthermore, fire characteristics like the ignition location and amount of combustible material available influence the fire behaviour.
This assumption of a flashover situation fire is conservative, as mentioned in the literature (van Herpen, 2014). Next, Appendix C.1 gives the same conclusion by comparing the total energy of a standard fire and a local car fire. Further research on this topic is necessary, as mentioned in 5.3.1 and 5.3.2.

5.4: Moisture design of the car park

As concluded in the paragraph about fire safety design, the car park will be designed as open. So, moisture can be present inside the car park. For a timber car park, this can be a problem in terms of durability, as indicated in paragraph 3.4. This paragraph discusses how to deal with the moisture exposure of timber elements in 5.4.1. Moreover, 5.4.2 shows examples of measures.

Five use classes (hazard classes) are defined in Table B-11 of Appendix B.2. Use classes 2, and 3 are of importance for this design. The lower the use class, the lower the natural durability of the timber element should be, as shown in Table B-12 of Appendix B.2. In addition, a lower use class results in a lower service class required, see Table B-13 of Appendix B.2. That gives higher k_{mod} values and lower k_{def} values so higher strength and less creep as shown in Tables B-5 and B-6 of Appendix B.2. Therefore, the cross-sectional dimensions will decrease. In addition, the technical service life can be higher, meaning those elements have to be replaced later, increasing the car park efficiency considerably based on the layering principle of Brand (paragraph 3.1).

5.4.1: Moisture exposure

The three main ways of moisture exposure are direct exposure of the upper parking level to weather influences, water transport by grooves of the wheels, and direct exposure through the open façade.

Unprotected timber elements must be assigned to use class 3, as stated in Eurocode 460: ”Situations in which the wood or wood-based product is above ground and exposed to the weather (particularly rain).” (NEN-EN 335, 2013).
Protected timber elements are in use class 2: “Situations in which the wood or wood-based product is under cover and not exposed to the weather (particularly rain and driven rain) but where occasional, but not persistent, wetting can occur.” (NEN-EN 335, 2013).

As the introduction of paragraph 5.4 presents, it is favourable to protect the timber elements and assign them as use class 2 to avoid larger cross-sections. More required material means a less sustainable design because more raw materials are necessary. Therefore, measures should be found to protect the timber elements and to be able to design them as use class 2.

For the façade timber elements, the most efficient and sustainable measure is a wooden protection panel, as indicated in the lessons learned in paragraph 4.3. Also, an open façade means not entirely open but at least one-third. So, the façade also protects against moisture ingress in the car park.

Considering the floor system moisture protection, multiple references in Chapter 4 use mastic asphalt. From the car park of Pollmeier and TUMWood (paragraph 4.5), it can be concluded that another solution is applying a roof against rainfall. However, this solution only benefits the upper floor level and does not protect the timber floor elements against moisture through the façade and via the grooves of the wheel. So, a water-resistant layer on each floor level is necessary next to the application of a roof. In addition, applying a roof means a high material use and, therefore, an increase in weight. So, it enlarges the load-bearing elements. In conclusion, a water-resistant layer will be applied on each level because only applying a roof is insufficient.

However, the benefit of combining the moisture protection function of a roof with solar panels or a green roof on top is an interesting topic for further research.

By applying these three measures, no timber element except for the wooden façade is directly influenced by rain. However, wetting can occur due to humid air in combination with the open façade. In addition, the open façade results in high natural ventilation to prevent flashover, creating a situation where the timber elements dry quickly. This ventilation helps avoid persistent wetting of the timber elements and ensures the elements are in use class 2.

5.4.2: Measures in moisture design

As concluded in the previous paragraph, a water-resistant layer should be applied on each level. The three examples of a water-resistant layer are mastic asphalt, a concrete layer, and a water-resistant coating.

A water-resistant layer of mastic asphalt

Mastic asphalt is used in the references of Chapter 4. Figure 5-10 shows a mastic asphalt application using the reference information from Appendix A.
The complete system is impervious to water due to the void fraction close to zero, combined with a water-resistant PMMA layer. This very low void faction also results in high durability. (Wang et al., 2017). Finally, mastic asphalt has favourable properties in fire spread resistance compared to timber (*Mastic Asphalt Footways, Car Parks & Service Decks; Technical Guide*, n.d.).

However, applying a mastic asphalt layer results in a very low re-mountability based on the investigated reference projects and the information gathered by Ballast Nedam Road Specialties B.V. The mastic asphalt attaches to the sealing membrane and the CLT panel by the high temperature of the fluid mastic asphalt during erection. So, during demounting, the floor will be damaged or should be completely removed. Removing the complete water-resistance layer results in much waste, handling, and especially more damaged CLT. Finally, small new mastic asphalt parts cannot connect to old adjacent floor parts. Next, erection requires heavy vehicles and manual work. Finally, mastic asphalt has a high self-weight, about 2400 kg/m3, comparable with concrete (Bazli et al., 2022).

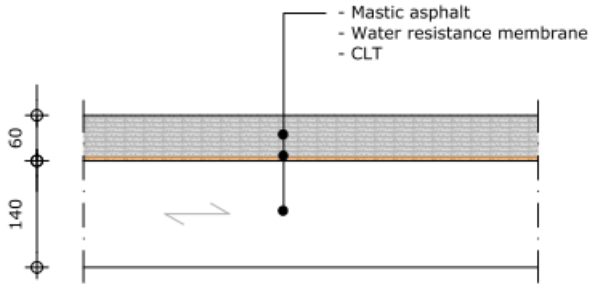

Figure 5-10: Lay-up CLT plus mastic asphalt floor system in mm

A water-resistant layer of concrete

Chapter 4 shows timber car parks with a pure concrete floor, eliminating the need for a completely watertight floor. But there are also timber-concrete composite floor systems in which the concrete protects the timber from moisture (*Timber Concrete Composites*, 2019). Systems like this can be prefabricated to ensure the re-mountability of the floor. This concrete layer will also contribute positively to the vibrational and fire resistance.
However, due to the prefabrication of the timber-concrete floor elements, the seams between the floor elements should be made watertight on-site using a sealant or coating. In addition, concrete has a higher permeability than the mastic asphalt system (Schänzlin & Dias, 2022). Improvement methods, like surface coating and integral mixing (Muhammad et al., 2015), should possibly be

included. Besides, prefabricated roughness should be applied to increase the concrete's roughness. Figure 5-11 shows a visualization of a water-resistant layer of concrete with indicative heights.

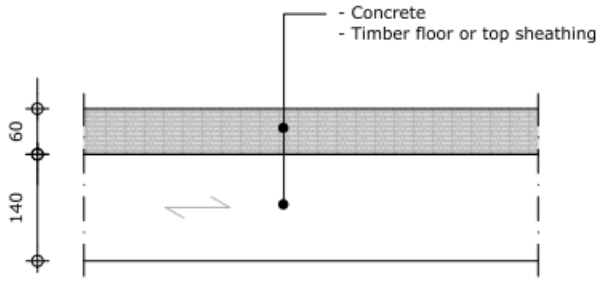

Figure 5-11: Lay-up timber plus concrete water-resistant layer in mm

A water-resistant layer of a coating

Figure 5-12 shows the system of a water-resistant coating. Using the Triflex Cryl Primer 222 (*Triflex Ondergrondtabel*, n.d.), it is possible to connect this water-resistant coating with the timber floor element. PMMA is the most suitable coating material for outside application because of its favourable resistance to weather influences (Pawar, 2016) compared to epoxy and polyurethane. The resulting thickness is about 5 mm, weighing about 19 kg/m2 (*Triflex ProPark Systeem, Variant 1*, n.d.) The configuration of the coating on the seams depends on its width.

In addition to the favourable properties in water resistance, the re-mountability potential is also good, as the Triflex technical manager indicates.
The coating can be removed using sanding and simple cutting hand tools. It requires removing about 20 cm of wearing and finishing layer around the seam. In the next application, a new coating can be placed at the seam, connecting with equal-strength chemical bindings with the adjacent coating.

A coating application's disadvantages are cracks in the timber plate material by deflection, swelling, or shrinkage. The second disadvantage is resin release from the timber. That resin can create blister formation, which damages the water-resistant layer. The cracks are only a problem if it is in the order of centimetres, which is impossible to take up for the PMMA. Based on CLT production company Derix's expectations, this order of values will not be reached, so applying a water-resistant coating on top of CLT will be fine. Nevertheless, there is no clear evidence because no test on coating performance on a CLT floor element has been conducted yet.

Appendix C.2 shows the only experiment conducted with a coating on timber. It concludes that the bonding stress is sufficient because all four specimens got cracks in the LVL. Further research is necessary to conclude if this is also the case for CLT and what the influence is for the ageing of the coating.

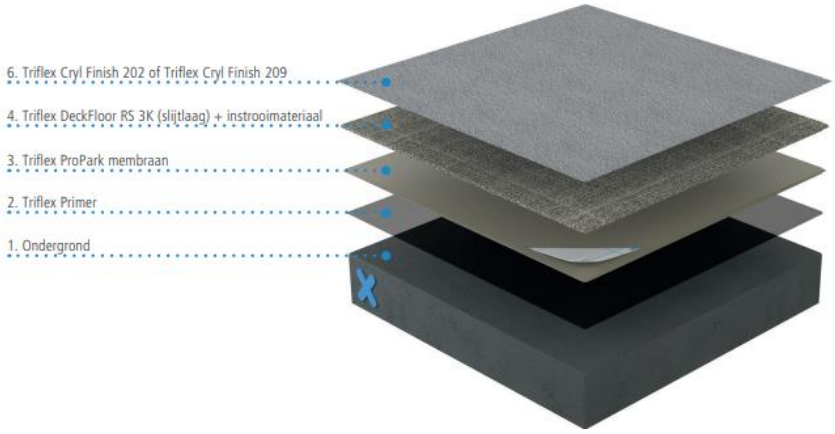

Figure 5-12: Lay-up Triflex coating (*Triflex DeckFloor Systeem, Variant 1*, n.d.)

Conclusion

Applying a water-resistant coating is the most favourable measure because it has the lowest weight per square meter and total height compared to the mastic asphalt and concrete system. Next, it has a high feasibility and most probably good water-resistant performance.

Suppose the top surface of the concluded potential floor system in Chapter 6 is made of timber. In that case, it will be assumed that a coating can be placed on top, with the annotation that further research is necessary to ensure this is possible.

If the most favourable floor design has a concrete top surface, an investigation into permeability improvement of the concrete should be done. Triflex is also possible on concrete, which has been applied multiple times, so no further research is necessary.

Chapter 6 Reference floor systems analysis and assessment

Before the preliminary and final designing of the global system and re-mountable connections, the floor systems with the highest potential should be known. Chapter 6 presents the reference floor systems and a first assessment. The general typologies of the floor systems will be given in 6.1. In paragraph 6.2, the specific floor systems are provided with additional information, their strengths and weaknesses in Appendix D. Based on the gained information, a determination of potential floor systems plus an assessment will be made in 6.3.

6.1: Typology floor systems

As stated in Chapter 1, this research focuses on the design of a timber car park. However, multiple types of floor systems are possible within a timber structure. Also, a combination of materials is possible. Assumed is that the columns and beams of the car park are made of timber. This results in the following three types of floor systems, based on the ones expressed by Kolb (Kolb, 2008).

I. Timber beam plus a top sheathing of a non-biobased material

As indicated in Figure 6-1, the timber beams are oriented in the longitudinal direction, and the non-biobased floor elements are in the transverse direction. Figure 6-2 visualizes the cross-section of the module in the transverse direction, with an undetermined joint between the timber beam and floor system I. The grid is based on the starting points (paragraph 5.1).

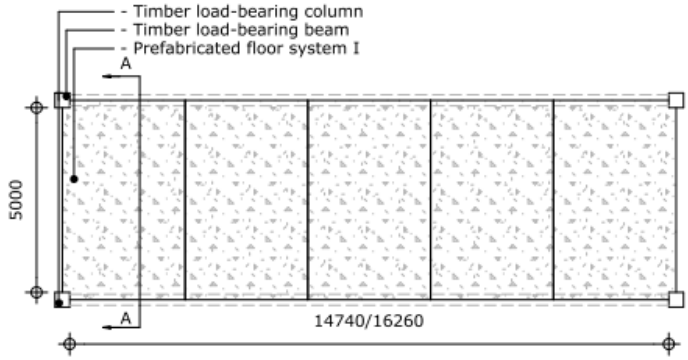

Figure 6-1: Car park module layout floor system I in mm

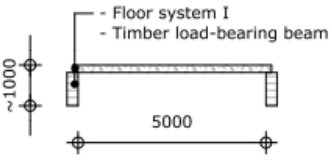

Figure 6-2: Cross-section A-A of floor system I in mm

II. Timber beam plus a top sheathing of timber

Figure 6-3 shows that the module layout for floor system II is comparable with Figure 6-1 for floor system I. Only the floor element is made of timber. The cross-section in the transverse direction with floor system II is shown in Figure 6-4. Metal fasteners can be used to connect the floor system with the timber beams of the module.

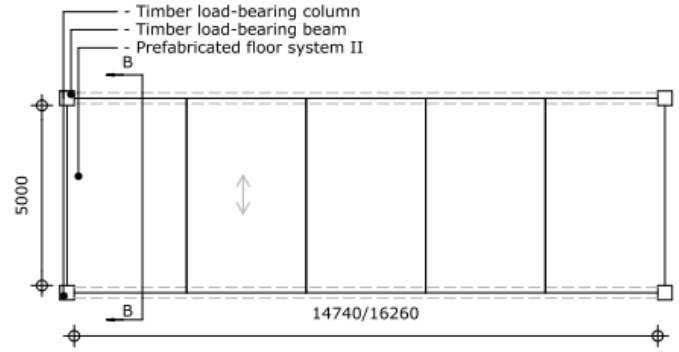

Figure 6-3: Car park module floor system II in mm

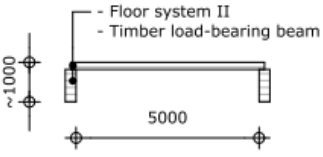

Figure 6-4: Cross-section B-B of floor system II in mm

III. Timber beam plus a timber composite floor

Due to the improved composite action, the rib floor has a higher structural performance than floor systems I and II. So, the maximum possible span is 14.74 or 16.26 meters instead of 5 meters, which makes it possible to change the module layout compared to floor systems I and II. Figure 6-5 shows that the timber beams of the module will be oriented in the transverse direction and the floor elements in the longitudinal direction. The number of elements per module is still variable. Figure 6-6 presents the longitudinal cross-section of floor system III.

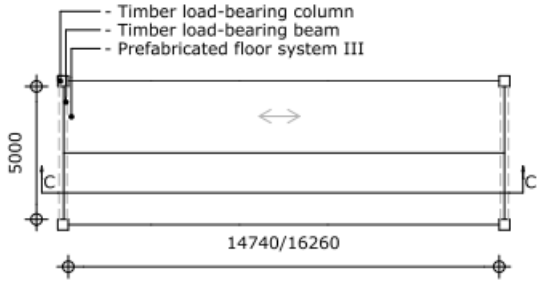

Figure 6-5: Car park module layout floor in mm

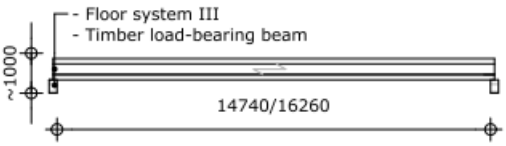

Figure 6-6: Cross-section C-C of floor system III in mm

6.2: Analysis of the reference timber floor systems

As mentioned in the introduction of this chapter, the alternatives corresponding to the type of floor systems will be discussed in this paragraph. Sub-paragraphs 6.2.1, 6.2.2, and 6.2.3 describe the alternatives for respectively floor systems I, II, and III, and they give a summary of the strengths and weaknesses based on the features presented in respectively Appendix D.1 to D.3.

6.2.1: Analysis of alternatives floor system I

Four types of alternatives correspond to floor system I using non-biobased floor elements. These alternatives are the prefab plus cast in-situ concrete floor, the prefab concrete floor, the CLT plus cast in-situ concrete floor, and the FRP floor.

Prefab plus cast in-situ concrete floor

The car park in Antwerp is the only available alternative corresponding to the prefab plus cast in-situ concrete floor.

- Floor system Park&Ride Antwerp (*Oosterweel Verbinding: Hout En Beton Op Park & Ride [Powerpoint-Slides]*, n.d.; *Park+Ride Antwerp / HUB* , n.d.)
  This system uses a combination of timber beams over 16.26 meters and prefab concrete elements over 7.5 meters. A concrete screed is cast on top to ensure the floor acts as one rigid system. Figure 6-7 presents a sketch of this floor system.

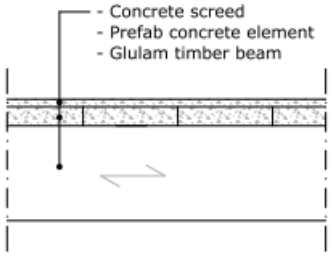

Figure 6-7: Lay-up floor system Park&Ride Antwerp

Prefab concrete floor

Two alternatives belong to the prefab concrete floor, namely the floor developed by the company Goldbeck and the one from the car park concept of Pollmeier and TUMWood of paragraph 4.5.

- Floor alternative of Goldbeck (*Parkhäuser*, n.d.)
  This alternative consists of prefab concrete elements placed on top of the steel beams and connected by shear studs with steel loops, as shown in Figures 6-8 and 6-9. Timber beams can replace the steel beams to make this alternative comparable with floor system I.

Figure 6-8: Goldbeck steel beam with shear studs connection (*Parkhäuser*, n.d.)

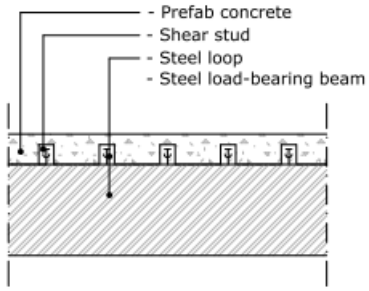

Figure 6-9: Sketch Goldbeck floor system

- Floor alternative of Pollmeier and TUMWood (*Development of Construction System for Multi-Storey Car Parks in BauBuche*, n.d.)
  This floor is made of reinforced pre-cast concrete elements and connected by a birdsmouth joint to the load-bearing timber beam. See Figures A-39 and A-42 of Appendix A and Figure 6-10.

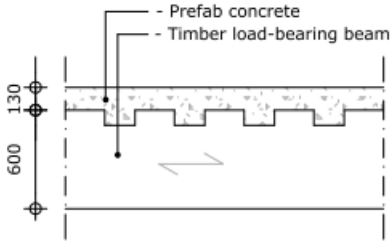

Figure 6-10: Lay-up floor system concept Pollmeier and TUMWood in mm

CLT plus cast in-situ concrete floor

Only the timber concrete composite floor of KLH corresponds to the CLT plus cast in-situ floor.

- Timber concrete floor alternative KLH (*Cross-Laminated Timber*, 2021; *Timber Concrete Composites*, 2019)
  The floor system of KLH consists of a CLT element and, on top, a cast in-situ concrete layer. The arrangement of both materials is shown in Figure 6-11. Three types of connections possible are possible, namely screws, grooves, and steel plates or strips. Figure 6-11 shows a combination of grooves and screws.

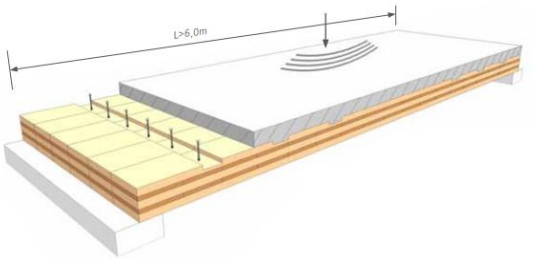

Figure 6-11: KLH timber-concrete composite floor (*Timber Concrete Composites*, 2019)

FRP floor system

As mentioned in 4.3, a lightweight floor is beneficial for the sustainability of the car park. That makes an FRP composite floor interesting to investigate. No reference floor system is available that combines an FRP floor with a timber beam. The only comparable reference is the Park4all floor system.

- Park4all FRP floor alternative (*Park4all - Parking Solutions*, n.d.)
  Park4all floor system consists of steel beams and GFRP floor elements. Replacing the steel beam with a timber beam makes a timber-FRP floor system corresponding to floor system I. FRP can connect with adjacent elements by bolts (Ascione et al., 2016), so the timber-FRP floor system has a connection type suitable for both materials. Figures 6-12 and 6-13 show the steel-GFRP composite floor system of Park4all.

Figure 6-12: Construction Park4all FRP floor system (*Park4all - Parking Solutions*, n.d.**)**

Figure 6-13: Steel-GFRP composite parking garage (*Park4all - Parking Solutions*, n.d.)

Table 6-1 shows the weaknesses and strengths per alternative of floor system 1.

Table 6-1: Strengths and weaknesses alternatives floor system I

Floor system I alternatives	Weaknesses	Strengths
General characteristics of the alternatives	- Low percentage biobased materials used	
Park&Ride Antwerp	- Low re-mountability level - Low prefabrication level - Long construction time - Small area floor elements - High self-weight - No composite action between floor and beam	- Non-combustible - Low moisture degradation risk - High vibrational resistance - Isotropic structural performance characteristics
Goldbeck	- High self-weight - No composite action between floor and beam	- Non-combustible - Low moisture degradation risk - High vibrational resistance - Isotropic structural performance characteristics - High re-mountability
Pollmeier and TUMwood	- High self-weight - No composite action between floor and beam	- Non-combustible - Low moisture degradation risk - High vibrational resistance - Isotropic structural performance characteristics - Re-mountable beam to floor connection options
KLH timber-concrete floor	- Low re-mountability level - Low prefabrication level - Long construction time - High self-weight	- Reduced combustible surface - Reduced moisture degradation risk - High vibrational resistance - Possibility for high re-mountability
Park4all	- Low stiffness - Small element area - Low machineability - Low fire resistance - Low moisture resistance - Anisotropic structural performance characteristics	- Lightweight - High re-mountability potential - High prefabrication level - High design freedom

6.2.2: Analysis of alternatives floor system II

Two types of alternatives correspond to the second floor system. These are a plate that can be made of CLT and LVL floor. Appendix D.2 presents the background of the alternatives related to floor system II. Below, the alternatives are introduced, and a summary of the strengths and weaknesses of the alternatives corresponding to floor system II is given.

CLT floor

There are two alternatives for the CLT floor: the X-lam of Derix and the CLT floor of Stora Enso.

- X-lam floor alternative of Derix (*X-Lam; Kruislaaghouten Bouwelementen in Groot Formaat Voor Daken, Vloeren En Wanden*, n.d.)
  Figure 6-14 shows the CLT floor called X-lam. It consists of at least three cross-laminated timber lamellae bonded by glue between the lamellae. Those lamellae are made of sawn timber with a minimum thickness of 20 mm.

Figure 6-14: Visualization X-lam element (*Environmental Product Declaration X-Lam*, 2022)

- CLT floor alternative of Stora Enso (*Cross-Laminated Timber (CLT)*, n.d.)
  The lay-up and characteristics of the CLT alternative of Stora Enso are similar to the previous alternative of Derix. Concluded, the same weaknesses and strengths belong to this alternative.

LVL floor

The Kerto Q panel of Metsäwood is the only LVL floor alternative.

- Kerto Q panel of Metsäwood (*Kerto® LVL for Load-Bearing Applications*, 2022; *Kerto® LVL Q-Panel*, n.d.)
  MetsäWood developed the Kerto Q panel to be applicable as a floor. This panel is made from LVL with approximately 20 per cent of the timber in a perpendicular direction, as shown in Figure 6-15.
  Compared to CLT, the thickness of the timber panels of the floor element is smaller due to the production process. The peeling technique is applied to produce the LVL veneers while the lamellae of CLT are sawn.

Figure 6-15: Visualization Kerto Q panel (*Kerto® LVL Q-Panel*, n.d.)

Table 6-2 presents the weaknesses and strengths of the alternatives corresponding to floor system II.

Table 6-2: Strength and weaknesses alternatives floor system II

Floor system II alternatives	Weaknesses	Strengths
General characteristics of the alternatives	- Low moisture resistance - Combustible character - Limited element area	- High percentage biobased materials used - High re-mountability potential - High prefabrication level - Fibres in both longitudinal and transverse direction - Lightweight
CLT floor Derix or Stora Enso	- No new weakness	- No new strenghts
LVL floor Metsäwood	- Limited element thickness	- No new strenghts

6.2.3: Analysis of alternatives floor system III

Three types of alternatives correspond to floor system III. These are the CLT plus glulam timber composite floor, the LVL timber composite floor, and the special timber cassette floors. The corresponding alternatives are listed and highlighted in this sub-paragraph. Appendix D.3 provides the alternatives' characteristics, strengths, and weaknesses.

CLT plus Glulam timber composite floor

Two companies developed a CLT plus glulam timber composite floor, namely KLH and Stora Enso.

- Timber-composite alternative of KLH (*Rib Panels*, n.d.; *Solid Wood Panels*, n.d.)
  KLH has developed an open timber composite floor system in which the ribs are made of glulam and the panels of KLH® solid wood, see Figure 6-16. The KLH® solid wood means a CLT panel.

Figure 6-16: Timber composite floor KLH (*Rib Elements*, 2019)

- Timber composite alternative of Stora Enso ("European Technical Assessment ETA-20/0893," 2020; *Rib Panels*, n.d.)
  Company Stora Enso has two types of glulam plus CLT rib floors: an open and a closed cross-section. See Figures 6-17 and 6-18. The rib floor consists of CLT panels and glulam ribs. There is no difference between the open CLT rib floor of Stora Enso and the open rib floor of KLH. So, the same weaknesses and strengths for the KLH rib floor belong to the open Stora Enso Rib floor.

Figure 6-17: Closed CLT rib floor Stora Enso (*Rib Panels*, n.d.)

Figure 6-18: Open CLT rib floor Stora Enso (*Rib Panels*, n.d.)

LVL timber composite floor

The two companies that developed LVL timber composite floors are Metsäwood and Stora Enso.

- LVL timber composite of Metsäwood (*Kerto - Ripa Technische Richtlijnen*, 2016; *Laminated Veneer Lumber (LVL) Bulletin; New European Strength Classes*, 2019)
  Metsäwood developed two types of timber composite floors made of LVL: the Ripa T and the Ripa Box. The difference between them is the presence of a bottom panel, see Figure 6-19.

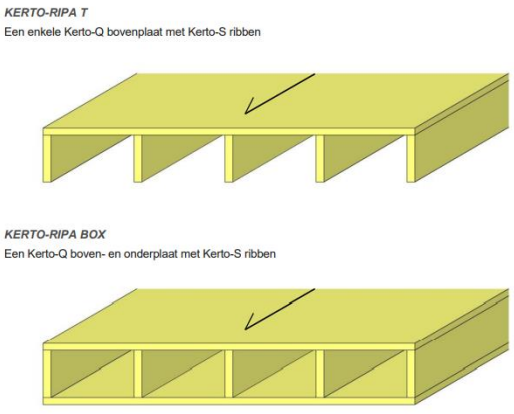

Figure 6-19: Kerto Ripa T and Kerto Ripa Box floor system (*Kerto - Ripa Technische Richtlijnen*, 2016)

- LVL timber composite alternative of Stora Enso (European Technical Assessment ETA 18/1132, 2021; Rib Panels, n.d.)
  Stora Enso has three types of LVL rib floor made of spruce: an open, semi-open, and closed cross-section, as shown in Figures 6-20,6-21, and 6-22. The panels of the LVL floor are made of LVL X, and the ribs of LVL S.

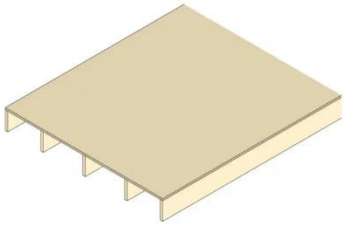

Figure 6-20: Open LVL rib floor Stora Enso (*Rib Panels*, n.d.)

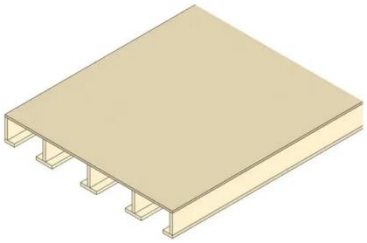

Figure 6-21: Semi-open LVL rib floor Stora Enso (*Rib Panels*, n.d.)

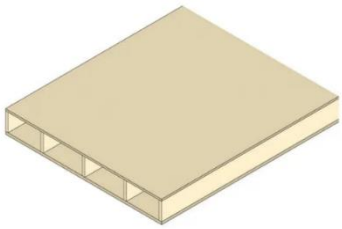

Figure 6-22: Closed LVL rib floor Stora Enso (*Rib Panels*, n.d.)

Special timber cassette floor

Two floor types correspond to the special timber cassette floor. These are the Lignatur floor and the Kielsteg floor.

- Lignatur (*Dragende Ideeën Met Hout*, 2016; "European Technical Assessment ETA-11/0137," 2021)
  Lignatur developed a floor system from sawn wood timber elements, as shown in Figure 6-23.

Figure 6-23: Lignatur® floor system (*Lignatur® Element*, n.d.)

- Kielsteg ("European Technical Assessment; ETA-18/1014," 2019; *Kielsteg - Light and Wide; The Handbook for the Wooden Roof and Floor Elements with Outstanding Performance*, 2019)
  The Kielsteg floor system consists of a curved OSB or plywood web in combination with timber top and bottom flanges. These can be made of softwood, glulam, or CLT. Figure 6-24 shows this alternative.

Figure 6-24: Kielsteg floor system (*Kielsteg - Light and Wide; The Handbook for the Wooden Roof and Floor Elements with Outstanding Performance*, 2019)

Table 6-3 presents the strengths and weaknesses corresponding to the alternatives of floor system III.

Table 6-3: Strengths and weaknesses alternatives floor system III

Floor system III alternatives	Weaknesses	Strengths
General characteristics of the alternatives	- Low moisture resistance - Combustible character	- High percentage biobased materials used - High re-mountability potential - High prefabrication level - Lightweight - Lamellae or veneers in both longitudinal and transverse direction - High composite action therefore large element area possible
KLH open rib floor	- Reduced fire resistance	- High natural ventilation - High accessibility connection rib to beam
Stora Enso closed rib floor	- Limited ventilation	- Improved fire resistance sheathing - Improved composite action - Holes inside floor can be used by installations
Metsäwood LVL open rib floor	- Limited thickness LVL sheathings and rib - Reduced fire resistance	- High natural ventilation - High accessibility connection rib to beam
Metsäwood LVL closed rib floor	- Limited thickness LVL sheathings and rib - Limited ventilation	- Improved fire resistance - Improved composite action - Holes inside floor can be used by installations
Lignatur	- Small element area - Limited ventilation - Low strength in transverse direction - Weak connection between adjacent floor element - High cost	- Improved fire resistance - Improved composite action - Holes inside floor can be used by installations
Kielsteg	- Small element area - Limited ventilation - Low strength in transverse direction - High cost - Low robustness	- Rigid connection with adjacent floor element - Improved fire resistance - Improved composite action - Holes inside floor can be used by installations

6.3: First assessment of potential floor systems

Sub-paragraph 6.3.1 presents a preliminary assessment. Based on that assessment, possible new floor designs are investigated in 6.3.2. Afterwards, the final step of the first floor system assessment is given in 6.3.3.

Floor system I	Floor system II	Floor system III
• Prefab concrete floor plus cast in-situ compression layer	• CLT floor	• Open CLT plus glulam rib floor
• Prefab concrete floor	• LVL floor	• Closed CLT plus glulam rib floor
• CLT plus cast in-situ concrete floor		• Open LVL rib floor
• FRP floor		• Semi-open LVL rib floor
		• Closed LVL rib floor
		• Lignatur
		• Kielsteg

6.3.1: Preliminary first assessment floor designs

Based on the strengths and weaknesses, some alternatives should be discarded to limit the number of floor systems in the preliminary design phase.

Appendix D.4.1 shows the reasoning behind the preliminary first assessment.
In conclusion, the following floor designs are left:

Floor system I	Floor system II	Floor system III
• Prefab concrete floor	• CLT floor	• Closed CLT plus glulam rib floor
• FRP floor	• LVL floor	• Closed LVL rib floor

6.3.2: Development of new floor designs

New floor designs can also be made based on the lessons learned in paragraph 4.3 and the strengths and weaknesses of the floor systems determined in paragraph 6.2.

Concrete has favourable moisture and fire resistance characteristics and high performance in structural dynamics. Those three features are not present in pure timber alternatives. On the other hand, timber is lightweight and a biobased material. These features concrete did not have. By correctly combining timber and concrete, all disadvantages of both materials can be lowered. The right fire and moisture resistance design is placing the concrete on top of the timber and using minimal concrete to create a maximum biobased percentage and lightweight floor. In addition, this layout also results in using the favourable strength characteristics of both materials for a situation with positive bending, as stated in 6.2.1.
The concrete layer should not be cast on-site to ensure a high feasibility and re-mountability level. Therefore, creating a complete prefabricated timber-concrete floor system in the factory is the most beneficial solution in terms of feasibility.
The combination of concrete and FRP is not favourable due to the limited floor size of FRP.

Summarizing there are new floor designs created as listed below.

- A complete prefabricated timber floor of system II with a concrete layer on top, see Figures 6-25 and 6-26.
- A complete prefabricated rib floor of system III with a concrete layer on top, see Figures 6-27 and 6-28.

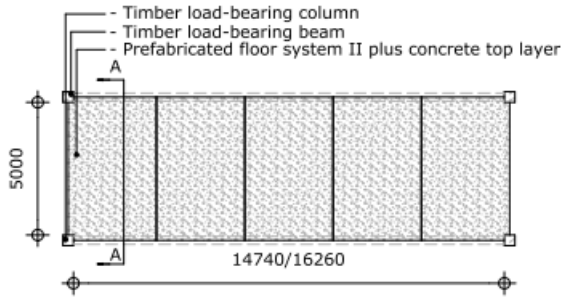

Figure 6-25: Global layout prefab timber floor system II plus a concrete top layer in mm

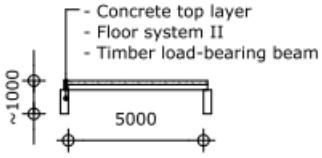

Figure 6-26: Cross-section A-A of the prefab timber floor system II plus a concrete top layer in mm

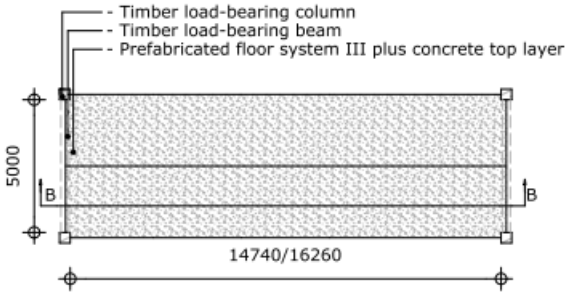

Figure 6-27: Global layout prefab timber floor system III plus a concrete top layer in mm

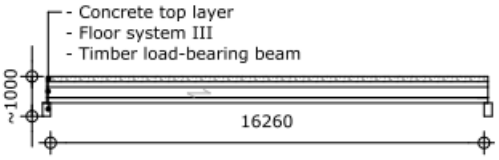

Figure 6-28: Cross-section B-B of the prefab timber floor system III plus a concrete top layer in mm

6.3.3: Final first assessment floor designs

The remaining alternatives undergo a second assessment to limit the number for the design phase. Appendix D.4.2 presents the reasoning behind this second part of the first floor design assessment. In conclusion, the following floor designs are left:

Floor system I	Floor system III	Floor system III	New floor system
• Prefab concrete floor	• CLT floor	• Closed CLT plus glulam rib floor	• Prefabricated closed CLT plus glulam rib floor with concrete top layer

The remaining floor designs are visualized in Figures 6-29 to 6-40. Additional required water-resistance or fire measures are determined in Chapter 7 per floor design.

- **Floor design 1: CLT floor**
  Figures 6-29 to 6-31 present the CLT floor system in combination with the load-bearing elements of the car park module.

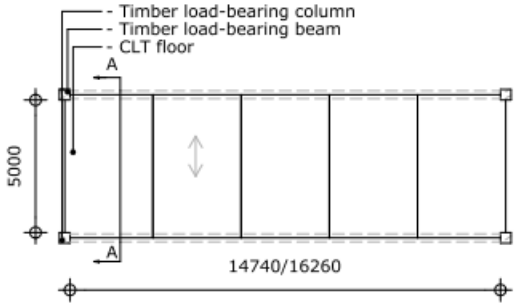

Figure 6-29: Top view floor design 1 CLT floor in mm

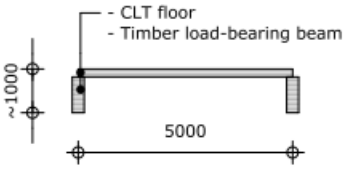

Figure 6-30: Cross-section A-A floor design 1 in mm

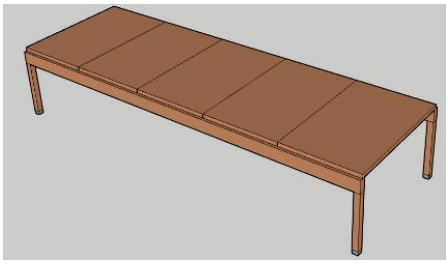

Figure 6-31: 3D view floor design 1

- **Floor design 2: Closed CLT plus glulam rib floor**
  Figures 6-32 to 6-34 show how this second alternative is placed with load-bearing elements in the car park module. The floor system is comparable to the closed rib floor of Figure 6-17.

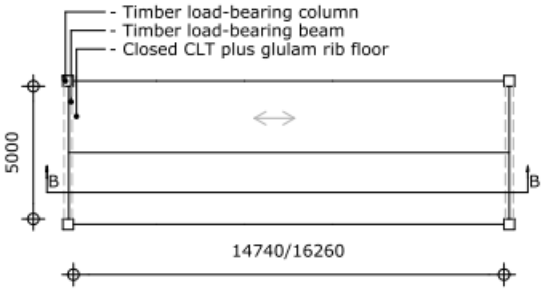

Figure 6-32: Top view floor design 2 closed CLT plus glulam rib floor in mm

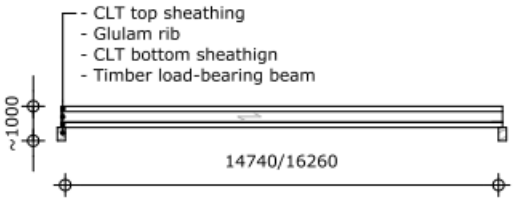

Figure 6-33: Cross-section B-B floor design 2 in mm

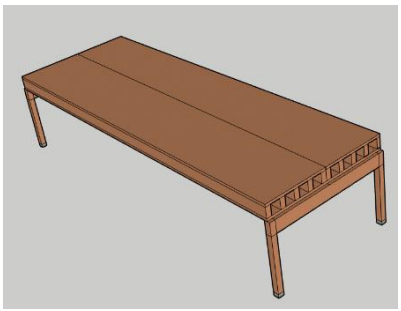

Figure 6-34: 3D view floor design 2

- **Floor design 3: Complete prefabricated closed CLT plus glulam rib floor with a concrete top layer**
  Figures 6-35 to 6-37 below present the third alternative. Also, this floor system looks like the closed rib floor of Figure 6-17, with the only difference being that a concrete layer is placed on top. The connection with the timber floor is still undetermined but made in the factory because the whole floor is one prefabricated element.

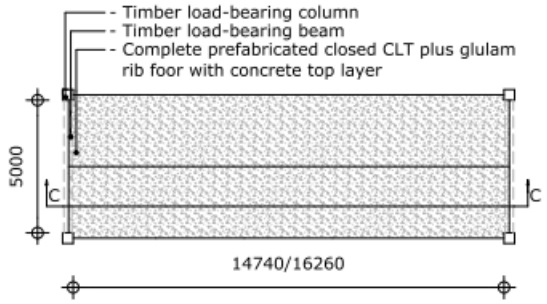

Figure 6-35: Top view floor design 3 complete prefabricated closed CLT plus glulam rib floor plus concrete in mm

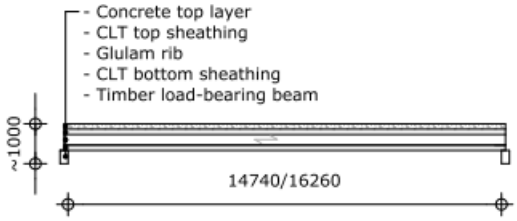

Figure 6-36: Cross-section C-C floor design 3 in mm

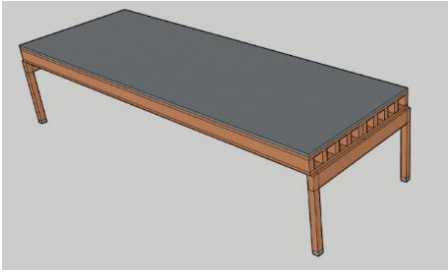

Figure 6-37: 3D view floor design 3

- **Floor design 4: Prefab concrete floor**
  Figures 6-38 to 6-40 present the prefab concrete floor in combination with the load-bearing elements of the car park module. This alternative looks like the references of Goldbeck and Pollmeier plus TUMWood showed in 6.2.1. However, the connection between the floor and the timber beam is still undetermined.

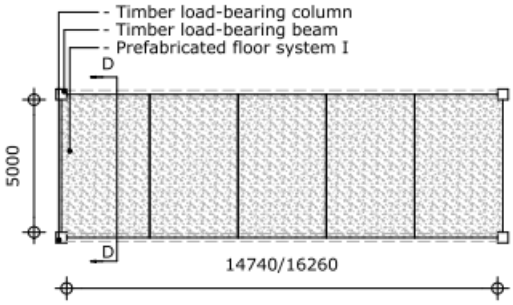

Figure 6-38: Top view floor design 4 prefab concrete floor in mm

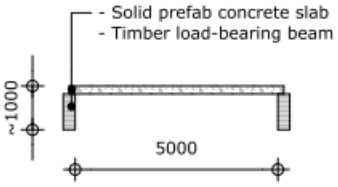

Figure 6-39: Cross-section D-D floor design 4 in mm

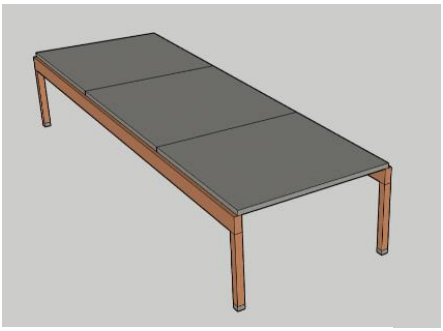

Figure 6-40: 3D view floor design 4

III Design phase

Chapter 7 Preliminary design

After gathering the floor design alternatives based on the first assessment, a preliminary design of the remaining floor systems is necessary to create background information for the second assessment through a multi-criteria analysis. This chapter presents the preliminary design of the four remaining potential floor designs. Paragraph 7.1 discusses the aspects related to moisture resistance. Then, in paragraph 7.2, the structural performance of the floor designs is considered, including the design of the load-bearing car park module beam. The check of the fire resistance for the four floor systems is given in paragraph 7.3. Paragraph 7.4 considers the total floor height optimizing potential by the connection design. Finally, paragraph 7.5 presents the concluding designs with remarks.

7.1: Preliminary moisture resistance design

First, the most favourable timber species will be determined. Then, the necessary measures per floor design are given, and the dimensional stability will be considered.
Spruce is the most common timber species based on the reference car parks in Chapter 4 and the reference floor systems in Chapter 6. Because of the limited transportation due to a growing area in Europe (NEN 5466, 2010). Limited transportation results in lower costs and higher sustainability. Spruce corresponds to the natural durability class 4 (NEN-EN 350, 2016). Table B-12 shows that this natural durability class is sufficient for a corresponding use class of 1 and 2. Use class 2 must be applied for all the timber elements except for the façade and wooden protection panels, as stated in paragraph 5.4.
In conclusion, using spruce as a timber species for the load-bearing elements is suitable according to its natural durability. Next, it is more environmentally friendly and cost-efficient due to the limited transportation. So, the timber elements in the potential floor designs are made of spruce.

The possible moisture resistance measures are already listed in subparagraph 5.4.2. The assessment of the possible measures concludes that a coating is most suitable on a top timber surface. Furthermore, applying a concrete top layer should ensure that this layer is specifically made watertight. That means floor designs 1 and 2 require a coating, and floor designs 3 and 4 require a watertight concrete top layer. The façade must protect the edges of the floor panels and beams.

For the concrete top surfaces in floor designs 3 and 4, dimensioning the reinforcement key to limit the crack widths to ensure sufficient water resistance.
Floor design 3 uses concrete on top of a timber rib floor. So, the concrete top layer should follow the dimensional changes of the timber rib floor, which gives a higher risk of crack formation, reducing the water resistance for the timber part of the floor. That makes appropriate reinforcing more important for this floor design compared to floor design 4.

Next, during the prefabrication of floor design 3, the moisture content in the connection zone between the CLT and concrete should be investigated to ensure no timber deterioration and concrete properties reduction (Siddika et al., 2021). Possible measures to improve the water-resistance are adjusting the water-to-cement ratio (w/c) of concrete, adding a vapour retarder, and applying a heater during the curing or drying period. Figure 7-1 presents the vapour retarder measure.

Literature shows a good performance of this measure, so it will be considered if floor design 3 becomes the final design. A w/c value 0.4 is most favourable for slabs to ensure sufficient workability. This w/c value also shows a favourable relative humidity and a Mould Growth Index during a year compared to a higher w/c of 0.6. So, the concrete top layer should have a w/c of about 0.4. (Baghdasarian et al., 2018)

To make the seams of concrete elements watertight, a sealant or a Triflex coating can be applied (*Triflex ProJoint Systeem* , n.d.; *Triflex ProPark Systeem, Variant 1*, n.d.). Depending on the type of connection and resulting seam width, the most suitable systems will be determined later.

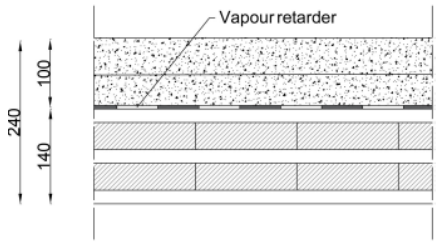

Figure 7-1: Cross-section concrete-CLT floor in mm
(Baghdasarian et al., 2018)

Due to the creep, swelling, and shrinkage, the deflections increase and the cross-section changes. These actions can damage the connections and reduce the sealant or Triflex performance.

Derix states swelling and shrinkage coefficients of 0.01% per moisture content change (MC%) parallel to the plane of the panel and 0.2% per MC% for the perpendicular to the plane of the panel (*X-Lam; Kruislaaghouten Bouwelementen in Groot Formaat Voor Daken, Vloeren En Wanden*, n.d.). Stora Enso indicates 0.02% to 0.04% per MC% in the panel direction and 0.24% per MC% perpendicular to the panel (*Cross-Laminated Timber (CLT)*, n.d.). Let's assume an average value of 0.02% in the panel direction and 0.22% perpendicular to the panel. For GLT, Stora Enso indicates a value of 0.01% parallel to the beam and 0.24% perpendicular to the beam.

In the assumed car park location Zandvoort (paragraph 5.1), the maximum difference in moisture content is 6.5%. Table 7-1 shows the corresponding values based on Figure 7-2.
Resulting in maximum CLT dimensional stability coefficients of 0.13% in the panel direction and 1.43% perpendicular to the panel direction. The ones of GLT are 0,065% parallel to the beam and 1.56% perpendicular to the beam.

Table 7-1: Determination yearly moisture content difference

	Summer	**Winter**
*Relative humidity (*Klimaatviewer*, n.d.)*	67%	85%
*Average temperature (*Klimaatviewer*, n.d.)*	17.2 °C	5 °C
Average moisture content	13%	19.5%

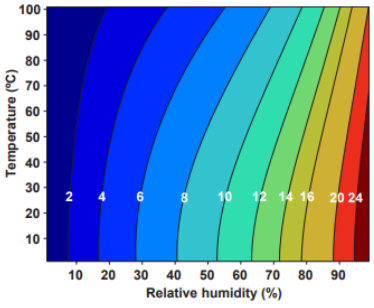

Figure 7-2: Moisture content as function of the temperature and relative humidity
(Glass & Zelinka, 2021)

The Triflex PMMA coating can face a maximum strain of about 1.8% (Zhou et al., 2021). Based on the calculated maximum strain from the results of Table 7-1, no cracking will occur due to the changes in relative humidity.

By satisfying the floor panels placed with average moisture content, the risk of cracks will be further reduced. When the CLT panel's moisture content difference becomes 7.5%, the maximum strain of 1.8% will be reached.

The Triflex coating is located on top of floor designs 1 and 2, so water accumulation above the crack is possible. Therefore, long-term wetting cannot be prevented, meaning moisture content above 20% can occur frequently. Because a relative humidity of 87% already gives a moisture content close to 20%, a situation with ponding water above the crack will further increase this value.
In conclusion, an use class 3 situation is present (NEN-EN 335, 2013), in which the natural durability of spruce may not be sufficient, as shown in Table B-12. So, biological degradation can occur, resulting in an irreversible reduction of the timber's structural performance. The technical service life will decrease, creating an unfavourable effect on sustainability. Namely, the technical service life governs over a functional service life in the case of a re-mountable structure. Next, the more strict kmod and kdef factor should be used, see Tables B-5 and B-6, unfavourably increasing the required cross-sectional areas and the total amount of timber in the car park.

In summary, maintenance of the Triflex coating is necessary to avoid biological degradation and to satisfy the initially determined technical service life. Furthermore, it is necessary to prevent the unfavourable increase in material use due to the larger required cross-section by a more strict kmod en kdef factor.
Next, assuming the CLT panel is installed at an average moisture content of 16%, cracks in the Triflex coating will occur from moisture contents below 8.5% and above 23.5% using the maximum difference of 7.5%.

7.2: Preliminary structural performance design

As indicated in the problem definition of paragraph 1.1 and the lessons learned in paragraph 4.3, it is beneficial for the profit of the car park to limit the floor height. This paragraph tries to find the most optimal cross-sections for the concluded floor designs of Chapter 6 to satisfy the structural performance requirements. Next, the supporting beam of the load-bearing car park module will also be designed. Namely, the height of this beam is also part of the total floor height, and its dimensions are valuable for the height optimization process considering the connection type in paragraph 7.5.

This paragraph will be divided into five sub-paragraphs. First, in 7.2.1, an introduction will be given to the applied loads, software, and criteria. Then, sub-paragraphs 7.2.2 to 7.2.5 cover the structural dimensioning of the four floor design. Finally, 7.2.6 covers the dimensioning of the supporting beam.

7.2.1: Introduction structural performance calculations

The floor systems will be modelled using the 3D RFEM software (*RFEM*, 2020) because the software provides deflectional and vibrational results for plates.

Paragraphs 5.1 and 5.2 provide the preliminary design's permanent and specific car park loads. Appendix E.1 determines the most severe locations of the point loads and the influence of spreading the point load out over a surface. Horizontal loads for stability assessment of the floors are not included because it is only a preliminary design. In addition, timber acts more favourably in normal force than in bending because that is in the grain orientation, and the vertical loads are perpendicular to the grain. The final design in Chapter 10 incorporates the horizontal loads.

The RFEM software applies the self-weight of the floor directly in the calculations. Table 7-2 presents the additional permanent, indicated by BNPC, and the variable loads of paragraph 5.2.

Table 7-2: Preliminary design loads on car park floor

Characteristic value permanent load		**Characteristic value variable load**	
Installations	0.25 kN/m^2	Surface load	2 kN/m^2
Water-resistant coating	0.19 kN/m^2	Point load	5 kN 2 times (Figure 5-2)
	q_g = 0.44 kN/m^2		

Due to vertical loads, bending is the most important strength criterion. Next, the low weight and corresponding stiffness also make the SLS criteria important to assess in the preliminary design. Therefore, global deflection and vibrational resistance become important due to vertical loads. SLS governs from spans of about 6 meters (Bazli et al., 2022). So, the strength criterion will only be applied for spans below 6 meters. This statement will be validated after the iteration process of floor design 1 with a span of 5 meters in 7.2.2.

Concluding, the following three structural assessment criteria will be applied:

- Global deflection
  The global deflection limit for the timber floor systems is 0.003*L for the frequent load combination applied in the preliminary design.
  Equations B.4 to B.7 must be used to calculate the final deflection from the initial deflection of RFEM. Paragraph 7.1 states the required use and service class. Table 7-3 presents the necessary parameters to calculate the global deflection, given in Appendix B.1 and B.2

  Table 7-3: Parameters final deflection calculation

k_{def}	0.8
Ψ_2	0.6

- Vibrational resistance
  The vibrational resistance can be checked in two ways: by the minimum eigenfrequency or by harmonic response analysis. The second option is a more detailed analysis, including damping and how the system responds to the dynamic loads resulting in increased deflections, accelerations, fatigue, and so on.

  As stated in paragraph 5.2, the minimum required eigenfrequency of the floor systems is 5 Hz. Equation 7.1 shows the equation to determine the eigenfrequency.

$$f[Hz] = \frac{1}{T[s]} = \frac{1}{2\pi}\sqrt{\frac{k\left[\frac{N}{m}\right]}{m_g[kg]}} \tag{7.1}$$

  Concrete has a higher self-weight than timber, resulting in a lower minimum eigenfrequency according to equation 7-1. In which parameter k is the element's stiffness, and m_g corresponds to the generalized mass. However, concrete behaves well in terms of vibrational resistance due to the high damping compared to timber, as shown in Table 7-4. Because damping is not included in equation 7-1, a comparison between timber and concrete based on minimum eigenfrequency according to equation 7-1 is inaccurate.
  So, the eigenfrequency of a concrete or timber-concrete floor element can be below 5 Hz but still perform well in practice due to the higher damping than timber.

This chapter covers the preliminary design, so only the minimum eigenfrequency will be determined to indicate the vibrational resistance performance. In the final design phase, a dynamic analysis will be carried out if the final floor designs have a damping influencing the vibrational resistance. So, is the final design floor design 3 or 4. Table 7-4 shows the damping ratios of the different materials in the remaining floor designs.

Table 7-4: Damping ratios materials

Timber	1% (NEN-EN 1995-1-1+C1+A1, 2011)
Timber-concrete composite	2.5% (NVN-CEN/TS 19103, 2021)
Reinforced concrete	5% (Papageorgiou & Gantes, 2010)

A harmonic analysis can be left out in the preliminary design by making a conservative assumption for both concrete using floor designs.

- Floor design 3 consists of timber and concrete. This floor system is comparable in design with floor design 2. The only difference is a thin concrete top layer.
  The minimum required height for the vibrational resistance for floor design 2 will also be sufficient for a timber-concrete floor design because concrete acts more favourable due to the higher damping. For the completeness of the preliminary design, the eigenfrequency of floor design 3 for this height will be determined in Appendix E.4.
- Floor design 4 consists of only concrete. According to Eurocode 1992, vibrations are not important for concrete elements. So, it will be assumed as a non-governing criterion. As mentioned for floor design 3, for the completeness of the preliminary design calculations. The eigenfrequency of floor design 4 will be determined in Appendix E.5.

- <u>Bending stress (if the span is shorter than 6 meters)</u>
  The glued laminated floor designs have the highest span in the transverse direction and support at those edges, visualized in Figures 6-29 and 6-38. So, the highest bending stresses are in this direction, modelled as the x-axis in the RFEM software.
  Tables B-7 and B-8 show the characteristic bending strength of the timber strength classes. This strength should be translated to a design bending strength using equation B-1 of Appendix B.2 and the values of Table 7-5 depending on the indicated service class 2.

Table 7-5: Safety factors design strength and stiffness values laminated timber elements

k_{mod}	0.8
γ_m	1.25

For all designs, the maximum strength class is assumed to be able to answer the research question of finding the most efficient floor system in structural performance. However, the final design phase will consider an optimization in the strength class. This investigation is important regarding cost optimization because higher strength classes result in higher costs due to the smaller availability of sufficient timber.

Finally, a length of 16.26 meters for the beam will be used as a starting point because it corresponds to the most optimal car park design indicated by BNPC. If the preliminary design shows that floor designs 2 and 3 cannot span this length, a value of 14.74 meters will be applied.

7.2.2: Structural performance floor design 1: CLT floor

Based on Appendix D.2, it can be concluded that CLT floor elements have a maximum width of about 3 meters. Most probably based on the maximum dimensions for road transport without special permission (*Grote Voertuigen*, n.d.). Applying this maximum width of 3 meters is most favourable to limit the number of floor elements and maximize the feasibility.
The span will be 5 meters according to the assumed car park module layout (paragraph 5.1). Next, CLT's highest strength class is C30, and it is possible to make with spruce ("European Technical Assessment ETA-14/0349," 2019)

Figure 7-3 visualizes the model of the floor system in the RFEM software. A 3D solid plate is modelled as a statically determined system. So, there is one supported edge with free translation in the x-direction and one fixed edge.

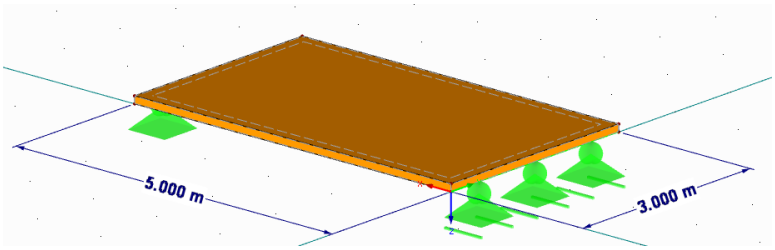

Figure 7-3: RFEM model CLT floor

A thickness of 100 mm is assumed as the starting point of the iteration process because this is the minimum value used in reference car parks, as Appendix A mentions.
The iteration process is presented in Appendix E.2.1, including visualizations of the results from RFEM.
Figure 7-4 shows the results of the iteration process, concluding that a thickness of 140 mm is most favourable with all unity checks below 1. Furthermore, Figure 7-5 visualizes this resulting cross-section of floor design 1.

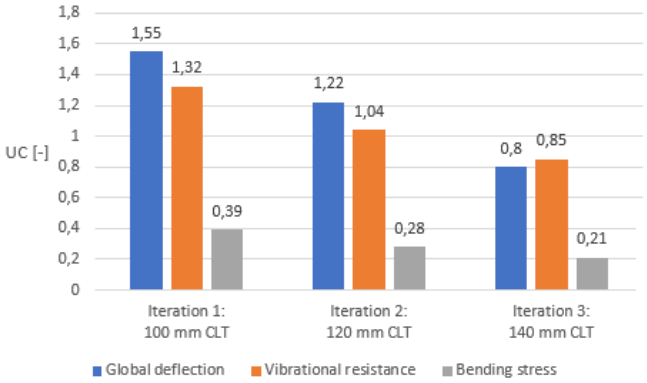

Figure 7-4: Unity check values iteration process floor design 1 CLT floor

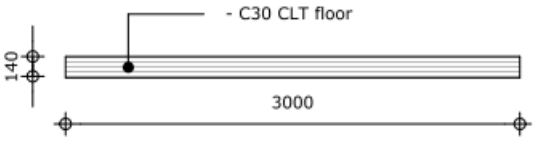

Figure 7-5: Most optimal cross-section floor design 1 in mm

7.2.3: Structural performance floor design 2: Closed CLT plus glulam rib floor

Appendix D.3 shows that rib floor elements have maximum widths of about 2.5 meters. This width will also be applied in the design because this corresponds to precisely one parking lot width (paragraph 5.1) and is acceptable for road transport (*Grote Voertuigen*, n.d.). As stated in sub-paragraph 7.2.1, a length of 16.26 will be assumed.

As indicated in 7.2.1, the results of the iteration process of floor design 1 should confirm the assumption to discard the bending stress criterion for a 16.26-meter floor. Figure 7-4 presents that

this assumption is correct because, for a 5-meter span, this criterion is already not governing. Concluding, only global deformation and vibrational resistance are considered.

A strength class C30 is the maximum possible strength class for the sheathings, indicated in sub-paragraph 7.1.2 and the reference of the Stora Enso rib floor ("European Technical Assessment ETA-20/0893," 2020). From that reference, the maximum strength class for the ribs is GL32h made of spruce, which corresponds with the assumed timber species in the previous part of this paragraph.

Figure 7-6 presents the model of this floor design in the RFEM software. 3D solid plates are used to model both the top and bottom sheathing and the ribs. The floor design has edge supports in a way that it is a statically determined system. So, a fixed edge and a free movable edge in the assumed x-direction is indicated at right in Figure 7-6.

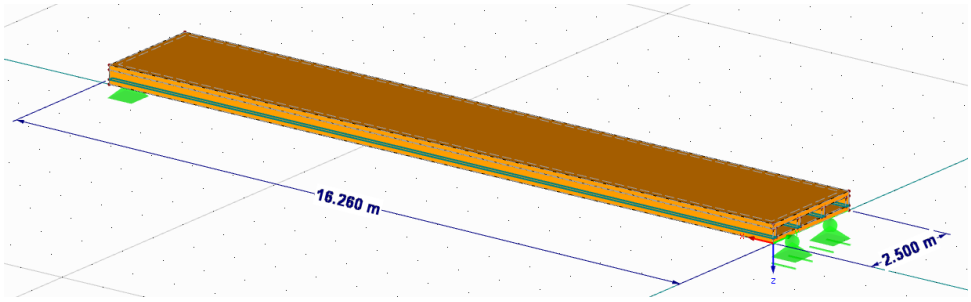

Figure 7-6: RFEM model closed CLT plus glulam rib floor

Appendix E-2.2 provides the iteration process to find the most optimal cross-section satisfying all requirements.

The minimum height of the rib floor is 220 mm ("European Technical Assessment ETA-20/0893," 2020), which is very small according to the resulting height of the CLT floor for one-third of the span. So, a total height of 400 mm will be assumed as a starting point in the iteration process using 100 mm thickness for both CLT sheathings and a glulam rib height of 200 mm.

Figure 7-7 presents the unity check values of the iteration steps.
Concluded, a span of 16.26 meters is possible, and the vibrational resistance is the governing criterion. A height of 900 mm is the minimum value to satisfy this governing criterion. Enlarging the rib width or the number of ribs has only a limited effect. See the difference between iterations 3 and 4.
Figure 7-8 visualizes the most optimal cross-section of floor design 2.

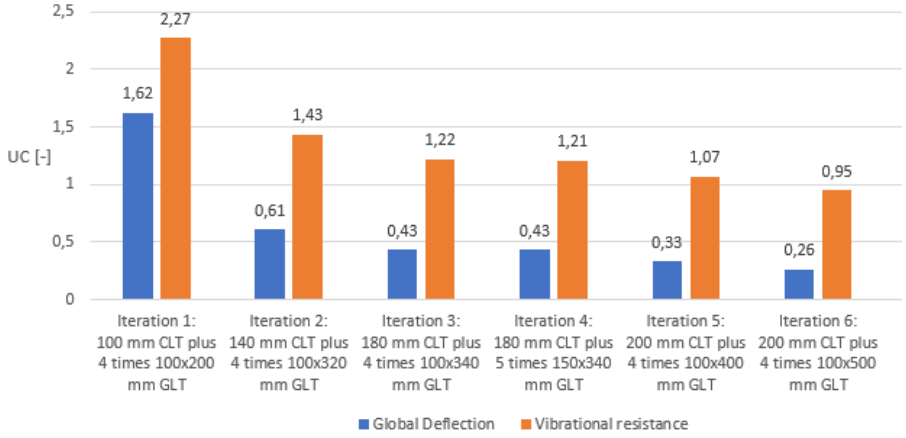

Figure 7-7: Unity check values iteration process floor design 2 closed CLT plus glulam rib floor

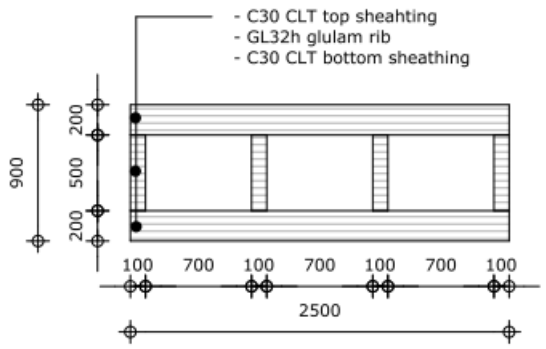

Figure 7-8: Most optimal cross-section floor design 2

7.2.4: Structural performance floor design 3: Closed CLT plus glulam rib floor with concrete top layer

This floor system is comparable to the previous one except for the concrete layer on top of the timber rib floor. Because it is a newly developed design, there are no dimensional limits indicated by a producer. So, the same dimensions as floor design 2 will be used, meaning a length of 16.26 meters and a width of 2.5 meters. The span of 16.26 meters is undoubtedly possible for this floor design because floor design 2 can be designed for this length with a governing vibrational resistance, as mentioned in 7.2.3. The concrete top layer of this floor design only increases the governing resistance.

Also, the same strength classes for the rib floor elements will be applied. So, C30 for both sheathings and GL32h for the ribs. For the concrete layer, a strength class C50/60 will be applied because this strength class is mostly used for prefab concrete elements, as BNPC indicates.

Below, Figure 7-9 shows the model for floor design 3. This model of the floor system is built up in the same way as floor design 2. The system is also statically determined.

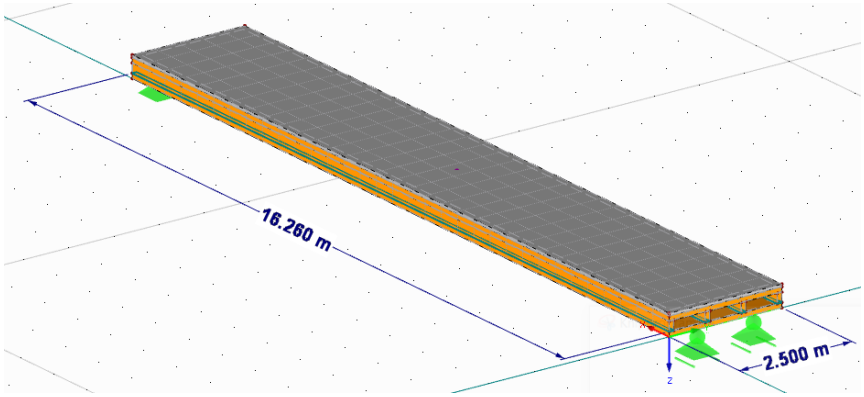

Figure 7-9: RFEM model closed CLT plus glulam rib floor with concrete top layer

The concrete layer thickness is minimally 50 mm (NVN-CEN/TS 19103, 2021). In the preliminary design, this minimum thickness will be assumed to limit the amount of non-biobased materials and weight.

As stated in 7.2.1, the minimum required height for the vibrational resistance of floor design 2 is also a conservative assumption for floor design 3. Sub-paragraph 7.2.3 shows that this is 900 mm. Next, the extra height of the concrete layer compared to floor design 2 can be translated into a sheathing thickness reduction of 20 mm and a rib height reduction of 10 mm, see Figure 7-11.

Appendix E.2.3 shows that this maximum cross-section has a minimum eigenfrequency of 4.97,

approximately 5 Hz. Considering the 2.5 times higher floor damping compared to floor design 2, according to Table 7-4, the conservative assumption is justified.

Only the global deflection criterion is left for a floor system with 16.26 meters span.
Figure 7-10 presents the results of the unity checks for global deflection calculated in Appendix E.2.3. A height of 510 mm is minimally required to satisfy the global deflection criterion, visualized in Figure 7-12. That makes the minimum required range for this floor system 510 mm to 900 mm.

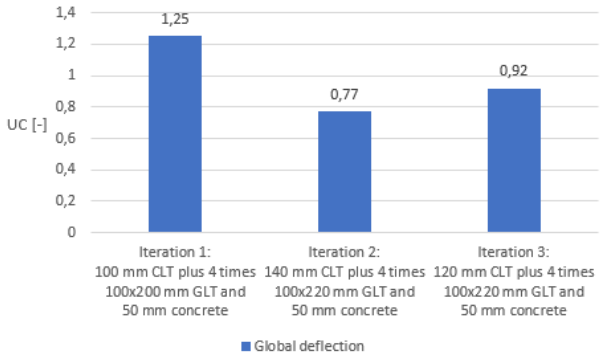

Figure 7-10: Unity check values iteration process floor design 3

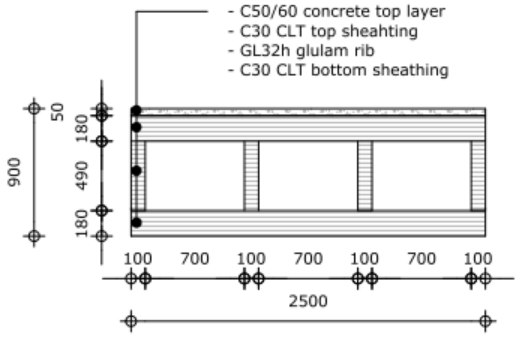

Figure 7-11: Maximum cross-section floor design 3 in mm

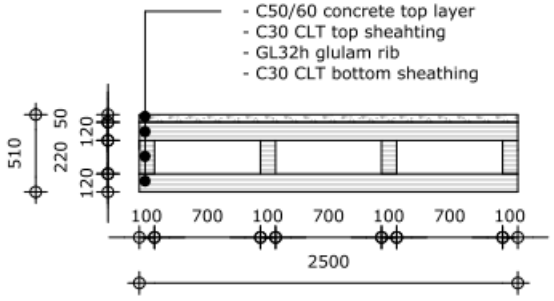

Figure 7-12: Minimum cross-section floor design 3 in mm

7.2.5: Structural performance floor design 4: Prefab concrete floor

This floor system looks like the CLT floor of 7.2.2. So, the prefab concrete floor spans 5 meters between the two supporting beams with a maximum width of 3 meters, see Figure 7-3.
A solid concrete slab is favourable over a hollow core slab because there is no need for a concrete compression layer to create a required cross-sectional area in strength and fire. So, there is no need to create a rigid connection between the concrete elements, favourable for the required high re-mountability potential.
Next, a massive concrete slab is cast in formwork in which the bottom side can be designed with the correct profile on the surface. On the other hand, a hollow core slab is created by pressing concrete in a mold. So, there is no possibility to create the required surface profile.

Compared to the indicated criteria in sub-paragraph 7.2.1, more criteria are important for a concrete resistance check.
The minimum required height for the global deflection will be determined as a starting point. Then, the bending and shear resistance will be determined with the possible required reinforcement. Next, the crack width control check will be carried out. Finally, the resulting first eigenfrequency will be determined. This eigenfrequency is not governing due to the high damping of the concrete, but it is checked for completeness of the design procedure.

The preliminary design of floor design 1 shows that the surface load governs over the two point loads. This floor system uses the same layout, so this type of variable load will be assumed to be governing. Next, the specific weight of concrete is 25 kN/m3. Because the floor is prefabricated, higher strength classes are possible compared to cast in situ, as indicated by BNPC. They mention that C50/60 is a standard prefab concrete strength, so it is also assumed in this verification procedure.

Appendix E.2.4 provides the preliminary design calculations. A height of 180 mm is the minimum required value for the global deflection. There is no shear reinforcement required for a cross-sectional height of 180 mm. A rebar diameter of 12 mm with spacing of 212 mm is minimally required to ensure sufficient bending resistance. Finally, no concrete cracking occurs because the cracking moment is larger than the bending moment for the serviceability limit state.
Despite the high concrete mass, the floor's first eigenfrequency satisfies the 5 Hz requirement. From Appendix E.2.4, it can be concluded that global deflection is the governing check.

Figure 7-13 presents the prefab floor cross-section without indicating the reinforcement.

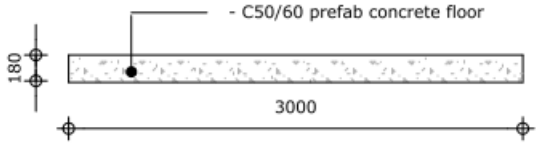

Figure 7-13: Most optimal cross-section solid prefab concrete slab in mm

7.2.6: Structural performance module beams

As indicated in the introduction of the structural performance in 7.2.1, the height of the beam also contributes to the total floor height. This sub-paragraph includes the determination of the most efficient supporting beam cross-sections of all four floor designs. The calculations are done in Appendix E.3.

The following assumptions are used in the preliminary design of the supporting beam.

- The reference car parks of Chapter 4 and Appendix A present two types of beams: a glulam beam and a Baubuche beam. So, both types are considered in the preliminary design. They have a maximum strength class of respectively GL32h and GL75 (*European Technical Assessment; ETA-14/0354*, 2018; *Gelamineerde Houtconstructies-Toepassing van Het Materiaal Voor Grote Overspanningen*, n.d.). Like the preliminary floor design, the final design phase considers if a lower strength class results in the same minimal dimensions.
- Chapter 4 indicates that tapered beams are suitable to guarantee sufficient slope. The required taper depends on the design of the water run-off. In the final design phase (Chapters 9 and 10), this aspect will be covered.
- A statically determined beam will be assumed because this is the most general configuration of a beam, and it ensures a favourable column length of more than one level (paragraph 4.3). This system can be changed in the final design phase of Chapter 10 if the connection is determined.
- It will be assumed that the beam carries the floor elements of two adjacent grids. Applying the surface load with the total span length results in the line load on the beam.
- A width of 300 mm is assumed because this is indicated as the producers' upper boundary width for BauBuche and for glulam. (*Gelamineerde Houtconstructies-Toepassing van Het Materiaal Voor Grote Overspanningen*, n.d.; *Product Overview, Tolerances and Finishes*, n.d.) However, this width is not the ultimate production width. Because there are options to create a higher width by, for example, block bonding.

Only vertical loads are assumed in the preliminary design of the floor systems. Therefore, the following two criteria will be applied, which correspond to vertical loading: bending stress and global deflection.

Bending stress

The bending strength is indicated in Table B-7 for glulam beams and Table B-10 for LVL beams. These values should be modified to a design load according to equation B.4 of Appendix B and the parameters indicated in Table 7-5. Bending will only be in the strong direction of the beam because there are only vertical loads. That leads to the check of equation 7.2.

$$\frac{\sigma_{m,y,d}[MPa]}{f_{m,y,d}[MPa]} \leq 1 \qquad (7.2)$$

Global deflection

According to paragraph 5.2 and sub-paragraph 7.2.1, the deflection limit is 0.003L. This limit corresponds to the final deflection. First, the initial deflections from the permanent and the live load should be translated into the final deflection, which should be done using equations B.5 to B.8 and the parameters of Table 7-3.

The resulting cross-sections of the beams are determined in Appendix E.3.1 to E.3.4 for respectively floor design 1 to floor design 4. Concluding from the calculations, global deflection is the governing criterion for all floor designs. Below, in Table 7-6, the concluding heights per floor design are given.

Table 7-6: Resulting heights supporting beams per floor design

	Floor design 1	**Floor design 2**	**Floor design 3**	**Floor design 4**
BauBuche beam height	1040 mm	560 mm	560-600 mm	1400 mm
Glulam beam height	1080 mm	560 mm	600-640 mm	1480 mm

7.3: Preliminary fire resistance design

This paragraph discusses the effect of the required fire resistance, stated in paragraph 5.3, on the preliminary design of the floor.
As indicated in paragraph 5.3, a compartment fire will be assumed because this is a conservative assumption. Therefore, the charring process present over the full 90 minutes of fire resistance should be applied.
The remaining cross-section can be determined using equation B.16 of Appendix B.2

The effect of a 90-minute fire will be determined for each floor design. This process will be done in sub-paragraphs 7.3.1 to 7.3.4, and the calculations are given in Appendix F. Only strength criteria should be checked in a fire situation (NEN-EN 1995-1-2+C2, 2011). Appendix B.2 shows how to calculate the design strength and actions in a fire situation.

7.3.1: Fire resistance floor design 1

From Appendix D.2, CLT's charring rate is 0.65 mm/min, and when the lamellae fall off, it is 1.3 mm/min for 25 mm. Next, Appendix B.2 presents that the heat-affected zone has a thickness of 7 mm.

Paragraph 7.2.2 shows that a 140 mm thick CLT element is required. A CLT plate with this thickness has a possible lamella arrangement, as shown in Figure 7-14 (*CLT by Stora Enso; Technical Brochure*, 2017).

Appendix F.1.1 presents that the total thickness reduction is 83.7 mm, including the heat-affected zone, meaning a remaining thickness of 56.3 mm based on the total thickness of 140 mm. This thickness reduction is summarized in Figure 7-14.

Finally, the CLT floor element will be checked on its bending resistance, as done in the structural performance analysis in paragraph 7.2. The results are calculated in Appendix F.1.1, which shows that the bending stress is below the resistance. So, a 140 mm floor has at least 90 minutes of fire resistance. This is most probably due to the governing SLS criteria in the preliminary design of sub-paragraph 7.2.2.

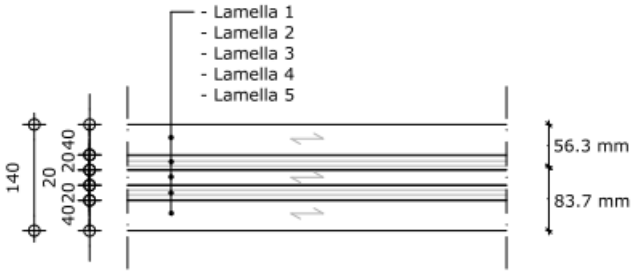

Figure 7-14: Lay-up for a 140 mm thick CLT panel in mm

7.3.2: Fire resistance floor design 2

This second floor design also has CLT panels on the top and bottom sides. They have a thickness of 200 mm. Assuming that the lay-up of these CLT sheathings is the same as for a CLT floor element with this thickness, the lamellae are stacked like Figure 7-15 (*CLT by Stora Enso; Technical Brochure*, 2017).

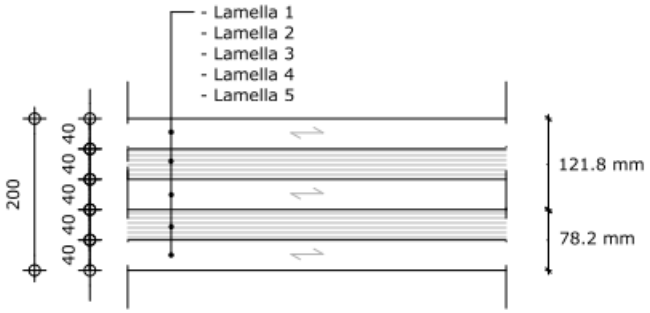

Figure 7-15: Lay-up for a 200 mm thick CLT bottom sheathing in mm

The right-hand side of Figure 7-15 presents the total thickness reduction of 78.2 mm. This reduction is smaller than for floor design 1 due to the larger lamellae thickness. A thickness of 121.8 mm is finally remaining, shown in Figure 7-15 and calculated in Appendix F.1.2.

Appendix F.1.2 also calculates the bending stress of the resulting cross-section. The bending stresses are far below the bending resistance because it also has a governing SLS criterion in the preliminary design of sub-paragraph 7.2.3, so this floor system has a 90-minute fire resistance.

7.3.3: Fire resistance floor design 3

The bottom surface of this floor system is made of timber, while the top surface is made of concrete. So, its bottom surface can still be reduced in thickness by the charring process.
Eurocode 1992 states the minimum required distance from the outer surface of the concrete to the centre of the reinforcement. This check should only be applied because the timber part mainly covers the strength of the rib floor due to the small thickness of the concrete layer.
Paragraph 5.3 states that a 90-minute fire resistance is necessary for a pure timber car park, which is also assumed for this floor design using a floor system with only the top surface made of concrete.

Because only the top surface of the floor is replaced by concrete, the minimum distance is 25 mm (NEN-EN 1992-1-2+C1, 2011).

As assumed in 7.2.3, the CLT sheathing thickness is 180 mm of the maximum cross-section. It has the lay-up of lamellas as shown in Figure 7-16, assuming the bottom sheathing is made of a 180 mm CLT element of Stora Enso (*CLT by Stora Enso; Technical Brochure*, 2017).

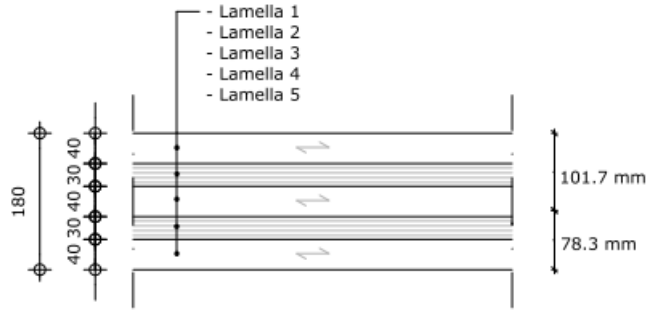

Figure 7-16: Lay-up for a 180 mm thick CLT bottom sheathing in mm

Figure 7-16 shows that the total thickness reduction is 78.3 mm for the maximum cross-section of floor design 3, as calculated in Appendix F.1.3. Meaning a remaining thickness of 101.7 mm.

The minimum cross-section of floor design 3 has a CLT sheathing thickness of 120 mm. Assuming that the CLT sheathing is made of a CLT element of Stora Enso (*CLT by Stora Enso; Technical Brochure*, 2017), the layup of the sheathing is according to Figure 7-17.

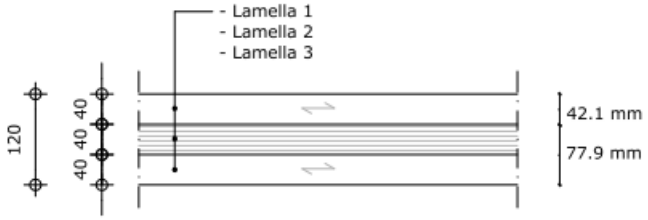

Figure 7-17: Lay-up for a 120 mm thick CLT bottom sheathing in mm

Again, the total thickness reduction and the remaining thickness are indicated on the right side of the CLT sheathing in Figure 7-17. They have a value of 77.9 mm and 42.1 mm, based on the calculations in F.1.3.

Appendix F.1.3 shows that the remaining cross-sections of the upper and lower bound can resist the bending moment for the same reason as indicated in 7.3.1 and 7.3.2.

7.3.4: Fire resistance floor design 4

Eurocode 1992 states that the minimum prefab concrete slab thickness for fire resistance of 90 minutes is 100 mm (NEN-EN 1992-1-2+C1, 2011). So, the plate of 200 mm used in this research is certainly sufficient. The reinforcement cover requirement is at least 20 mm (NEN-EN 1992-1-2+C1, 2011), so the reinforcement can easily be designed to satisfy this requirement.

7.3.5: Fire resistance beams

Appendix F.2.1 to F.2.4 shows the preliminary fire resistance assessment of the supporting beams per floor design. Both glulam and Baubuche beam has a charring rate of 0.7 mm/min (*European Technical Assessment; ETA-14/0354*, 2018; *Gelamineerde Houtconstructies-Toepassing van Het Materiaal Voor Grote Overspanningen*, n.d.).

In conclusion, the results of Appendix F.2 show that all beams have sufficient fire resistance. So, the dimensions of Table 7-6 are sufficient for fire resistance. The reason is most probably comparable

with the one for the floor systems. The beam is over-dimensioning in terms of the ultimate limit state to reach a sufficient serviceability limit state resistance.

7.4: Preliminary connections design

As indicated in Chapter 6, all types of timber floors can be made re-mountable because several timber-timber connections can be re-mountable, like dowels, bolts, and carpentry joints. BNPC also uses re-mountable connections between the TT-slabs in their re-mountable ModuPark design. Concluding, all floor designs can be designed re-mountable in some way. So, investigating this topic in the preliminary design has no benefit. However, there is a possibility to connect the rib floor with the supporting beam as suspended support, which might give a lower height of the total floor system.

Floor designs 2 and 3 use a timber rib floor. The difference in connection is shown in Figures 7-19 and 7-20. These figures are cross-sections A-A of the top view in Figure 7-18.
Figure 7-19 shows the traditional configuration like the ones in Appendix E.4. The adjusted connection is shown in Figure 7-20.

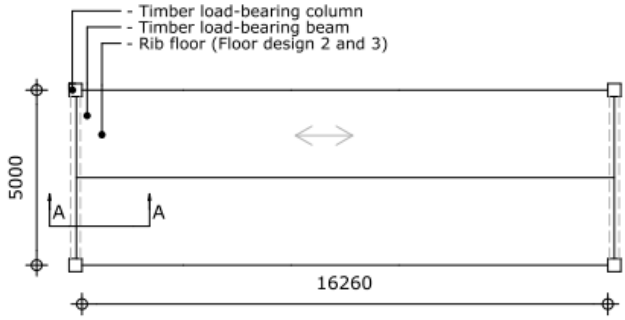

Figure 7-18: Top view global layout floor rib floor

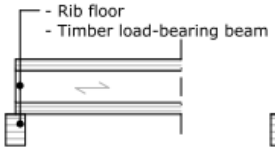

Figure 7-19: Section A-A rib floor placed on top of the supporting beam

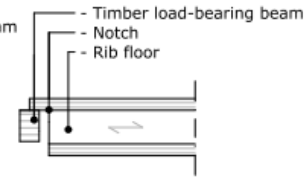

Figure 7-20: Section A-A rib floor suspended support

The free height is the distance between the top surface of the lower floor level and the bottom surface of the lowest element of the upper floor level. The installation zone is also affecting the free height. Figures 7-21 and 7-22 show the traditional connection. The free height is from the top floor surface to the bottom beam surface in Figure 7-21 because this beam passes the driveway in the grids indicated in Figure 1-2. And to the installation bottom surface in Figure 7-22 near the parking grids. Also, for the suspended support, the bottom surface of the installation zone is the lowest floor surface, as shown in Figure 7-23. This installation zone has a height of 300 mm, as indicated by BNPC. So, the height benefit is only present in the grid where the beam crosses the driveway, and the height improvement is about 200 mm to 300 mm based on Table 7-6 and paragraphs 7.2.3 and 7.2.4. In conclusion, for only three beams, there is a height saving. Next, suspended support also has some unfavourable characteristics.

- The small area between the column and rib floor, see Figure 7-20, is prone to moisture degradation (paragraph 3.4).
- The potential of installations inside the rib reduces because they should pass the beam.
- Third, the relatively thin connection part of the suspended rib floor has low robustness. During a fire or in case of other damage, the connection's resistance becomes insufficient earlier.
- Fourth, adjusting the length is almost impossible because the suspended part should be cut off.

Due to the above reasons, this suspended connection will not be applied in the final design phase.

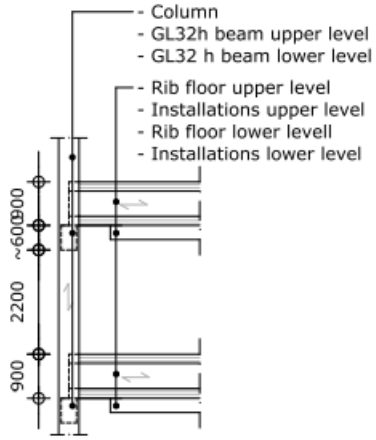

Figure 7-21: Rib floor on beam connection at driveway crossing in mm

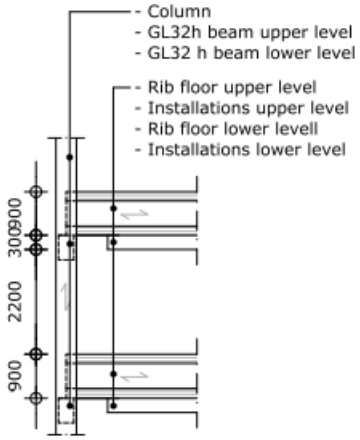

Figure 7-22: Rib floor on beam connection at parking girds in mm

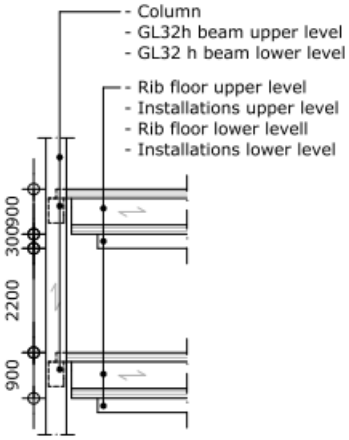

Figure 7-23: Suspended rib floor connection with installations in mm

7.5: Conclusion preliminary design floor systems

Combining the resulting floor height with the beam height and thickness of a required water resistance layer gives the total floor heights of Table 7-7. Appendix E.4 presents the visualizations of those floor systems. Based on the results, the weight of the floor system is the main governing parameter for the total floor height because it increases the beam height significantly.

A span of 16.26 meters is used for floor designs 2 and 3 because they can reach this length, resulting in the car park's highest area efficiency.
Applying a shorter length, 14.74 meters instead of 16.26 meters, can change the difference in heights between the floor designs. Because for floor designs 2 and 3, the span reduces. For floor designs 1 and 4, the beam length reduces. In addition, the total self-weight and variable load reduces because of the smaller area for all floor designs. A second calculation step in this preliminary design is necessary to find the effect of changing the length. Nevertheless, it reduces the car park efficiency, so it is not included in this research.

Comparing the results of Table 7-7 with the dimensions of the reference car parks, Table 4-1 leads to the following conclusions:

- The thickness of floor design 1 is comparable to that of the car park Studen. However, the beam's cross-sectional area is smaller. This research uses a 1.26-meter larger beam span, which can cause part of the difference because the parameter length is power four in the deflection equation E.22. In addition, the column's V-form reduces the beam's span further. Finally, this research uses only strength class GL32h, and in the Studen Car park, it is GL24h, GL28k, and GL32k. (Zaugg, 2018)
- Floor design 4 can be compared with the Park & Ride Antwerp and the concept of Pollmeier plus TUMWood. Park & Ride Antwerp has a larger floor span but two beams per column, resulting in a logically larger prefab floor thickness and a comparable beam cross-section. On the other hand, the concept of Pollmeier and TUMWood has half of the span compared to floor design 1. Resulting in a slightly smaller thickness of the floor. Next, much lower beam dimensions are applied in that design. The smaller floor thickness and span can partly cause this difference, combined with the more fixed connection of the beam with the column compared to this research.

Table 7-7: Preliminary resulting heights floor designs

		Floor design 1	Floor design 2	Floor design 3	Floor design 4
Beam height	**BauBuche** **Glulam**	1040 mm 1080 mm	560 mm 560 mm	560-600 mm 600-640 mm	1400 mm 1480 mm
Governing criterion beam		Global deflection	Global deflection	Global deflection	Global deflection
Floor height		140 mm	900 mm	510-900 mm	180 m
Governing criterion floor		Vibrational resistance	Vibrational resistance	Vibrational resistance	Global deflection
Coating		5 mm	5 mm	0 mm	0 mm
Total height		1185 mm / 1225 mm	1465 mm / 1465 mm	1070-1110 mm / 1500-1540 mm	1580 mm / 1660 mm

Chapter 8 Assessment of the potential floor systems

In Chapter 7, four designs are made that fulfil the requirements of structural performance, fire and moisture resistance. Those designs are visualized in Appendix E.4. This chapter assesses the most suitable floor design, focusing on the re-mountability and structural performance mentioned in the research goal.
First, in paragraph 8.1, the set-up of the multi-criteria analysis is given. Then, 8.2 presents the assessment of the preliminary floor designs. Finally, 8.3 provides the conclusion of the MCA for a certain ranking of criteria and a sensitivity analysis.

8.1: Set-up of the multi-criteria analysis

The set-up of the multi-criteria analysis consists of determining the criteria, multi-criteria method, and weight factors given in 8.1.1 to 8.1.2.

8.1.1: Determination of the criteria

Based on the research goal, research question, and performance-influencing aspects covered in the theoretical analysis (part I of the report), the main topics for the multi-criteria analysis of designs are feasibility, structural performance, sustainability, and costs.
The corresponding criteria and sub-criteria for the multi-criteria analysis of the floor systems are given in Table 8-1. An explanation of these criteria with their sub-criteria is given in Appendix G.1.

Table 8-1: Criteria assessment floor systems

Main *Criteria*	Sub-criteria
Construction time	Number of elements
	On-site handlings
	Quality control
MEP installations	Integration of installations
	Machineability
Future-proof	Adjustability
	Re-mountability
	Re-mounting damage
	Technical service life
	Waste
Structural height	Floor height
Structural weight	Floor weight
Environmental impact	Material sustainability
Moisture resistance	Protection performance
	Design influence
Production cost	Material cost
	Handlings and coordination

8.1.2: Determination multi-criteria method

A multi-criteria analysis requires weight factors for the criteria and scores for the floor designs per criterion. This paragraph determines which method of valuing those two aspects is most suitable to apply in this research.

There are two options to express the performance of an alternative, namely quantitatively values and qualitatively. Both types of expressions can be linked to some of the Table 8-1 criteria.
Applying the “verwachtingswaardemethode” (Ministerie van Financien, 1992) makes combining

qualitative and quantitative scores in a multi-criteria analysis possible. The qualitative performances can be translated to a value based on Table 8-2. The columns in this table represent the position in the ranking for a certain criterion, from high performance to low performance. So, score 1 means the score for the alternative, which is the best-performing one on this criterion. Row four of Table 8-2 must be used in this assessment process with four alternatives. The difference between consecutive values will increase, making steps into the lowest position. This increasing step size makes an alternative with large advantages and disadvantages less suitable than an alternative that scores medium on all criteria. Large disadvantages are unwanted, so this principle is favourable to use.
If multiple alternatives have the same score on a sub-criterion, then the average value should be determined based on the ranking position of those alternatives.

Table 8-3 presents the criterium values for the quantitative criteria. It shows a high difference in value between the positions for qualitative criteria of Table 8-2. Assuming only qualitative values makes comparing the floor designs more valuable. Because the floor designs are only preliminary, the quantitative values are also preliminary. Moreover, the quantitative performances of the floor designs, like resulting floor heights, can easily be translated into ranking positions to make the scores qualitative.

Table 8-2: Qualitative score values
(Ministerie van Financien, 1992)

Number of alternatives	Position 1	Position 2	Position 3	Position 4
1	1	x	x	x
2	1	0.75	x	x
3	1	0.89	0.61	x
4	1	0.94	0.79	0.52

Table 8-3: Quantitative score values
(Ministerie van Financien, 1992)

Number of alternatives	Position 1	Position 2	Position 3	Position 4
1	1	x	x	x
2	1	0	x	x
3	1	0.5	0	x
4	1	0.67	0.33	0

The determination of weight factors (W_i) according to the “verwachtingswaardemethode” is given in equation 8.1. The parameter i represents the position of the criterion on the ranking of importance. Sub-script 1 corresponds to the most important criterion. Next, parameter j is the total number of criteria. (Ministerie van Financien, 1992).

$$W_i = \Sigma \frac{1}{j*(j-(i-1))} \tag{8.1}$$

Table 8-4 indicates the resulting weight factors corresponding to a certain number of criteria based on equation 8.1. These weight factors should be used for the main criteria, the eight criteria of Table 8-1. In addition, it should also be used to weigh the sub-criteria for each main criterion, as determined in Appendix G.1.

Table 8-4: Weight factors per alternative in function of the number of criteria

	Most important							*Least important*
Number criteria	**W_1**	**W_2**	**W_3**	**W_4**	**W_5**	**W_6**	**W_7**	**W_8**
1	1	-	-	-	-	-	-	-
2	0.75	0.25	-	-	-	-	-	-
3	0.61	0.28	0.11	-	-	-	-	-
4	0.52	0.27	0.15	0.06	-	-	-	-
5	0.46	0.26	0.16	0.09	0.04	-	-	-
6	0.41	0.26	0.16	0.10	0.06	0.03	-	-
7	0.37	0.23	0.15	0.11	0.07	0.04	0.02	-
8	0.34	0.21	0.15	0.11	0.08	0.05	0.03	0.02

8.2: Multi-criteria assessment of the floor designs

The first part of the assessment procedure is determining which beam type is most suitable because sub-paragraph 7.2.6 presents two types of timber beams. This assessment is done in Appendix G.2.1; the results with the corresponding conclusion are given in 8.2.1. Sub-paragraph 8.2.2 provides the results of the floor system assessment.

8.2.1: Multi-criteria assessment supporting beams

Table 8-5 below summarises the assessment procedure done in Appendix G.2.1.

Table 8-5: Criterion rankings per supporting beam type

	BauBuche beam	Glulam beam
Height	1	2
Weight	2	1
Material environmental impact	2	1
Production cost	2	1

Only the resulting floor height is beneficial for the BauBuche beam. But this benefit is between 0 mm and 80 mm. That gives a minimal positive effect on the total car park height and ramp length. For a 4-storey car park, this is only 320 mm. In addition, for a ramp using a maximum slope of 14% (NEN 2443, 2013). The possible shortening of the ramp per level is about 300 mm.

In conclusion, the glulam beam is beneficial over the BauBuche beam. Only if marginal gains for height improvement should be found in the design, then a BauBuche beam is more favourable.

8.2.2: Multi-criteria assessment floor systems

Appendix G.2.2 presents the reasoning behind the floor system assessment, and Table G-36 summarises the concluding ranking positions per criterion. These ranking positions on each criterion are translated to criterium scores in Table 8-6 based on row 4 of Table 8-2.

Table 8-6: Criterion scores per floor design

Main criterion	Sub-criterion	Floor design 1	Floor design 2	Floor design 3	Floor design 4
Construction time	Number of elements	0.65	0.97	0.97	0.65
	On-site handlings	0.65	0.65	0.97	0.97
	Quality control	0.97	0.97	0.52	0.79
MEP installations	Integration of installations	0.65	0.97	0.97	0.65
	Machineability	1	0.87	0.87	0.52
Future-proof	Adjustability	1	0.94	0.79	0.52
	Re-mountability	1	0.65	0.65	0.94
	Re-mounting damage	0.65	0.65	0.97	0.97
	Technical service life	0.52	0.79	1	0.94
	Waste	0.65	0.65	0.97	0.97
Structural height	Floor height	1	0.87	0.87	0.52
Structural weight	Floor weight	1	0.94	0.79	0.52
Environmental impact	Material sustainability	1	0.94	0.79	0.52
Moisture resistance	Protection performance	0.97	0.97	0.65	0.65
	Design influence	0.94	0.65	0.65	1
Production cost	Material cost	1	0.79	0.52	0.94
	Handlings and coordination	1	0.94	0.52	0.79

8.3: Conclusion of the multi-criteria analysis

This paragraph shows the conclusions of the multi-criteria analysis. However, this conclusion depends on the ranking of importance for the main criteria. This ranking will be determined in 8.3.1. The corresponding results are given in 8.3.2. Finally, 8.3.3 shows the sensitivity analysis outcomes.

8.3.1: Primary ranking of importance for the main criteria

As indicated in the paragraph introduction, multiple rankings of importance for the criteria are possible because the needs and requirements can differ between clients.
In this sub-paragraph, one possible ranking of importance is given. This primary ranking is based on the research question of paragraph 1.3, which states that this research tries to find the most suitable design based on structural performance and feasibility.

An overview of the main criteria with their corresponding topic is given below in Table 8-7 to ensure the criteria can be ranked. The problem definition (paragraph 1.1) indicates the following important topics: structural performance, feasibility, sustainability and durability. Next, costs are also important for the competitiveness of the design. So, those five topics are linked to the main criteria.

Table 8-7: Relationships topics and main criteria

	Feasibility	Structural performance	Cost	Sustainability	Durability
Construction time	X		X		
MEP installations	X				
Future-proof	X			X	
Structural height		X			
Structural weight	X	X	X		
Environmental impact				X	
Moisture resistance					X
Production cost			X		

Table 8-8 presents the pairwise comparison results to determine the ranking positions. In a pairwise comparison, the importance of a criterion to another criterion is investigated. The criterion with the highest importance scores 1; the other criterion 0. Summing up the total scores per criterion results in the ranking of importance, shown in the most right column of Table 8-8. The mutual comparisons are explained below the Table 8-8.

Table 8-8: Pairwise comparison results main criteria

	Construction time	MEP installations	Future-proof	Structural height	Structural weight	Environmental impact	Moisture resistance	Production cost	Total
Construction time	X	1	1	0	0	1	1	1	5
MEP installations	0	X	1	0	0	1	1	1	4
Future-proof	0	0	X	0	0	1	1	1	3
Structural height	1	1	1	X	1	1	1	1	7
Structural weight	1	1	1	0	X	1	1	1	6
Environmental impact	0	0	0	0	0	X	0	1	1
Moisture resistance	0	0	0	0	0	1	X	1	2
Production cost	0	0	0	0	0	0	0	X	0

Mutual comparisons:

- The floor height mainly determines the car park efficiency (paragraph 1.1). Therefore, this criterion is favourable over the other criteria.
- Feasibility is the most important criterion for determining the most suitable re-mountable floor design. Therefore, the criteria corresponding to feasibility (Table 8-1) are more important than the remaining criteria.
- Combining the load-bearing timber load-bearing structure with a heavy floor negatively influences the structure dimensions, reducing the feasibility and car park efficiency. Therefore, the floor weight criterion is considered more important than the other feasibility criteria: construction time, MEP installations, and future-proof.
- Moisture degradation can limit the technical service life of the timber, so it lowers the sustainability of the timber. Therefore, moisture resistance design is more important than the environmental impact.
- The production cost only partly determines the total cost of the structure because criteria like feasibility and good moisture resistance will also affect the total cost. So, the production cost has a limited effect on the total cost. Therefore, it has the lowest importance.
- If the car park is not competitive for its first application, there is never a second application. Because the criterion future-proof only covers aspects related to the potential for the second use, it will be ranked less important than the construction time and MEP installations criteria.
- Criteria construction time is assumed to be more important than MEP installations because it covers the whole process from factory to erection on-site. So, saving time in the complete process is more important than only on-site. Next, lowering the number of elements is also beneficial for the detailing optimization corresponding to the criterion MEP installations.

The concluding ranking of importance is shown below in Table 8-9.

Table 8-9: Ranking of importance main criteria

Ranking of importance	Main criteria
Most important	Structural height
	Structural weight
	Construction time
	MEP installations
	Future-proof
	Moisture resistance
	Environmental impact
Least important	Production cost

8.3.2: Results primary ranking

Table G-37 of Appendix G.3.1 presents the weighted scores per criterion for the four floor designs based on the ranking of importance given in Table 8-9. Below, Table 8-10 summarises the resulting weighted scores from a high value to a low value.

Table 8-10: Summary results multi-criteria analysis

Concluding position	Alternative	Total weighted score
1	Floor design 1	0.925
2	Floor design 2	0.880
3	Floor design 3	0.819
4	Floor design 4	0.598

Based on the total values of Table 8-11, floor design 1 is the most favourable design due to its highest resulting weighted value, but Table G-37 shows that the total unweighted score is also the highest. The second-best is floor design 2, then floor design 3, and floor design 4 has the lowest score.

The difference in weighted scores between the best and second-best floor designs is 0.045, as shown in Table 8-10. The lower bound of the total weighted score is 0.52 because this is the lowest criterion score, shown in Table 8-2, and the sum of the weight factors is always 1. Therefore, a difference of 0.045 is 9.4% on a total weighted score range of 0.52 to 1.

In addition, Figure 8-1 shows a visualization on a logarithmic scale of all the results of Table 8-10 together. It shows that the blue line corresponding to floor design 1 is well-performing on the criteria with a high score, but the lines are close to each other in the figure except for the yellow line of floor design 4. Therefore, Appendix G.3.1 presents the logarithmic radar plots per floor design pair.

Figure 8-1: Weighted criterion scores primary ranking

Checking the uncertainty of the given conclusion is done in Appendix G.3.2 by a sensitivity analysis. Some criteria are changed from positions and corresponding weight factors to see the difference in the outcome. This change is only done if there is an arguable possibility to do this, meaning position 8 can never become position 1. Table 8-7 presents the topics per main criteria that help switch the positions meaningfully.
Based on Appendix G.3.2, the only way to get another most favourable floor design is the situation in which the main criterion construction time has the highest ranking position. In this case, floor design 2 has the highest score and floor design 1 has the second-highest score. This score of floor design 1 is only 0.021 lower than floor design 2. On all other analyses, floor design 2 has the second-highest score.

In conclusion, floor design 1 is the most favourable floor design because it has the highest score in every situation except for one sensitivity analysis. Floor design 2 scores very close results compared to floor design 1, so this floor system is a good second alternative.

8.3.3: Results secondary rankings

Sub-paragraph 8.3.2 assumes that the main criteria of structural performance and feasibility have the highest ranking positions based on the research question. However, cost, sustainability, and durability can also be the most important criteria for clients. Therefore, this paragraph shows the results for the cases in which cost and sustainability are assumed to be most important.

Assuming the cost is most important. Production cost, structural weight, and construction time should be placed at the top of the ranking, according to Table 8-7. The other criteria do not directly influence the cost and will be assumed in the same order of importance as in Table 8-9. Appendix G.3.2 presents in Table G-42 the scores per criterion for the floor designs on the new rankings. Table 8-11 shows that floor design 1 is still the most favourable alternative.

Table 8-11: Summary results secondary ranking on costs

Concluding position	Alternative	Total weighted score
1	Floor design 1	0.934
2	Floor design 2	0.870
3	Floor design 3	0.736
4	Floor design 4	0.679

If sustainability is the most important criterion, ranking position 1 must be for sub-criteria environmental impact and ranking position 2 for future-proof, based on Table 8-7. Environmental impact is on position 1 because it is linked to sustainability already for first use instead of future-proof. The other criteria do not directly influence sustainability and remain in the same order as Table 8-9.
Floor design 1 is again the most favourable floor system with the highest weighted score, as shown in Table G-43 and summarized in Table 8-12 below. In conclusion, if sustainability is the most important criterion, floor design 1 and floor is the best alternative.

Table 8-12: Summary results secondary ranking on sustainability

Concluding position	Alternative	Total weighted score
1	Floor design 1	0.925
2	Floor design 2	0.855
3	Floor design 3	0.813
4	Floor design 4	0.629

Next, durability can also be the most important topic. That results in the ranking and results of Table G-44 and the corresponding summary of Table 8-13 using the topic relationship of Table 8-7. Again floor design 1 has the highest score.

Table 8-13: Summary results secondary ranking on durability

Concluding position	Alternative	Total weighted score
1	Floor design 1	0.932
2	Floor design 2	0.865
3	Floor design 3	0.778
4	Floor design 4	0.640

In conclusion, floor design 1 is the best alternative for the other three secondary rankings of the main criteria. This conclusion gives again extra certainty to the statement that floor design 1 is the most favourable one to apply in a timber car park mentioned in paragraph 8.3.2.

Chapter 9 Final design - global layout

The most suitable floor system is known, so the final design of the re-mountable car park can be made, including satisfying the re-mountable character of the car park.
This chapter presents the final design of the global layout, meaning the positioning of the elements and installations. The goal of this chapter is:
Find the most optimal global layout in terms of feasibility and structural performance.

This goal is directly related to the main research goal, including the two main aspects: feasibility and structural performance.

An introduction for determining the optimal global layout will be given in paragraph 9.1. Next, the boundary conditions are listed in paragraph 9.2. Subsequently, paragraph 9.3 determines the design of installations present in the grids. Finally, paragraph 9.4 assesses the possible layouts and gives the conclusions.

9.1: Recap and introduction global layout design

Chapter 8 concludes that floor design 1 is the most favourable for the given ranking in the importance of the criteria in Table 8-9.
Four grids of 16.26 meters by 5 meters will be incorporated in this design, as mentioned in Chapter 1 and visualized in Figures 1-1 and 1-2 by the grey area. Figure 9-1 shows these four grids in detail. The length of 16.26 meters corresponds to the length between the outer faces of the column, while the width of 5 meters corresponds to the column centre to column centre distance.

Table 9-1 below lists the elements and products in a grid. It can be separated into three groups: main load-bearing elements, drainage system, and electrical system.

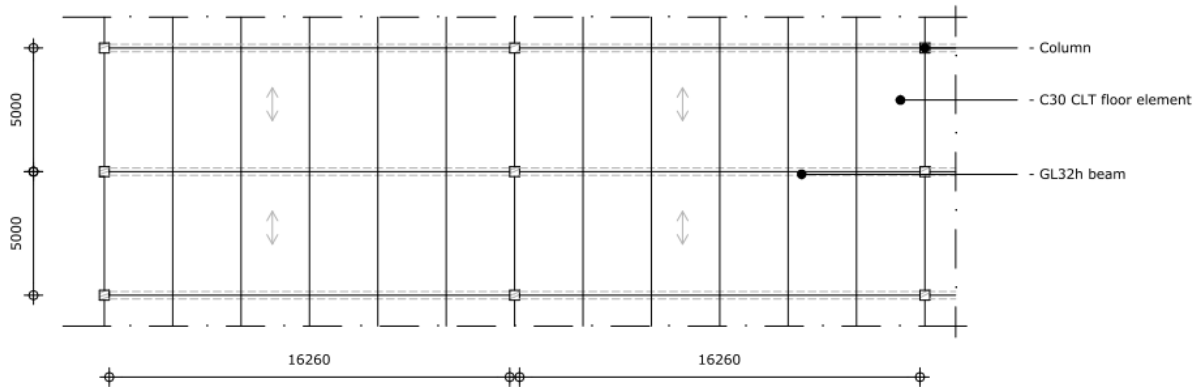

Figure 9-1: Top view investigated grids in mm

Table 9-1: Products and elements list

Load-bearing elements	Drainage system	Electrical system
CLT floor element	Gutter	Electrical products (e.g. lights)
Glulam beam	Vertical and horizontal duct	Cable system
Column	Overflow protection	

Next, some design issues are related to the drainage and electrical system. For example, a sufficient slope should be created for the drainage system to avoid a waterfall at the edge of the car park. These topics will be covered in detail design (paragraph 9.3).

9.2: Boundary conditions

Boundary conditions will guide the assessment of the most suitable global layout. The boundary conditions are divided into four parts: transportation, feasibility, production, and the starting points plus requirements of Chapter 5 and Appendix B.

Transportation

The maximum transportation sizes and weights are given below in Table 9-2 for regular transport. Exceptional transport results in higher costs and limitations and routing and planning, leading to more unfavourable feasibility.

Table 9-2: Maximum transportation dimensions (Kuiper & Ligterink, 2013; Overzicht Maten En Gewichten in Nederland, 2012; Reefer Trailer, n.d.)

Width (dividable - individable) [m]	2.55 – 3
Length [m]	≈16.88 - 22
Height (Including reduction trailer height [m]	2.7
Weight (Including reduction empty truck weight) [tonnes]	27.3

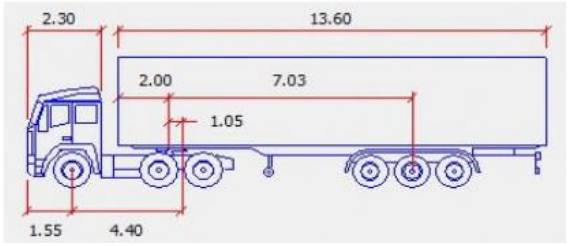

Figure 9-2: Truck with trailer dimensions (*Nader Onderzoek MFA Overtuinen*, 2017)

In length, the truck plus trailer should be maximally 16.5 meters. However, the load may protrude at the front and end of the trailer to a maximum length of 22 meters. The protruding length at the end of the trailer is maximally 0.5 times the length between the last axle and the end of the trailer, with a maximum protruding length of 5 meters (*Overzicht Maten En Gewichten in Nederland*, 2012). Protrusion in front of the truck is impossible for the beam elements with a long span. They should be positioned under an angle to pass the truck's cabin or placed horizontally above it. However, the trailer should support these beams, reducing the efficiency of the available trailer volume.

An example truck is shown in Figure 9-2. Applying the requirements gives a maximum length of the trailer of 16.88 meters.

The remaining volume to be used for loads given in Table 9-2 is summarized in Figures 9-3 and 9-4.

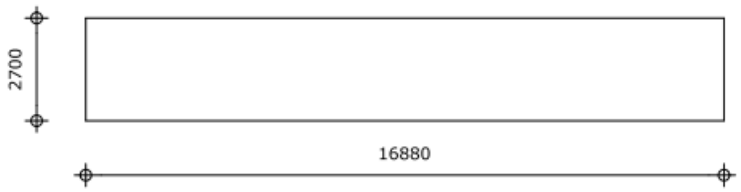

Figure 9-3: Length direction view maximum loading area trailer in mm

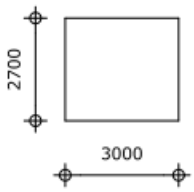

Figure 9-4: Cross-sectional view maximum loading area trailer in mm

Feasibility

Below, the feasibility boundary conditions are indicated based on the information gathered by the BNPC supervisors and the lessons learned from paragraph 4.3.

- The sizes of the elements should be optimized instead of the weight per handling
- Limit the number of actions during mounting and demounting
- Limit the number of manual actions, so strive for the highest prefabrication level
- Limit the necessary duration of heavy vehicles and equipment per handling

Finally, the re-mountability of the possible connections affects the feasibility largely.
There are two main types of connections in timber: metal fasteners and carpentry joints. The main types of metal fasteners are screws, bolts, and dowels.

Table 9-3 presents the type of connections and their relative re-mountability potential. Concluding that the bolt and dowel have the highest re-mountability and feasibility potential.

Table 9-3: Comparison re-mountability potential connection types

Type of connection	Relative re-mountability and feasibility potential	Background potential assessment
Screw	Low	- Irreversible damage - Risk to get stuck - Low maximum diameter
Bolt	High	- Reusable predrilled hole - High maximum diameter
Dowel	High	- Reusable predrilled hole - High maximum diameter
Carpentry joint	Low	- Risk to get stuck by dimensional instability

Additionally, only a screw and a bolt can take up tensile stresses, which makes the bolt more favourable over a dowel.

The final limitation of the re-mountable joint is based on the water-resistant Triflex coating on top and the drivability of the floor elements. Because the Triflex coating is about 5 mm thick, the nuts of the bolt on top of the floor elements make applying a Triflex coating impossible. Because the coating cannot be placed over the nut, and cars cannot drive over the nut without damaging their tires. In conclusion, protruding parts on top of the floor element must be avoided.

Production

Production limits will also affect the design freedom of the grids. For the timber glulam beam and CLT panel, the maximum dimensions are given in Table 9-4. Glulam beams have no clear limitation in cross-sectional dimension due to the freedom in the number of the lamella and glueing them together. As mentioned in sub-paragraph 7.2.6, a width of 300 mm is a given upper limit by producers, but this is not the ultimate possible width. The same principle holds for height and length; the ultimate dimension is not unlimited, but there is no fixed boundary. However, the boundaries are certainly higher than the applied 1080 millimetres in height and 16.26 meters in length.

Table 9-4: Maximum dimesions floor and beam element (*CLT by Stora Enso; Technical Brochure*, 2017; *Gelamineerde Houtconstructies-Toepassing van Het Materiaal Voor Grote Overspanningen*, n.d.)

	CLT panel	Glulam beam
Width [mm]	2950	> 300
Length [mm]	16000	> 16260
Thickness/height [mm]	320	> 1080

General requirements

The requirements and starting points mentioned in Chapter 5 and Appendix B.1 are still valid for the final design phase.

9.3: Detail design drainage and electrical system

The drainage and electrical system must be known to assess the final global system. This paragraph focuses on the design of these details.

Drainage system design

As mentioned in paragraph 4.3, a curved or tapered beam can give a sufficient slope in the floor. Figures 9-5 and 9-6 show both systems. For a curved beam, the tip of the panel has no contact with the beam. Connecting the panel to the beam gives stress concentration, and this gap is prone to moisture degradation. So, the tapered beam of Figure 9-7 will be applied because this problem is not present in a tapered beam.

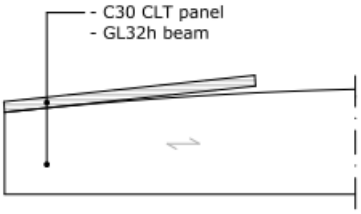

Figure 9-5: Curved beam with CLT panel

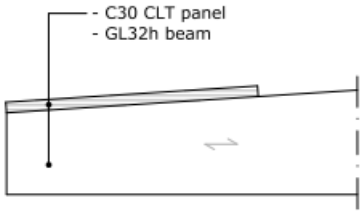

Figure 9-6: Tapered beam with CLT panel

The beam of Figure 9-7 shows the tapered design. There is a taper from both sides of the beam to limit the total height of the beam. Because one continuous taper over the full length of the beam gives twice as much extra height (Δh) of the beam compared to the design of Figure 9-7, see equation 9-1.

Using the slope requirement of Appendix B.1, the total height increment is rounded up to 130 mm based on the preliminary floor design of Table E-23, as calculated in Equation 9.1.

$$\Delta h[mm] = 1\% * \frac{1}{2} * l[mm] + u_{fin,tot}[mm] = 0.01 * \frac{1}{2} * 16260 + 46.76 = 128.06\,mm \quad (9.1)$$

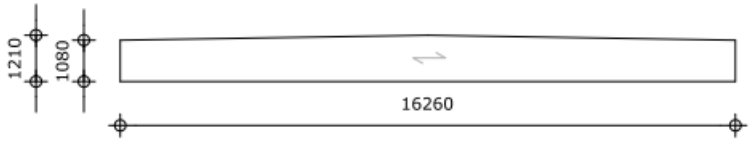

Figure 9-7: Tapered beam preliminary design in mm

This design raises the following issue, namely the number of CLT panels. Because one panel cannot be placed partly on both sides of the taper, this problem is exaggeratedly shown in Figure H-1. So, an even number of CLT panels should be positioned on both sides.

This length is about 8.13 per side, so applying three panels per side is possible with an extra margin of 0.87 meters based on the minimum transportation width of 3 meters, as visualized in Figure H-2. An extra margin is necessary to span half of the column thickness due to the net distance of 16.26 meters. But this distance is most probably smaller than 0.87 meters, which is favourable for the transportation potential.

Figures 9-8 and 9-9 show that the centre two CLT panels must have an edge under an angle of 1 degree. So, both panel edges become perfectly vertical.

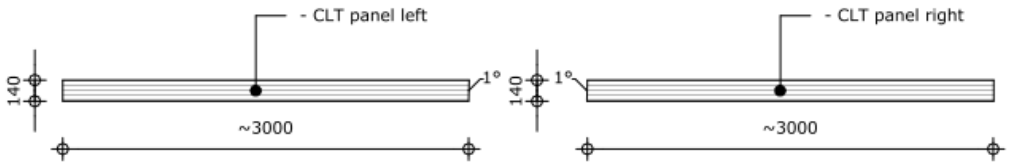

Figure 9-8: Centre CLT panel design in

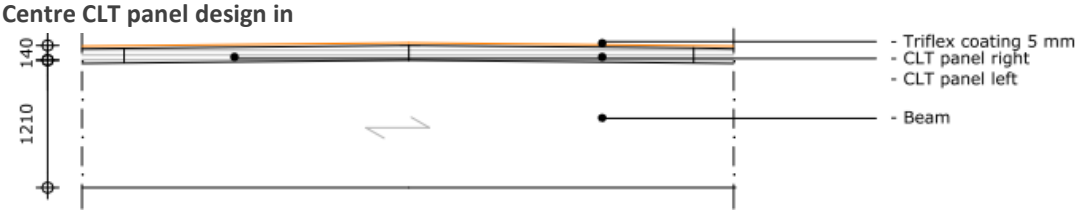

Figure 9-9: Tapered beam layout with centre CLT panels in mm

In conclusion, the water flows to both sides of the car park grid.
A gutter will collect and transport the water to the vertical drainage pipe. Next, the water from the vertical drainage pipe should be collected in a collection duct. This vertical drainage system and collection duct have standard dimensions in the ModuPark car parks of BNPC. Because this system is functioning well, as indicated by BNPC, and there is no limitation to apply in a timber car park. This system is assumed to be the drainage design of the re-mountable timber car park. This collection duct runs to both ends of the grid, shown in Figure 9-10, where it transports the water to ground level.

Appendix H.1.1 shows that the most favourable collection duct design has two ducts at both sides of the grids, as Figure 9-10 shows. It creates the lowest duct length, which minimises the risk of leakages. Next, the ducts in a two-duct configuration (Figure H-3) are also less visible, creating a higher aesthetical value. The only disadvantage is the collection duct crosses the beams on both sides per grid, see Figures 9-10 and H-5. Appendix H.1.1 determines that these openings create no problem for the preliminary design values. But it must be reviewed after the final design phase. To create a sufficient slope in the collection duct (Van De Ven et al., 2007), an opening area of 150 mm x 150 mm will be assumed. So, a 25 mm tolerance is available next to the 125 mm duct.

Finally, at the edges of the car park, a thicker panel edge is applied to ensure there is no chance for water to flow from the edge, creating a waterfall. This elevated panel edge will be connected to the CLT panel by screws because it is a permanent connection.
The gutter is covered with the Triflex coating as applied on the floor. Due to the small thickness of the Triflex layer, this design is well-suitable. Appendix H.1.1 presents the visualization of the detailed drainage system. Figure 9-11 presents a smaller version of the visualization for a car park edge panel with all aspects included.

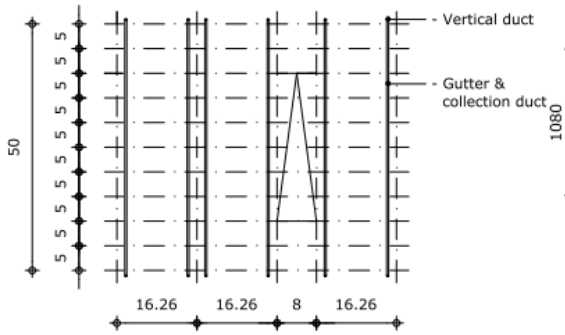

Figure 9-10: Top view grid lines with drainage system in mm

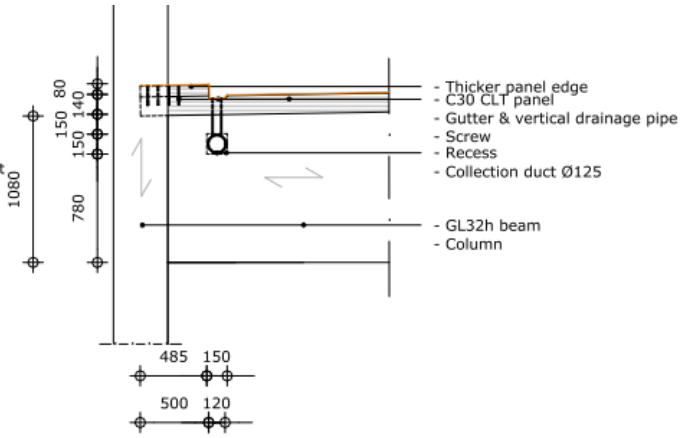

Figure 9-11: Edge panel drainage system design in mm

Electrical system design

The electrical system can be applied in two ways:

1. Using two central electrical systems per grid through the whole car park at a distance of one-third of the length of the grid. See Figures 9-12 to 9-14. A favourable system is the VEKO one of Figure 9-15 (*Richard Parking LED*, n.d.). It is an energy-saving LED system, and the lights or other electrical products can easily be connected to the cable duct. So, the suspension of the cable duct is also functioning for the light system, creating a high feasibility potential.

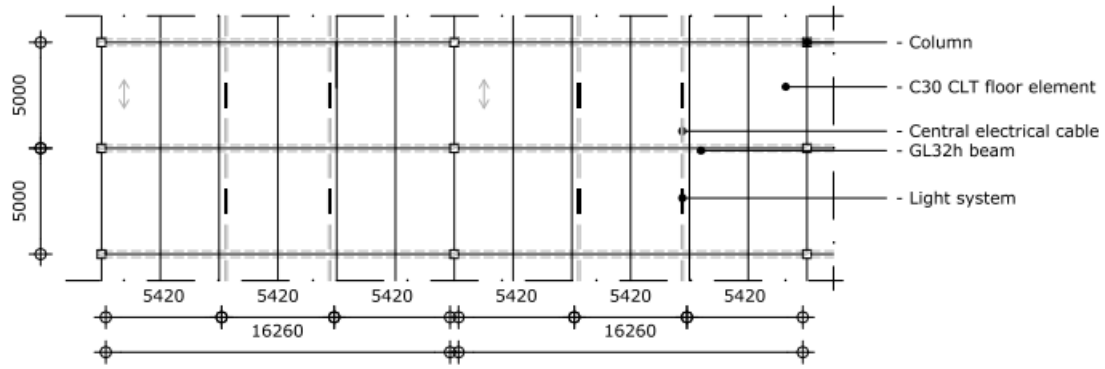

Figure 9-12: Alternative 1 electrical system two central cables in mm

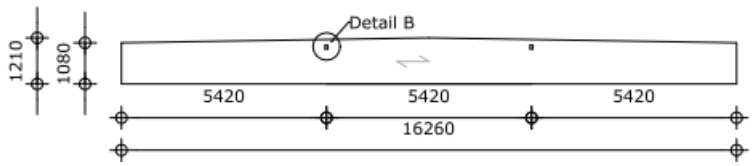

Figure 9-13: Side view beam with recesses in mm

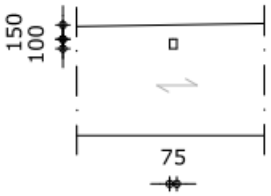

Figure 9-14: Detail B in mm

Figure 9-15: Example Veko light system (*RAI P4 Amsterdam*, n.d.)

2. A central cable duct with a branch per grid. See Figure 9-16. This system requires cable fastening and light system fastening.

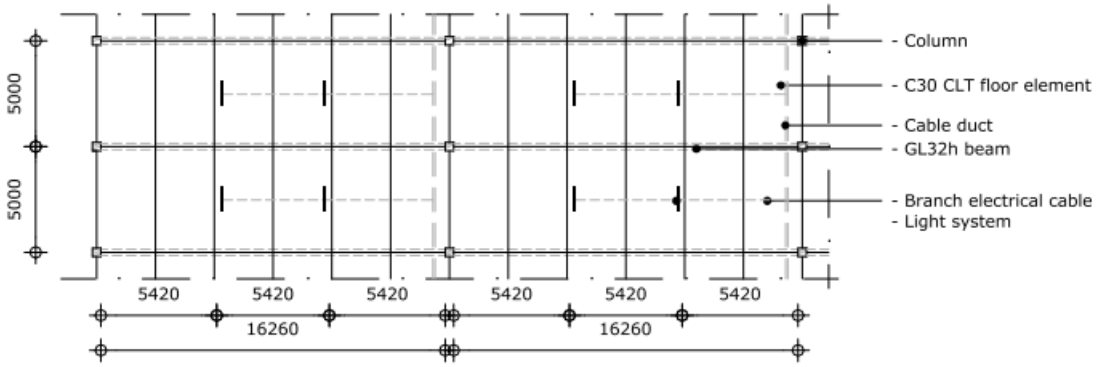

Figure 9-16: Alternative 2 cable duct with branches in mm

Figure 9-16 presents a higher length of cables and a higher number of connections for alternative 2 than alternative 1 of Figure 9-12, meaning more connections should be made or demounted. So, it is less favourable in terms of feasibility. Next, the higher length of cables or ducts will also result in lower aesthetics.

Another difference between the alternatives is the position of the recess. Applying a central cable duct is most optimal to position it at the edge of a grid, as shown in Figure 9-16. So, there is a short cable distance between the duct and a possible charging unit for electric cars. However, it requires a larger recess because the water collection duct is also positioned there. And it raises the requirement for good moisture protection of the cable duct to prevent short circuits.

In the case of the VEKO system, the required recesses are shown in Figures 9-13 and 9-14. These recesses are smaller than the one of the drainage system, and that opening already fits the structural performance requirements, assuming the same top height of 150 mm.

Third, both systems require a cable duct at the end of the car park, where the systems should go vertically to ground level.

Finally, the amount of suspensions with corresponding fasteners of the VEKO system is favourable over the alternative with a central cable duct and branches. So, it has a higher feasibility potential.

In conclusion, two central VEKO systems per grid will be applied due to the more advantages. The cable duct can possibly be favourable when using charging units. Nevertheless, it is unclear if electric cars are allowed in a timber car park due to their unknown influence on the fire behaviour.

9.4: Assessment and decision final global layout

As a starting point in assessing the global layout, the system of the preliminary design is assumed. This layout is visualized in Figures 9-1 and 9-17.

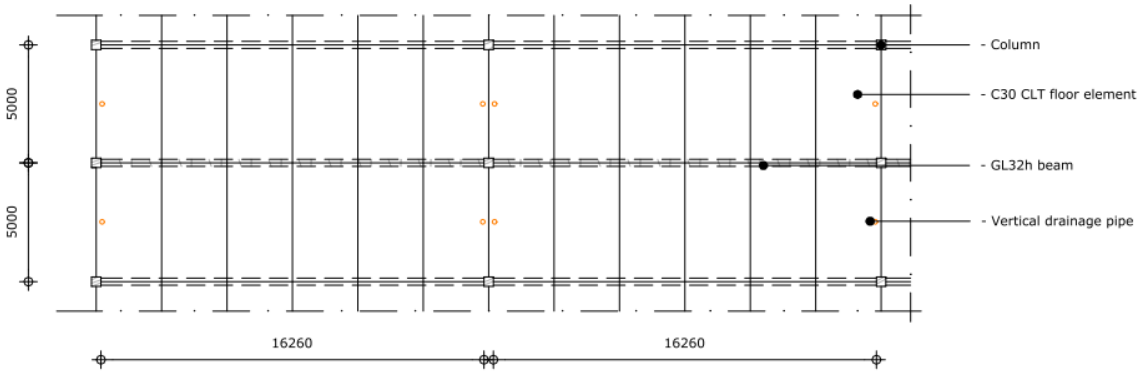

Figure 9-17: Drainage system preliminary layout in mm

Global layout optimization solution 1

Table 7-7 shows that the largest part of the floor height comes from the beam height. So, applying an extra beam reduces the span and improves the floor height. Another difference is the floor panel area of about 2.5 meters x 8 meters instead of 3 meters x 5 meters. This option became possible due to the decreased span from 5 to 2.5 meters.

The most logical position of this extra beam is at half the span, so each beam gets half of the load compared to the preliminary design. This design results in the beam being positioned between two parking lots. This layout is shown in Figures 9-18 and 9-19, assuming two extra column supports or two additional beam supports.

Like the preliminary design, the load-bearing elements are assumed to be separate elements arriving at the construction site.

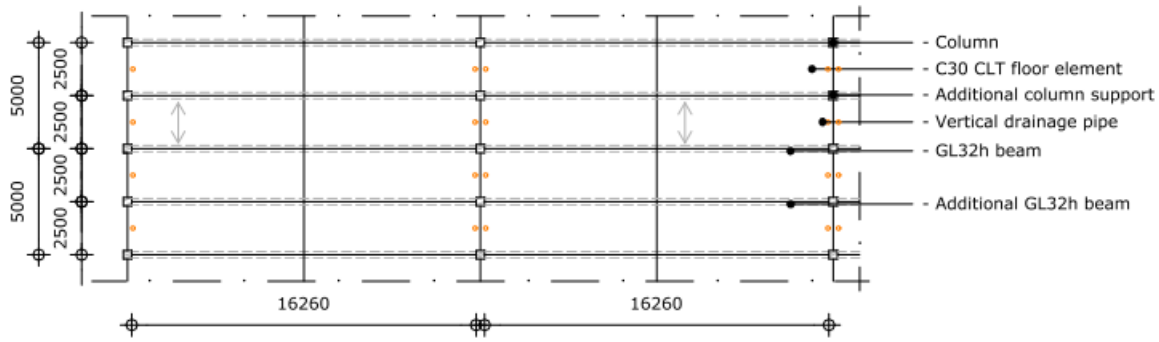

Figure 9-18: Global layout optimization solution 1 column support in mm

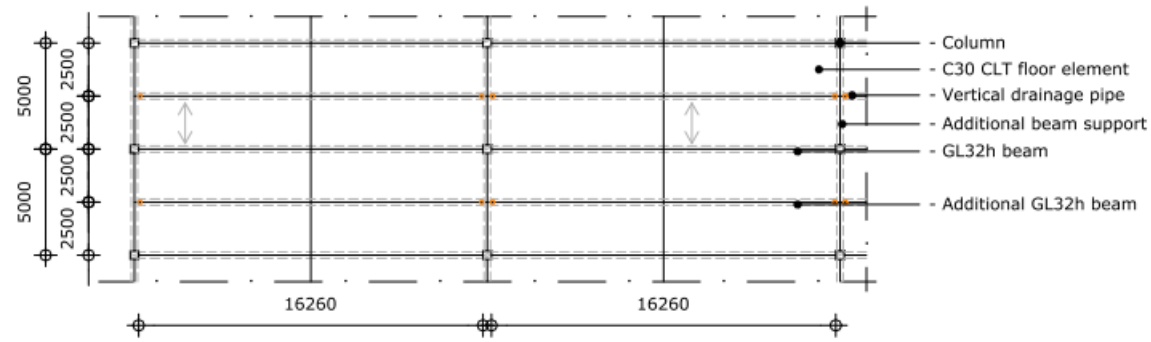

Figure 9-19: Global layout optimization solution 1 beam support

Appendix H.1.2.1 explains the advantages and disadvantages that are summarized in Table 9-5.

Table 9-5: Assessment global layout optimization solution 1

Advantages	Disadvantages
- Longitudinal beam height optimization - Floor height optimization - Floor panel area optimization - Seam length reduction with Triflex demounting optimization	- Extra support system for new beam by column or secondary supporting beam - Increased number of connections - Extra column: - Reduced social safety - Blocking of driveway - Increased number of drainage details - Extra beam: - Extra steel necessary - Less natural ventilation - Conflict beam and vertical drainage pipe - Further increased number of connections or vertical drainage pipes - Increased damage and leakage risk water collection duct or beam recess prone to degradation

Comparing the advantages and disadvantages of Table 9-5 ensures that applying an extra beam is not favourable compared to the preliminary global layout. The total height improves, and the number of elements stays the same, but the feasibility, fire, and durability performance are reduced.

Global layout optimization solution 2

The major disadvantage of global layout optimization solution 1 is the reduced feasibility. To improve this aspect, a complete prefabricated grid part of 2.5 meters by 16.26 meters is assumed as global layout optimization solution 2, including two glulam floor beams and CLT floor panels. This prefabricated element is within the dimensional transportation limits of Table 9-2. Figure 9-20 shows this global layout with the beam support. Because the column support is not possible, as mentioned for optimization solution 1.

Because each prefab grid part consists of two beams, meaning there are two beams next to each other per support, as visualized in Figure 9-21.

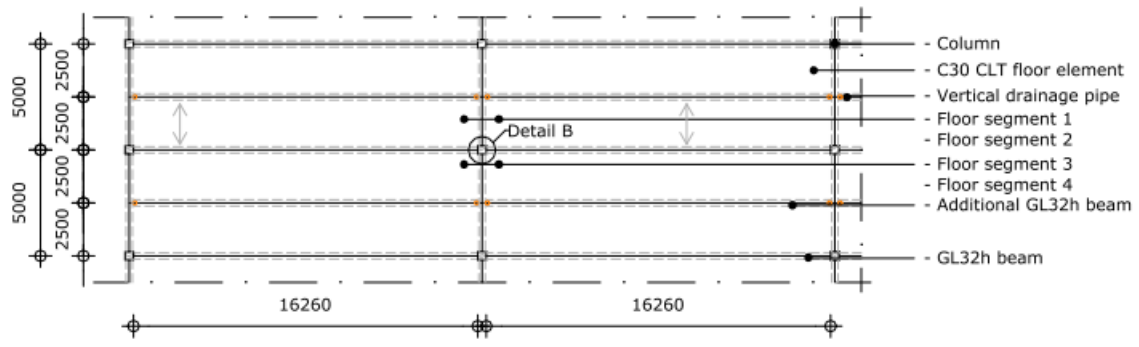

Figure 9-20: Global layout optimization solution 2 beam support in mm

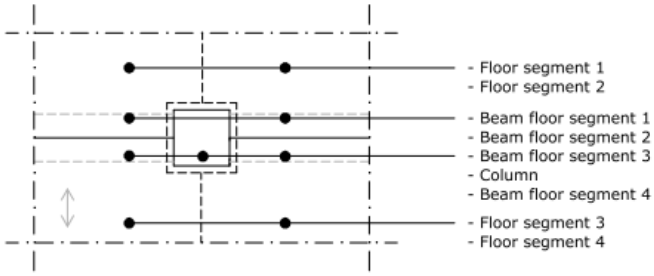

Figure 9-21: Detail B floor,beam, and column orientation

Appendix H.1.2.2 presents the background of the global layout optimization 2 assessment, which is summarized in Table 9-6.

Table 9-6: Assessment global layout optimization solution 2

Advantages	Disadvantages
- Longitudinal beam height optimization - Floor height optimization - Floor area optimization - Increasing prefabrication level - Seam length reduction with Triflex demounting optimization	- Extra support system for new beam by column or secondary supporting beam - Extra bending in columns - Reduced transport potential - Extra beam: - Extra steel necessary - Less natural ventilation - Conflict beam and vertical drainage pipe - Further increased number of connections or vertical drainage pipes - Increased damage and leakage risk water collection duct or beam recess prone to degradation

Compared to global layout optimization 1, the disadvantage in the number of re-mountable connections is now improved to an equal performance with the preliminary design.
However, the transportation potential of global layout optimization 2 is reduced compared to global layout optimization 1 and the assumed starting global layout. This results in more truck movements, which unfavourably affects the environment. In addition, the disadvantages concerning the beam support are still present. The design of the beams results in extra bending in the connections and supports, so more material should be used.

In conclusion, global layout optimization 2 has some important advantages, like height reduction and increased prefabrication level, but also disadvantages in feasibility, durability, and sustainability. So, the assumed global layout, as applied in the preliminary design, is assumed to be more favourable than global layout optimization solution 2.

The columns cannot be positioned at another distance from each other because of the parking lot width of 2.5 meters mentioned in paragraph 5.1. Therefore, no other global layout option is possible, so the preliminary global layout will be used as the final global layout.

Chapter 10 Final design – dimensioning and detailing

Based on the determined final global layout in Chapter 9. The final dimensioning and detailing of the load-bearing structure with a focus on the re-mountability of the connections is the next step for achieving a final design of a re-mountable timber car park. This chapter includes the dimensioning and detailing of this final design phase. First, the necessary background for the design procedure will be given in paragraph 10.1. Paragraph 10.2 presents the design of the floor system, which means the final dimensioning of the floor and beam element combined with the re-mountable floor-to-floor and floor-to-beam connection.
Then, the column will be designed with the related column-to-beam and column-to-column connection in paragraph 10.3. Paragraph 10.4 includes the design of the secondary details. Finally, 10.5 shows the mounting and demounting sequence.

10.1: Background final design process

This paragraph provides the background information necessary for the final design process.

10.1.1: Determination wind and imperfection loads

Wind loads create horizontal forces in the longitudinal and transverse direction next to the vertical upwards and downwards forces. Appendix H.2 determines the values for the wind loads based on the assumed location of the car park in paragraph 5.1 and the assumed global dimensions of Figure 1-1 in the problem statement (paragraph 1.1).

Table 10-1 presents the resulting horizontal wind loads as a line load by applying the assumed closed façade height of 2.27 meters, calculated in Appendix H.2. Negative loads mean suction and positive loads compression.

The vertical wind loads are given as a surface load in Table 10-2. The positive loads are in the downward direction, and the negative loads are in the upward direction.

Table 10-1: Horizontal wind loads

Zone	**A**	**B**	**C**	**D**	**E**
$c_{pe,10}$ factor	**-1.2**	**-0.8**	**-0.5**	**+0.8**	**-0.5**
$Q_{wind,level\ 4}$ [kN/m]	-3.05	-2.03	-1.27	2.03	-1.27
$Q_{wind,level\ 3}$ [kN/m]	-2.81	-1.87	-1.17	1.87	-1.17
$Q_{wind,level\ 2}$ [kN/m]	-2.40	-1.60	-1.00	1.60	-1.00
$Q_{wind,level\ 1}$ [kN/m]	-1.93	-1.29	-0.81	1.29	-0.81

Table 10-2: Vertical wind loads

c_f factor	**0.2**	**-1**
$Q_{wind,level\ 4}$ [kN/m^2]	0.22	-1.12
$Q_{wind,level\ 3}$ [kN/m^2]	0.21	-1.03
$Q_{wind,level\ 2}$ [kN/m^2]	0.18	-0.88
$Q_{wind,level\ 1}$ [kN/m^2]	0.14	-0.71

Also, imperfections create horizontal loads. Based on Eurocode 5 (NEN-EN 1995-1-1+C1+A1, 2011), the imperfection is 0.17 degrees for a total height of about 14 meters using a skewness of h/333. Applying the total floor load of 1.88 kN/m^2 based on sub-paragraph 7.2.1 and Appendix E.3.1 gives the horizontal loads of Table 10-3 using the global car park dimensions of Figure 1-1.

Table 10-3: Second order horizontal loads

	Transverse second order load	**Longitudinal second order load**
Surface load [kN/m^2]	0.0056	0.0056
Width [m]	56.78	50
Line load [kN/m]	0.32	0.28

10.2.1: Layout stability system

Global stability should be ensured in the whole car park. The diaphragm action of the floor will ensure horizontal stability. That means the individual floor elements act as one rigid plate to transfer the horizontal loads from the façade to the vertical stability systems. Sub-paragraph 10.2.3 covers the design of the horizontal stability system.

For the vertical stability system, the ModuPark concept of BNPC is the most suitable solution. Figure 10-1 shows in the bold lines the vertical stability systems of the ModuPark concept. Sub-paragraphs 10.4.1 and 10.4.2 cover the design of the vertical bracing system.

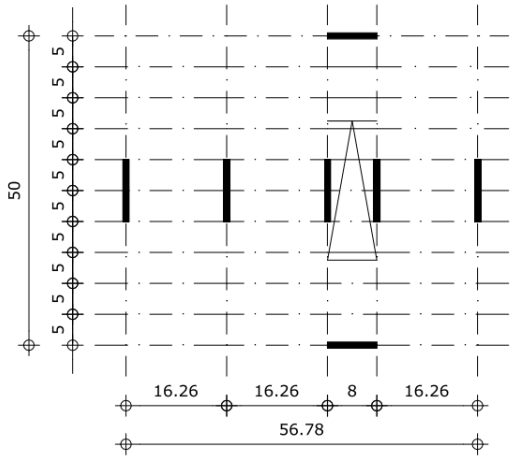

Figure 10-1: Car park floor plan with bold lines indicating the vertical stability system in m

10.2: Final design floor system

Paragraph 10.2 covers the floor system's design, including the floor and beam elements. First, the final dimensions of both elements are determined in 10.2.1 and 10.2.2. Then, the horizontal stability system is investigated in 10.2.3. The corresponding loads of this horizontal stability system should be known to design the floor-to-floor connection and floor-to-beam connection in 10.2.4.

10.2.1: Final dimensioning floor element

Compared to the preliminary design of the floor element, only the presence of a vertical load is different. Chapter 9 states that the final floor system has six panels per grid. Assume the conservative maximum width of 3 meters, equal to the preliminary design. Sub-paragraph 10.3.3 reviews this assumption based on the final column dimension.

Appendix H.3.1 presents the final design calculation of the floor elements.
The presence of the vertical wind load will not affect the design of the floor system because it does not affect the governing load configuration, as shown in Table H-9 of Appendix H.3.1.

As mentioned in paragraph 7.2, the optimization in the strength class will be included in the final design phase. The preliminary strength class C30 is not optimal because applying C24 results in the same minimum required thickness. This strength class is also available for a CLT panel (*CLT by Stora Enso; Technical Brochure*, 2017). So, strength class C24 will be applied in the final design due to the higher availability and reduced cost of a lower strength class.

Figure 10-2 presents the final floor element design. If, based on sub-paragraph 10.3.2, the floor element width can be reduced, it does not affect the resistances of the floor element, as shown in Appendix H.3.1.

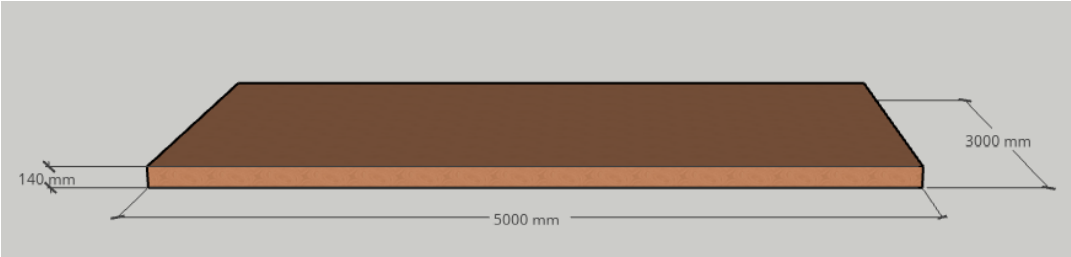

Figure 10-2: 3D view final design CLT floor element

10.2.2: Final dimensioning beam

The final beam design differs from the preliminary design by the possible contribution of the wind load and the tapered design with a corresponding reduction in the bending resistance.

A hinged connection between the beam and column will be assumed because otherwise, a more significant large bending moment will be generated in the column. This bending moment will increase the column's minimum required dimension, reducing the car park efficiency. Because Appendix B.1 states that the protrusion of a column in a parking lot has a maximum value of 200 mm. In addition, a hinged connection is favourable in terms of minimizing the manual actions required on-site.

Appendix H.3.2 presents the final design of the beam. The same variable loads are present for the design of the beam as for the design of the floor. Because the wind load is again not affecting the final design. The reduction of the taper will also not affect the resulting height because bending is not the governing unity check.
In conclusion, a cross-section of 300x1080 mm for a strength class GL32h is minimally required. The taper of 130 mm, calculated in equation 9.1, is still valid due to the unchanged global deflection.

Strength class optimization results in a larger cross-sectional area, as shown in Appendix H.3.2. Applying a strength class GL24h gives a minimum height of 1130 mm.
The differences are small, but the research question states that this research should find the most suitable design in terms of structural performance. To answer this question most accurately, a GL32h beam should be applied. Nevertheless, the recommendations will indicate that a lower strength class of the beam will result in a small increase in floor height.

Figures 10-3 and 10-4 show the final design of the beam.

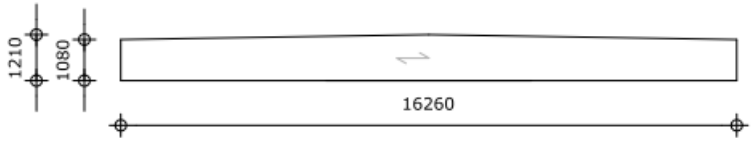

Figure 10-3: Final design beam in mm

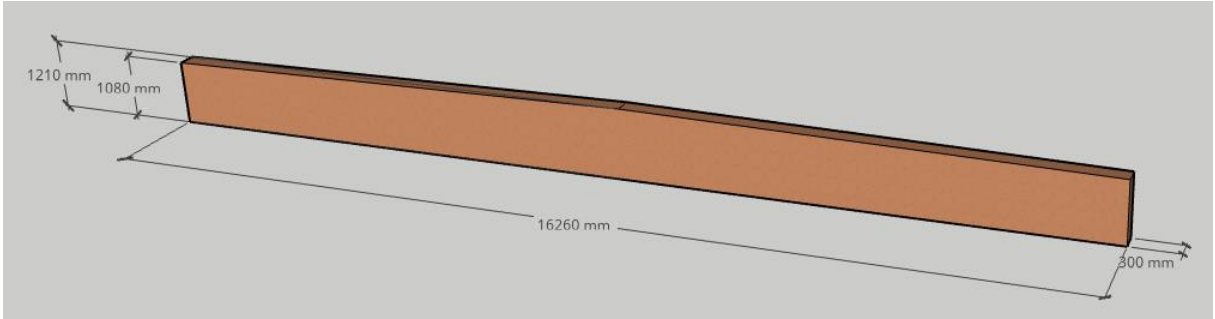

Figure 10-4: 3D view final beam design

10.2.3: Horizontal stability system

The diaphragm action of the floor ensures horizontal stability. Figures 10-5 and 10-6 show the two possible diaphragm actions based on the wind from the transverse and longitudinal directions.

If the following condition of equation 10.1 is satisfied, then the deep beam theory can be applied. Parameter b is the depth of the diaphragm, and l is the length of the diaphragm.

$$2b[m] \leq l[m] \leq 6b[m] \tag{10.1}$$

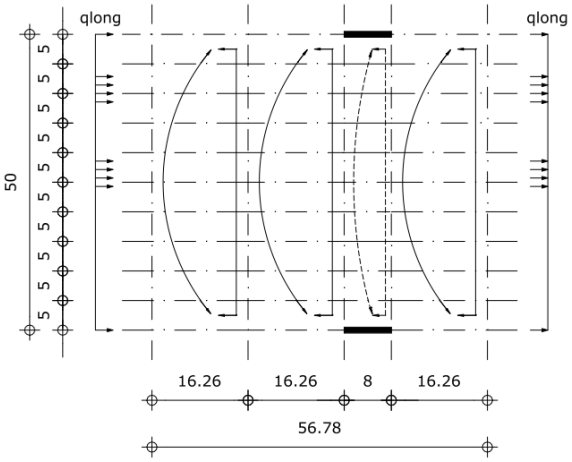

Figure 10-5: Longitudinal diaphragm action in m

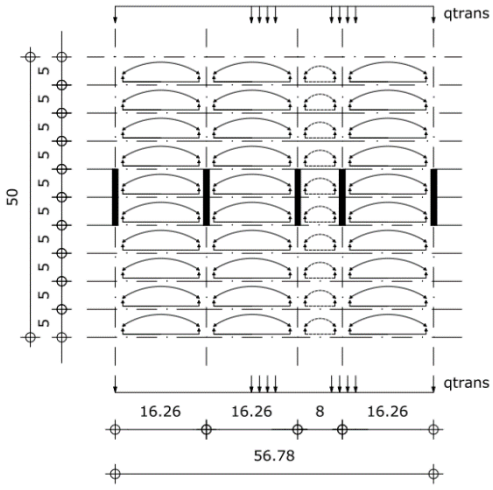

Figure 10-6: Transverse diaphragm action in m

Based on Figures 10-5 and 10-6, Table 10-4 shows the parameters b and l of both systems. Both systems satisfy the above condition. Appendix H.3.3 provides the deep beam calculation results of the diaphragm action in both directions.

Table 10-4: Values parameters b and l

	Transverse	Longitudinal
L [m]	16.26	50
b [m]	5	16.26

The stiffness of a diaphragm is calculated by the parameter EI, which is Young's modulus times the moment of inertia. The ramp grid, shown in Figure 10-5, has a height of 8 meters in the moment of inertia equation, while the other three grids have a value of 16.26 meters. A two times larger height means eight times larger stiffness. So, the contribution of the ramp grid is negligible in the longitudinal diaphragm actions due to the presence of three grids with an eight times larger stiffness.

Also, the ramp design is outside this research's scope. Therefore, the overall diaphragm action of this grid is not included in this research. This assumption is conservative because the floor area is much smaller than the other grids.

10.2.4: Final design floor system connections

There are two different connections to be made in the floor system: between the floor panels and between the floor panel and the beam.

As mentioned in the boundary conditions of paragraph 9.2, the goal is to limit the number of actions on-site, and the connection should be re-mountable. So, a bolt or a dowel are the two options left. However, as indicated in paragraph 9.2, a bolt has a tensile strength due to the clamped characteristic of the bolt head and nut, which the dowel does not have. Therefore, a bolt is the used

type of fastener. This decision raises the point of attention that the bolt head or nut cannot protrude on top of the floor.

Next, getting as few bolts in the floor-to-floor connection is favourable for feasibility. This connection must take up only the transverse shear force and the longitudinal wind load, as shown in Figures H-24 and H-25 and should ensure a similar deflection of two adjacent panels. The floor-to-beam connection can be designed to take up the other loads of Figures H-24 and H-25.

Sub-paragraph 10.2.4.1 gives the design conclusions of the floor-to-floor connection, and 10.2.4.2 presents the same for the floor-to-beam connection.

Figure 10-7 shows the investigated cross-sections in the floor system.

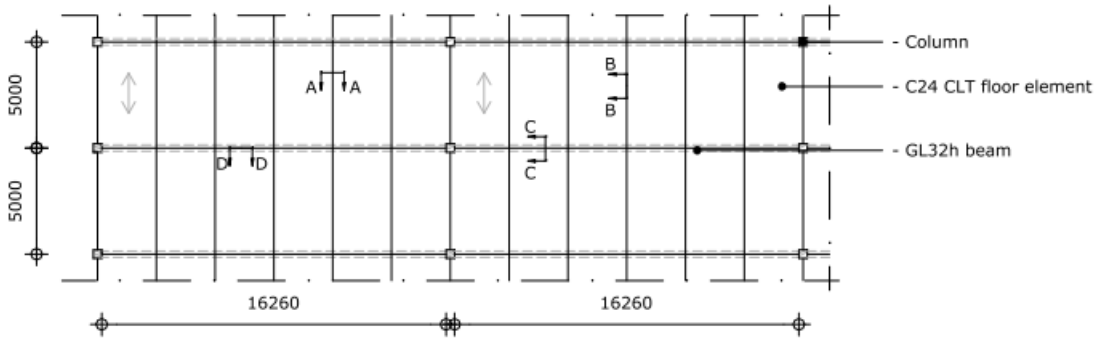

Figure 10-7: Cross-sectional views floor-to-floor and floor-to-beam connection in mm

10.2.4.1: Final design floor-to-floor connection

The floor-to-floor connection is required because two adjacent panels should deform similarly. Otherwise, cracks occur in the Triflex coating along the seam and driving cars hit the edge of the undeformed panel, creating unfavourable damage.

Figures 10-8 to 10-10 present the final floor-to-floor beam design. The design reasoning and calculations are given in Appendix H.3.4.
Next, to the two indicated loads from the horizontal loads, the concentrated wheel load will also affect this connection. Recesses should be made to be able to tighten the bolt and to prevent a protruding bolt part. The recess filling material cannot be lightweight material like PIR isolation due to the limited stiffness and compression stress resistance (*IKO Enertherm ALU*, 2020). Another option is applying a C24 CLT timber block with equal weight to the other floor volume. This option is the most suitable one because it can take up the concentrated wheel load. Second, it has the same dimensional stability as the surrounding floor. Third, this solution is also favourable from an environmental point of view to ensure a high biobased material level.

This connection can achieve a high re-mountability potential because the floor panels should be installed and demounted vertically due to the block in the horizontal direction by the columns. This movement is possible when the bolt is not installed. But the Triflex coating on top of this connection is the only part that should be removed during demounting and renewed during re-mounting. Table H-17 and Figures H-31 to H-36 present this connection's demounting and re-mounting steps.
A recess of 90mm x 120mm is assumed, so a hand or equipment can enter the tightening recess. In addition, a tapered edge of the recess results in a guiding system for the filling timber block. At the bottom of the recess, the area is assumed to be 100x100 mm. However, the resulting bolt length is 200 mm, as Figure 10-8 shows. So, one recess will be 220 mm at the bottom to install the bolt from that side.

Concluding Appendix H.3.4, one M16 bolt is sufficient to resist the loads. The depth of the bolt on each floor should be minimally 50 mm. A recess should be made using a timber filling block at the bolt's position.

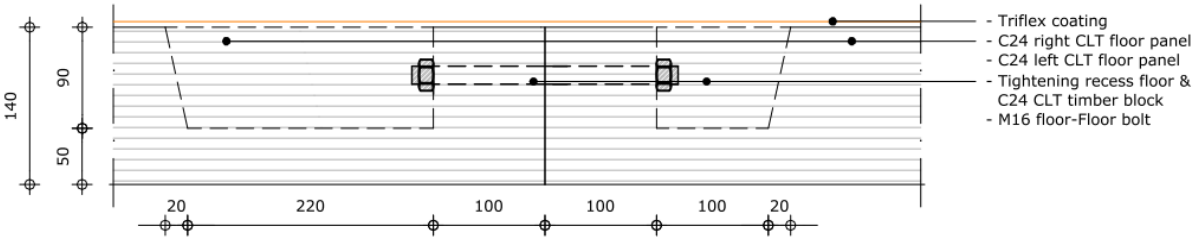

Figure 10-8: Cross-section A-A final design floor-to-floor connection in mm

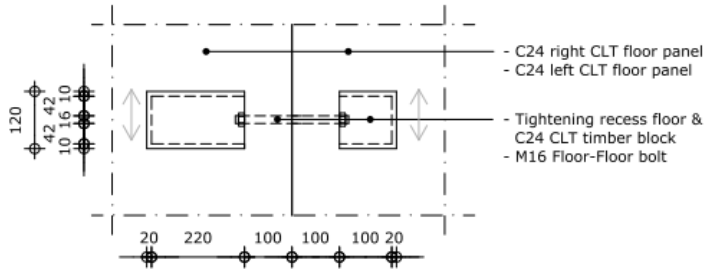

Figure 10-9: Top view final design floor-to-floor connection in mm

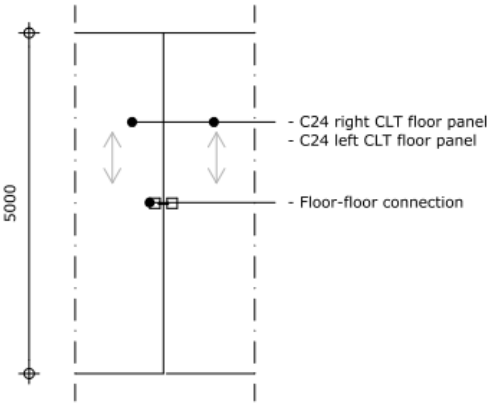

Figure 10-10: Position floor-to-floor connection per seam in mm

Paragraph 7.1 presents a limited shrinkage and expansion of 0.04%, so 1.2 mm for a 3-meter wide CLT panel, meaning no seam is required. Therefore, no special Triflex coating should be applied at the connection of the two floor panels in the width direction.

10.2.4.2: Final design floor-to-beam connection

Due to the mentioned benefits of the floor-to-floor connection of sub-paragraph 10.2.4.1, a comparable bolt connected with recesses on both ends will be applied as the floor-to-beam connection. Also, the re-mountability steps, as shown in Table H-17 and Figures H-31 to H-36, for the floor-to-floor connection are valid for this floor-to-beam connection.

Figures 10-11 to 10-14 present the final design of this connection, as designed in Appendix H.3.5. Due to the vertical orientation of the floor and beam, the M20 bolt is also in the vertical direction. Meaning there should be a tightening recess in the floor and beam. Like the floor-to-floor connection, the recess edge in the floor will be tapered to ensure accurate positioning of the filling material, which is assumed to be a C24 CLT timber block for the floor and GL32h for the beam. Due to the biobased character, structural performance, and dimensional stability, as concluded in 10.2.4.1.
Two bolts connect the panel to the beam on each end of the CLT panel. See Figure 10-12. This design produces high rotational stiffness and should create sufficient resistance to present loads.

Concluded from the design calculations of the floor-to-beam connection in Appendix H.3.5, four M20 bolts are required to take up the shear force from the tensile chord of the longitudinal diaphragm action plus the vertical wind force. The remaining eight M20 bolts can resist the shear force from the transverse diaphragm action combined with the vertical wind force.

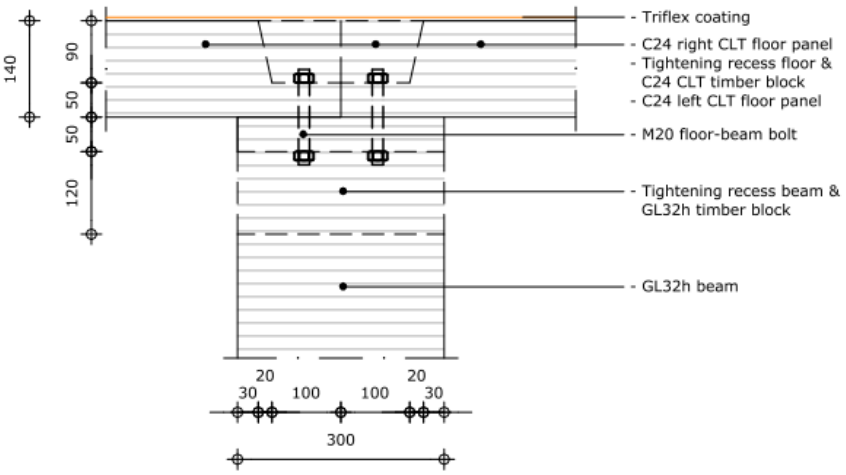

Figure 10-11: Cross-section C-C final design floor-to-beam connection beam in mm

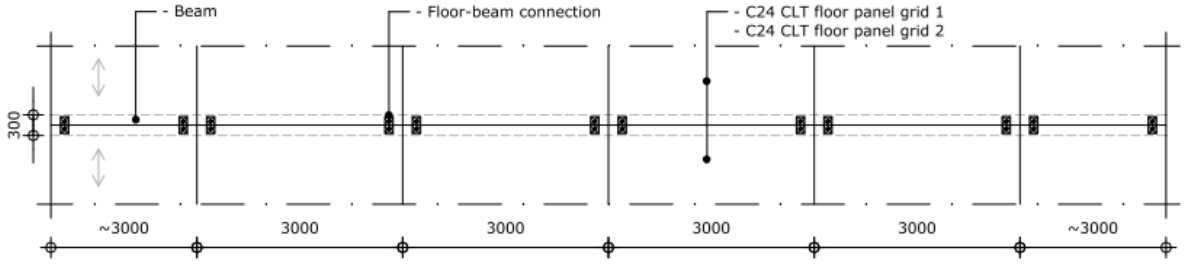

Figure 10-12: Positioning floor-to-bbeam connections in mm

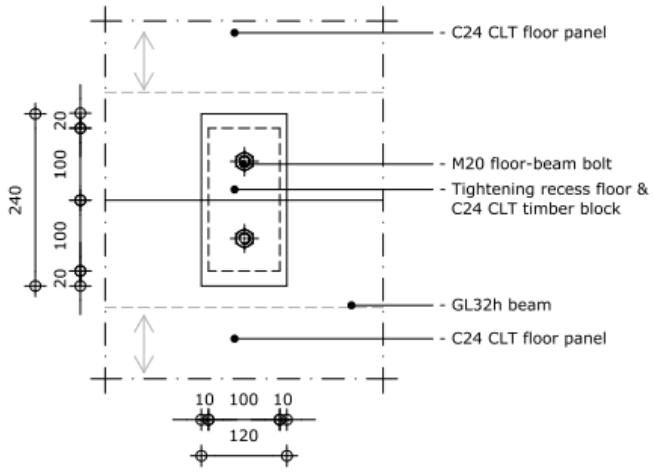

Figure 10-13: Top view final design floor-to-beam connection in mm

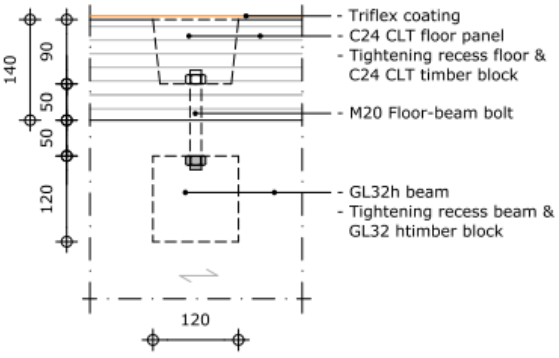

Figure 10-14: Cross-section D-D final design floor-to- beam connection in mm

The minimum required tolerance between the two CLT panels is 2 mm, based on the values of Paragraph 7.1. So, the panels can be placed directly next to each other to prevent the necessity of a special seam coating.

10.3: Final design column and corresponding connections

This paragraph covers the design of the column, which was not included in the preliminary design. Next, the re-mountable connections corresponding to the column will be designed.

First, the column-to-beam connection will be introduced in sub-paragraph 10.3.1 because it probably affects the column design calculations by creating a bending moment due to the eccentricity in the connection. Then, the column will be dimensioned in sub-paragraph 10.3.2 based on the known compression force and bending moment. Afterwards, the assumed beam and floor dimensions will be reviewed based on the known column width in 10.3.3. Next, sub-paragraph 10.3.4 covers the finalizing steps for the beam-to-column connection. Then, a review of the drainage detail should be done in 10.3.5. Finally, sub-paragraph 10.3.6 designs the column-to-column connection.

10.3.1: Introduction column-to-beam connection

The lessons learned in paragraph 4.3 state that it is beneficial from a feasibility point of view to use a corbel or steel shoe and secure them horizontally independent from large vehicles like cranes. So, the beam should rest on this corbel or shoe element, and the crane can move to the next grid. Resulting in the optimal use of large vehicles, which are costly and environmentally unfriendly in emissions and hindrance. So, the time-consuming manual actions are not in the critical time path.

The reference projects in Antwerp, Bad Aibling, and Malmö, investigated in Appendix A, use a corbel. Figures A-2, A-24, and A-33 visualize their corbel connection. The timber car park in Studen (Figure A-16) has beams passing through the column, but this is an unfavourable carpentry joint, as mentioned in paragraph 9.2.

Applying a completely protruding corbel next to the column is unfavourable because it affects the free height, so each total floor level height increases with the height of the corbel. See Figures 10-15. Hanging the beam on the corbel does not impact the total level height, as shown in Figure 10-16.

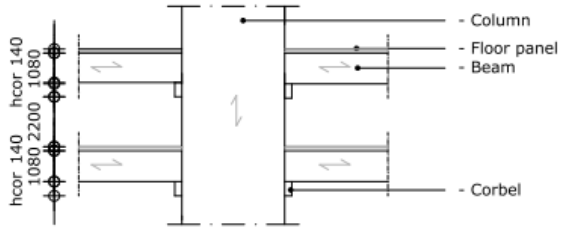

Figure 10-15: Column-to-beam connection protruding corbel in mm

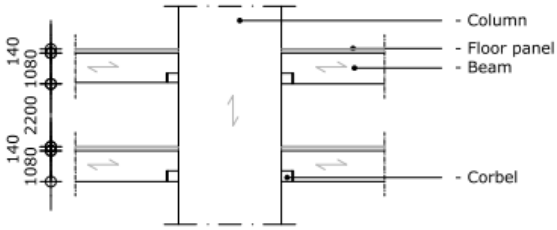

Figure 10-16: Column-to-beam connection corbel with hanging beam in mm

Another solution is applying steel instead of timber. Like Figure 10-17, a steel shoe is a possible solution. However, the fire safety of this connection is low because the steel connection parts are exposed to the environment and by an increasing steel temperature, the strength and stiffness reduce significantly (NEN-EN 1993-1-2+C2, 2011). The connection's strength and stiffness depend only on the steel shoe, so the connection has a low redundancy. Covering the steel end plate is possible by making a recess in the beam, but the shoe flange cannot be protected because the beam should be erected vertically. So, moving the shoe flange horizontally in a beam recess is impossible.

In conclusion, hanging the beam on the corbel, like in Figures 10-16 and 10-18, is the most suitable type of beam-to-column connection.

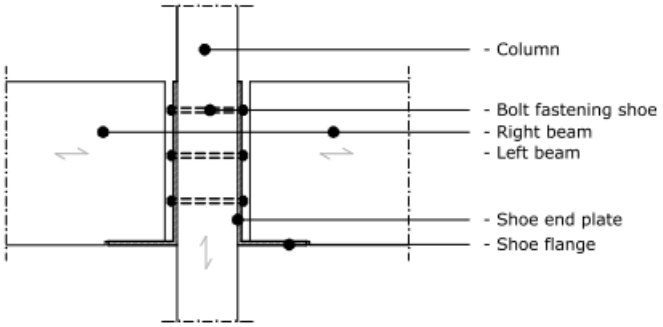

Figure 10-17: Steel shoe column-to-beam connection

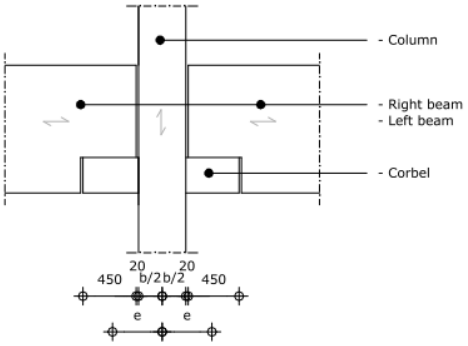

Figure 10-18: Eccentricity column-to-beam connection in mm

The connection of Figure 10-16 gives an eccentricity (e), shown in Figure 10-18.
Assuming the corbel has an equal width as the beam, the minimum contact area between the beam and the corbel is 300mm x 450mm. This area is calculated using the design value of the glulam beam's perpendicular compression strength and the beam's line load from Table E-23. The column will probably be wider than 300 mm, based on the reference project column dimensions, meaning the length of the corbel of 450 mm is a conservative assumption.
There is also a standard BNPC erection tolerance between two prefabricated timber elements of 20 mm, as shown in Figure 10-18. This value is larger than the maximum extension of the glulam beam according to the timber's dimensional stability given in paragraph 7.1.

10.3.2: Dimensioning of the column

The preliminary layout of the column-to-beam connection is known, so designing the column cross-sectional area is possible.
Two configurations are assumed: a centre column with only a compression force and an edge column facing half the compression force with a bending moment.

Appendix H.4.1 shows the design assumptions and calculates the minimal required cross-sectional dimensions. A glued laminated column with strength class GL32h will be used as a starting point because the expected cross-section cannot be produced as sawn timber. The ultimate limit state criteria will govern the column design, so the resistance in a fire situation is most probably governing.

The column cross-sections for a lower strength class GL24h will also be checked to optimise the cost.

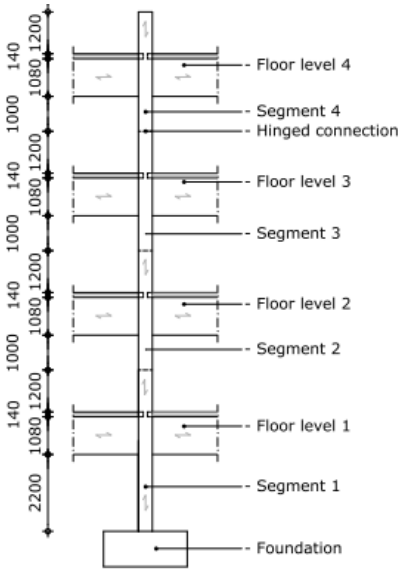

Figure 10-19: Column segments in mm

Table 10-5 presents the resulting cross-sectional dimensions for a GL32h column. Applying an optimization in strength class using GL24h results in the cross-sectional dimensions of Table 10-6.

All segments have an equal final cross-section because Tables H-33 and H-34 of Appendix H.4.2 show that segment 4 governs all segments due to the large bending moment present. Applying a cross-sectional reduction in the lower segment reduces the flexibility of the load-bearing structure for changing car park dimensions. In addition, the aesthetics of the column is reduced by the higher number of cross-sectional changes.

A strength class optimization from GL32h to GL24h increases the cross-sectional area by 20 mm in both directions. See the tables below. Therefore, the most optimal column design uses a GL32h strength class.

Table 10-5: Resulting column dimensions final design GL32h

Floor segment	Final cross-section [mm]
1	360x360
2	360x360
3	360x360
4	360x360

Table 10-6: Resulting column dimensions final design GL24h

Floor segment	Final cross-section [mm]
1	380x380
2	380x380
3	380x380
4	380x380

Figure 10-20 presents the final design of the column. The final dimensions are smaller than the maximum column dimensions for parking lot protrusion. See Figure 10-21. So, this column satisfies the maximum parking lot design efficiency.

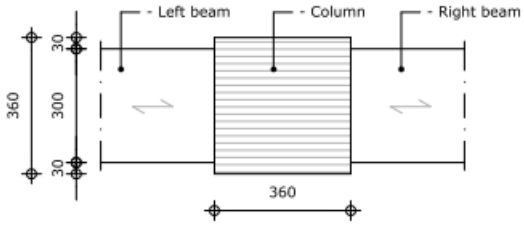

Figure 10-20: Final column cross-section in mm

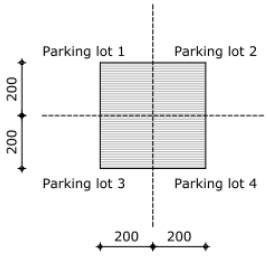

Figure 10-21: Maximum parking lot protruding area column in mm

10.3.3: Review of the final beam and floor design

As determined in the previous sub-paragraph 10.3.2, the final column width is 360 mm. So, the beam width can also be adjusted to 360 mm instead of 300 mm from the final design process in 10.2.2.

Table H-35 of Appendix H.4.2 presents that a height of 1040 mm is the new minimally required height for a GL32h beam. Next, a GL24h beam has a minimum height of 1090 mm, based on Table H-36. Applying the same taper design calculation procedure results in a height increment of 130 mm, as calculated in equation H.32.

Next, the calculations in Appendix H.4.2 conclude that the minimum beam's fire resistance does not influence the resulting cross-sections.
So, the GL32h beam results in the most favourable cross-sectional dimensions.
The final beam cross-section is 360 mm x 1040 mm at the edges and 360 mm x 1170 mm at the centre of the beam, as visualized in Figure 10-22.

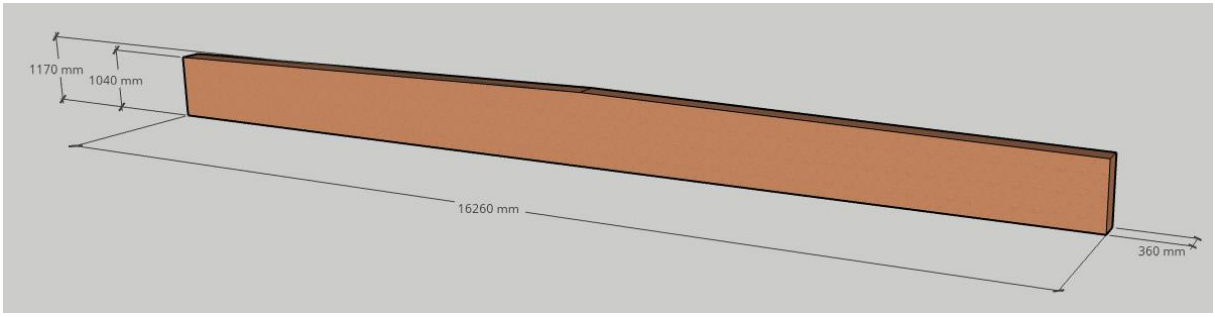

Figure 10-22: 3D view final dimensioning beam element mm

The final column width of 360 mm results in a total grid length of 16.62 meters, so each of the six CLT floor panels should have a length of 2.77 meters, as shown in Figure 10-23.

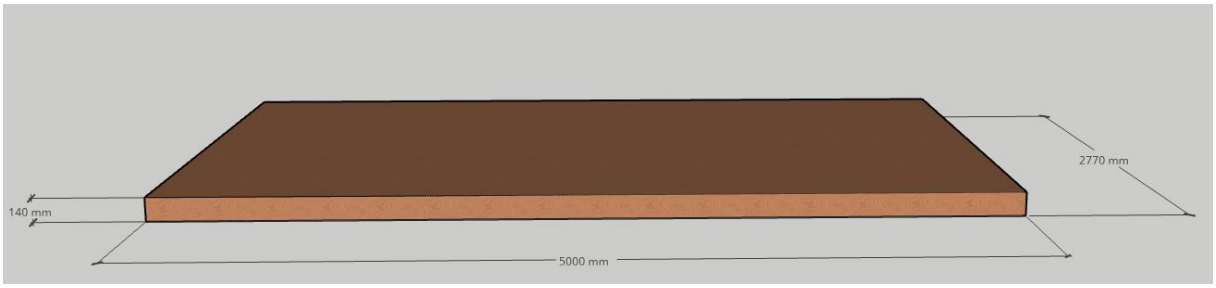

Figure 10-23: 3D view final dimensioning floor element in mm

10.3.4: Final design column-to-beam connection

All design verifications and calculations according to the column-to-beam connection are provided in Appendix H.4.3.

The resulting corbel area should be 360x420 mm instead of the preliminary 300x450 mm based on the increased width and the use of an elevated corbel edge, as shown in Figure 10-25. This elevated corbel edge prevents the beam's horizontal movement during execution. It has a cross-section of 400x120x45, which is also visualized in Figures 10-25 to 10-27. A taper is applied on the internal surface of the elevated edges to ensure accurate positioning of the beam by assuming the bottom thickness is 60 mm, and the top thickness is 45 mm.

The corresponding minimum height of the corbel is 600 mm, determined by applying the bending moment and shear resistance verification. In which the shear resistance is governing.
This shear resistance check should also be made for the reduced beam height on top of the corbel, with an extra reduction factor k_v (NEN-EN 1995-1-1+C1+A1, 2011). This results in a minimum required beam height of 750 mm in combination with a recess slope of 1:6. Figures 10-26 to 10-28 show the final column-to-beam connection design with the adjusted beam layout, including this slope of 1:6.
This slope is necessary to limit the stress concentration at the corbel recess's corner, as shown in Figure 10-26.

Next, the connection between the corbel and the column should be designed. A recess in the column creates a possibility to transfer the shear force from the corbel to the column as a compression force parallel to the grain. The GL32h column has a high strength for this type of loading. Therefore, this type of connection is chosen. The bending moment should be resisted by bolts connecting the corbel to the column. Three rows with each of three M24 bolts, shown in Figure 10-26 and 10-27, results in sufficient resistance.

Due to the protruding corbel below the beam, the level height increases slightly to a total height of 3.69 m instead of 3.42 m.

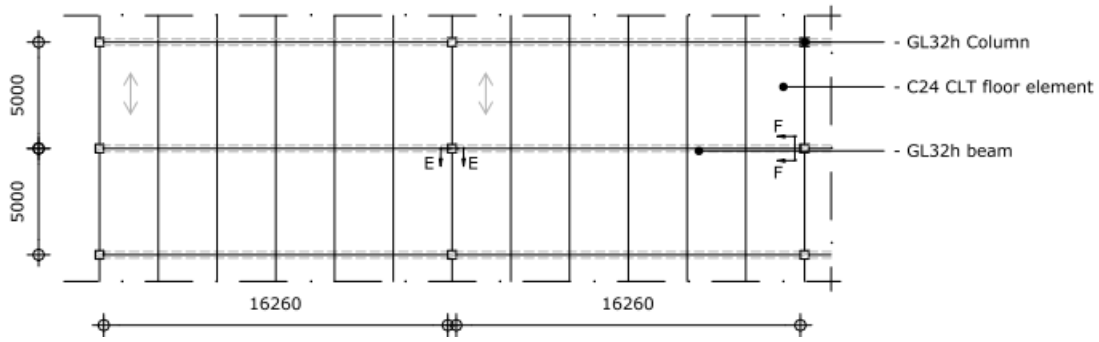

Figure 10-24: Top view investigate module with cross-sections indicated in mm

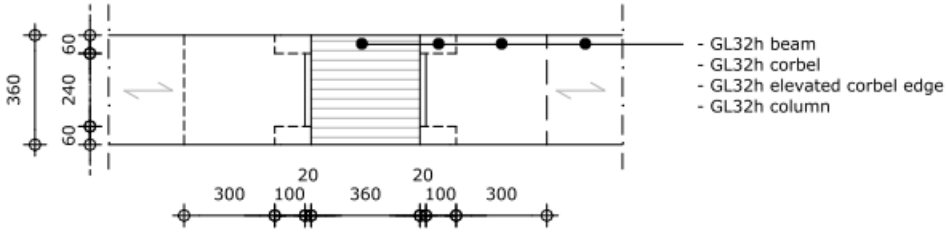

Figure 10-25: Top view column-to-beam connection in mm

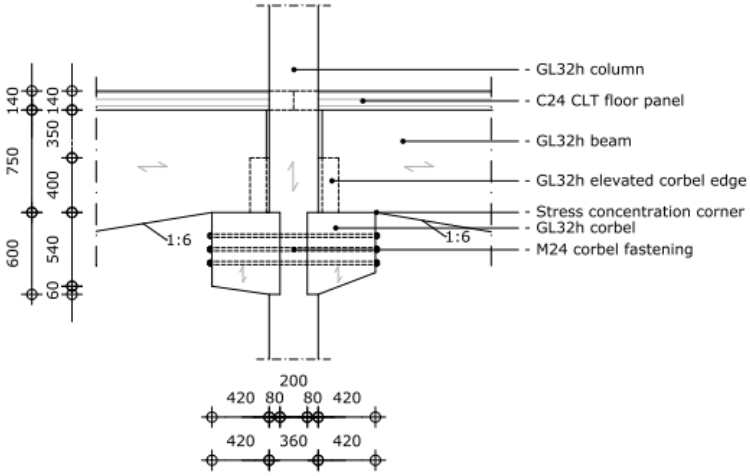

Figure 10-26: Cross-section E-E column-to-beam connection in mm

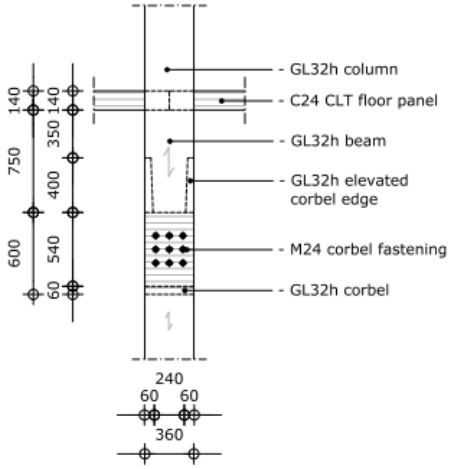

Figure 10-27: Cross-section F-F column-to-beam connection in mm

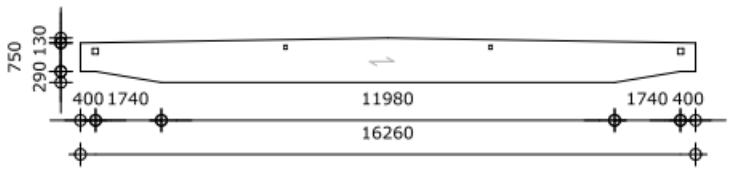

Figure 10-28: Adjusted final beam design in mm

10.3.5: Review of the drainage detail

As Figure 10-28 shows, the drainage recess is located at the corbel recess zone of the beam. The applied height of the beam is the minimum height to ensure sufficient shear resistance. This means that this recess can not be positioned above the corbel, or the beam height at this position should increase, which unfavourably increases the total floor height.

So, the drainage recess should be moved next to the corbel with a length of 420 mm, assuming a centre position of 575 mm from the beam end. Appendix H.4.4 presents that the shear resistance is sufficient at this position. So, the recess and gutter will move 195 mm to the centre of the beam compared to the beam design of Figure 10-28.
This movement is relatively small compared to the parking lot length of 5.13 meters (NEN 2443, 2013). Therefore, the new gutter position does not affect the parking possibility.

Figures 10-29 and 10-30 show the new drainage system design.

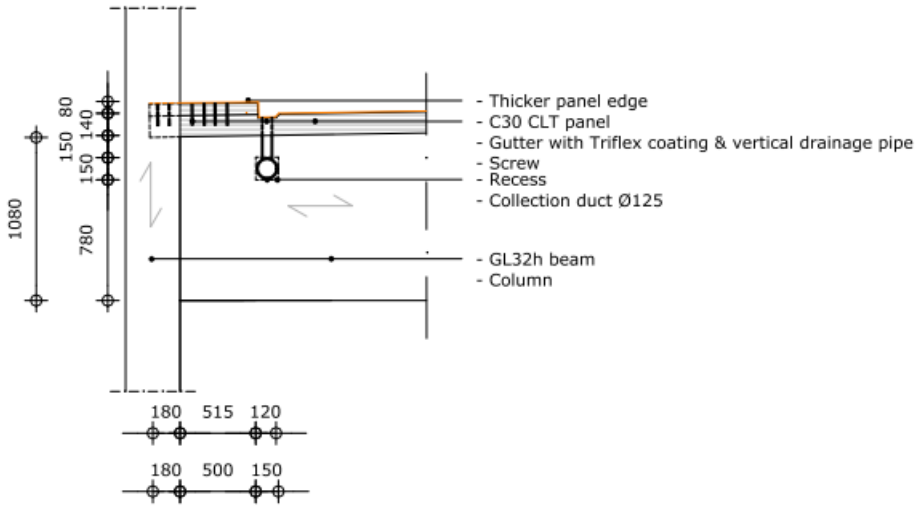

Figure 10-29: Updated drainage design edge column in mm

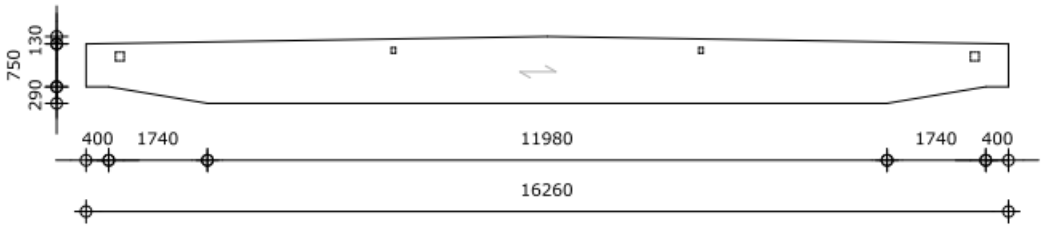

Figure 10-30: Updated drainage recess position final beam design in mm

10.3.6: Final design column-to-column connection

The connection between two column segments is at 1.2 meters, visualized in Figure 10-19. The reason is that fall protection can be installed before manual actions per floor level are required. This results in optimizing the number of actions on-site. In addition, this design ensures the connection design will not be affected by a water flow from the floor element.

Figures 10-31 and 10-32 show the most optimal design of the column-to-column connection. As sub-paragraph 10.3.2 states, the column faces a compression force and bending moment. But assuming the column-to-column connection as a hinge, as mentioned in sub-paragraph 10.3.3, there is no bending moment at this connection, resulting in a simpler connection in terms of feasibility.
At the contact area, a steel end plate will be applied to ensure the edges of the contact zone are open. Hence, there is ventilation in this contact zone possible, and it creates the possibility of protecting the timber against moisture. Another solution is applying a more durable type of timber like azobe than spruce, which results in a higher cost due to the lower availability, as indicated in paragraph 7.1.

This gap between the elements will be assumed to be 20 mm in height based on the tolerance indicated by BNPC, as mentioned in 10.3.1.

The compression force will be translated to the lower segment by contact stresses, so the slotted-in steel plate should only take up the shear force at the connection. Bolts secure this steel plate. Appendix H.4.4 calculates that two M16 bolts on each column end are necessary to give sufficient resistance to the connection. Furthermore, the steel plate dimensions satisfy the minimum required bolt, end, and edge distances. Finally, the end plate should have a thickness of 50 mm.

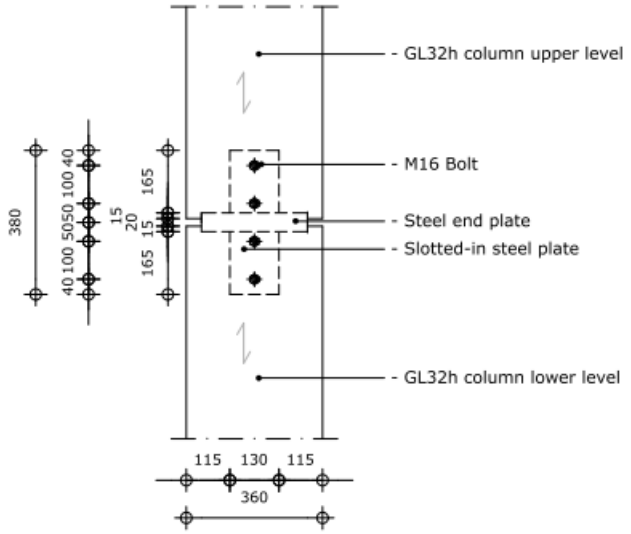

Figure 10-31: Side view column-to-column connection in mm

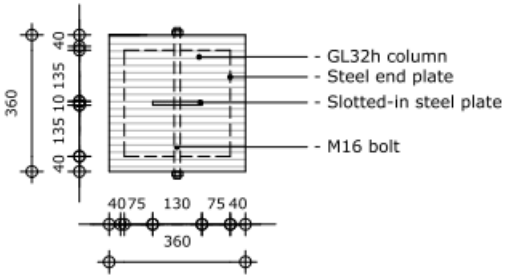

Figure 10-32: Top view column-to-column connection in mm

10.4: Design secondary details

Finally, some secondary details are covered in the grid that should still be designed. For example, the bracing system with corresponding connection, as done in 10.4.1 and 10.4.2. Then, the Integra fencing with connection is investigated in 10.4.3, and the wood protection panel in 10.4.4.

10.4.1: Bracing system design

The bracing system can be designed based on the horizontal loads considered in the horizontal stability design of sub-paragraph 10.2.3 and Appendix H.3.3. Those horizontal loads should be transported to the foundation by the bracing system.

Cables are mainly used as bracing elements. Also, Studen and Bad Aibling's reference projects (Appendix A) use this type of vertical bracing system.
This research uses a special cable type called "Willems anker" (*Willems Anker 2017 Specificaties*, 2017), shown in Figure 10-33, which consists of two round steel parts per total length screwed somewhere in the centre of the span to a coupling element. This coupling element allows pre-strengthening of the cable to make sure higher stability can be achieved.
Because the serviceability limit state governs the horizontal timber load-bearing elements' resistance, as concluded from paragraph 10.2, this type of bracing is more beneficial in a timber structure.

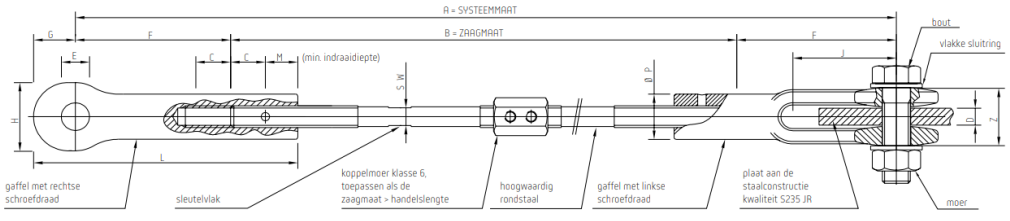

Figure 10-33: Visualization of a "Willems Anker"(*Willems Anker 2017 Specificaties*, 2017)

The characteristic of a cable is that it can only take up tension forces.
Next to the cable, a secondary timber beam should be positioned horizontally in these bracing grids to ensure the horizontal loads can be taken up. Figure 10-34 shows the global layout of the transverse bracing system with the governing cable depending on the wind direction.

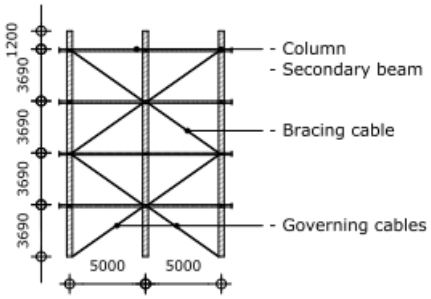

Figure 10-34: Global layout transverse bracing system in mm

Appendix H.5.1 presents the bracing design according to the stability system design of Figure 10-1.

In conclusion, the cables for the vertical bracings in the transverse direction should have a diameter meter of 31 mm, also satisfying the fire situation if the steel temperature stays below 700 °C. The governing longitudinal bracing cable is positioned in the façade of the ramp grid, which is not investigated in this research. Further research in the ramp grid should find an optimal design for this bracing system with a corresponding connection.

10.4.2: Final design connection bracing with load-bearing system

The horizontal force from the diaphragm should be translated to the bracing cables by connecting the column with the cable. Figures 10-36 and 10-37 show the final design of this connection.

The detailing of the transverse bracing connection is done in Appendix H.5.2.
Four M27 bolts are sufficient to resist the shear force in the connection. Preventing a conflict with the elevated corbel edge is necessary, which is done by positioning the bolts in a 32 mm recess in the column.
That means the column width at this position is reduced by 64 mm. At this position, the column is covered by the beam and floor. So, Appendix H.5.2 provides the check of the column on its resistance in a non-fire situation, which gives a satisfying unity check of 0.73. Next, the “Willems Anker” connection to the primary steel plate can only be done by one M33 bolt.

For the secondary slotted-in steel plate, there are three M20 bolts necessary in the beam and one M20 bolt in the primary slotted-in steel plate. The secondary beam should increase to a 140x120 mm cross-section to ensure the required resistance and minimum edge distances.
Finally, the thicknesses of the two types of steel plates are assumed to be 10 mm, satisfying the requirements calculated in Appendix H.5.2.

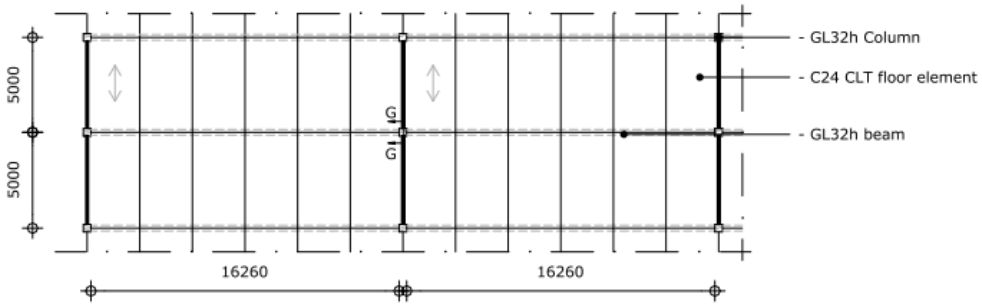

Figure 10-35: Top view investigated module with cross-sections indicated in mm

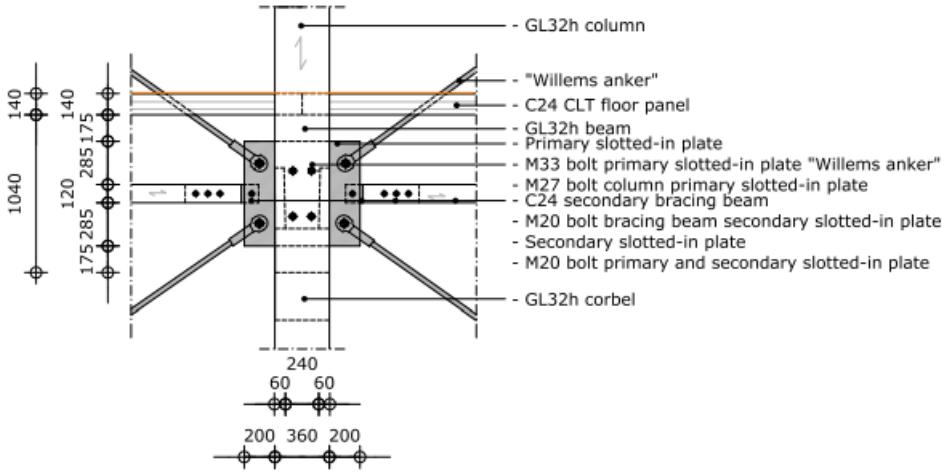

Figure 10-36: Cross-section G-G column-bracing connection in mm

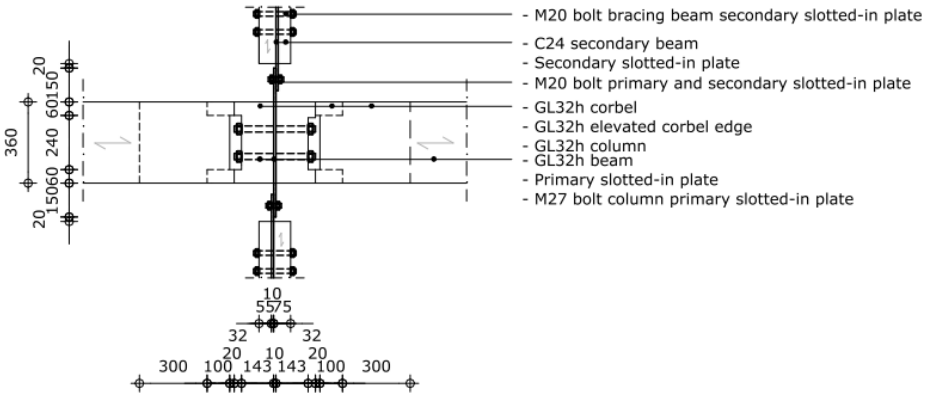

Figure 10-37: Top view column-bracing connection in mm

10.4.3: Integra system

BNPC uses a standard type of fence called Integra (*INTEGRA-Pw*, n.d.). The producer standardizes the connection between the fence and the column. They indicate that the type 4 connection (*Data Sheet De/En 210 - INTEGRA-Pw 943 Concrete Connection Type 4*, n.d.) also applies to a timber column, as shown in Figures 10-38 and 10-39. Only the anchorage should be changed because this is a typical concrete anchor, which should resist a collision force of 50 kN. For example, four M16 bolts at a 230 mm distance from each other give sufficient resistance for a thick-walled steel-to-timber connection, using the axial resistance of a bolt in a steel-to-timber connection. See Figure 10-40.

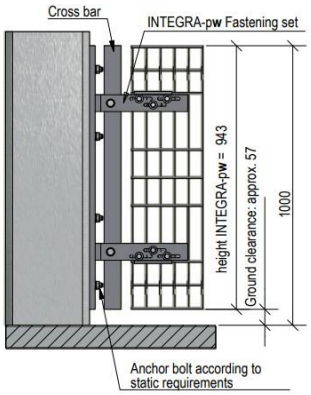

Figure 10-38: Type 4 Integra connection (*Data Sheet De/En 210 - INTEGRA-Pw 943 Concrete Connection Type 4*, n.d.)

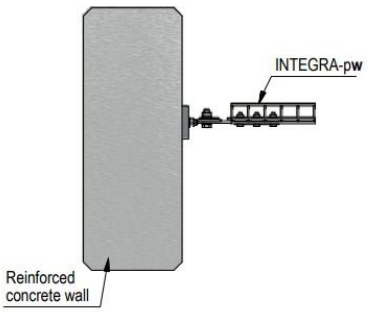

Figure 10-39: Top view integra connection (*Data Sheet De/En 210 - INTEGRA-Pw 943 Concrete Connection Type 4*, n.d.)

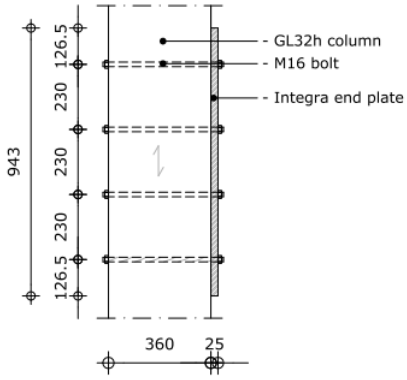

Figure 10-40: Integra anchorage design in mm

10.4.4: Wood protection panel

Figures A-26 and A-28 show the wooden protection of the edge column to ensure it is an element in use class 2 instead of use class 3 using Table B-11.

Any wood species with high natural durability should be used for this application. Durability class 1 or 2 should be applied, as shown in Table B-12, for hazard class 3. An example is oak (*Houtsoort: Eiken, Europees*, n.d.), located in durability class 2. Or azobe (*Houtsoort: Azobé*, n.d.), in durability class 1. The decision on timber species will depend on the availability of the species with corresponding costs. So, this is probably time-dependent and project-specific.

The total width of the wood protection panel will be assumed as three times the column width, based on the reference project shown in Figure A-28 and Figure 10-41.

A re-mountable connection of the protection to the column will be applied to create a potential for a car park expansion. The panels should have the same height as the column, governing 4.62 meters for column segment 1. Furthermore, the thickness will be assumed to be 50 mm. This panel has no constructive function, so the minimum bolt dimension and number can be applied. BNPC indicates that this is 16 mm. For example, four M16 bolts over the height will be applied to ensure a high protection performance by preventing openings in the connection, as visualized in Figure 10-42.

Figure 10-41: Wood protection panel reference project Bad Aibling

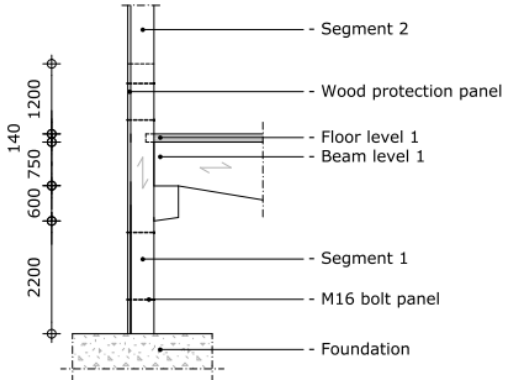

Figure 10-42: Wood based panel connection in mm

10.5: Mounting and demounting sequence

This paragraph summarises the mounting and demounting sequence of the car park module in Figure 1-1. Figure 10-43 presents the order of grids in the construction process. Because the ramp grid consists of vertical stability systems in both directions, this grid is constructed first. Then the adjacent grids are erected, with grids 2a and 2b together because they are next to each other on the same side of the stable core. First, all four levels will be constructed per grid to limit the number of crane movements and optimize the layout of the construction site. Otherwise, during a long construction time, there is very less space for storage available, so a large construction site should be necessary.

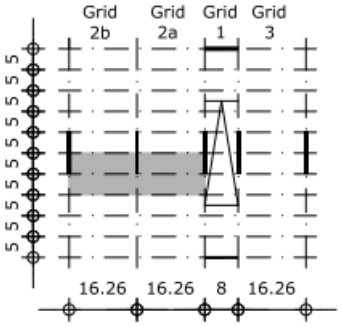

Figure 10-43: Erection order grids in m

Below, Figure 10-44 shows the mounting and demounting sequence per level, which is visualized in Appendix H.6. And on the bottom, the activities that should be done per grid. However, before the car park is going to be erected, there are already activities done. Figure 10-44 links those activities to prefabrication and starting points. The prefabricated timber products should be temporarily protected from moisture, mainly applied with a foil. Because during transport and storage on-site, they are exposed to direct weather influences. The sequence of Figure 10-44 indicates when the temporary moisture protection can be removed or should be installed again.

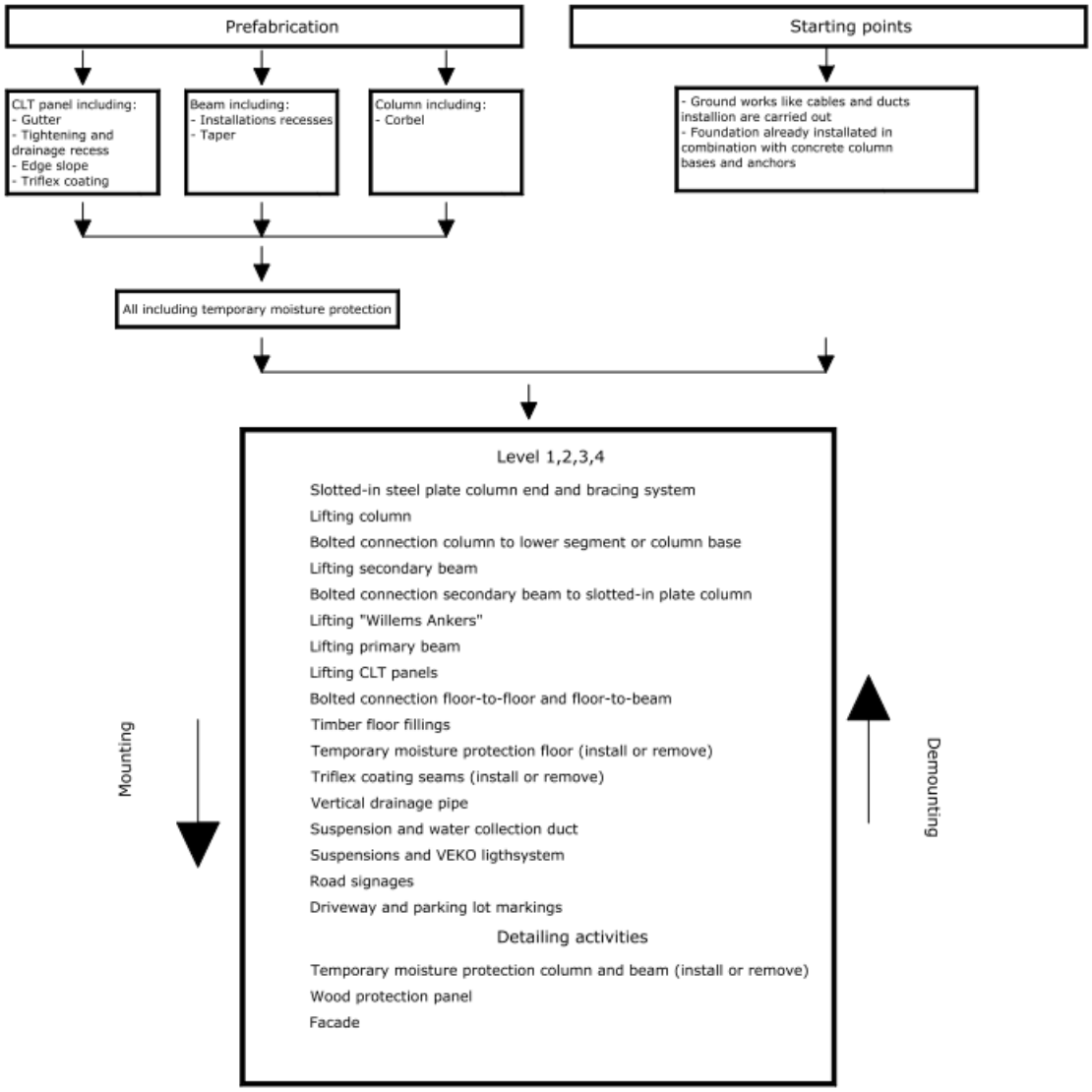

Figure 10-44: Order (de)mounting sequence

Below, three annotations are given for the completeness of the listed sequence.

- During demounting, the Triflex coating should not completely be removed, but only a strip of 20 cm, as indicated in sub-paragraph 5.4.2.
- Next, when the wood protection panel and façade are removed, the column and beam should be temporarily protected from moisture. For the floor, this is necessary when the coating on the seam is removed and the floor panels are demounted.
- Finally, the drainage system is most probably end-of-life by demounting. This system is well accessible and demountable, according to Brand (Brand, 1995). However, the light system has a second application potential due to the longer technical service life, as BNPC indicates.

IV Results phase

Chapter 11 Discussion

Chapter 11 gives a discussion about the research done. So, discussing the outcome of the multi-criteria analysis and the design procedures.
The final floor system is determined based on the multi-criteria analysis of Chapter 8. Paragraph 11.1. covers the discussion of this analysis. Second, the limitations of the research are covered in 11.2.

11.1: Validation of the multi-criteria analysis

Based on the multi-criteria analysis, the CLT floor of floor design 1 is chosen as the most suitable alternative. Sub-paragraphs 8.3.2 and 8.3.3 already perform a sensitivity analysis to check for the validity of this multi-criteria outcome and especially the influence of the weight factors. The focus was on the main research question in determining the weight factors. So, assuming feasibility and structural performance as most important. In addition, the weight factors of the main and sub-criteria are also related to the lessons learned from the reference projects. So, the information gathered is directly translated to the weight factors.

Table 11-1 shows the outcome of the adjusted rankings of the main criteria. Only for sensitivity analysis 1, there is another most suitable design. Namely, floor design 2, representing the timber rib floor. There is only a small difference of 4.4% compared to the chosen floor design 1. Sensitivity analysis 2 also has a small difference but favours floor design 1. All other rankings have a larger difference between floor designs 1 and 2 in favour of floor design 1. Mostly about five to ten per cent because the minimum total floor design score is 0.52 based on the minimum criterion score of 0.52 and the total sum of weight factors of 1.

Floor design 2 has a slightly more favourable feasibility performance than floor design 1, whose corresponding main criteria get the highest weight factor in sensitivity analysis 1. So, only if feasibility is much more important than structural performance floor design 2 is more favourable. Because sensitivity analysis 2 has one of the two structural performance criteria as the most important and the other less important than the feasibility criteria. This ranking results already in floor design 1 as the most suitable alternative. In summary, the conclusion gets improved certainty.

Table 11-1: Resulting scores multi-criteria analysis

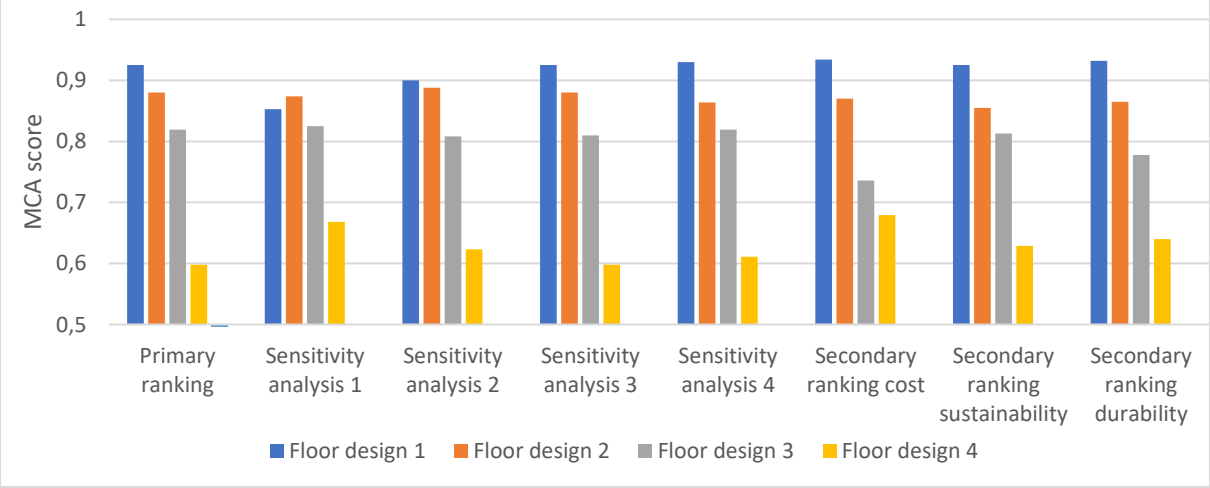

Below will be discussed if the chosen method, weight factors and assumptions can have affected the outcome.

The "verwachtingswaarde method" can combine a qualitative and quantitative assessment. However, it is assumed to apply only a qualitative assessment instead of a combination of qualitative and quantitative. Tables 8-2 and 8-3 show that the quantitative assessment scores differ for positions 2,3 and 4 compared to a qualitative assessment. Applying qualitative and quantitative assessments will result in a larger score difference because the quantitative assessment's weight factors differ more than the qualitative assessment's. Because the assessment is only based on a preliminary design, the accuracy of the knowledge gathered is not maximal. So, applying large score differences gives too much weight to the ranking outcome, resulting in a reduced certainty of the conclusion. Nevertheless, on the criteria suitable for a quantitative assessment: floor height, floor weight, environmental impact, and product cost, the most suitable floor design 1 gets the highest score. So, the resulting score of this floor design will not change. Only the score of the other alternatives will decrease, meaning a higher difference with the second-best alternative.

Next, the number of main- and sub-criteria can influence the resulting weight factor per criteria, affecting the score per alternative. This aspect's impact is hard to determine because it depends on multiple factors, like how many extra criteria and the scores per new criteria. However, the completeness of the criteria is checked by supervisors in terms of feasibility, as well as engineers of BNPC for the design, to cover all the aspects of the design and erection process.

Finally, the outcome of the research is consistent with the reference projects, which also use a comparable load-bearing system with almost equal cross-sections, as concluded in paragraph 7.5.

11.2: Research potential and limitations

This research focuses on the design of four grids, including the connection with upper or lower levels able to copy multiple times in a complete car park, and no total car park area limitations are present due to the assumption of a flashover situation. Therefore, the outcome of this research is applicable to any size and layout of a car park, which increases the potential of the research design.

The limitations of this research are related to the following topics:

- Fire safety design
- Moisture resistance design
- Preliminary and final calculation procedures
- The quantitative assessment of the durability and sustainability performance
- Re-mountable connection design

For traditional car parks made of steel and concrete, like the ModuPark, the fire behaviour is exactly known. So, applying the requirements for an open car park is sufficient to ensure no flashover will occur. However, combustible timber contributes to the fire and lets the fire expand faster. That means the fire characteristic of the car park is different compared to a traditional car park. Modelling this new fire characteristic is impossible because there is only software developed for a car park made of steel (*CaPaFi Version 2.1*, 2010). That means the fire behaviour in a timber car park cannot be modelled. However, the temperatures and fire expansion will most probably be higher than in a traditional car park due to the extra combustion of timber. Therefore, preventing flashover by an open façade cannot be satisfied. Also, the performance of possible fire growth limitation measures, like sprinklers, cannot be determined. So, the fire safety design of the timber car park should be investigated more thoroughly in the future to design the structure more accurately. In addition, to be able to assess valuable measures.

Therefore, this research uses a conservative assumption that a flashover situation will occur and the timber elements should achieve the full 90 minutes of fire resistance.

The potential of the Triflex coating on a timber floor panel is only based on a small test conducted by BNPC and Triflex. This test had a positive result. Nevertheless, a long-term ageing test should also ensure that the CLT-Triflex bonding is sufficient for the total technical service life.
This research does not conduct this test because of limitations in time. This moisture resistance solution is applied in the research because, interviewing all corporate companies, like Triflex and CLT manufacturers, no design issues are indicated by using their expectations for the practical application.

Only the natural vibration resistance is checked in both the preliminary and final design phases for all floor designs. However, this check does not include the damping ratio of the material. This assumption is not a problem for timber due to the negligible damping ratio, but concrete has a five times higher damping ratio. So, a dynamic analysis should be made to determine the benefit of concrete on structural performance. However, building a dynamic analysis model for the four remaining floor systems in the preliminary design takes too much time. Therefore, an upper and lower bound of the floor height is indicated for the timber concrete composite floor, and the prefab concrete floor already fits the natural vibration limit.
Because a CLT panel is designed in the final design phase, no dynamic model is applied due to the assumption that the damping is negligible in the case of a pure timber floor system, so only a simplified and conservative natural vibration check is performed.

The requirements, safety factors, and load values applied in the design phases correspond to the Dutch codes and guidelines. So, this design cannot directly be moved to another country without checking the difference in regulations.

Next, there is limited quantitative durability and sustainability assessment made for the final design due to time limitations. Only a simplified environmental cost comparison is applied in the multi-criteria analysis between glulam, CLT and concrete. Furthermore, the beam alternatives are compared qualitatively instead of quantitative using literature. The assessment in a qualitative way is also done for the design influence on the durability and the re-mountability potential, meaning there is a higher uncertainty than a comparison based on real quantitative numbers.

Finally, regarding the re-mountable connection design, one suitable connection type is investigated based on the scope of paragraph 2.1 and given the boundary conditions of paragraph 9.2. However, it cannot be ensured that this is the only possible type of connection. Further research on a specific connection, including an assessment study, is required to determine the most suitable connection based on the assumed requirements and preferences.

Chapter 12 Concluding remarks

This chapter presents the research conclusion in paragraph 12.1, and Appendix I shows the corresponding visualizations. Second, the recommendations are given in paragraph 12.2.

12.1: Conclusion

Sub-paragraph 12.1.1 presents the concluding answers to the sub-research questions, and 12.2.2 the final answers to the main research question.

12.1.1: Conclusion sub-research questions

Below, the answers to each of the sub-research questions of sub-paragraph 1.3.1 are given.

- ***How are the current structures of re-mountable and non-remountable timber car parks made?***

Re-mountable timber car parks are still not constructed worldwide, so this research focuses on reference timber car parks that are not specifically designed to be re-mountable. Five references are investigated using only timber or combining timber with concrete. These references are the Park & Ride car park in Antwerp (*Park+Ride Antwerp / HUB* , n.d.), car park Studen (Zaugg, 2018), Sege Park Malmö (Rosholm, 2021), car park Bad Aibling (*B&O Wooden Multi-Storey Car Park, Bad Aibling*, n.d.), and car park design Pollmeier and TUMWood (*Development of Construction System for Multi-Storey Car Parks in BauBuche*, n.d.). They are using, for example, monolithic and fixed joints or connections, including screws and carpentry joints which face a high risk of becoming stuck. Next, the multiple times applied mastic asphalt on the CLT floors creates low and unfavourable re-mountability. Table 12-1 summarises the structures corresponding to these reference projects.

Table 12-1: Design summary reference projects

References	Main load-bearing beam	Floor system
Park & Ride Antwerpen	GLT: 360 mm x 1400 mm	Prefab concrete deck plus compression layer: ≈ 400 mm
Car Park Studen	GLT: 200 mm x 960 mm	CLT panel: 140 mm Mastic asphalt: 55 mm
Sege Park Malmö	GLT: unknown height	CLT panel: unknown height Mastic asphalt: 60 mm
Car Park Bad Aibling	GLT & Baubuche: 240 mm x 680-840 mm, 240 mm x 600-760 mm	CLT: 100 mm Mastic asphalt: 70 mm
Car Park Pollmeier and TUMWood	240 mm x 600 mm Baubuche beam	Prefab concrete: 130 mm

All the references show measures for protecting timber at vulnerable moisture deterioration locations. For example, the façade made of steel in the park Studen or protecting the timber columns with wood protection panels, done in the car parks Bad Aibling, Sege Park, and Pollmeier with TUMWood. Next, the top surface of the floors can face direct moisture from the rain or grooves of the wheels. The references with a timber floor system have all mastic asphalt moisture protection. Another applied solution is a complete concrete floor, which is less prone to moisture degradation than timber due to the absence of the biobased character and the reduced hygroscopic behaviour.

Regarding fire safety design, all car parks are designed to be open for natural ventilation to reduce the fire growth risk. There are also additional measures applied to limit the fire growth. The Sege Park uses a sprinkler to limit fire growth, car park Bad Aibling hot gas panels, and the design of Pollmeier and TUMWood smart concrete element design combined with the prevention of cavities.

- ***What are the constructive requirements corresponding to an open re-mountable car park made of timber?***

Eurocode 2443 (NEN 2443, 2013) lists the design regulations for a car park, which is used as a starting point for the design phases. The resulting optimal grid size is 16.26 meters longitudinal by 5 meters transverse, for which different global layouts of the load-bearing elements are possible.

Next, the category F car park loads (NEN-EN 1991-1-1+C1+C11, 2019) should be used. This category contains a surface load of 2 kN/m^2 and two point loads of 5 kN.

Because timber is applied, the requirements from Eurocode 1995 (NEN-EN 1995-1-1+C1+A1, 2011) correspond to this design. Next, timber is a lightweight material with a relatively low stiffness compared to concrete and steel. That makes the serviceability limit state requirements most important for the timber floor system. Those requirements are a deflection limit of 0.003 times the length and a first eigenfrequency limit of 5 Hz.

The timber species should be determined based on the applicable use class and its durability class to ensure sufficient natural durability. In the case of direct exposure to weather influences, use class 3 is the applicable one. Inside the car park, when the timber elements are covered, it is use class 2.
In the case of fire resistance, the façade should be at least one-third open to make it an open car park. Furthermore, the timber elements should have a conservative 90 minutes of fire resistance due to the highest floor level above 5 meters.

- ***What measures can be taken against the performance-affecting aspects of timber at a global and detailed level to ensure an appropriate technical lifetime and resistance?***

This research considers two main performance-affecting aspects: fire and moisture resistance.

The main fire measure is designing the car park with an open façade to create natural ventilation to limit the chance for flashovers. No other measures to reduce the fire growth risk, like concrete barriers, sprinklers, and covering of timber surface, are included in the design. Namely, the effect of the measures is unknown in a timber car park due to the lack of available modelling software. In addition, those measures also create disadvantages for the design. Concrete is a less favourable material in terms of sustainability and weight. Next, a sprinkler reduces the feasibility. Finally, coverage measures have a low performance under the influence of moisture combined with an increasing cost level.

Moisture resistance measures should be applied on the façade and at the top of each floor. On the façade, the possibilities are applying a wood protection panel or using a non-natural material like steel or concrete in the façade. The wood protection panel is the chosen most sustainable solution compared to the use of non-biobased materials. See Figure 12-1. There are three main alternatives for floor protection: concrete finishing, mastic asphalt finishing, and water-resistant Triflex coating finishing. The weight of the floor and height should be limited in optimizing the structural performance, feasibility and car park profit. The Triflex coating is beneficial in these aspects, meaning the coating system shown in Figure 12-2 is chosen as the most optimal solution.

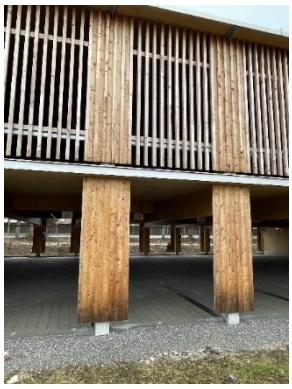

Figure 12-1: Wood protection panel

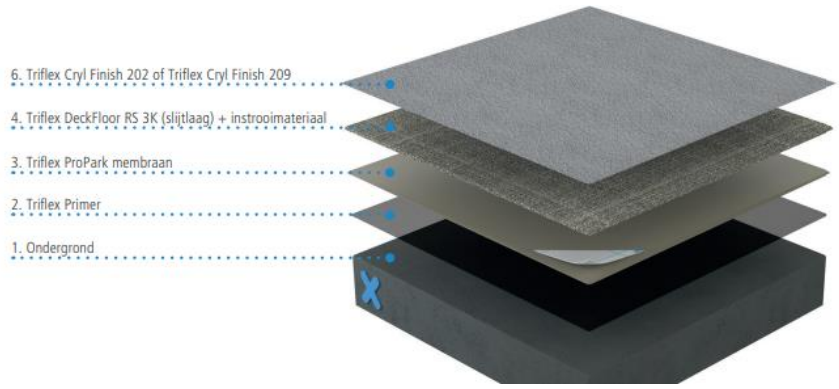

Figure 12-2: Triflex coating moisture protection (*Triflex DeckFloor Systeem, Variant 1*, n.d.)

- ***What is the potential of a combination of materials in the floor system?***

Two different materials are present in the available floor systems: timber and concrete.
Concrete has a favourable fire and moisture resistance performance compared to timber. Next, on structural performance, the good characteristics of concrete are the weak characteristics of timber. However, timber is a biobased material which is not valid for concrete. Furthermore, concrete's self-weight is much higher than timber. So, smart combining both materials can give a floor system that reduces the disadvantages of both materials.

The most favourable combination of timber and concrete in a floor system is applying concrete on top of the timber. Because the concrete is in compression for a positive bending moment, no tensile cracks will occur, and timber has a good tensile resistance. In addition, in this way, the concrete can act as moisture protection.

- ***Which type of long-span floor system is most suitable in the open timber re-mountable car park?***

The most suitable type of floor system is a 140 mm thick CLT panel with a span of 5 meters combined with glulam beams over a length of 16.26 meters, as shown in Figure I-2 of Appendix I. After two assessments, first based on mutual comparisons and second on the multi-criteria analysis, this floor system has the highest score of 0.925 on the primary ranking in the multi-criteria analysis. Moreover, it also has the highest score on all secondary rankings and three of the four sensitivity analyses. Therefore, the decision for this floor system as the most suitable one has a low uncertainty.

The first assessment of the existing available floor systems and the generated new floor designs are based on comparing their characteristics. Then, four floor systems are left, namely the CLT floor, timber rib floor, timber-concrete rib floor, and a prefab concrete floor.

After preliminary designing those four floor systems, the remaining floor designs are assessed based on structural performance, feasibility, sustainability, durability, and cost criteria.
Applying a CLT floor is the most suitable long-span floor system alternative because it has the lowest height, weight, and cost. Combined with no clear disadvantages on feasibility.

- ***Which type of global load-bearing structure fits the best within the structural performance and feasibility boundary conditions?***

Applying beams every 5 meters to span from column to column over 16.26 meters combined with CLT floor panels of 5 meters x 2.77 meters is the most optimal global design, as indicated in Figure I-1.
The elements of this most optimal global layout are all individual elements to improve the transportation potential. The advantages of this layout are the favourable feasibility due to the reduced number of elements and the favourable drainage design compared to a smaller grid. Next, the height of this system is only slightly larger than by applying a smaller span of 2.5 meters. A larger span will result in an unfavourable height increase.

- ***What are the most feasible types of re-mountable connections in the car park module?***

A bolted connection is the most favourable type of a re-mountable connection. Due to wood's natural character, it has a lower dimensional stability than synthetic materials like concrete and steel. So, a carpentry joint has a low potential to be good re-mountable because it can become stuck. Next, screws can also get stuck in the timber and create irreversible damage to the timber each time it is applied. A dowel has its disadvantage that it cannot take up tension forces. Those problems are not present in a bolted connection due to the predrilled holes and the presence of a head and/or nuts. The only limitation is the hindrance of the bolt head or nut on the floor's top surface to the coating's performance and driveability. So, recesses should be made to ensure a smooth top surface. The floor-to-floor, floor-to-beam, column-to-column, and column-to-bracing connection uses a bolted connection. Those connections are shown in Figures I-3, I-4, I-8 and I-10.

The dependency on large vehicles during the erection of the load-bearing elements connections must be as much as possible limited in time to prevent environmental hindrance plus emissions and increasing cost. So, the beam-to-column connection, visualized in Figures I-6 and I-7, uses a corbel on which the beam rests, and the corbel's elevated edges prevent sideways translation and rotation.

12.1.2: Conclusion main research question and research goal

Before answering the main research question, the stated goal of paragraph 1.2 will be reviewed.

Research goal:
To design a re-mountable car park made of timber, focusing on the structural performance and feasibility of the car park module and important details like the floor system and the re-mountable connections.

This goal is achieved by successfully making a final car park design using only timber load-bearing elements and creating re-mountable connections.
As a concise conclusion, it is possible to design a re-mountable car park made of timber by applying a CLT floor, creating bolted or console connections and using a Triflex coating on the CLT floor top surface.

Below, the answer to the main research question will be given.

Main research question

What is the most suitable design for a timber re-mountable car park, including global structure and details based on structural performance and feasibility?

The most suitable timber re-mountable car park design combines the sub-research questions' results. Appendix I presents the 2D and 3D visualizations of the final re-mountable timber car park design.

Concluding the floor system investigation process, applying a 5-meter by 16.26 meters grid with separate CLT floor panels, glulam beams, and columns results in the most efficient global layout, as shown in Figure I-1 of Appendix I. The C24 CLT floor system must have a thickness of 140 mm and an area of 2.77 meters by 5 meters. Next, the optimal GL32h glulam beams cross-section is 360x1040 mm with a taper creating a height increment of 130 mm. Combining the floor system with the required glulam beam cross-section has the smallest height, visualized in Figure I-2. In addition, it has a low weight, meaning it creates an optimal design for the other load-bearing elements, and the production cost is favourable. In terms of feasibility, it acts moderately compared to the other three investigated floor designs in the multi-criteria analysis with no clear disadvantages.

Re-mountability can be applied in a timber car park using the following connections.
The CLT panels are connected with bolts to the adjacent panels and beams, creating the highest feasibility. However, floor and beam recesses are necessary to ensure the bolts can be tightened without conflicting the coating performance and driveability. After the erection, they should be filled with timber blocks as a sustainable solution and to create sufficient structural performance. See Figures I-3 and I-4.
The beam-to-column connection must be designed to be least dependent in time on large vehicles because they are environmentally unfriendly and costly. So, it consists of a beam resting on a corbel with elevated edges. Those elevated edges prevent translation and rotation of the beam during erection. This connection is shown in Figures I-6 and I-7.
Finally, the column segments are connected by bolts at a distance of 1.2 meters above the top surface of the floor to ensure that the final fall protection can be installed before manual actions occur, creating a safe and feasible optimization. This connection consists of a slotted-in steel plate and an end plate, creating a possibility of ventilation and protecting the column from moisture. Figure I-8 shows this connection.

The floor panels are covered with a Triflex coating of 5 mm thick to ensure moisture protection of the timber floor panel. This option is chosen to limit the weight of the floor and create a high re-mountability. The façade, which is at least one-third open and combined with durable wood protection panels, acts as a sustainable moisture resistance measure to ensure the edge columns are also in use class 2. This favourable use class limits the amount of timber necessary and makes the application of spruce possible for the timber load-bearing elements. Spruce is favourable because of its high availability in Western Europe, reducing material costs and transportation distance.
In terms of drainage, the applied tapered beams easily create the required slope in the floor to ensure sufficient water drainage. The water is further drained using gutters, vertical drainage pipes and collection ducts. This drainage system is shown in Figures I-7 and I-12.

Regarding fire resistance, the façade must be at least one-third open to ensure an open car park design, creating natural ventilation. This measure is the only applied one because the performance of other measures is unfavourable in terms of feasibility and cost. However, due to the unknown effect of the combustible timber on preventing a flashover by natural ventilation, the car park is designed according to this conservative flashover situation. This conservative assumption only increases the column dimensions because the serviceability limit state governs the floor system and beam design.

12.2: Recommendations

Below, a list of recommendations is presented. Those recommendations are based on the scope (paragraph 2.1) and the knowledge gaps faced during research, mentioned in 12.2.1. In addition, the relevant recommendations for policymakers are given in 12.2.2 and the ones for BNPC in 12.2.3.

12.2.1: Recommendations further research

Based on the scope and the research steps done, the recommendations for further research are:

- The ramp grid with corresponding elements should be designed and dimensioned for a complete re-mountable timber car park design.
- Next, investigating the application of re-mountability combined with timber in the foundation is necessary for further research to get a complete re-mountable timber car park design.
- The façade has an important function in the fire and moisture resistance of the car park. So, finding the most optimal façade design is a valuable topic for further research.
- The design aspects and behaviour of the performance-affecting aspects are completely different for an underground car park. So, investigating the difference with the outcome of this research is an important topic for further research.
- Sub-paragraph 6.3.3 states that the CLT floor panel and rib floor alternatives will be taken into the preliminary design instead of the LVL variants because of the larger possible element sizes. In Chapter 8, it is concluded that the CLT floor system 1 is the most beneficial design. This floor system can also be produced in LVL, so further research should determine if the LVL variant also satisfies all requirements.
- No scientific research is available on the use of FRP in floor systems in a car park. By improving the knowledge, the potential of an FRP floor system can increase, making it a valuable topic for further research.
- The Triflex coating on the seams is the only part of the design that is not completely re-mountable because a strip of 20 cm around the seam becomes waste during demounting. Further research can investigate if another solution is creating a higher re-mountability.
- As indicated in the discussion (paragraph 11.2), further research on a complete alternative assessment study per detail can increase the certainty of the resulting final design.

During the investigation of the fire safety design of an open re-mountable timber car park, the following knowledge gap and recommendation appeared.

- No specific software is available for modelling an open car park fire made of timber due to the different fire behaviour of timber compared to incombustible steel and concrete. Therefore, applying the available software for steel is not possible. So, developing a new software tool for using timber in an open car park is necessary to get a more accurate insight into fire behaviour. And the performance of fire growth reduction measures.

Corresponding to the moisture design. There are two recommendations:

- Detailed tests, including long-term behaviour tests, should ensure the Triflex coating is performing well in combination with timber.
- The potential benefit of a roof for moisture protection with solar panels can be investigated.

The final recommendations for further research are related to the calculation procedures.

- Dynamic analysis should be done next to the check on natural vibration because the damping should be included for the completeness of the vibrational design.

12.2.2: Recommendations policymakers

The recommendation for the policymakers is:

- Stimulate the number of requested timber car parks instead of car parks with traditional materials. This increase in projects leads to a higher need for investigation and innovation in timber car parks. Resulting in a higher knowledge and experience level.

12.2.3: Recommendations Ballast Nedam Park & Connect

Finally, there are three recommendations for Ballast Nedam Park & Connect.

- The focus during the final design phase was on the smallest cross-sections possible. However, applying optimization in the combination of cost and cross-sectional dimensions is not included but can benefit the competitiveness of the overall re-mountable car park design. This optimization process is not applied because gathering real cost values for the materials and strength classes was difficult, and they are time-dependent, so applying them makes this research less generalizable. However, the required cross-section for lower strength classes is indicated in this research.
- If the design should also be applied in countries other than the Netherlands, the differences in codes and regulations should be investigated, which can result in a different final design.
- An LCA and BCI calculation should be made to prove the timber car park's sustainability and durability level. These results can be important information for clients to assess and compare this car park design with others, especially the ones with non-biobased materials. However, it is not included in this design due to time limitations.

Bibliography

Structural design manual CLT Rib Panels . (2022). https://www.storaenso.com/-/media/documents/download-center/documents/product-specifications/wood-products/rib-panel-technical/structural-design-manualclt-rib-panelsv021-sep-2022.ashx

Ahmed, S., & Arocho, I. (2021). Feasibility Assessment of Mass Timber as a Mainstream Building Material in the US Construction Industry: Level of Involvement, Existing Challenges, and Recommendations. *Practice Periodical on Structural Design and Construction*, *26*(2). https://doi.org/10.1061/(ASCE)SC.1943-5576.0000574

Altin Karataş, M., & Gökkaya, H. (2018). A review on machinability of carbon fiber reinforced polymer (CFRP) and glass fiber reinforced polymer (GFRP) composite materials. *Defence Technology*, *14*(4), 318–326. https://doi.org/10.1016/J.DT.2018.02.001

Alzamora Guzman, V., & Brøndsted, P. (2015). Effects of moisture on glass fiber-reinforced polymer composites. *Journal of Composite Materials*, *49*(8), 911–920. https://doi.org/10.1177/0021998314527330/FORMAT/EPUB

Amir, N., Abd. Majid, A. A., & Ahmad, F. (2016). Effects of Hybrid Fibre Reinforcement on Fire Resistance Performance and Char Morphology of Intumescent Coating. *MATEC Web of Conferences*, *38*. https://doi.org/10.1051/matecconf/20163803001

Ascione, L., Caron, J.-F., Godonou, P., van IJselmuijden, K., Knippers, J., Mottram, T., Oppe, M., Sorensen, M. G., Taby, J., & Tromp, L. (2016). *Prospect for new guidance in the design of FRP*. https://eurocodes.jrc.ec.europa.eu/sites/default/files/2021-12/ReqNo_JRC99714_lbna27666enn.pdf

Baghdasarian, Z., Christianto, S., & Kusuma, C. (2018). *Moisture Safety Evaluation of CLT-Concrete Composite Slab* [Chalmers University of Technology]. www.tcpdf.org

Bazli, M., Heitzmann, M., & Ashrafi, H. (2022). Long-span timber flooring systems; A systematic review from structural performance and design considerations to constructability and sustainability aspects. *Elsevier*.

Blaß, H. J., & Sandhaas, C. (2017). *PRINCIPLES FOR DESIGN*. https://doi.org/10.5445/KSP/1000069616

B&O Holzparkhaus, Bad Aibling . (n.d.). HK Architekten. Retrieved December 8, 2022, from https://www.hkarchitekten.at/de/projekt/bo-holzparkhaus-bad-aibling/

B&O Wooden multi-storey car park, Bad Aibling. (n.d.). HK Architekten. Retrieved December 13, 2022, from https://www.hkarchitekten.at/en/project/bo-holzparkhaus-bad-aibling/

Bouwbesluit 2012. (2011).

Brancart, S., Paduart, A., Vergauwen, A., Vandervaeren, C., Laet, L. De, & Temmerman, N. De. (2017). Transformable structures: Materialising design for change. *International Journal of Design and Nature and Ecodynamics*, *12*(3), 357–366. https://doi.org/10.2495/DNE-V12-N3-357-366

Brand, S. (1995). *How Buildings Learn; What Happens after They're Built*. Penguin Books.

Buchanan, A. H. (2000). Fire performance of timber construction. *Progress in Structural Engineering and Materials*, *2*, 278–289.

Buck, D., Wang, X., Hagman, O., & Gustafsson, A. (2015). Comparison of different assembling techniques regarding cost, durability, and ecology - a survey of multi-layer wooden panel

assembly load-bearing construction elements. *BioResources*, *10*(4), 8378–8396. https://doi.org/10.15376/biores.10.4.8378-8396

Cadorin, J. F., Franssen, J. M., Pintea, D. I., Zaharia, R., Cajot, L. G., Vassart, O., Hanus, F., & Thauvoye, C. (2018). *Ozone* (3.0.4). ArcelorMittal.

Cambier, C., Elsen, S., Galle, W., Lanckriet, W., Poppe, J., Tavernier, I., & Vandervaeren, C. (2019). *Building a Circular Economy Design Qualities to Guide and Inspire Building Designers and Clients*. https://www.vub.be/arch/files/circular_design_qualities/VUB%20Architectural%20Engineering%20-%20Circular%20Design%20Qualities%20(2019.12).pdf

CaPaFi version 2.1. (2010). Bouwen met staal.

CLT by Stora Enso; Technical brochure. (2017). https://www.storaenso.com/-/media/documents/download-center/documents/product-brochures/wood-products/clt-by-stora-enso-technical-brochure-en.ashx?mode=brochure#page=34

Cross-laminated timber. (2021). https://www.klh.at/wp-content/uploads/2019/10/kreuzlagenholz-07-2021-us-k.pdf

Cross-laminated timber (CLT). (n.d.). Stora Enso. Retrieved November 2, 2022, from https://www.storaenso.com/en/products/mass-timber-construction/building-products/clt#Tf4d02c92-02e9-4899-9270-3f7e842882e3

Data Sheet De/en 210 - INTEGRA-pw 943 Concrete connection type 4. (n.d.).

de Feijter, M. P., & Breunese, A. J. (2007). *Onderzoek brand parkeergarage Lloydstraat, Rotterdam*.

de Witte, L., & van der Graaf, P. J. (2021). *Onderzoek sprinklerinstallatie parkeergarage*.

Development of construction system for multi-storey car parks in BauBuche. (n.d.). Retrieved September 6, 2022, from www.holz.tum.de

Dragende ideeën met hout. (2016, May). Lignatur® . https://shuttle-storage.s3.amazonaws.com/laminatedtimbersolutions/DOWNLOADS/Lignatur-imagebook.pdf?1562158024

Environmental Product Declaration X-lam. (2022). https://www.mrpi.nl/epd-files/epd/1.1.00281.2022_MRPI-EPD_X-LAM%20-Cross%20laminated%20timber-Norwegian%20market_FINAL.pdf

Ermakov, V., & Stepanova, E. (2020). Moisture content and its influence on glued timber structures. *IOP Conference Series: Materials Science and Engineering*, *869*(5). https://doi.org/10.1088/1757-899X/869/5/052015

European Technical Assessment ETA 18/1132. (2021). In *Eurofins*. EOTA. https://www.storaenso.com/-/media/documents/download-center/certificates/wood-products-approvals-and-certificates/eta/etalvl-rib-panel181132-23122021.ashx

European Technical Assessment ETA-11/0137. (2021). In *Austrian Institute of Construction Engineering*. EOTA. https://www.lignatur.ch/fileadmin/ablage/downloads/Das-Element/eta-11-0137-lignatur-en.pdf

European Technical assessment ETA-14/0349. (2019). In *Austrian Institute of Construction Engineering*. EOTA. https://www.cltcz.info/wp-content/uploads/CLT_ETA-14-0349_en.pdf

European Technical Assessment; ETA-14/0354. (2018).

European Technical Assessment; ETA-18/1014. (2019). In *Deutches Institut für Bautechnik*. EOTA.

European Technical Assessment ETA-20/0893. (2020). In *ETA-Danmark A/S*. EOTA. https://www.storaenso.com/-/media/documents/download-center/certificates/wood-products-approvals-and-certificates/eta/clt-rib-panels-by-stora-enso_eta.ashx

Fennell, P., Driver, J., Bataille, C., & Davis, S. J. (2022). Going net zero for cement and steel. *Nature*. https://media-nature-com.tudelft.idm.oclc.org/original/magazine-assets/d41586-022-00758-4/d41586-022-00758-4.pdf

Framework Circulair Bouwen versie 1.0. (2019, July). *Platform CB'23*. https://platformcb23.nl/images/downloads/20190704_PlatformCB23_Framework_Circulair_Bouwen_Versie_1.0.pdf

Gao, Y., Chen, J., Zhang, Z., & Fox, D. (2013). An advanced FRP floor panel system in buildings. *Composite Structures*, *96*, 683–690. https://doi.org/10.1016/j.compstruct.2012.09.033

Gelamineerde houtconstructies-Toepassing van het materiaal voor grote overspanningen. (n.d.). Retrieved March 14, 2023, from https://www.derix.de/data/Gelamineerde_houtconstructies_Derix_NL.pdf

Gillon, J. (2002). Acid attack. *Nature 2002 415:6874*, *415*(6874), 847–847. https://doi.org/10.1038/415847A

Gjutasfalt i P-huset Sege Park . (2021, December 7). Parkering Malmö. https://www.pmalmo.se/Om-parkering-Malmo/mediarum/aktuella-nyheter/gjutasfalt_i_P-huset/

Glass, S. V, & Zelinka, S. L. (2021). *Wood Handbook; Wood as an Engineering Material* (Vol. 4). United States Department of Agriculture Forest Service. https://www.fpl.fs.usda.gov/documnts/fplgtr/fplgtr282/chapter_04_fpl_gtr282.pdf

Grote voertuigen. (n.d.). CROW. Retrieved March 27, 2023, from https://kennisbank-crow-nl.tudelft.idm.oclc.org/public/gastgebruiker/WBASVV/Turborotondes/Grote_voertuigen/8296

Hamerlinck, A. F., Breunese, A., Noordijk, L. M., Jansen, D. W. L., & van Oerle, N. J. (2011). Richtlijn Brandveiligheid Stalen Parkeergarages. In *Bouwen met staal*. https://docplayer.nl/13183486-Richtlijn-brandveiligheid-stalen-parkeergarages.html

Hessels, T., & Ebus, J. (2020). *De brand in de Singelgarage te Alkmaar*. www.ifv.nl

Het Nieuwe Normaal van 0.2 bijna naar 0.3. (2022). Cirkelstad. https://www.cirkelstad.nl/het-nieuwe-normaal-van-0-2-bijna-naar-0-3/

Hildebrandt, J., Hagemann, N., & Thrän, D. (2017). The contribution of wood-based construction materials for leveraging a low carbon building sector in europe. *Sustainable Cities and Society*, *34*, 405–418. https://doi.org/10.1016/J.SCS.2017.06.013

Hilster, D., Leestemaker, L., & Hoen, A. (2020). *Veiligheid en elektrische personenauto's - Actualisatie factsheet 2020*.

Houtsoort: Azobé. (n.d.). Centrum Hout. Retrieved July 5, 2023, from https://www.houtinfo.nl/node/312

Houtsoort: Eiken, Europees. (n.d.). Centrum Hout. Retrieved July 5, 2023, from https://www.houtinfo.nl/node/278

IKO enertherm ALU. (2020). https://www.isolatiewereld.nl/wp-content/uploads/2021/01/Iko-Enertherm-Alu-productblad-isolatiewereld.pdf

INTEGRA-pw. (n.d.). Projekt w. Retrieved June 8, 2023, from https://www.projekt-w.de/en/integra-pw-en/

Introduction to timber & fire . (n.d.). CTI Firehub. Retrieved October 11, 2022, from https://timberfirehub.co.uk/introduction-to-timber-fire/

ISO 15686-1. (2000). *Gebouwen en constructies - Planning van de levensduur - Deel 1: Algemene principes en kader*. ISO.

Kerto® LVL for load-bearing applications. (2022). https://www.metsagroup.com/contentassets/f8ff384a208d4786959efa4bca9fab2c/kerto_lvl_for_load-bearing_applications3.pdf

Kerto® LVL Q-panel. (n.d.). Metsä Group. Retrieved October 18, 2022, from https://www.metsagroup.com/nl/metsawood/producten-en-diensten/producten/kerto-lvl/kerto-lvl-q-panel/

Kerto - Ripa Technische Richtlijnen. (2016). Metsä wood Holland. https://docplayer.nl/60911911-Kerto-ripa-technische-richtlijnen-metsa-wood.html

Kielsteg - Light and wide; The handbook for the wooden roof and floor elements with outstanding performance. (2019).

Klimaatviewer. (n.d.). Koninklijk Nederlands Meteorologisch Instituut. Retrieved March 1, 2023, from https://www.knmi.nl/klimaat-viewer

Kolb, J. (2008). *Systems in Timber Engineering Loadbearing Structures and Component Layers*. Birkhäuser . https://doi.org/10.1007/978-3-7643-8690-0

Kuiper, E., & Ligterink, N. E. (2013). *Voertuigcategorieën en gewichten van voertuigcombinaties op de Nederlandse snelweg op basis van asses-combinaties en as-lasten*. https://legacy.emissieregistratie.nl/erpubliek/documenten/05%20Verkeer%20en%20vervoer/2013%20(TNO)%20Beladingsgraden%20vrachtverkeer%20WiM.pdf

Laminated veneer lumber (LVL) bulletin; New European strength classes. (2019). Studiengemeinschaft Holzleimbau e.V., Federation of Finnish Woodworking Industries. https://puutuoteteollisuus.fi/images/pdf/LVL_bulletin_eng.pdf

Leidraad meten van circulariteit version 3.0. (2022). In *Platform CB'23*. https://platformcb23.nl/images/downloads/2022/final/Leidraad_Meten-van-circulariteit-3.pdf

Lignatur® element. (n.d.). Lignatur®. Retrieved October 27, 2022, from https://www.lignatur.ch/en/product/lignatur-element

Lucherini, A., Razzaque, Q. S., & Maluk, C. (2019). Exploring the fire behaviour of thin intumescent coatings used on timber. *Fire Safety Journal*, *109*, 102887. https://doi.org/10.1016/J.FIRESAF.2019.102887

Martinez, M. (n.d.). *Wat is nu de beste oplossingsrichting in een parkeergarage*. Saval. Retrieved August 1, 2023, from https://www.saval.nl/blog/de-beste-oplossingsrichting-parkeergarage/

Mastic Asphalt Footways, Car Parks & Service Decks; Technical Guide. (n.d.). Mastic Asphalt Council. Retrieved January 18, 2023, from https://masticasphaltcouncil.co.uk/paving-technical-guide/

Maundrill, Z. C., Dams, B., Ansell, M., Henk, D., Ezugwu, E. K., Harney, M., Stewart, J., & Ball, R. J. (2023). Moisture and fungal degradation in fibrous plaster. *Construction and Building Materials*, *369*, 130604. https://doi.org/10.1016/J.CONBUILDMAT.2023.130604

Meetmethode Circulair vastgoed - Building Circularity Index versie 1.0. (2022). In *BCI*. https://bcigebouw.nl/wp-content/uploads/2022/03/2022-Whitepaper-Building-Circularity-Index-V1.0.pdf

Ministerie van Financien, afdeling B. en instrumentatie. (1992). *Evaluatiemethoden: een introductie* (4th ed.). SDU Uitgeverij.

Muhammad, N. Z., Keyvanfar, A., Abd. Majid, M. Z., Shafaghat, A., & Mirza, J. (2015). Waterproof performance of concrete: A critical review on implemented approaches. *Construction and Building Materials*, *101*, 80–90. https://doi.org/10.1016/j.conbuildmat.2015.10.048

Nader onderzoek MFA Overtuinen. (2017). https://www.planviewer.nl/imro/files/NL.IMRO.0479.STED3838BP-0301/b_NL.IMRO.0479.STED3838BP-0301_tb3.pdf

NEN 2443. (2013). *Parkeren en stallen van personenauto's op terreinen en in garages*. Nederlands Normalisatie-instituut.

NEN 5466. (2010). *Kwaliteitseisen voor hout (KVH 2010) - Op uiterlijke kenmerken gesorteerd Europees naaldhout*. Nederlands Normalisatie-instituut.

NEN 6008+A1. (2020). *Betonstaal*. Nederlands Normalisatie-instituut.

NEN 6055. (2011). *Thermische belasting op basis van het natuurlijk brandconcept - Bepalingsmethode*. Nederlands Normalisatie-instituut.

NEN 6069+A1+C1. (2019). *Beproeving en klassering van de brandwerendheid van bouwdelen en bouwproducten*. Nederlands Normalisatie-instituut.

NEN 6090. (2017). *Bepaling van de vuurbelasting*. Nederlands Normalisatie-instituut.

NEN-EN 335. (2013). *Duurzaamheid van hout en op hout gebaseerde producten - Gebruiksklassen: Definities, toepassing op massief hout en op houtachtige plaatmaterialen*. Nederlands Normalisatie-instituut.

NEN-EN 338. (2016). *Hout voor constructieve toepassingen - Sterkteklassen*. Nederlands Normalisatie-instituut.

NEN-EN 350. (2016). *Duurzaamheid van hout en houtachtige producten - Beproeving en classificatie van de weerstand tegen biologische agentia, de doorlaatbaarheid van water en de prestaties van hout en houtachtige materialen*. Nederlands Normalisatie-instituut.

NEN-EN 460. (1994). *Duurzaamheid van hout en op hout gebaseerde produkten. Natuurlijke duurzaamheid van massief hout. Richtlijn voor de eisen aan de duurzaamheid van hout voor toepassing in risicoklassen*. Nederlands Normalisatie-instituut.

NEN-EN 1990+A1+A1/C2. (2019). *Eurocode: Grondslagen voor het constructief ontwerp*. Nederlands Normalisatie-instituut.

NEN-EN 1990+A1+A1/C2/NB. (2019). *Grondslagen van het constructief ontwerp*. Nederlands Normalistie-instituut.

NEN-EN 1991-1-1+C1+C11. (2019). *Eurocode 1: Belastingen op constructies – Deel 1-1: Algemene belastingen – Volumieke gewichten, eigen gewicht en gebruiksbelastingen voor gebouwen*. Nederlands Normalisatie-instituut.

NEN-EN 1991-1-1+C1+C11/NB. (2019). *Algemene belastingen – Volumieke gewichten, eigen gewicht en gebruiksbelastingen voor gebouwen*. Nederlands Normalisatie-instituut.

NEN-EN 1991-1-2+C3. (2019). *Algemene belastingen – Belasting bij brand*. Nederlands Normalisatie-instituut.

NEN-EN 1991-1-2+C3/NB. (2019). *Nationale bijlage bij NEN-EN 1991-1-2+C3: Eurocode 1: Belastingen op constructies - Deel 1-2: Algemene belastingen - Belasting bij brand*. Nederlands Normalisatie-instituut.

NEN-EN 1991-1-3+C1+A1/NB. (2019). *Algemene belastingen - Sneeuwbelasting*. Nederlands Normalisatie-instituut.

NEN-EN 1991-1-4+A1+C2. (2011). *Eurocode 1: Belastingen op constructies - Deel 1-4: Algemene belastingen - Windbelasting*. Nederlands Normalisatie-instituut.

NEN-EN 1991-1-4+A1+C2/NB+C1. (2020). *Algemene belastingen - Windbelasting*. Nederlands Normalisatie-instituut.

NEN-EN 1991-1-7+C1+A1. (2015). *Algemene belastingen - Buitengewone belastingen: stootbelastingen en ontploffingen*. Nederlands Normalisatie-instituut.

NEN-EN 1991-1-7+C1+A1/NB. (2019). *Belastingen op constructies - Deel 1-7: Algemene belastingen - Buitengewone belastingen*. Nederlands Normalisatie-instituut.

NEN-EN 1992-1-1+C2. (2011). *Eurocode 2: Ontwerp en berekening van betonconstructies - Deel 1-1: Algemene regels en regels voor gebouwen* . Nederlands Normalisatie-instituut.

NEN-EN 1992-1-1+C2/NB+A1. (2020). *Nationale bijlage bij NEN-EN 1992-1-1+C2 Eurocode 2: Ontwerp en berekening van betonconstructies - Deel 1-1: Algemene regels en regels voor gebouwen*. Nederlands Normalisatie-instituut.

NEN-EN 1992-1-2+C1. (2011). *Eurocode 2: Ontwerp en berekening van betonconstructies - Deel 1-2: Algemene regels - Ontwerp en berekening van constructies bij brand*.

NEN-EN 1993-1- 1+C2+A1. (2016). *Eurocode 3: Ontwerp en berekening van staalconstructies - Deel 1-1: Algemene regels en regels voor gebouwen*. Nederlands Normalisatie-instituut.

NEN-EN 1993-1-2+C2. (2011). *Eurocode 3: Ontwerp en berekening van staalconstructies - Deel 1-2: Algemene regels - Ontwerp en berekening van constructies bij brand* . Nederlands Normalisatie-instituut.

NEN-EN 1993-1-8+C2. (2011). *Eurocode 3: Ontwerp en berekening van staalconstructies - Deel 1-8: Ontwerp en berekening van verbindingen*. Nederlands Normalisatie-instituut.

NEN-EN 1995-1-1+C1+A1. (2011). *Ontwerp en berekening van houtconstructies - Deel 1-1: Algemeen - Gemeenschappelijke regels en regels voor gebouwen*. Nederlands Normalisatie-instituut.

NEN-EN 1995-1-2+C2. (2011). *Eurocode 5: Ontwerp en berekening van houtconstructies - Deel 1-2: Algemeen - Ontwerp en berekening van constructies bij brand*. Nederlands Normalisatie-instituut.

NEN-EN 12845+A1. (2019). *Vaste brandblusinstallaties - Automatische sprinklerinstallaties - Ontwerp, installatie en onderhoud*. Nederlands Normalisatie-instituut.

NEN-EN 14080. (2013). *Houtconstructies - Gelijmd gelamineerd hout en gelijmd massief hout*. Nederlands Normalisatie-instituut.

NEN-EN 14081-1+A1. (2019). *Houtconstructies - Op sterkte gesorteerd hout met rechthoekige doorsnede - Deel 1: Algemene eisen*. Nederlands Normalisatie-instituut.

Nu sätts trästommen på plats i Sege Park . (2021, May 28). Parkering Malmö. https://www.pmalmo.se/Om-parkering-Malmo/mediarum/pressmeddelanden/nu-satts-trastommen-pa-plats-i-sege-park/

NVN-CEN/TS 19103. (2021). *Eurocode 5: Ontwerp en berekening van houtconstructies - Constructief ontwerp van constructies van hout-beton-composiet - Algemene regels en regels voor gebouwen*. Nederlands Normalisatie-instituut.

Oosterweel verbinding: hout en beton op Park & Ride [Powerpoint-slides]. (n.d.). CIT Blaton. Retrieved December 5, 2022, from https://www.citblaton.be/en/projects/oosterweel-linkerover

Overzicht maten en gewichten in Nederland. (2012). https://www.transportscanner.nl/wp-content/uploads/2021/04/2-B-1097b-Overzicht-maten-en-gewichten.pdf

Papageorgiou, A. V., & Gantes, C. J. (2010). Equivalent modal damping ratios for concrete/steel mixed structures. *Computers & Structures*, *88*(19–20), 1124–1136. https://doi.org/10.1016/J.COMPSTRUC.2010.06.014

Park+Ride Antwerp / HUB . (n.d.). ArchDaily. Retrieved December 5, 2022, from https://www.archdaily.com/985070/park-plus-ride-antwerp-hub

Park4all - Parking solutions. (n.d.). Park4all. Retrieved November 3, 2022, from https://www.park4all.com/

Parkeergarage TU Delft P-Sports. (n.d.). Ballast Nedam Park&Connect. Retrieved September 2, 2022, from https://www.bnparking.nl/modulaire-parkeergarages/parkeergarage-tu-delft-p-sports/

Parkhäuser. (n.d.). Goldbeck GmbH. Retrieved November 7, 2022, from https://cms.goldbeck.de/fileadmin/goldbeck.de/00_newsroom/prospekte/goldbeck_pros_parkhaus.pdf

Pawar, E. (2016). A Review Article on Acrylic PMMA. *IOSR Journal of Mechanical and Civil Engineering (IOSR-JMCE) e-ISSN*, *13*(2), 1–4. https://doi.org/10.9790/1684-1302010104

Pieters, K. (2019, December 11). *Park&Ride krijgt langzaam vorm: eerste van 874 houten dwarsliggers geplaats*. HLN. https://www.hln.be/zwijndrecht/park-en-ride-krijgt-langzaam-vorm-eerste-van-874-houten-dwarsliggers-geplaatst~a87a5397/

Plaschke, P. (2021). Webbinarium - Parkering Malmö bygger parkeringshus i trä [Powerpoint-slides]. In *Parkering Malmö*. https://www.pmalmo.se/Om-parkering-Malmo/mediarum/webbinarier/

Principes bij circulair detailleren. (2020, January 26). https://www.nieman.nl/publicatie/principes-bij-circulair-detailleren/

Process Data set: glued laminated timber. (2022). German Federal Ministry for Housing, Urban Development and Building.

https://oekobaudat.de/OEKOBAU.DAT/datasetdetail/process.xhtml?uuid=73366123-98d1-4fb1-9edc-37ba4ba57331&version=00.03.000&stock=OBD_2021_II&lang=en

Process Data set: Laminated veneer board. (2018). German Federal Ministry for Housing, Urban Development and Building. https://oekobaudat.de/OEKOBAU.DAT/datasetdetail/process.xhtml?uuid=b50f7b36-d9aa-40c5-b839-4925a1500952&version=20.20.120&stock=OBD_2021_II&lang=en

Product overview, tolerances and finishes. (n.d.). Retrieved April 4, 2023, from https://www.pollmeier.com/nl/dam/jcr:019693ff-d954-4515-9a47-9fc6764adaf8/2022-12_EN_BauBuche_02_Produktuebersicht.pdf

Proença, M., Garrido, M., Correia, J. R., & Gomes, M. G. (2021). Fire resistance behaviour of GFRP-polyurethane composite sandwich panels for building floors. *Composites Part B*, *224*.

Purba, C. Y. C., Pot, G., Viguier, J., Ruelle, J., & Denaud, L. (2019). The influence of veneer thickness and knot proportion on the mechanical properties of laminated veneer lumber (LVL) made from secondary quality hardwood. *European Journal of Wood and Wood Products*. https://doi.org/10.1007/s00107-019-01400-3

Puri, R. G., & Khanna, A. S. (2017). Intumescent coatings: A review on recent progress. *Journal of Coatings Technology and Research*, *14*(1), 1–20. https://doi.org/10.1007/s11998-016-9815-3

RAI P4 Amsterdam. (n.d.). Veko Lightsystems. Retrieved July 14, 2023, from https://www.veko.com/nl/projecten/parkeergarages.html?view=project&id=6:rai-p4-amsterdam&catid=24

Reefer trailer. (n.d.). DSV. Retrieved June 23, 2023, from https://www.dsv.com/nl-nl/diensten/transportmodaliteiten/wegtransport/trailer-types/reefer-trailer

Reinprecht, L. (2016a). *Wood Deterioration, Protection and Maintenance*. John Wiley & Sons, Incorporated.

Reinprecht, L. (2016b). Wood Durability and Lifetime of Wooden Products. In *Wood Deterioration, Protection and Maintenance* (pp. 1–27). John Wiley & Sons, Ltd. https://doi.org/10.1002/9781119106500.ch1

RFEM (5.24.01). (2020). Dlubal Software GmbH.

Rib elements. (2019). https://www.klh.at/wp-content/uploads/2019/09/klh-rib-elements-en.pdf

Rib Panels. (n.d.). Stora Enso. Retrieved October 28, 2022, from https://www.storaenso.com/en/products/mass-timber-construction/building-products/rib-panels#Ted6aad89-1d58-49a0-bb0c-da4f7cad7cd9

Richard Parking LED. (n.d.). VEKO Lightsystems. Retrieved July 13, 2023, from https://www.veko.com/nl/producten/led-lijnverlichting/richard-parking-led.html

Rijksoverheid. (n.d.). *Nederland circulair in 2050*. Retrieved August 30, 2022, from https://www.rijksoverheid.nl/onderwerpen/circulaire-economie/nederland-circulair-in-2050

Rosholm, J. (2021, August 26). *Lägre klimatpåverkan när p-hus byggs i trä*. Svensk Byggtjänst. https://byggkoll.byggtjanst.se/artiklar/2021/augusti/lagre-klimatpaverkan-nar-p-hus-byggs-i-tra/

Rosmuller, N., van der Graaf, P. J., & Hessles, T. F. T. (2021). *Brandveiligheid van parkeergarages met elektrisch aangedreven voertuigen*. www.ifv.nl

Schänzlin, J., & Dias, A. (2022, May). Design of timber-concrete composite structures. *International Conference on Timber Bridges*.

Schut, E., Crielaard, M., & Mesman, M. (2015). *Beleidsverkenning circulaire economie in de bouw*.

Siddika, A., Mamun, M. A. Al, Aslani, F., Zhuge, Y., Alyousef, R., & Hajimohammadi, A. (2021). Cross-laminated timber–concrete composite structural floor system: A state-of-the-art review. *Engineering Failure Analysis*, *130*, 105766. https://doi.org/10.1016/J.ENGFAILANAL.2021.105766

Solid Wood Panels. (n.d.). KLH Massivholz GmbH. Retrieved October 28, 2022, from https://www.klh.at/en/manufacture-assembly/

Sustainable Construction Information Portal. (n.d.). German Federal Ministry for Housing, Urban Development and Building. Retrieved April 21, 2023, from https://www.oekobaudat.de/no_cache/en/database/search.html

Sweden's largest multi-storey solid wood car park . (2022, September 28). Binderholz GmbH. https://www.binderholz.com/en-us/news/details/swedens-largest-multi-storey-solid-wood-car-park/

Terlouw, K. (2019). *The fire safety of car parks Focussing on structural damage*.

Timber Concrete Composites. (2019). https://www.klh.at/wp-content/uploads/2019/10/klh-timber-concrete-composites.pdf

Triflex DeckFloor systeem, variant 1. (n.d.). Triflex Nederland. Retrieved February 8, 2023, from https://www.triflex.nl/download/5235/Triflex%20DeckFloor%20systeem,%20variant%201%20-%2020220523.pdf

Triflex Ondergrondtabel. (n.d.). Triflex Nederland. Retrieved February 8, 2023, from https://www.triflex.nl/download/5334/20210506%20Ondergrondtabel%20NL.pdf

Triflex ProJoint systeem . (n.d.). Triflex Nederland. Retrieved May 8, 2023, from https://www.triflex.nl/download/4723/Triflex%20ProJoint%20systeem.pdf

Triflex ProPark systeem, variant 1. (n.d.). Triflex Nederland. Retrieved February 9, 2023, from https://www.triflex.nl/download/5236/Triflex%20ProPark%20systeem,%20variant%201%2020220405.pdf

Uitgebreide toelichting BCI gebouw. (n.d.). BCI. Retrieved September 12, 2022, from https://bcigebouw.nl/uitgebreide-toelichting/

van Dam, J., & van den Oever, M. (2019). *Catalogus biobased bouwmaterialen 2019 : Het groene en circulaire bouwen*. https://doi.org/10.18174/461687

van de Leur, P. (2015). *Onderzoek richtlijn brandveiligheid parkeergarages*.

Van De Ven, F. H. M., Visser, W., & Biron, D. J. (2007). *Publicatie Publicatie "Ontwatering in stedelijk gebied."* www.bouwrijp.nl

van der Lught, P. (2021). *Houtbouwmythes ontkracht; het onderscheid tussen fabels en feiten*.

van Herpen, R. (2014). *Brandveiligheid natuurlijk geventileerde parkeergarages - consequenties van het autobrandscenario*. https://www.nieman.nl/wp-content/uploads/2014/03/bip-03-03-2014-p15-19.pdf

van Herpen, R. (2021, October 19). *Brandrisico van open parkeergarages*. Brandveilig.Com. https://www.brandveilig.com/artikel/brandrisico-van-open-parkeergarages-70027

Wang, M., Hu, D., Xiao, L., & Shang, F. (2017). Developments of Gussasphalt System on Steel Deck Pavement. *World Journal of Engineering and Technology*, *05*(03), 141–147. https://doi.org/10.4236/wjet.2017.53b016

Willems Anker 2017 Specificaties. (2017). https://willemsanker.nl/server/multimediaserve/200/?hash=db96e87ac09c25605f65d435321c049db17cd2b1ff0bbb068f53fdd9c283c425

X-lam; Kruislaaghouten bouwelementen in groot formaat voor daken, vloeren en wanden. (n.d.). Retrieved November 2, 2022, from https://www.derix.de/data/DERIX_X_Lam_Brosch_NL_2019_03_WEB.pdf

Zaugg, M. (2018). Dawn of a New Era-World First Timber-Built Car Park. In *8e Forum International Bois Construction FBC*. http://www.forum-boisconstruction.com/conferences/91_FBC2018_Zaugg.pdf

Zhao, X., Korey, M., Li, K., Copenhaver, K., Tekinalp, H., Celik, S., Kalaitzidou, K., Ruan, R., Ragauskas, A. J., & Ozcan, S. (2022). Plastic waste upcycling toward a circular economy. *Chemical Engineering Journal*, *428*, 1385–8947. https://doi.org/10.1016/j.cej.2021.131928

Zhou, J., Heisserer, U., Duke, P. W., Curtis, P. T., Morton, J., & Tagarielli, V. L. (2021). The sensitivity of the tensile properties of PMMA, Kevlar® and Dyneema® to temperature and strain rate. *Polymer*, *225*, 123781. https://doi.org/10.1016/J.POLYMER.2021.123781

Appendices

A: References car parks

The information about the car parks is determined based on literature and drawings. Those references are analysed in four parts: general info about the grid and durability measures, load-bearing structure, floor system, and connections.

A.1: Park & Ride Antwerp Belgium

The first car park is made of concrete and timber, and it is located in Antwerp, Belgium. (*Oosterweel Verbinding: Hout En Beton Op Park & Ride [Powerpoint-Slides]*, n.d.; *Park+Ride Antwerp / HUB* , n.d.; Pieters, 2019)

General info:

- The total length of the timber beams is 18 meters, and the span between the columns is 16,26 meters. Next, the distance between the timber beams is about 7.5 meters.
- Because of the low amount of timber and large distance between the timber beams, the risks concerning a fire increase limitedly compared to a complete concrete car park. The timber beam is most probably dimensioned on serviceability limit state criteria, so the cross-sectional dimension is most probably sufficient in a fire for the strength criteria like bending.

Load bearing structure:

- Concrete columns are combined with glued laminated timber beams of 360 mm width in the longitudinal direction, as shown in Figures A-1 and A-2. However, the dimensions of the cross-sections are not available.

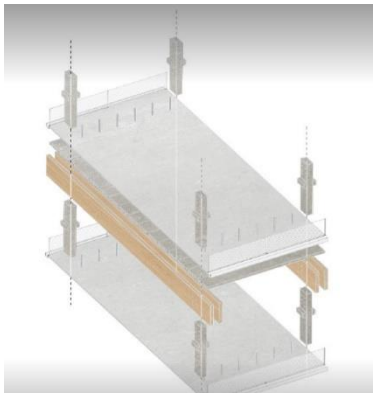

Figure A-1: Elements load-bearing system (*Park+Ride Antwerp / HUB* , n.d.)

Figure A-2: Inside view car park Antwerp

Floor system:

- Prefab concrete elements are placed on top of the timber beams to make a floor system. The dimensions are unknown.
- On top of the prefab concrete deck, a structural concrete screed is cast in situ to ensure the complete floor acts as one rigid element and to get the right finishing surface. This floor system is visualized in Figures A-1, A-2, and A-3. The space between the beam and floor at both sides, visualized in Figure A-3, is used for installation equipment like cables.

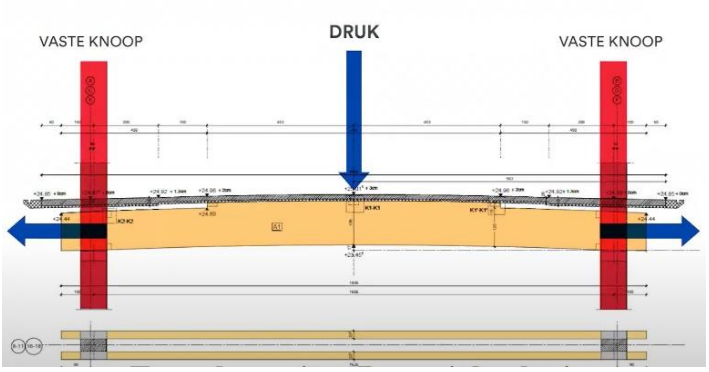

Figure A-3: Cross-section beam plus floor (*Oosterweel Verbinding: Hout En Beton Op Park & Ride [Powerpoint-Slides]*, n.d.)

Connections:

- The timber beams are placed on corbels at the columns. And the prefab floor rests on the horizontal middle part of the timber beam. See Figures A-3, A-4, and A-5. Neoprene layers will be used on the corbels to ensure a good force transfer between the flexible timber and the stiff concrete.
- The timber beams are connected for stability by a steel element with metal fasteners. These are located at multiple positions over the span. Figures A-4 and A-5 visualize this connection.

Figure A-4: Connection between timber beams and column (*Oosterweel Verbinding: Hout En Beton Op Park & Ride [Powerpoint-Slides]*, n.d.)

Figure A-5: Timber beam plus prefab connection (Pieters, 2019)

A.2: Car Park Studen Switzerland

The second car park discussed is the Autotranspo car park in Studen Switzerland. (Zaugg, 2018)

General information:

- A grid of 5.1 meters by 15 meters is used in the design, as shown in Figure A-6.
- The timber elements are not directly exposed to moisture due to hot-dip galvanized steel façade pillars, beams, access ramps, and stair towers, see Figure A-7. In addition, on all levels, the bottom part of the column is protected from moisture. For the bottom level, this is done by concrete. The columns on the other levels have an aluminium covering. Those protections are shown in respectively Figures A-8 and A-9.

- The area per level of the car park is designed according to the maximum compartment size of the Swiss fire safety regulations. So, no measures are applied to ensure a local fire. Therefore, the load-bearing elements will be designed to meet the fire resistance requirements.

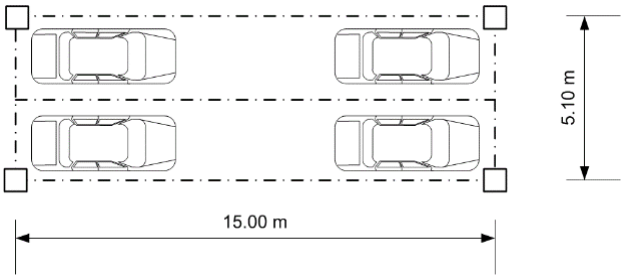

Figure A-6: Grid car park Studen

Figure A-7: Car park façade Studen (Zaugg, 2018)

Figure A-8: Column to foundation connection

Figure A-9: Column protection second, and third car park level

Load-bearing structure:

- V-formed pillars used for the vertical load-bearing structure are made of LVL and glulam, see Figure A-10. On the bottom car park level, the LVL is placed in the vertical direction and on the other levels in the horizontal direction, as visualized in Figures A-11 and A-12. But in both situations, the load is perpendicular to the grain direction, so there is no difference in strength.
- In the longitudinal direction, there are coupled multi-span glued laminated joists of 200 mm x 960 mm with a length of 15 meters. This joist is visualized in Figures A-13 and A-16.
- In the transverse direction, there are also joists between the pillars to transfer the horizontal loads from the wind bracing, see Figures A-16 and A-17.
- Horizontal loads in the longitudinal direction are taken up by pillars and in the transverse direction by wind bracing of steel bars, visualized in Figure A-17.

Figure A-10: V-form pillars (Zaugg, 2018)

Figure A-11: LVL beam bottom level

Figure A-12: LVL beam first level

Figure A-13: Connection joist-joist

Floor system:

- The floor system is made of CLT panels with a span of 5.1 meters and a width of 2.5 meters.
- These panels consist of the following materials: five-ply cross-laminated timber with a thickness of 140 mm, sealing membrane, separation layer, and on top two layers of mastic asphalt with a 30 mm and 25 mm thickness. This floor system is visualized in Figures A-14 and A-15.

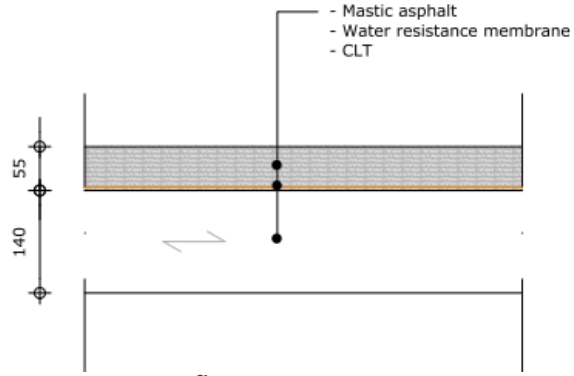

Figure A-14: Lay-up floor system

Figure A-15: Floor surface mastic asphalt

Connections:

- An articulated carpentry joint secured with dowels and screws connects the longitudinal joists at a certain distance from the column, shown in Figures A-13 and A-17.
- A carpentry joint makes the joist-to-pillar connection. See Figures A-10 and A-16. The joist rests on the pillar, but metal fasteners like dowels are used for extra stiffness and stability.

- Slotted-in steel plates are used to connect two pillar segments, the wind bracing to the pillar and the transverse joist to the pillar. Figure A-17 shows these connections. Next, Figure A-18 presents the connection between the joist and the façade column using slotted-in steel plates.

Figure A-16: Connection pillar to beam (Zaugg, 2018)

Figure A-17: Erection CLT floor (Zaugg, 2018)

Figure A-18: Façade column to joist connection

A.3: Sege Park Malmö Sweden

The third design is the timber car park Sege Park in Malmö, Sweden. (*Gjutasfalt i P-Huset Sege Park* , 2021; *Nu Sätts Trästommen På Plats i Sege Park* , 2021; Plaschke, 2021; Rosholm, 2021)Klik of tik om tekst in te voeren.

General info:

- Multiple grids are used in this car park, with a maximum of about 5 meters x 7.5 meters, see Figure A-19. That also means that the columns are located at the end and beginning of the parking lots, as shown in Figures A-19 and A-20.
- For durability, the columns in the façade are protected from moisture by cover boards made of durable timber. The connection from the beam to the column has gaps to allow drainage in combination with the sealing mastic asphalt. Only a part of the floor area is protected by a roof with solar panels.
- There are measures taken to improve fire safety, like sprinklers and paintings, to improve the fire resistance of the timber elements to the required level. Next, timber plugs are used to cover the dowels to increase the fire resistance of the joints.

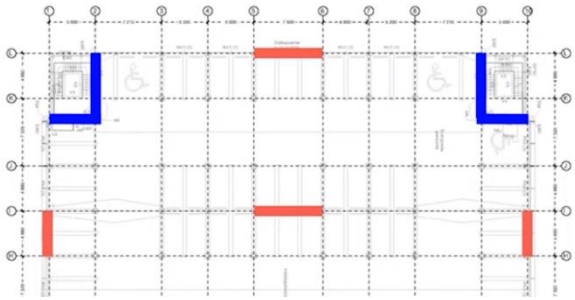

Figure A-19: A part of the Sege Park Malmö grid (Plaschke, 2021)

Figure A-20: Load-bearing system Sege Park (Rosholm, 2021)

Load bearing structure:

- The columns and beams are made of glued laminated timber with unknown dimensions. Those beams are orientated in the transverse direction.

- Steel bracings and the CLT walls of the staircase ensure stability. In Figure A-21, the blue lines are the staircase walls, and the red lines indicate the steel bracings.
- Figure A-21 visualizes that the columns have a length of three and a half levels.

Figure A-21: Erection of columns and walls (*Nu Sätts Trästommen På Plats i Sege Park* , 2021)

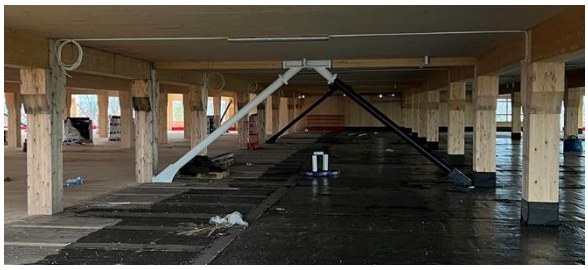

Figure A-22: Installation water resistanct mastic asphalt layer (*Gjutasfalt i P-Huset Sege Park* , 2021)

Floor system:

- The floor system is made of cross-laminated timber with on top a membrane plus mastic asphalt. This mastic asphalt consists of 2 layers of 30 mm. The erection is shown in Figure A-22. This floor system is approximately the same as shown in Figure A-14.

Connections:

- The connection of the column to the concrete foundation is made by anchor bolts plus a shear lug in combination with a knife plate and dowels, see Figure A-23.
- There are two different types of connections between the beam and the column.
  Inside the car park is the joint made of consoles. Consoles make a contact area between the beam and the column, transferring vertical loads directly as normal force. Those cleats are connected to the column by fully threaded screws. The beam is also secured to the column by screws. This joint is visualized in Figure A-24.
  In the façade, the connection is made of a knife plate plus an end plate secured with dowels, see Figure A-25. No cleats are used due to the risk of unwanted trapped water. So, the end plate is beneficial for water drainage and fire protection.
- Column-to-column connections are made by steel plates like the car park in Studen.

Figure A-23: Column to concrete connection (Plaschke, 2021)

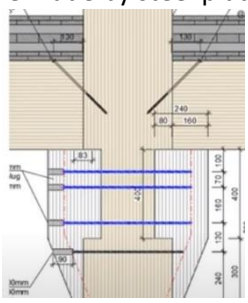

Figure A-24: Inside column to beam connection (Plaschke, 2021)

Figure A-25: Façade column to beam connection (Plaschke, 2021)

A.4: Car park Bad Aibling Germany

The fourth reference car park is the one from Bad Aibling. *of Construction System for Multi-S*(*B&O Wooden Multi-Storey Car Park, Bad Aibling*, n.d.)

General info:

- A grid of about 2.5 meters by 16.5 meters is used in this car park. This grid corresponds to a column on both parking lot edges (paragraph 5.1). See Figures A-27 and A-30 for the grid of this car park.
- Timber plates protect all columns on both levels from direct rainfall. See Figures A-26 and A-29. Also, the edges of the floors and the top of the column on the first level are protected, as shown in Figures A-28 and A-29.
- Timber elements in the width direction between the beams are used as a measure against the flow of hot gases, visualized in Figure A-30. This limits the spread of fire. Next, the relatively small width of the car park and the open façade result in a high level of ventilation. Therefore, the risk of a compartment fire is reduced. So, applying a costly sprinkler system has a low advantage.

Figure A-26: Car park Bad Aibling Germany (*B&O Wooden Multi-Storey Car Park, Bad Aibling*, n.d.)

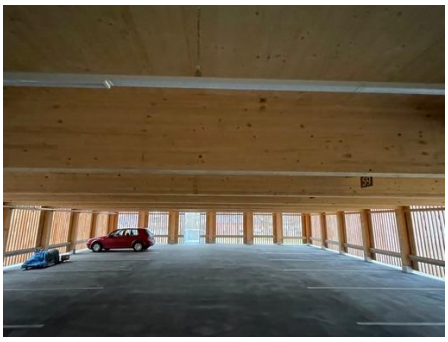

Figure A-27: Inside view second level

Figure A-28: Column protection first level

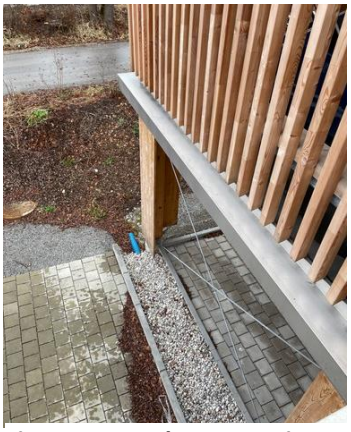

Figure A-29: Edge protection of the floor

Load bearing structure:

- For the load-bearing structure, glued laminated columns in combination with tapered timber beams are used, as visualized in Figures A-28, A-30, A-31, and A-33. The roof beam is made of glued laminated timber GL24h, and the floor beam is made of BauBuche GL75.
- The columns have dimensions of 240 mm by 240 mm. Next, the tapered timber beams are 240 mm by 600-760 mm for the floor and 240 mm x 680-840 mm for the roof, which means a taper of about 2%. Dimensions of 240 mm x 120-280 mm are used for the beams at the ends of the car park in the transverse direction. Those beams are placed in the longitudinal direction. Figures A-30 and A-32 show those beams.

- Stability is guaranteed by steel bracings in the façade and by timber walls inside the car park, as shown in respectively Figures A-30 and A-32.

Figure A-30: Load bearing structure of the Bad Aibling car park

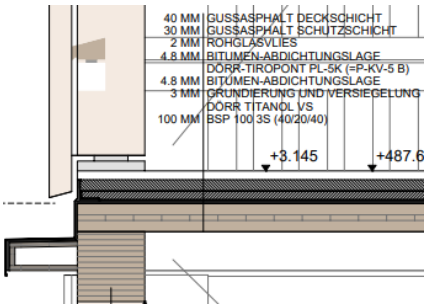

Figure A-31: Floor system of the Bad Aibling car park

Figure A-32: Load-bearing structure bottom level plus stability wall

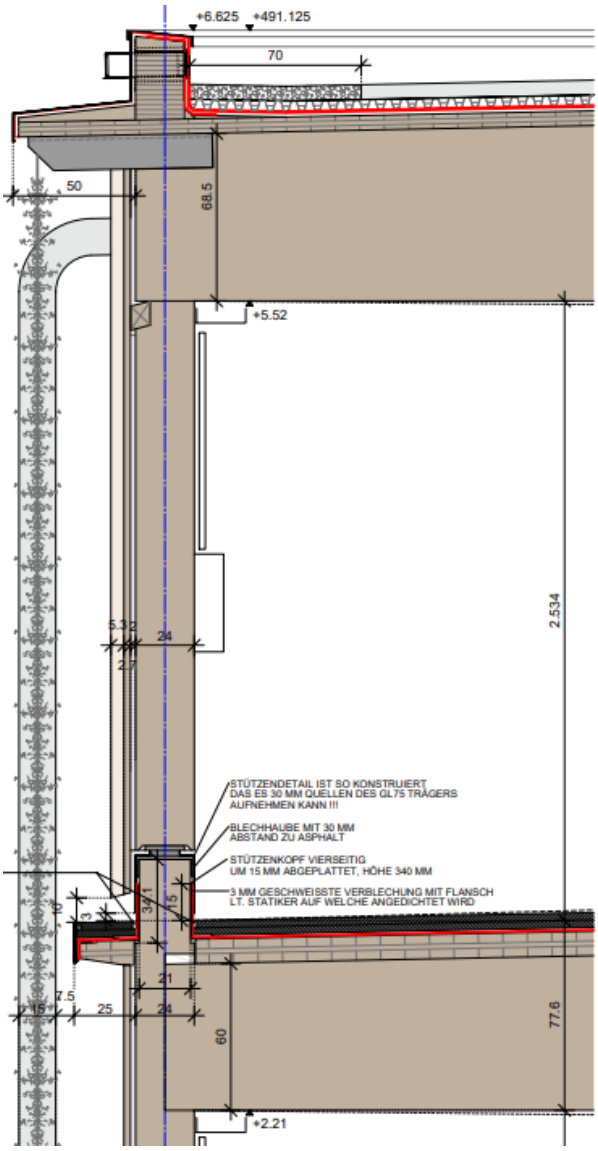

Figure A-33: Beams-to-column connection

Floor system:

- The floor system consists of a 100 mm thick CLT element. On top is a sealing and separation layer, plus 70 mm of mastic asphalt. This system corresponds with the shown layout in Figure A-14, but the dimensions differ slightly.

Connections:

- The foundation-to-column connection is made by a steel element plus dowels. See Figure A-34.
- A steel element plus dowels are used between the columns, shown in Figure A-35.
- The timber beam on the first level is connected to the column by a carpentry joint with most probably extra secureness. This joint is shown in Figures A-33 and A-37.
- On the second level, the beam rests on top of the column and is probably extra secured. Figure A-36 shows this connection.

Figure A-34: Connection foundation to column (*B&O Wooden Multi-Storey Car Park, Bad Aibling*, n.d.)

Figure A-35: Connection between columns (*B&O Wooden Multi-Storey Car Park, Bad Aibling*, n.d.)

Figure A-36: Connection between timber beam and column level 2 (*B&O Wooden Multi-Storey Car Park, Bad Aibling*, n.d.)

Figure A-37: Connection between timber beam and column level 1 (*B&O Wooden Multi-Storey Car Park, Bad Aibling*, n.d.)

A.5: Car park design Pollmeier and TUMWood

The final timber car park is only a concept made by Pollmeier and TUMWood. (*Development of Construction System for Multi-Storey Car Parks in BauBuche*, n.d.)

General info:

- The design uses a grid of 2.5 meters by 16.5 meters, shown in Figure A-38.
- All timber elements are coated to give protection against moisture, and a roof is designed to protect the upper level against moisture.
- The fire safety of this car park is focused on limiting the fire spread to achieve a fast extinguishing potential. For example, the concrete floor acts as a barrier, and there are no cavities in the timber elements. So, only a low number of elements will be affected by the fire. The columns are most probably designed to resist the fire loads after the required fire resistance time to prevent progressive collapse.

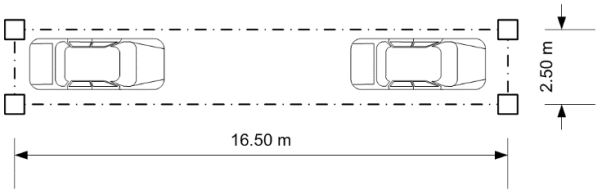

Figure A-38: Grid car park

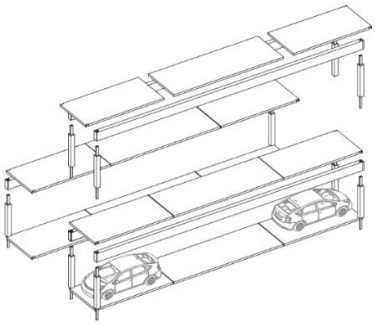

Figure A-39: Load-bearing elements of the modules (*Development of Construction System for Multi-Storey Car Parks in BauBuche*, n.d.)

Load-bearing structure:

- The modules are made of beams and posts in BauBuche GL75, visualized in Figure A-39. A 240 mm x 600 mm cross-section is used for the beams, and the posts are 240 mm x 240 mm. Those beams span 16.5 meters in the longitudinal direction.
- Stability is created in the transverse direction by the stairwell walls of reinforced concrete. In the longitudinal direction, diagonal steel elements are used to create stability.

Floor system:

- The floor is made of prefabricated reinforced concrete panels on top of the load-bearing timber beams. Those panels have a thickness of 130 mm, as shown in Figures A-39, A-40, and A-41. They extend across the entire floor.

Figure A-40: Inside render of the car park (*Development of Construction System for Multi-Storey Car Parks in BauBuche*, n.d.)

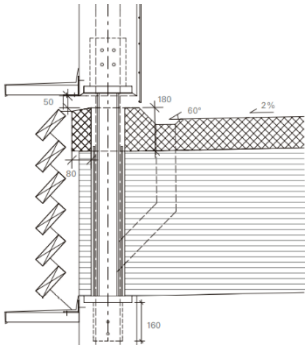

Figure A-41: Connection of the beam and floor to column (*Development of Construction System for Multi-Storey Car Parks in BauBuche*, n.d.)

Connection:

- A connection with birdsmouth joints is used between the timber beams and prefab concrete slab to form a rigid structure. On the ramps, extra secureness is created by screws.
- Hollow steel profiles make the connection between the posts slotted into each other. Subsequently, the joint is secured with low-shrinkage expansive mortar and dowels.
  These hollow steel profiles go through the timber beam and concrete slab. This connection is visualized in Figures A-41 and A-42.

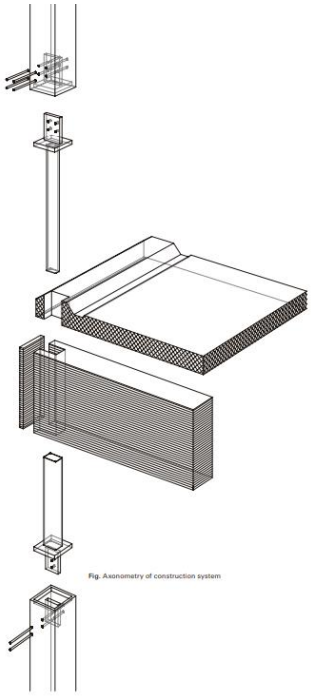

Figure A-42: Connection beam and slab to column (*Development of Construction System for Multi-Storey Car Parks in BauBuche*, n.d.)

B: Addition requirements and material properties

All additional important requirements and the introduction of the timber material properties are given in this Appendix.

B.1: Additional general requirements

The National Annex of Eurocode 1990 provides the following requirements. (NEN-EN 1990+A1+A1/C2/NB, 2019)

- Category F gives ψ-factors are ψ_0 is 0.7, ψ_1 is 0.7, and ψ_2 is 0.6, as stated in Table NB.2. In addition, for snow and wind loads ψ_0 is 0, ψ_1 is 0.2, and ψ_2 is 0.
- Equation B.1 should be used to calculate the ULS design load, and equation B.2 to determine the SLS design load.

$$\gamma_g * G_k + \gamma_Q * Q_{1,k} + \Sigma\, \gamma_{Q,i} * \psi_{0,i} * Q_{i,k} \quad \text{(B.1)}$$

$$G_k + \psi_{1,1} * \ Q_{1,k} + \Sigma\, \psi_{2,i} * Q_{i,k} \quad \text{(B.2)}$$

- Table B-1 shows the possible values of the factors using CC2, as stated in paragraph 5.2.

Table B-1: Partial safety factors

Factor	Value
γ_g *favorable*	0.9
γ_g *unfavorable*	1.2
γ_Q *favorable*	0
γ_Q *unfavorable*	1.5

The National Annex of Eurocode 1991 provides the loads corresponding to a car park. (NEN-EN 1991-1-1+C1+C11/NB, 2019)

- For a car weight of less than 25 kN, a static 10 kN horizontal braking force must be applied.

From the National Annex of the Eurocode 1991-1-3, it can be concluded that no additional snow loads should be taken into account during the design phase. (NEN-EN 1991-1-3+C1+A1/NB, 2019)

National Annex of the Eurocode 1991-1-4 provides the requirements for wind load calculations. (NEN-EN 1991-1-4+A1+C2/NB+C1, 2020)

- The red box in Table B-2 shows the applicable loads based on the defined location in paragraph 5.1. These loads should be multiplied by coefficients based on the layout of the façade and roof. For designing the main load-bearing elements factor $c_{pe,10}$ should be applied instead of $c_{pe,1}$ for elements with an area smaller than 1 m^2. Next, the values provided in Table B-3 correspond to the façade and in Table B-4 to this research's roof or floor element. (NEN-EN 1991-1-4+A1+C2, 2011).

Table B-2: Wind loads [kN/m2] (NEN-EN 1991-1-4+A1+C2/NB+C1, 2020)

Hoogte	Gebied I			Gebied II			Gebied III	
m	Kust	Onbebouwd	Bebouwd	Kust	Onbebouwd	Bebouwd	Onbebouwd	Bebouwd
1	0,93	0,71	0,69	0,78	0,60	0,58	0,49	0,48
2	1,11	0,71	0,69	0,93	0,60	0,58	0,49	0,48
3	1,22	0,71	0,69	1,02	0,60	0,58	0,49	0,48
4	1,30	0,71	0,69	1,09	0,60	0,58	0,49	0,48
5	1,37	0,78	0,69	1,14	0,66	0,58	0,54	0,48
6	1,42	0,84	0,69	1,19	0,71	0,58	0,58	0,48
7	1,47	0,89	0,69	1,23	0,75	0,58	0,62	0,48
8	1,51	0,94	0,73	1,26	0,79	0,62	0,65	0,51
9	1,55	0,98	0,77	1,29	0,82	0,65	0,68	0,53
10	1,58	1,02	0,81	1,32	0,85	0,68	0,70	0,56
15	1,71	1,16	0,96	1,43	0,98	0,80	0,80	0,66
20	1,80	1,27	1,07	1,51	1,07	0,90	0,88	0,74

Table B-3: Cpe-factors façade rectangular floor plan from Table NB.6 – 7.1 (NEN-EN 1991-1-4+A1+C2/NB+C1, 2020)

Zone	A		B		C		D		E	
h/d	$C_{pe,10}$	$C_{pe,1}$	$C_{pe,10}$	$C_{pe,1}$	$C_{pe,10}$	$C_{pe,1}$	$C_{pe,10}$	$C_{pe,1}$	$C_{pe,10}$	$C_{pe,1}$
5	−1,2	−1,4	−0,8	−1,1	−0,5		+0,8	+1,0	−0,7	
≤ 1	−1,2	−1,4	−0,8	−1,1	−0,5		+0,8	+1,0	−0,5	

Table B-4: Cpe- factors open roof from Table 7.6 (NEN-EN 1991-1-4+A1+C2, 2011)

Dakhelling α	Blokkering φ	Globale kracht-coëfficiënten c_f	Zone A	Zone B	Zone C
0°	Maximaal voor alle φ	+ 0,2	+ 0,5	+ 1,8	+ 1,1
	Minimaal voor $\varphi = 0$	- 0,5	- 0,6	- 1,3	- 1,4
	Minimaal voor $\varphi = 1$	- 1,3	- 1,5	- 1,8	- 2,2
5°	Maximaal voor alle φ	+ 0,4	+ 0,8	+ 2,1	+ 1,3
	Minimaal voor $\varphi = 0$	- 0,7	- 1,1	- 1,7	- 1,8
	Minimaal voor $\varphi = 1$	- 1,4	- 1,6	- 2,2	- 2,5
10°	Maximaal voor alle φ	+ 0,5	+ 1,2	+ 2,4	+ 1,6
	Minimaal voor $\varphi = 0$	- 0,9	- 1,5	- 2,0	- 2,1
	Minimaal voor $\varphi = 1$	- 1,4	- 1,6	- 2,6	- 2,7
15°	Maximaal voor alle φ	+ 0,7	+ 1,4	+ 2,7	+ 1,8
	Minimaal voor $\varphi = 0$	- 1,1	- 1,8	- 2,4	- 2,5
	Minimaal voor $\varphi = 1$	- 1,4	- 1,6	- 2,9	- 3,0
20°	Maximaal voor alle φ	+ 0,8	+ 1,7	+ 2,9	+ 2,1
	Minimaal voor $\varphi = 0$	- 1,3	- 2,2	- 2,8	- 2,9
	Minimaal voor $\varphi = 1$	- 1,4	- 1,6	- 2,9	- 3,0
25°	Maximaal voor alle φ	+ 1,0	+ 2,0	+ 3,1	+ 2,3
	Minimaal voor $\varphi = 0$	- 1,6	- 2,6	- 3,2	- 3,2
	Minimaal voor $\varphi = 1$	- 1,4	- 1,5	- 2,5	- 2,8
30°	Maximaal voor alle φ	+ 1,2	+ 2,2	+ 3,2	+ 2,4
	Minimaal voor $\varphi = 0$	- 1,8	- 3,0	- 3,8	- 3,6
	Minimaal voor $\varphi = 1$	- 1,4	- 1,5	- 2,2	- 2,7
OPMERKING Positieve waarden duiden op een netto neerwaartse windbelasting, negatieve waarden duiden op een netto opwaartse windbelasting.					

Below, the needed requirements based on the impact loads and explosions are listed. Based on Eurocode 1991-1-7 and the corresponding national annex. (NEN-EN 1991-1-7+C1+A1, 2015; NEN-EN 1991-1-7+C1+A1/NB, 2019)

- Requirements about explosions need not be included.

The car park layout requirements are provided below. (NEN 2443, 2013)

- The minimum width of a one-way driving lane is 2.75 meters, and in two directions, it is 5.5 meters.
- For 70 degrees parking, the column-free zone at the end of the parking lot must be determined by a line perpendicular to the parking lot. From the point where this line intersects with the edge of the parking lot, a tolerance of 0.5 meters must be assumed.
- To ensure sufficient water run-off towards the drainage. The floor must have a minimum slope of 5 mm per meter. Meaning a gradient of 0.5 per cent or 0.29 degrees. But BNPC uses a steeper slope of 10 mm per meter.
- Columns must be located at an extra distance of 0.15 meters from the parking lot if positioned within 0.5 meters from the driving lane or more than 1.5 meters from the driving lane. If columns are on both sides of the parking lot, an extra tolerance of 0.35 meters must be applied.
- The maximum protrusion of a column is 0.5 meters at the end of the parking lot, which does not function as an entrance.
- Between two parking lots in the longitudinal, the maximum protrusion of a column is 0.2 meters in length and width.
- The view lines through the car park must be open, and hidden spaces must be prevented to ensure social safety.

All requirements based on the use of timber are discussed below.

- The structural timber belongs to a reaction to fire class D-s2,d0. This class is also valid for glulam elements. (NEN-EN 14081-1+A1, 2019) (NEN-EN 14080, 2013)
- The deviation in straightness for elements laterally supported at distance L should be maximal L/500 for laminated elements or LVL and L/300 for the other elements. (NEN-EN 1995-1-1+C1+A1, 2011)
- For timber floors, a damping factor of 0.01 must be used. (NEN-EN 1995-1-1+C1+A1, 2011)
- Non-separating load-bearing elements should be designed for fire influence from both sides. (NEN-EN 1995-1-2+C2, 2011)

For concrete, the global deflection limit is L/250 (NEN-EN 1992-1-1+C2, 2011)

Below, the requirements for an open car park are listed based on NEN 2443 (NEN 2443, 2013).

- At least two opposite walls must have non-closing openings.
- The façades of at least two with non-closing openings must be located at a maximum distance of 54 meters.
- The lowest floor should be placed less than 1.3 meters below ground level.
- At least one of the following requirements must be met.
    - The minimum non-closing openings must be 1/3 of the total façade area of that compartment.
    - The total non-closing opening area in each of the walls must be at least 2.5% of the gross floor area of that compartment.
- Openings are assumed to be open if the distance to adjacent buildings at these openings is at least 5 meters.

B.2: Timber material properties

Besides the functional requirements, timber material properties-related aspects should be known. These properties are discussed below based on NEN-EN 1995-1-1. (NEN-EN 1995-1-1+C1+A1, 2011)

- Factor k_{mod} must be included in the calculations for the strength design value, shown in equation B.3. This factor includes the influence of the load duration and moisture content.

$$X_d = k_{mod} * \frac{X_k}{\gamma_m} \quad \text{(B.3)}$$

  The value of k_{mod} depends on the type of timber, service class, and load duration class. Table B-5 shows these values.
- Factor k_{def} includes the creep deformation based on the service class. This factor should be used in the calculation step to go from the initial deflection to the final deflection, presented in equations B.4 to B.7. The values of k_{def} are given in Table B-6 below.

$$u_{fin}[mm] = u_{fin,G}[mm] + u_{fin,Q1}[mm] + \Sigma u_{fin,Qi}[mm] \quad \text{(B.4)}$$

$$u_{fin,G}[mm] = u_{inst,G}[mm](1 + k_{def}) \quad \text{(B.5)}$$

$$u_{fin,Q,1}[mm] = u_{inst,Q,1}[mm](1 + \psi_{2,1}k_{def}) \quad \text{(B.6)}$$

$$u_{fin,Q,i}[mm] = u_{inst,Q,i}[mm](\psi_0 + \psi_{2,1}k_{def}) \quad \text{(B.7)}$$

Table B-5: Values k_{mod} (NEN-EN 1995-1-1+C1+A1, 2011)

Materiaal	Norm	Klimaat-klasse	Belastingsduurklasse				
			Blijvend	Lang	Middellang	Kort	Zeer kort
Gezaagd hout	EN 14081-1	1	0,60	0,70	0,80	0,90	1,10
		2	0,60	0,70	0,80	0,90	1,10
		3	0,50	0,55	0,65	0,70	0,90
Gelijmd gelamineerd hout	EN 14080	1	0,60	0,70	0,80	0,90	1,10
		2	0,60	0,70	0,80	0,90	1,10
		3	0,50	0,55	0,65	0,70	0,90
LVL	EN 14374, EN 14279	1	0,60	0,70	0,80	0,90	1,10
		2	0,60	0,70	0,80	0,90	1,10
		3	0,50	0,55	0,65	0,70	0,90
Multiplex	EN 636						
	Type EN 636-1	1	0,60	0,70	0,80	0,90	1,10
	Type EN 636-2	2	0,60	0,70	0,80	0,90	1,10
	Type EN 636-3	3	0,50	0,55	0,65	0,70	0,90
OSB	EN 300						
	OSB/2	1	0,30	0,45	0,65	0,85	1,10
	OSB/3, OSB/4	1	0,40	0,50	0,70	0,90	1,10
	OSB/3, OSB/4	2	0,30	0,40	0,55	0,70	0,90
Spaanplaat	EN 312						
	Type P4, Type P5	1	0,30	0,45	0,65	0,85	1,10
	Type P5	2	0,20	0,30	0,45	0,60	0,80
	Type P6, Type P7	1	0,40	0,50	0,70	0,90	1,10
	Type P7	2	0,30	0,40	0,55	0,70	0,90
Vezelplaat, hard	EN 622-2						
	HB.LA, HB.HLA 1 of 2	1	0,30	0,45	0,65	0,85	1,10
	HB.HLA1 or 2	2	0,20	0,30	0,45	0,60	0,80
Vezelplaat, medium	EN 622-3						
	MBH.LA1 of 2	1	0,20	0,40	0,60	0,80	1,10
	MBH.HLS1 of 2	1	0,20	0,40	0,60	0,80	1,10
	MBH.HLS1 of 2	2	–	–	–	0,45	0,80
Vezelplaat, MDF	EN 622-5						
	MDF.LA, MDF.HLS	1	0,20	0,40	0,60	0,80	1,10
	MDF.HLS	2	–	–	–	0,45	0,80

Table B-6: Values k_{def} (NEN-EN 1995-1-1+C1+A1, 2011)

Materiaal	Norm	Klimaatklasse		
		1	2	3
Gezaagd hout	EN 14081-1	0,60	0,80	2,00
Gelijmd gelamineerd hout	EN 14080	0,60	0,80	2,00
LVL	EN 14374, EN 14279	0,60	0,80	2,00
Multiplex	EN 636			
	Type EN 363-1	0,80	–	–
	Type EN 363-2	0,80	1,00	–
	Type EN 363-3	0,80	1,00	2,50
OSB	EN 300			
	OSB/2	2,25	–	–
	OSB/3, OSB/4	1,50	2,25	–
Spaanplaat	EN 312			
	Type P4	2,25	–	–
	Type P5	2,25	3,00	–
	Type P6	1,50	–	–
	Type P7	1,50	2,25	–
Vezelplaat, hard	EN 622-2			
	HB.LA	2,25	–	–
	HB.HLA1, HB.HLA2	2,25	3,00	–
Vezelplaat, medium	EN 622-3			
	MBH.LA1, MBH.LA2	3,00	–	–
	MBH.HLS1, MBH.HLS2	3,00	4,00	–
Vezelplaat, MDF	EN 622-5			
	MDF.LA	2,25	–	–
	MDF.HLS	2,25	3,00	–

- The material factor γ_m is 1.3 for sawn timber and connections, 1.25 for laminated timber, 1.2 for LVL, and 1.3 for joints.
- Tables B-7 to B-10 show the strength classes of timber for respectively glued laminated timber, softwood, hardwood, and LVL.

Table B-7: Values strength classes glued laminated timber (NEN-EN 14080, 2013)

Property	Symbol	Glulam strength class						
		GL 20h	GL 22h	GL 24h	GL 26h	GL 28h	GL 30h	GL 32h
Bending strength	$f_{m,g,k}$	20	22	24	26	28	30	32
Tensile strength	$f_{t,0,g,k}$	16	17,6	19,2	20,8	22,3	24	25,6
	$f_{t,90,g,k}$	0,5						
Compression strength	$f_{c,0,g,k}$	20	22	24	26	28	30	32
	$f_{c,90,g,k}$	2,5						
Shear strength (shear and torsion)	$f_{v,g,k}$	3,5						
Rolling shear strength	$f_{r,g,k}$	1,2						
Modulus of elasticity	$E_{0,g,mean}$	8 400	10 500	11 500	12 100	12 600	13 600	14 200
	$E_{0,g,05}$	7 000	8 800	9 600	10 100	10 500	11 300	11 800
	$E_{90,g,mean}$	300						
	$E_{90,g,05}$	250						
Shear modulus	$G_{g,mean}$	650						
	$G_{g,05}$	540						
Rolling shear modulus	$G_{r,g,mean}$	65						
	$G_{r,g,05}$	54						
Density	$\rho_{g,k}$	340	370	385	405	425	430	440
	$\rho_{g,mean}$	370	410	420	445	460	480	490

Table B-8: Values strength classes softwood (NEN-EN 338, 2016)

	Class	C14	**C16**	**C18**	C20	C22	**C24**	C27	**C30**	C35	C40	C45	C50
Strength properties in N/mm²													
Bending	$f_{m,k}$	14	**16**	**18**	20	22	**24**	27	**30**	35	40	45	50
Tension parallel	$f_{t,0,k}$	7,2	**8,5**	**10**	11,5	13	**14,5**	16,5	**19**	22,5	26	30	33,5
Tension perpendicular	$f_{t,90,k}$	0,4	**0,4**	**0,4**	0,4	0,4	**0,4**	0,4	**0,4**	0,4	0,4	0,4	0,4
Compression parallel	$f_{c,0,k}$	16	**17**	**18**	19	20	**21**	22	**24**	25	27	29	30
Compression perpendicular	$f_{c,90,k}$	2,0	**2,2**	**2,2**	2,3	2,4	**2,5**	2,5	**2,7**	2,7	2,8	2,9	3,0
Shear	$f_{v,k}$	3,0	**3,2**	**3,4**	3,6	3,8	**4,0**	4,0	**4,0**	4,0	4,0	4,0	4,0
Stiffness properties in kN/mm²													
Mean modulus of elasticity parallel bending	$E_{m,0,mean}$	7,0	**8,0**	**9,0**	9,5	10,0	**11,0**	11,5	**12,0**	13,0	14,0	15,0	16,0
5 percentile modulus of elasticity parallel bending	$E_{m,0,k}$	4,7	**5,4**	**6,0**	6,4	6,7	**7,4**	7,7	**8,0**	8,7	9,4	10,1	10,7
Mean modulus of elasticity perpendicular	$E_{m,90,mean}$	0,23	**0,27**	**0,30**	0,32	0,33	**0,37**	0,38	**0,40**	0,43	0,47	0,50	0,53
Mean shear modulus	G_{mean}	0,44	**0,50**	**0,56**	0,59	0,63	**0,69**	0,72	**0,75**	0,81	0,88	0,94	1,00
Density in kg/m³													
5 percentile density	ρ_k	290	**310**	**320**	330	340	**350**	360	**380**	390	400	410	430
Mean density	ρ_{mean}	350	**370**	**380**	400	410	**420**	430	**460**	470	480	490	520

NOTE 1 Values given above for tension strength, compression strength, shear strength, char. modulus of elasticity in bending, mean modulus of elasticity perpendicular to grain and mean shear modulus have been calculated using the equations given in EN 384.

NOTE 2 The tension strength values are conservatively estimated since grading is done for bending strength.

NOTE 3 The tabulated properties are compatible with timber at moisture content consistent with a temperature of 20 °C and a relative humidity of 65 %, which corresponds to a moisture content of 12 % for most species.

NOTE 4 Characteristic values for shear strength are given for timber without fissures, according to EN 408.

NOTE 5 These classes may also be used for hardwoods with similar strength and density profiles such as e.g. poplar or chestnut.

NOTE 6 The edgewise bending strength may also be used in the case of flatwise bending.

Table B-9: Values strength classes hardwood (NEN-EN 338, 2016)

	Class	D18	D24	D27	D30	D35	D40	D45	D50	D55	D60	D65	D70	D75	D80
Strength properties in N/mm²															
Bending	$f_{m,k}$	18	**24**	27	**30**	35	**40**	45	**50**	55	**60**	65	**70**	75	80
Tension parallel	$f_{t,0,k}$	11	**14**	16	**18**	21	**24**	27	**30**	33	**36**	39	**42**	45	48
Tension perpendicular	$f_{t,90,k}$	0,6	**0,6**	0,6	**0,6**	0,6	**0,6**	0,6	**0,6**	0,6	**0,6**	0,6	**0,6**	0,6	0,6
Compression parallel	$f_{c,0,k}$	18	**21**	22	**24**	25	**27**	29	**30**	32	**33**	35	**36**	37	38
Compression perpendicular	$f_{c,90,k}$	4,8	**4,9**	5,1	**5,3**	5,4	**5,5**	5,8	**6,2**	6,6	**10,5**	11,3	**12,0**	12,8	13,5
Shear	$f_{v,k}$	3,5	**3,7**	3,8	**3,9**	4,1	**4,2**	4,4	**4,5**	4,7	**4,8**	5,0	**5,0**	5,0	5,0
Stiffness properties in kN/mm²															
Mean modulus of elasticity parallel bending	$E_{m,0,mean}$	9,5	**10,0**	10,5	**11,0**	12,0	**13,0**	13,5	**14,0**	15,5	**17,0**	18,5	**20,0**	22,0	24,0
5 percentile modulus of elasticity parallel bending	$E_{m,0,k}$	8,0	**8,4**	8,8	**9,2**	10,1	**10,9**	11,3	**11,8**	13,0	**14,3**	15,5	**16,8**	18,5	20,2
Mean modulus of elasticity perpendicular	$E_{m,90,mean}$	0,63	**0,67**	0,70	**0,73**	0,80	**0,87**	0,90	**0,93**	1,03	**1,13**	1,23	**1,33**	1,47	1,60
Mean shear modulus	G_{mean}	0,59	**0,63**	0,66	**0,69**	0,75	**0,81**	0,84	**0,88**	0,97	**1,06**	1,16	**1,25**	1,38	1,50
Density in kg/m³															
5 percentile density	ρ_k	475	**485**	510	**530**	540	**550**	580	**620**	660	**700**	750	**800**	850	900
Mean density	ρ_{mean}	570	**580**	610	**640**	650	**660**	700	**740**	790	**840**	900	**960**	1020	1080

NOTE 1 Values given above for tension strength, compression strength, shear strength, char. modulus of elasticity in bending, mean modulus of elasticity perpendicular to grain and mean shear modulus, have been calculated using the equations given in EN 384.

NOTE 2 The tabulated properties are compatible with timber at moisture content consistent with a temperature of 20 °C and a relative humidity of 65 %, which corresponds to a moisture content of 12 % for most species.

NOTE 3 Characteristic values for shear strength are given for timber without fissures, according to EN 408.

NOTE 4 The edgewise bending strength may also be used in the case of flatwise bending.

Table B-10: Values strength classes LVL (*Laminated Veneer Lumber (LVL) Bulletin; New European Strength Classes*, 2019)

Table 2:
Strength class for LVL without crossband veneers (LVL-P)

	Property [a]	Symbol	Unit	Strength class LVL 32 P	LVL 35 P	LVL 48 P	LVL 50 P	LVL 80 P
Bending strength	Edgewise, parallel to grain (depth 300 mm)	$f_{m,0,edge,k}$	N/mm²	27	30	44	46	75
	Flatwise, parallel to grain	$f_{m,0,flat,k}$	N/mm²	32	35	48	50	80
	Size effect parameter	s	–	0,15	0,15	0,15	0,15	0,15
Tension strength	Parallel to grain (length 3 000 mm)	$f_{t,0,k}$	N/mm²	22	22	35	36	60
	Perpendicular to grain, edgewise	$f_{t,90,edge,k}$	N/mm²	0,5	0,5	0,8	0,9	1,5
Compression strength	Parallel to grain for service class 1	$f_{c,0,k}$	N/mm²	26	30	35	42	69
	Parallel to grain for service class 2 [b]	$f_{c,0,k}$	N/mm²	21	25	29	35	57
	Perpendicular to grain, edgewise	$f_{c,90,edge,k}$	N/mm²	4	6	6	8,5	14
	Perpendicular to grain, flatwise (except pine)	$f_{c,90,flat,k}$	N/mm²	0,8	2,2	2,2	3,5	12
	Perpendicular to grain, flatwise, pine	$f_{c,90,flat,k,pine}$	N/mm²	MDV [c]	3,3	3,3	3,5	– [d]
Shear strength	Edgewise parallel to grain	$f_{v,0,edge,k}$	N/mm²	3,2	3,2	4,2	4,8	8
	Flatwise, parallel to grain	$f_{v,0,flat,k}$	N/mm²	2,0	2,3	2,3	3,2	8
Modulus of elasticity	Parallel to grain	$E_{0,mean}$ [e]	N/mm²	9 600	12 000	13 800	15 200	16 800
	Parallel to grain	$E_{0,k}$ [f]	N/mm²	8 000	10 000	11 600	12 600	14 900
	Perpendicular to grain, edgewise	$E_{c,90,edge,mean}$ [g]	N/mm²	MDV [c]	MDV [c]	430	430	470
	Perpendicular to grain, edgewise	$E_{c,90,edge,k}$ [h]	N/mm²	MDV [c]	MDV [c]	350	350	400
Shear modulus	Edgewise, parallel to grain	$G_{0,edge,mean}$	N/mm²	500 [i]	500 [i]	600	650	760
	Edgewise, parallel to grain	$G_{0,edge,k}$	N/mm²	300 [i]	350 [i]	400	450	630
	Flatwise, parallel to grain	$G_{0,flat,mean}$	N/mm²	320 [i]	380 [i]	380	600	850
	Flatwise, parallel to grain	$G_{0,flat,k}$	N/mm²	240 [i]	270 [i]	270	400	760
Density		ρ_{mean}	kg/m³	440	510	510	580	800
		ρ_k	kg/m³	410	480	480	550	730

The use classes (hazard classes) are shown in Table B-11 to determine the required timber species. Table B-12 gives the relationship between the use class (hazard class) and the appropriate durability classes. Subsequently, Table B-13 shows the link between the use and service class.

Table B-11: Use classes (NEN-EN 335, 2013)

Use class	General use situation [a]	Occurrence of biological agents [b, c]				
		Disfiguring fungi	Wood-destroying fungi	Beetles	Termites	Marine borers
1	Interior, dry	-	-	U	L	-
2	Interior, or under cover, not exposed to the weather. Possibility of water condensation	U	U	U	L	-
3	Exterior, above ground, exposed to the weather. When sub-divided: **3.1** limited wetting conditions **3.2** prolonged wetting conditions	U	U	U	L	-
4	Exterior in ground contact and/or fresh water	U	U	U	L	-
5	Permanently or regularly submerged in salt water	U[d]	U[d]	U[d]	L[d]	U

U = ubiquitous in Europe and EU territories
L = locally present in Europe and EU territories

[a] Border line and extreme cases of use of wood and wood-based products exist. This can cause the assignment of a use class that differs from that defined in this standard (see Annex B).

[b] It may not be necessary to protect against all biological agents listed as they may not be present or economically significant in all service conditions in all geographic regions, or may not be able to attack some wood-based products due to the specific constitution of the product.

[c] See Annex C.

[d] The above water portion of certain components can be exposed to all of the above biological agents.

Table B-12: Relationship use (hazard) class and durability class (NEN-EN 460, 1994)

Hazard class	Durability class				
	1	2	3	4	5
1	o	o	o	o	o
2	o	o	o	(o)	(o)
3	o	o	(o)	(o) — (x)	(o) — (x)
4	o	(o)	(x)	x	x
5	o	(x)	(x)	x	x

Key

o	natural durability sufficient.
(o)	natural durability is normally sufficient, but for certain end uses treatment may be advisable (see annex A).
(o) — (x)	natural durability may be sufficient, but depending on the wood species, its permeability (see **6.1**), and end use (see annex A), preservative treatment may be necessary.
(x)	preservative treatment is normally advisable, but for certain end uses natural durability may be sufficient (see annex A).
x	preservative treatment necessary.

NOTE. Sapwood of all wood species should be regarded as durability class 5.

Table B-13: Correlation service class and use class (NEN-EN 335, 2013)

Service class according to EN 1995-1-1	Possible corresponding use class according to EN 335:2012
Service class 1	Use class 1
Service class 2	Use class 1 Use class 2 if the component is in a situation where it could be subjected to occasional wetting caused by e.g. condensation
Service class 3	Use class 2 Use class 3 or higher if used externally

There are two parts to consider in calculating fire's effect on timber performance. First, adjust the required strength ($f_{d,fi}$) and stiffness ($S_{d,fi}$) shown in the following two equations B.8 and B.9. Second, determine the charring depth discussed later.

- In equations B.8 and B.9 below, parameter f_{20} and S_{20} means the 20%-fractional value of the strength and stiffness at room temperature. Also, a different specific fire modification ($k_{mod,fi}$) and material factor ($\gamma_{m,fi}$) should be used with the following values in the preliminary design phase of Table B-14.

Table B-14: Values parameters fire strength adjustment (NEN-EN 1995-1-2+C2, 2011)

$k_{mod,fi}$	1
$\gamma_{m,fi}$	1

$$f_{d,fi}[MPa] = k_{mod,fi} * \frac{f_{20}[MPa]}{\gamma_{m,fi}} \quad \text{(B.8)}$$

$$S_{d,fi}[MPa] = k_{mod,fi} * \frac{S_{20}[MPa]}{\gamma_{m,fi}} \quad \text{(B.9)}$$

- The 20%-fractional value of the strength and stiffness must be determined by multiplying the regular strength and stiffness by factor k_{fi}, as shown in equations B.10 and B.11. The value of this factor depends on the type of timber used, as provided in Table B-15. (NEN-EN 1995-1-2+C2, 2011)

$$f_{20}[MPa] = k_{fi} * f_k[MPa] \quad \text{(B.10)}$$

$$S_{20}[MPa] = k_{fi} * S_{05}[MPa] \quad \text{(B.11)}$$

Table B-15: k_{fi} factors (NEN-EN 1995-1-2+C2, 2011)

Gezaagd hout	1,25
Gelijmd gelamineerd hout	1,15
Houtachtige plaatmaterialen	1,15
LVL	1,1
Verbindingen met verbindingsmiddelen, op afschuiving belast, met koppelplaten van hout of houtachtig plaatmateriaal	1,15
Verbindingen met verbindingsmiddelen, op afschuiving belast, met koppelplaten van staal	1,05
Verbindingen met op trek belaste verbindingen	1,05

In addition, the partial safety factors γ_g and γ_Q are 1, and the variable loads should be multiplied by ψ_1 or ψ_2, given in this paragraph. Equation B.12 show the formula from Eurocode 1990 for an accidental situation (NEN-EN 1990+A1+A1/C2, 2019). Parameter P and A_d can be neglected because no prestressing is present, and A_d is covered in the charring rate.

$$\Sigma G_{k,j}"+"P"+"A_d" + "(\psi_{1,1} \; or \; \psi_{2,1}) * Q_{k1}" + "\Sigma\psi_{2,i} * Q_{ki} \quad \text{(B.12)}$$

As mentioned, the charring of the timber surface should also be considered from 300°C. This charring process will lead to a reduced effective cross-section, calculated by one of the following equations B.13 and B.14. In which $d_{char,0}$ means the one-dimensional charring depth and $d_{char,n}$ means the notional charring depth, which includes the effects of corners and cracks. (NEN-EN 1995-1-2+C2, 2011)

$$d_{char,0}[mm] = \beta_0[\frac{mm}{min}] * t[min] \quad \text{(B.13)}$$

$$d_{char,n}[mm] = \beta_n[\frac{mm}{min}] * t[min] \quad \text{(B.14)}$$

- The charring rate factors β_0 and β_n depend on the type of wood, density, and if the element is laminated. The values are shown in Table B-16 for a standard fire curve.

Table B-16: Charring rate factors (NEN-EN 1995-1-2+C2, 2011)

	β_0 mm/min	β_n mm/min
a) Naaldhout en beuken		
Gelijmd gelamineerd hout met een karakteristieke volumieke massa van ≥ 290 kg/m³	0,65	0,7
Gezaagd hout met een karakteristieke volumieke massa van ≥ 290 kg/m³	0,65	0,8
b) Loofhout		
Gezaagd of gelijmd gelamineerd loofhout met een karakteristieke volumieke massa van 290 kg/m³	0,65	0,7
Gezaagd of gelijmd gelamineerd loofhout met een karakteristieke volumieke massa van ≥ 450 kg/m³	0,50	0,55
c) LVL		
met een karakteristieke volumieke massa van ≥ 480 kg/m³	0,65	0,7
d) Panelen		
Houten betimmering	0,9 [a]	–
Triplex	1,0 [a]	–
Houtachtige plaatmaterialen anders dan triplex	0,9 [a]	–

[a] De waarden gelden voor een karakteristieke volumieke massa van 450 kg/m³ en een plaatdikte van 20 mm; zie 3.4.2(9) voor andere diktes en volumieke massa's.

- The total reduced cross-section is the charring depth plus the heat-affected zone. This heat-affected zone must be determined by multiplying the factors k_0 and d_0, see equation B.15 Factor k_0 depends on the time, which has a value of 1 in case of an exposure longer than 20

minutes, necessary for this research based on the mentioned fire resistance in paragraph 5.3. Factor d_0 has a value of 7 mm. (NEN-EN 1995-1-2+C2, 2011)

$$HAZ[mm] = k_0[-] * d_0[mm] \quad \text{(B.15)}$$

- Concluded, the reduction of the cross-section is d_{ef}. This value is calculated for one exposed surface. In the case of more exposed surfaces, this cross-sectional reduction value (d_{ef}) should be applied to all exposed surfaces, as calculated by equation B.16.

$$d_{ef}[mm] = d_{char}[mm] + k_0[-] * d_0[mm] \quad \text{(B.16)}$$

Based on the "Bouwbesluit" (*Bouwbesluit 2012*, 2011), the fire classes corresponding to a building with a remaining use function are given in Table B-17.

Table B-17: Fire classes (*Bouwbesluit 2012*, 2011)

In contact with indoor air	**Fire Class**
Extra protected escape route	B
Protected escape route	D
Remaining	D
In contact with open air	**Fire class**
Extra protected escape route	C
Protected escape route	D
Remaining	D

B.3: Concrete design properties and requirements

This Appendix provides the properties to design a concrete floor element.

Table B-18 presents concrete strength classes with the corresponding strength and stiffness characteristics (NEN-EN 1992-1-1+C2, 2011).

Table B-18: Values strength classes concrete (NEN-EN 1992-1-1+C2, 2011)

Sterkteklassen voor beton														
f_{ck} (MPa)	12	16	20	25	30	35	40	45	50	55	60	70	80	90
$f_{ck,cube}$ (MPa)	15	20	25	30	37	45	50	55	60	67	75	85	95	105
f_{cm} (MPa)	20	24	28	33	38	43	48	53	58	63	68	78	88	98
f_{ctm} (MPa)	1,6	1,9	2,2	2,6	2,9	3,2	3,5	3,8	4,1	4,2	4,4	4,6	4,8	5,0
$f_{ctk,0,05}$ (MPa)	1,1	1,3	1,5	1,8	2,0	2,2	2,5	2,7	2,9	3,0	3,1	3,2	3,4	3,5
$f_{ctk,0,95}$ (MPa)	2,0	2,5	2,9	3,3	3,8	4,2	4,6	4,9	5,3	5,5	5,7	6,0	6,3	6,6
E_{cm} (GPa)	27	29	30	31	33	34	35	36	37	38	39	41	42	44
ε_{c1} (‰)	1,8	1,9	2,0	2,1	2,2	2,25	2,3	2,4	2,45	2,5	2,6	2,7	2,8	2,8
ε_{cu1} (‰)	3,5									3,2	3,0	2,8	2,8	2,8
ε_{c2} (‰)	2,0									2,2	2,3	2,4	2, 5	2,6
ε_{cu2} (‰)	3,5									3,1	2,9	2,7	2,6	2,6
n	2,0									1,75	1,6	1,45	1,4	1,4
ε_{c3} (‰)	1,75									1,8	1,9	2,0	2,2	2,3
ε_{cu3} (‰)	3,5									3,1	2,9	2,7	2,6	2,6

Eurocode 1991 states that the self-weight of concrete plus reinforcement is about 25 kN/m^3 (NEN-EN 1991-1-1+C1+C11, 2019).

In sub-paragraph 7.2.5.1, it is indicated that B500 reinforcing steel will be used because this is the most used reinforcing steel.
The modulus of elasticity of reinforcement steel is 200 GPa, and the corresponding partial safety factor is 1.15 (NEN-EN 1992-1-1+C2, 2011).
The yield strength of B500 reinforcement steel is 500 MPa (NEN 6008+A1, 2020), and applying the partial safety factor results in a design yield strength of 435 MPa.

Because the floor of an open car park is alternately dry and wet, subsequently de-icing salts can be present. Next, the assumed location of the car park (paragraph 5.1) is close to the sea. So, the corresponding environmental classes of a concrete car park floor element are XC3, XD3, XS1, and XF4. (NEN-EN 1992-1-1+C2, 2011).

The maximum crack width and the minimum concrete cover can be determined based on the environmental classes. Table B-18 presents the maximum crack width for the different environmental classes. The column of Table B-18 for no fixation should be used because the connections will not be monolithic. This non-monolithic connection is to ensure a re-mountable structure.
So, based on Table B-19, it can be concluded that 0.20 mm is the maximum crack width.

Table B-19: Maximum crack width requirements (NEN-EN 1992-1-1+C2/NB+A1, 2020)

Milieuklasse	Elementen met betonstaal en/of voorspanstaal zonder aanhechting	Elementen met een combinatie van betonstaal en voorspanstaal met aanhechting	Elementen met uitsluitend voorspanstaal met aanhechting
	Frequente belastingscombinatie	Frequente belastingscombinatie	Frequente belastingscombinatie
X0, XC1	$w_{max} \leq 0{,}40$ mm [a]	$w_{max} \leq 0{,}30$ mm	$\Delta\sigma_p \leq \xi$ 275 MPa
XC2, XC3, XC4	$w_{max} \leq 0{,}30$ mm	$w_{max} \leq 0{,}20$ mm	$\Delta\sigma_p \leq \xi$ 175 MPa
XD1, XD2, XD3, XS1, XS2, XS3	$w_{max} \leq 0{,}20$ mm	$w_{max} \leq 0{,}10$ mm	$\Delta\sigma_p \leq \xi$ 75 MPa
[a] Voor milieuklasse X0 en XC1 heeft de scheurwijdte geen invloed op de duurzaamheid; deze grens is gesteld om een in het algemeen aanvaardbaar uiterlijk te verkrijgen. Bij afwezigheid van voorwaarden ten aanzien van het uiterlijk mag deze beperking zijn afgezwakt.			

Equation B.17 presents the formula for the occurring crack width (NEN-EN 1992-1-1+C2, 2011). The parameters α, β, and τ_{bm} are listed in Table B-20. This table is provided by the concrete courses of the TU Delft Civil Engineering Bachelor and Master.

$$w_{\max}\,[mm] = \frac{1}{2} * \frac{f_{ctm}[MPa]}{\tau_{bm}[MPa]} * \frac{\emptyset[mm]}{\rho_{s,eff}[-]} * \frac{1}{E_s[MPa]} * (\sigma_s[MPa] - \alpha * \sigma_{sr}[MPa] + \beta * \varepsilon_{cs} * E_s[MPa]) \quad \text{(B.17)}$$

Table B-20: Values parameter equation maximum crack width

	crack formation stage	stabilised cracking stage
short term loading	$\alpha = 0{,}5$ $\beta = 0$ $\tau_{bm} = 2{,}0\, f_{ctm}$	$\alpha = 0{,}5$ $\beta = 0$ $\tau_{bm} = 2{,}0\, f_{ctm}$
long term or dynamic loading	$\alpha = 0{,}5$ $\beta = 0$ $\tau_{bm} = 1{,}6\, f_{ctm}$	$\alpha = 0{,}3$ $\beta = 1$ $\tau_{bm} = 2{,}0\, f_{ctm}$

C: Fire resistance assumption and Triflex test results

In Appendix C.1, the check of fire resistance assumption is given. Second, Appendix C.2 gives the coating bonding strength test results.

C.1: Comparison of a standard fire and local fire

Two possible options for a fire scenario in a car park are a local fire and a standard fire, as stated in sub-paragraph 5.3.1. It also states that a standard fire will be assumed because a local fire cannot be completely ensured. However, it should be checked that the assumption of a standard fire is conservative. This check is possible by comparing both scenarios' total fire energy for the indicated fire resistance in sub-paragraph 5.3.1. The total fire energy is the area below the firepower graph. The graphs with the firepower over time for both scenarios are shown below in Figures C-1 and C-2.

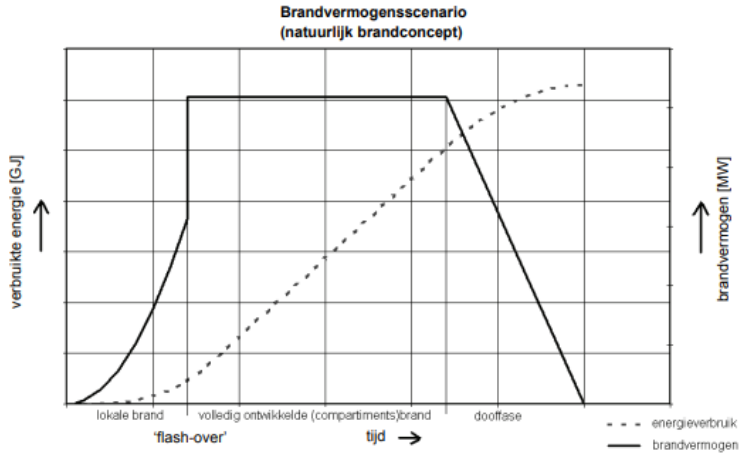

Figure C-1: Firepower standard fire scenario (NEN 6055, 2011)

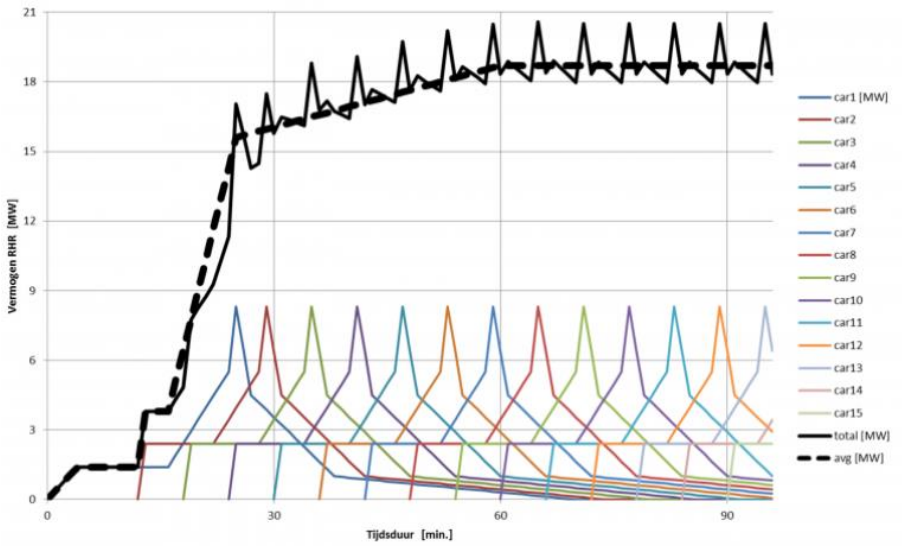

Figure C-2: Firepower local car fire (van Herpen, 2021)

Applying the Ozone software (Cadorin et al., 2018) can develop a firepower curve.
The following steps are necessary to produce a firepower curve: define compartment size, define compartment elements, and define a fire.

1) Define compartment

As stated in the starting points, the free height is assumed to be 2.2 meters. Combined with a beam height of about 1 meter, based on Table 4.1, it gives a total height of 3.2 meters. The maximum compartment area of the car park is assumed to be 50x56.78 m^2, shown in Figure 1-1. Table C.1 shows an overview of the compartment dimensions.

Table C-1: Model compartment dimensions

H	3.2 meters
L	50 meters
B	56.78 meters

2) Define compartment elements

The software provides fire characteristics for normal wood, as shown in Figure C-3. This material will be used for the floor, ceiling, and walls. Based on the reference car parks, a CLT floor has a thickness of about 120 mm. So, this thickness will also be assumed in the model for the floor and ceilings. Paragraph 5.3 mentions that there should be no walls inside the car park. So, the walls in this software are the façade elements. They have an opening of 33%, the minimum value based on Eurocode 2443 (NEN 2443, 2013). For a height of 3.2 meters, this is 1.07 meters. Figure C-4 shows how the opening is located in the façade, assuming the opening of the façade is in the middle.

Material	Thickness	Unit mass	Conductivity	Specific Heat	Rel Emissivity	Rel Emissivity
	cm	kg/m³	W/mK	J/kgK	Hot Surface	Cold Surface
Normal Wood	12	450	0.1	1113	0.8	0.8

Figure C-3: Model fire characteristics timber (Cadorin et al., 2018)

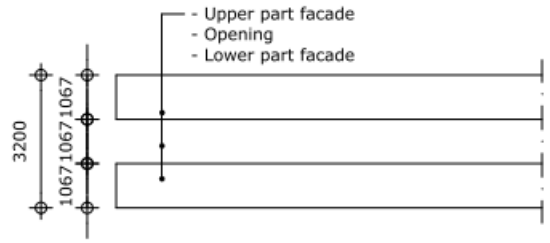

Figure C-4: Model facade layout in mm

3) Define a fire

The National Annex of Eurocode 1991-1-2 (NEN-EN 1991-1-2+C3/NB, 2019) gives reference to fire growth rate, firepower, and fire load.
However, none of those references corresponds to a timber car park. Therefore, the following assumptions are made:

- There are two ways in which the fire can expand in the pre-flashover phase due to the use of timber in the ceiling and floor and the travelling character of a car fire. So, it will be assumed that the fire growth rate is at least moderate, which means a fire growth rate of 300 seconds.
- The firepower is assumed to be high because the cars and the structural timber elements will contribute to the fire. Therefore, the assumption of the firepower is 500 kW/m^2.
- The amount of timber contributing to the fire should be known to determine the fire load correctly.
  This value still needs to be discovered. Therefore, a corresponding value of a library will be used. It has a mean value of 1500 MJ/m^2 and an 80% fraction of 1824 MJ/m^2 (NEN-EN 1991-1-2+C3/NB, 2019). Below, a justification of this assumption is given.

NEN 6090 (NEN 6090, 2017) provides indicative values for the fire load of timber, which is 333 MJ/m^2 for a timber floor thickness of 25 mm. This value is certainly present because, as mentioned in step 2, the floor thickness of a CLT floor in the references is about 140 mm. Also, the cars give a fire load. For a medium car, this is 9500 MJ (de Feijter & Breunese, 2007). The approximate fire load per area is 327 MJ/m^2, as calculated in equation C.1. Based on two cars with parking lot dimensions in paragraph 5.1.

$$q_f \left[\frac{MJ}{m^2}\right] = \frac{Q_f[MJ]}{A[m^2]} = \frac{2*9500}{16.26*2.5} = 467\ MJ/m^2 \quad \text{(C.1)}$$

Table C-2 presents all fire loads together, with a resulting value of 1133 MJ/m^2 for the mean firepower. This value is already close to the value of 1500 MJ/m^2. Based on the extrapolation of the values in NEN 6090 (NEN 6090, 2017), a timber floor and ceiling thickness of 38.2 mm results in 1500 MJ/m^2. Based on the references, this thickness is most probably less than half of the element thickness. So, it can be assumed that this thickness is reachable in reality.

Table C-2: Assumed fire loads timber car park

Floor	333 MJ/m^2
Ceiling	333 MJ/m^2
Cars	467 MJ/m^2
Total	1133 MJ/m^2

Conclusion

Based on the above set-up of the model, the firepower graph of Figure C-5 is produced by Ozone.

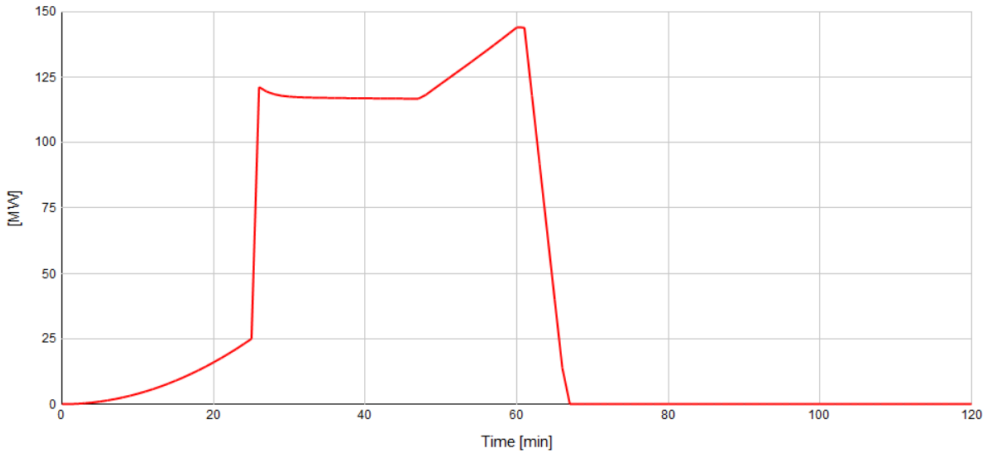

Figure C-5: Resulting firepower graph (Cadorin et al., 2018)

Figures C-2 and C-5, with their modelled values, are placed in one graph, visualized in Figure C-6. From that figure, it can be concluded that the area below the line of the standard fire is much larger than the area below the line of the local car fire scenario. So, the assumption of considering a standard fire is conservative.

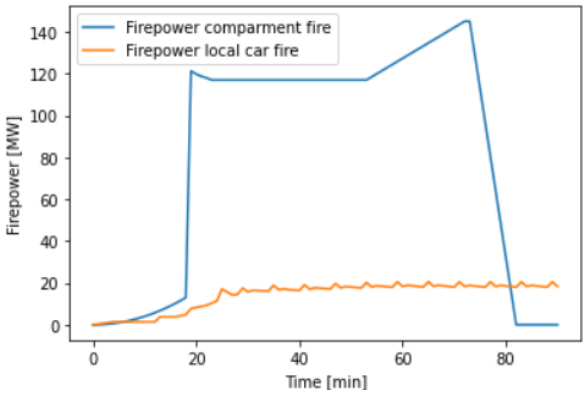

Figure C-6: Comparison firepower graph of a standard fire and a local fire

C.2: Results bonding test Triflex

Figures C-7 show the results of the bonding strength test of the Triflex primers with a Kerto-Ripa LVL plate. Moreover, Figure C-8 shows the test samples.

Hechtsterktemeting Matest

ALGEMEEN

Segment: BTL ☐ CCP ■ DDS ☐ WIS ☐ Acquisitie/offerte ☐

Projectnaam: Underlayment P2
Projectnummer:
Plaats: Schiphol

Applicateur: Aanwezig: D. Bast
Opdrachtgever: Balast-Nedam
Op verzoek van: dhr. T. Hienekamp / dhr. R. Verhagen
Datum: 29-8-2016
Uitgevoerd door: Emiel van Leeuwen

Opmerkingen: Dolly = 1963,495 mm²

METINGEN

Tijdstip: tot uur Luchtvochtigheid % Vocht% ondergr. %
Temperatuur ondergrond °C Luchttemp. °C Dauwpunttemp. °C

Locatie meting	1. A	Waarde 2,61	kN
Opbouw ondergrond	Kerto-Ripa, fineerhout	Waarde 1,329	N/mm²
Breukvlak:	Volledig in het fineerhout, Hechting tussen Triflex Cryl Primer 222 en fineerhout is groter dan tussen de fineerlagen onderling		

Locatie meting	1. B	Waarde 2,57	kN
Opbouw ondergrond	Kerto-Ripa, fineerhout	Waarde 1,308	N/mm²
Breukvlak:	Volledig in het fineerhout, Hechting tussen Triflex Cryl Primer 222 en fineerhout is groter dan tussen de fineerlagen onderling		

Locatie meting	2. A	Waarde 2,34	kN
Opbouw ondergrond	Kerto-Ripa, fineerhout	Waarde 1,191	N/mm²
Breukvlak:	Volledig in het fineerhout, Hechting tussen Triflex Pox Primer R 103 (350gr/m2) + instrooiing 0,3 - 0,8 mm en fineerhout is groter dan tussen de fineerlagen onderling		

Locatie meting	2, B	Waarde 2,31	kN
Opbouw ondergrond	Kerto-Ripa, fineerhout	Waarde 1,176	N/mm²
Breukvlak:	Volledig in het fineerhout, Hechting tussen Triflex Pox Primer R 103 (500 gr/m2) + instrooiing 0,3 - 0,8 mm en fineerhout is groter dan tussen de fineerlagen onderling		

Figure C-7: Results Triflex bond strength test

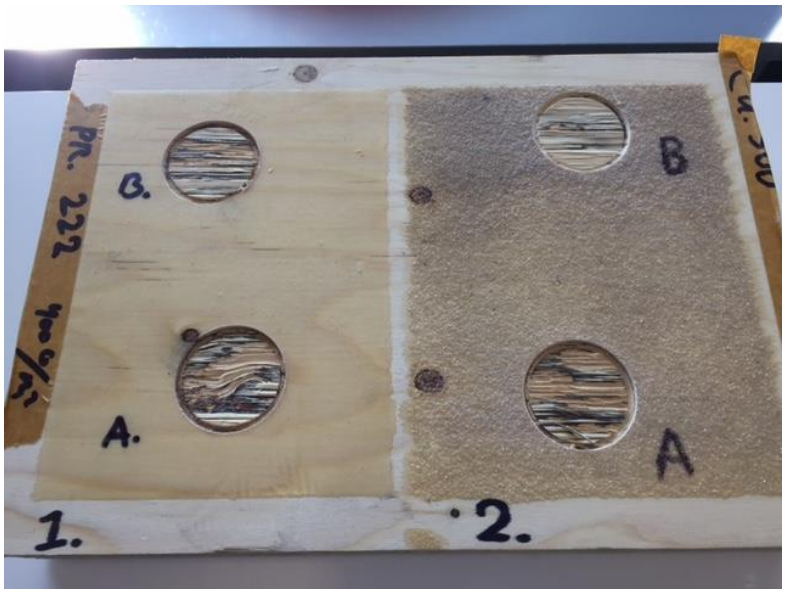

Figure C-8: Test samples bond strength test Triflex

D: Characteristics alternatives floor systems

For each alternative corresponding to floor systems I, II, and III, the features like species, dimension, strength class, fire resistance, and possible connections are listed in this Appendix.

D.1: Characteristics alternatives floor system I

All the alternatives corresponding to the floor system I have a common weakness, as stated below.

Weakness corresponding to all alternatives of floor system I

- All alternatives have a low percentage of biobased materials compared to timber floor systems II and III.

Floor system Park&Ride Antwerp (*Oosterweel Verbinding: Hout En Beton Op Park & Ride [Powerpoint-Slides]*, n.d.; *Park+Ride Antwerp / HUB* , n.d.)

- This alternative combines prefab concrete elements over 7.5 meters with a width of about 1 meter with a timber beam of 16.26 meters. A concrete screed is cast on top of the prefab floor panel to ensure the floor acts as one rigid system. See Figures 4-1, 4-2 of paragraph 4.2, and Figure A-2 of Appendix A.1.
- Most probably, the floor thickness is larger than 120 mm. That means the system has a minimum fire resistance of REI120, which meets the most strict fire requirement. (NEN-EN 1992-1-2+C1, 2011)
- Paragraph 4.2 and Appendix A.1 mention that the prefab elements rest on the timber beams. Next, the in-situ cast floor is monolithically connected to the prefab element to form one rigid floor element.

Weaknesses

- The cast in-situ concrete top layer results in a low re-mountability and prefabrication level because concrete cannot be re-mounted in the same conditions as initially.
- The cast in-situ concrete also results in a long construction time due to the high number of actions required, like installation of formwork and propping, and also the long hardening time.
- Third, the number of prefab concrete elements is large per span, as presented in Figure A-2 of Appendix A. So, an increased amount of crane movements is required.
- Furthermore, as shown in Figure 6-7, the complete floor is made of concrete, which results in a large self-weight of the floor. This high weight results in a large cross-section for the load-bearing elements like timber beams and columns.
- Finally, a weakness of the overall floor system is the missing composite action because there is no rigid connection between the floor and the beam, so the structural performance is not optimized.

Strengths

- Concrete has favourable characteristics in fire compared to timber because it is a non-combustible material.
- Due to the non-biobased nature of concrete, it is less prone to degradation by moisture.
- Also, in terms of structural performance, it is performing well. The high mass of concrete is stated as a weakness, but it improves the vibrational resistance. Concrete is an isotropic material, so the strength in all directions is equal, which is beneficial for stabilizing the structure because it can take up loads from all directions.

Floor system Goldbeck (*Parkhäuser*, n.d.)

- This alternative consists of prefab concrete elements placed on the steel beams and connected by shear studs with steel loops.
- The prefab concrete elements have a length of 8 meters and a width of 2.5 meters.
- Most probably, the height of the concrete panel is larger than 120 mm, which means the fire resistance is REI120. This value also meets the most strict requirement. (NEN-EN 1992-1-2+C1, 2011)
- Shear studs are placed at a regular distance on top of the steel beams. See Figures 6-8 and 6-9 of sub-paragraph 6.2.1. The prefab concrete element is connected to the beam using steel loops around the shear studs. The concrete slabs can easily be taken out because no permanent connection is made between the steel beam and the concrete slab.

Weaknesses

- Figure 6-9 shows that the floor system is completely made of concrete, so the floor's self-weight is high, resulting in larger cross-sections of the timber beams and columns.
- The floor system is not rigidly connected to the timber beam, so there is almost no composite action. Therefore, not the full structural performance potential of this design is used.

Strengths

- A high resistance against fire can be achieved for this complete concrete due to the non-combustible fire characteristics of concrete.
- Concrete is a non-biobased material, so there is limited degradation by moisture.
- In terms of structural performance, concrete acts well in vibrational resistance due to its large self-weight. It is also an isotropic material, so the strength in all directions is equal, which is beneficial for stabilizing the structure because it can take up loads from all directions.
- The connection of the floor to the beams is easy to make from a feasibility point of view. This type of connection gives the floor system also high re-mountability potential because the connection between the beam and floor can be demounted without damaging the elements.
- Medium-large floor elements of 2.5 meters by 8 meters are used. So, two elements should be used to span the required length of 16 meters.

Floor alternative of Pollmeier and TUMWood (*Development of Construction System for Multi-Storey Car Parks in BauBuche*, n.d.)

- This floor is made of reinforced pre-cast concrete elements and connected by a birdsmouth joint to the load-bearing timber beam.
- As shown in Figure A-39 of Appendix A.5, three floor elements are required for one grid of 2.5 meters by 16.5 meters. That means the elements are 2.5 meters by 5 to 6.5 meters.
- The prefab concrete element is 130 mm thick.
- Based on the thickness mentioned above of 130 mm, the fire resistance of the floor is larger than the maximum fire resistance requirement of REI120. (NEN-EN 1992-1-2+C1, 2011)
- The concrete elements are connected to the timber beams using birdsmouth joints, presented in Figure 6-10 of sub-paragraph 6.2.1.2. At the ramps, screws are used to make an extra rigid connection.

Weaknesses

- As mentioned for the previous floor systems of Goldbeck and the car park in Antwerp, a complete concrete floor system has a large self-weight that results in larger cross-sections of the load-bearing elements.
- The birdsmouth joint gives very limited composite action. Some composite action can be achieved by using the screws on the ramps.

Strengths

- As stated for the previous floor systems of Goldbeck and the car park in Antwerp, concrete has favourable features regarding fire, moisture resistance, and structural performance.
- The connection of the floor and the timber beam is made by Birdsmouth joints, as indicated in Figure 6-10. From a feasibility point of view, the connection between the slab and the beam can be erected easily. In addition, this connection between the floor and the timber beams is also re-mountable because no permanent connection is made.

Timber concrete floor alternative KLH (*Cross-Laminated Timber*, 2021; *Timber Concrete Composites*, 2019)

- The floor system of KLH consists of a timber CLT element and, on top, a cast in-situ concrete layer.
- For the smallest span of 6.5 meters, the minimum height is 240mm, based on a preliminary design made by KLH for a load of 5.8 kN/m^2. Then, it consists of 160mm of CLT plus 80mm of concrete.
- The maximum production dimensions of the CLT are 16.5 meters by 2.95 meters by 0.5 meters.
- The mentioned floor thicknesses above are the minimum values to reach R60 fire resistance.
- Three types of shear connections can be used between concrete and timber: grooves, screws, and perforated steel plates. In addition, a combination of connections is also possible.

Weaknesses

- Due to the use of cast in-situ concrete, the floor system has a relatively long construction time. It requires the installation of formwork and has a long hardening time. Propping may also be required during execution. Also, a limited prefabrication level corresponds to this floor system due to the casting of the concrete on-site. Next, the concrete cannot be re-mounted in the same condition as initially, so the re-mountability level of this floor system is limited.
- Concrete has a higher self-weight than timber. So, the in-situ cast layer makes the floor heavier, making the cross-sections of the load-bearing elements larger.

Strengths

- The arrangement of timber and concrete is optimal because it uses the strengths of both materials efficiently. Therefore, the concrete is less susceptible to cracking. So it can achieve higher moisture resistance.
- Concrete is isotropic, and CLT has higher strength characteristics in its weak direction than sawn timber. Therefore, the complete floor has relatively good properties in both directions, which is favourable for stabilising the structure.

- Also, concrete improves the fire resistance compared to a pure CLT floor due to its favourable fire characteristics.
- In addition, due to the large self-weight of concrete, the floor system has a lower susceptibility to vibration than a completely CLT floor.
- There are multiple options to connect the timber floor system with a timber beam in a re-mountable way using, for example, bolts, carpentry joints, and dowels. Therefore, this floor system has an improved re-mountability potential compared to pure concrete alternatives.

FRP floor alternative Park4all (*Park4all - Parking Solutions*, n.d.)

- Park4all floor system consists of steel beams and GFRP floor elements.
- Based on Figures 6-12 and 6-13 of sub-paragraph 6.2.1.4, the floor system's height is limited. Next, the maximum possible span is also limited. These small dimensions are due to the low stiffness and the limitations in the manufacturing (Proença et al., 2021). The required fire resistance will be larger. So, measures should be taken to satisfy the fire requirement.
- FRP can be connected to steel and timber by glue or by bolts. (Ascione et al., 2016)

Weaknesses

- The floor system is highly susceptible to deformations and vibrations due to the moderate modulus of elasticity of FRP combined with the small cross-section. FRP panels have a small maximum element area based on that aspect and the small production sizes of the pultrusion or molding process. This results in a high number of handling required to install the complete floor, and extra beams are needed. So, the FRP has low performance in terms of feasibility.
- Next, an unprotected FRP element has a very limited fire resistance (Proença et al., 2021). And protection against moisture should be applied to ensure reliable performance in a high-humidity environment. (Alzamora Guzman & Brøndsted, 2015)
- Third, FRP is an anisotropic material, so the strength characteristics in the transverse are lower than in the longitudinal direction.
- Finally, changing the dimensions requires special or heavy equipment (Altin Karataş & Gökkaya, 2018). This aspect lowers the re-mountability potential.

Strengths

- The high strength-to-weight ratio results in a very lightweight floor. Therefore, the other load-bearing elements can be designed smaller.
- Next, bolts can connect FRP panels (Ascione et al., 2016), giving them a high re-mountability potential. This re-mountability potential is not the case when connected by glue.
- FRP elements should be made in the controlled environment of a factory so it has a high prefabrication level. The pultrusion or molding process gives a high freedom in cross-section.

D.2: Characteristics alternatives floor system II

All alternatives corresponding to this floor system II have two same weaknesses and three same strengths, as listed below.

Weaknesses corresponding to all alternatives of floor system II

- As discussed in paragraphs 3.4 and 5.4, all complete timber floor systems should be protected with a waterproofing layer like a coating, mastic asphalt, or concrete. This measure

can reduce the feasibility due to the increase in on-site actions and lower the re-mountability potential, as indicated in paragraph 5.4.
- The fire resistance is limited compared to concrete due to the combustible behaviour of timber, as stated in paragraphs 3.4 and 5.3. Fire measures should probably be applied to ensure sufficient fire resistance of REI90. These measures can reduce the prefabrication level and the re-mountability potential. By using timber floor elements, the fire can spread more heavily through the car park than concrete.

Strengths corresponding to all alternatives of floor system II

- Only biobased materials are used in the alternatives of floor system II, which are beneficial for the environmental problems, as indicated in Chapter 3. The possible protection measures against moisture and fire can reduce the percentage of biobased materials used.
- Multiple re-mountable timber-to-timber connections are possible, like bolts, screws, and carpentry joints. So, all alternatives have a certain re-mountability potential.
- A high prefabrication level is possible for a pure timber application due to the possibility of producing the timber elements in the factory. It is also relatively easy in timber to create recesses, holes, attached corbels, and so on already in the factory.
- CLT and LVL have improved strength characteristics in both longitudinal and transverse directions for an anisotropic material like timber due to the orientation of lamellae or veneers in both directions.

X-lam floor alternative of Derix (*X-Lam; Kruislaaghouten Bouwelementen in Groot Formaat Voor Daken, Vloeren En Wanden*, n.d.)

- This flooring alternative is a CLT system, with each lamella thickness between 20 and 40 mm. In addition, it is made of spruce.
- The number of panels is always odd to provide stability in case of moisture and temperature changes (Buck et al., 2015).
- There are two variants possible, namely L-plates and X-plates. X-plates have a higher percentage of timber orientated in the transverse direction.
- The maximum dimensions are a thickness of 400 mm, a width of 3.5 meters, and a length of 17.8 meters. However, the span goes up to 7 meters for an application as a floor element.
- A strength class C24 corresponds to the timber used in this alternative.
- In the case of fire, the charring rate for a standard fire curve is 0.65 mm per minute. The resulting fire resistance depends on the thickness of the CLT floor.

Weaknesses

- Due to the limited thickness of about 300 mm to 400 mm and the corresponding moderate strength class, the maximum element area is 2.5 meters by 7 meters. So, at least three elements should be used in a grid of approximately 5 meters by 15 to 16 meters. This layout is not the most optimal in terms of feasibility compared to the previous alternatives in sub-paragraph 6.2.1.

Strengths

- CLT is a lightweight material compared to concrete, and the maximum thickness is 400mm, which minimizes the load from the floor system on the load-bearing structure. So, the cross-sections of the load-bearing structure will be limited.

CLT floor alternative of Stora Enso (*Cross-Laminated Timber (CLT)*, n.d.)

- Spruce is used as a timber species for the CLT lamellae. And the maximum lamella thickness is 80 mm.
- There are two variants possible, namely L-plates and C-plates. C-plates have a higher percentage of timber orientated in the transverse direction.
- The CLT panel has a maximum dimension of 2.95 meters by 16 meters and a maximum thickness depending on the type of CLT floor. The maximum thickness of a type C floor is 160 mm, and for the L-variant, it is 320 mm. The CLT can only reach approximately 7 meters for a floor application.
- A strength class of C24 belongs to the CLT floor.
- A reaction to the fire class of D-s2, d0 corresponds to this type of floor.
- The resistance to fire is given in a charring rate for a standard fire curve. For floors, the cover layer has a charring rate of 0.65 mm/min; when the lamellae fall off, it is 1.3 mm/min for 25 mm.

- **Kerto Q panel of Metsäwood** (*Kerto® LVL for Load-Bearing Applications*, 2022; *Kerto® LVL Q-Panel*, n.d.)e curve. For floors, the cover layer has a charring rate of 0.65 mm/min; when the lamellae fall off, it is 1.3 mm/min for 25 mm.

Kerto Q panel of Metsäwood (*Kerto® LVL for Load-Bearing Applications*, 2022; *Kerto® LVL Q-Panel*, n.d.)

- The LVL floor belongs to a strength class of LVL 36 C for thicknesses between 27 mm and 75 mm. Below 27 mm, it has the strength properties of LVL 32 C.
- The maximum production dimensions of the floor are a thickness of 75 mm, a width of 2.5 meters, and a length of 20 meters. As stated for the CLT alternatives, a car park floor can most likely not reach the maximum production length due to the limited thickness combined with the stiffness.
- The alternative has a reaction to the fire class of D-s1, d0.
- In the case of fire, the charring rate for a standard fire curve of the cover plate is 0.7 mm per minute.

Weaknesses

- LVL plates have a low maximum thickness of 75 mm compared to CLT in combination with a moderate strength class. This results in a shorter maximum span possible. So, more floor elements are necessary, which is unfavourable in terms of feasibility.

Strengths

- LVL is a lightweight material with a very limited thickness, resulting in less load acting on the load-bearing elements than heavier materials like concrete. Therefore, the cross-sections of the load-bearing structure can probably be designed to be smaller.

D.3: Characteristics alternatives floor system III

All alternatives belonging to floor system III have two general weaknesses and five strengths.

Weaknesses corresponding to all alternatives of floor system III

- As discussed in paragraph 5.4, all complete timber floor systems should be protected with a waterproofing layer like a coating, mastic asphalt, or concrete. This measure can reduce the feasibility due to the increase in on-site actions and lower the re-mountability potential, as indicated in paragraph 5.4.
- The fire resistance of timber is lower than concrete due to the combustible character of timber, as stated in paragraphs 3.4 and 5.3. Probably, fire measures should be applied to ensure sufficient fire resistance. By using timber floor elements, the fire can spread more heavily through the car park than concrete.

Strengths corresponding to all alternatives of floor system III

- Only biobased materials are used in the alternatives, which benefit the environmental problems, as indicated in Chapter 3. The possibly required protection measures against moisture and fire can reduce the percentage of biobased materials used.
- Multiple re-mountable timber-to-timber connections like carpentry joints, bolts, and screws are possible. So, the timber systems have a re-mountability potential.
- A high prefabrication level is possible for a pure timber application due to the possibility of producing the timber elements in the factory. It is also relatively easy in timber to create recesses, holes, attached corbels, and so on already in the factory.
- Timber is a lightweight construction material, so the load on the load-bearing elements reduces by applying a pure timber floor. So, the required cross-section of the beam and column are more optimized. Especially the height of the beam can be reduced compared to heavier floor systems.
- Due to the glued connections between the ribs and the panels, composite action is created between these elements. This results in improved structural characteristics, so a large span combined with a limited height is possible. Therefore, a lower number and fewer significantly large elements are required per grid, which is good for the feasibility and the car park efficiency.
- CLT and LVL have improved strength characteristics in both longitudinal and transverse directions for an anisotropic material like timber due to the orientation of lamellae or veneers in both directions.

Timber composite alternative of KLH (*Rib Panels*, n.d.; *Solid Wood Panels*, n.d.)

- This alternative uses a glulam rib and a KLH® solid wood top sheathing (CLT). Spruce is used as a timber species for the floor system.
- The glulam rib has a strength of GL 28c, and the strength class of the CLT panel is variable.
- This floor system has dimensions up to 16.5 meters by 2.5 meters and a height of approximately 600 mm.

- Fire resistance of at least REI30 can be reached by the system. For higher resistances, additional measures are necessary.
- A glued connection is used to connect the ribs to the panel.
- The floor elements can be connected to adjacent floor elements with screws.

Weaknesses open CLT plus glulam rib floor

- The fire resistance is low compared to the other rib floors because the cross-section is open, which means all timber elements of the floor are exposed to the fire.

Strengths open CLT plus glulam rib floor

- This floor system has good natural ventilation because there is no bottom sheathing, so the timber dries faster, which is beneficial for moisture resistance.
- Next, the ribs of the floor can be connected to the transverse beam of the module with relatively high rigidity by using joist hangers with metal fasteners due to the good accessibility of the ribs. This joint creates a higher stiffness of the floor.

Timber composite alternative of Stora Enso ("European Technical Assessment ETA-20/0893," 2020; *Rib Panels*, n.d.)

- This rib floor uses a glulam rib and CLT for the top and bottom panels. A strength class of up to GL 32 can be reached for the ribs. The CLT panels have a maximum strength class of C30.
- The maximum length is 13 to 16.5 meters, depending on the cross-section of the rib floor. The maximum height is about 600 mm, and the maximum width is 3.5 meters.
- The closed CLT design has a fire resistance of REI90. For the open alternative, additional measures are required to reach the resistance of REI90. Both types of rib floors need measures to achieve a fire resistance of REI120.
- In both rib floors, the panel and web are connected by glue.

Weaknesses closed CLT plus glulam rib floor

- The bottom panel can protect the other elements of the floor against moisture. But when the moisture is inside the floor system, it cannot get out easily due to the limited ventilation. So, the timber is a long time wet, and therefore it degrades faster.

Strengths closed CLT plus glulam rib floor

- In a fire, the bottom panel functions as a fire protection measure. Because the ribs and the top panel are not directly exposed to the fire until the bottom panel falls off. Next, it improves the structural performance because the composite action is increased, and the ribs are also stabilized on the bottom.
- Hollow cores are created inside the floor. These spaces are useful for installations. Due to the ease of creating recesses and holes, as stated in the general strengths of floor system III, the application of installations inside has a higher potential to be possible.
- Finally, the closed rib floor can be placed on the transverse beam. See Figures 6-5 and 6-6. So, the crane can move away when the connection is made, which is good from a feasibility point of view.

LVL timber composite of Metsäwood (*Kerto - Ripa Technische Richtlijnen*, 2016; *Laminated Veneer Lumber (LVL) Bulletin; New European Strength Classes*, 2019)

- Kerto Ripa T and Kerto Ripa Box systems use LVL panels as ribs and sheathings. Those systems have a width of 2.4 meters and can span up to 20 meters. The rib and the panel have a maximum thickness of 75 mm and 43 mm, respectively. For the total height, the maximum is 600mm.
- The rib is in class LVL 48 P, and the panels in LVL 36 C
- Fire resistance of REI60 can be reached without measures for the Ripa box. For the Ripa T, additional measures are already necessary to reach REI30. Higher fire resistance requires additional measures for both systems.
- Screws are possible to connect the floor elements.

Weaknesses open cross-section LVL

- The ribs and sheathing of this alternative have a limited thickness compared to the CLT plus glulam rib floor. But the strength characteristics are a bit higher. However, the maximum strength and stiffness of the panel are limited compared to the CLT plus glulam rib floor. This lower structural performance reduces the possible span, which is disadvantageous from a feasibility point of view.
- Because the cross-section is open, the rib and top panel are exposed to fire. So, both floor parts are directly damaged in case of a fire. Due to the limited thickness of the rib and panel, charring results faster in failure of the floor compared to CLT.

Strengths open cross-section LVL

- The open cross-section variant has higher moisture resistance than the closed variant due to the natural ventilation possible compared to the closed cross-section.
- Next, the connections between the floor and transverse timber beam for the open cross-section can be made with high rigidity by using joist hangers and metal fasteners due to the good accessibility of the ribs.

Weaknesses closed cross-section LVL

- As stated for the open cross-section, the ultimate strength of the closed LVL rib floor is limited compared to the closed CLT plus glulam rib floor due to the limited thickness of the ribs and sheathing.
- The closed cross-section creates a lower moisture resistance than the open design because the moisture in the floor's holes cannot go out easily. So, the timber is longer wet, and it degrades therefore faster.

Strengths closed cross-section LVL

- The fire resistance is higher than for an open cross-section due to the protection of the rib and top panel by the bottom panel.
- High composite action between the rib and sheathings is possible due to the glued connection, which is beneficial for structural performance.
- Next, the floor system can be placed easily on the transverse beam. See Figures 6-5 and 6-6. So, the execution processes like crane movement and execution of the connection should not be done at the same time. This efficiency is beneficial for feasibility.

- Finally, the hollow cores inside the floor can be used for installations. This solution has extra potential due to the ease of creating recesses and holes, as stated in the general strengths of floor system III.

- **LVL timber composite alternative of Stora Enso** (European Technical Assessment ETA 18/1132, 2021; Rib Panels, n.d.)a potential due to the ease of creating recesses and holes, as stated in the general strengths of floor system III.

LVL timber composite alternative of Stora Enso (European Technical Assessment ETA 18/1132, 2021; Rib Panels, n.d.)

- Like the Metsäwood LVL alternatives, the floor systems of Stora Enso consist of the same products and are fabricated similarly.
- All open, semi-open, and closed LVL rib floor variants can probably span up to 20 meters and have a maximum width of 2.4 meters. The rib has a maximum thickness of 75 mm. And the panel has a maximum thickness of 43 mm. Next, the maximum total height is 600mm.
- The resulting strength class is LVL 48 P for the rib and LVL 36 C for the panels.
- The open LVL design has a fire resistance of REI30, including a protective layer on the bottom part of the cross-section. The closed LVL rib floor has a higher fire resistance.
- The panel and rib are connected by glue for all three types of cross-sections.

Almost all characteristics of both LVL floor types of Stora Enso are the same as for the alternatives of Metsäwood. Therefore, the same strengths and weaknesses for the Metsäwood variants correspond to these alternatives. The semi-open variant combines the open and closed alternatives' features, so the stated strengths and weaknesses are more average. These average properties can be beneficial depending on the importance of the strengths and weaknesses.

Lignatur (*Dragende Ideeën Met Hout*, 2016; "European Technical Assessment ETA-11/0137," 2021)

- Sawn wood spruce ribs and flanges are used to make the lignatur floor elements.
- The lignatur floor element can span 16 meters, has a maximum width of 1 meter, and a maximum height of 360mm.
- A strength class C24 corresponds to this floor system
- The Lignatur system can be designed for fire resistance up to REI90.
- Carpentry and screw joints can easily connect the floor elements, as shown in Figure 6-23 of sub-paragraph 6.2.3.

Weaknesses

- The maximum width of 1 meter for this floor system is relatively small. So, a high number of elements should be used per grid. This high number is unfavourable from a feasibility point of view.
- Next, the sawn wood elements are only in the longitudinal direction and have a maximum strength class of C24. Therefore, it is doubtful if the 16 meters span can be reached for car park loads.
- Also, the connection between the floor elements with carpentry joints, as shown in Figure 6-23, has limited structural performance because the depth of the carpentry joint in the floor is very short.

- Like the other types of closed rib floors, the moisture resistance is lower than for the open variants due to the hindrance of ventilation by the sheathings and the timber plates at the ends of the square holes in the floor, as shown in Figure 6-23.
- Fourth, because of the special design, the cost is higher than the standard rib floor designs due to the higher production costs.

Strengths

- As mentioned for the other types of closed rib floors, the fire performance is improved compared to the open variants due to a bottom flange. So, the bottom sheathing protects the inner part of the floor.
- High composite action between the rib and sheathings is possible due to the glued connection, which is beneficial for structural performance.
- As indicated for the closed cross-section rib floors, they can easily be placed on the transverse beam, as shown in Figures 6-5 and 6.6.
- Fourth, installations can probably be placed inside the floor. However, due to the transverse blocks in the holes, shown in Figure 6-23, this is more difficult compared to the LVL and CLT plus glulam rib floor.

Kielsteg ("European Technical Assessment; ETA-18/1014," 2019; *Kielsteg - Light and Wide; The Handbook for the Wooden Roof and Floor Elements with Outstanding Performance*, 2019)

- This Kielsteg floor system consists of a curved OSB or plywood web in combination with timber top and bottom flanges.
- The plywood strength class corresponds to class F35 to F70 parallel to the grain and F10 to F15 perpendicular to the grain. The modulus of Elasticity is class E140 to E100 parallel to the grain and E5 to E20 perpendicular to the grain. The OSB webs are in class OSB/3.
- The maximum width of a floor element is 1.2 meters, and the maximum height is 380 mm for plywood webs or 800 mm for OSB webs.
- The fire resistance is up to REI60.
- In the length direction, the joints are made by finger joints. And in the width direction by glued or screw joints. Joint boards can be added to the floor to create a diaphragm floor system.

Weaknesses

- Like the other closed rib floors, moisture can be trapped in the spaces between the ribs. This trapped moisture makes it more vulnerable to moisture degradation.
- The maximum width of this floor system is 1.2 meters. Therefore, a higher number of elements are required per gird. This high number is not optimal based on feasibility. In addition, this floor system has a lower robustness than the other rib floors. The sheathings are placed between the ribs instead of the ribs glued on their top and bottom sides to the continuous sheathings. So, damage to the top or bottom flanges largely affects the floor's performance. The bottom flange can also not function as fire protection because the whole floor system no longer performs if it falls off.
- Finally, the cost is higher than for the standard rib floor designs due to the higher production costs of this special design.

Strengths

- The floor elements are connected by each other using a timber plate on top of two adjacent elements, and they should be fastened with glue or screws. See the recess on top in Figure 6-24. In addition, timber boards can be fastened on top of the floor systems. This connection can create diaphragm action. The floor elements can be connected on the bottom by placing the right bottom flange on top of the left bottom flange. See the recess at the bottom of Figure 6-24. This connection can be secured by glue or screws. Using glue in the top and bottom flange connection is not favourable for the re-mountability potential.
- Next, the closed cross-section is beneficial in fire resistance and composite action, as mentioned before in Appendix D.3.
- Third, this floor system can be placed on the transverse timber beam like the other closed types of cross-sections, shown in Figures 6-5 and 6-6. This connection is positive for the feasibility of the structure.
- Fourth, installations can probably be placed inside the floor. However, the curved webs make this more challenging than the LVL and CLT plus glulam rib floors.

D.4: Background first assessment floor desings

Below, the background of the first assessment of the floor designs is given. Appendix D.4.1 gives the reasoning behind the discarded floor designs of the preliminary first assessment.

D.4.1: Reasoning preliminary first assessment floor designs

First, the alternatives with cast in-situ concrete are discarded. Because based on sub-paragraph 6.2.1, the construction time and re-mountability potential of cast in-situ concrete are disadvantageous. Those topics are important for the design. See the problem definition and the research goal of paragraph 1.2.

Second, A high level of composite action optimises the structural performance of the cross-section, resulting in a lower floor height. Closed rib floors have a higher level of composite action than open or semi-open cross-sections. In addition, the bottom sheathing is favourable for fire resistance and creates holes for installations. The only disadvantage is the moisture accumulation inside the rib floor. However, internal ventilation can be improved, for example, by using products that take up moisture. So, closed rib floor designs are beneficial over open or semi-open rib floor designs. That means all floor system III designs using open or semi-open rib floors are discarded.

Compared to engineered timber like LVL, CLT, or glulam, the lignatur floor system has limited strength due to using sawn wood and a strength class of only C24. Next, it has a limited maximum floor element area compared to the other types of rib floors. Therefore, this system will not be included in the following research phase. Also, the Kielsteg floor is not favourable because of the limited floor element area and the low robustness, explained in 6.2.3.3, compared to the remaining closed rib floors with CLT plus glulam and LVL.

D.4.2: Reasoning second part first assessment floor designs

References of Chapter 4 present CLT floors with a thickness of about 100 to 140 mm for a design like Figures 6-3 and 6-4. LVL has a lower maximum thickness of 75 mm. However, it has improved structural characteristics compared to CLT, as indicated in Appendix D.2. So, there is a potential that these applications are possible in LVL. However, this potential is not very high because the structural characteristics are not twice as high, based on Tables B-8 and B-10. While the maximum thickness of LVL is half compared to the applied CLT thickness.

Only the CLT floor system II will be designed in the preliminary design instead of the LVL floor system II. Because the much larger maximum thickness results in higher maximum strength and stiffness values possible. If this CLT floor system II becomes the most beneficial floor design, then further research can conclude if LVL floor system II is also applicable.
For the same reason, the closed CLT plus glulam rib floor will be used in the preliminary design instead of the closed LVL rib floor. If this will be the most beneficial floor system, then further research can investigate whether this is also possible by using a closed LVL rib floor.

FRP panels are possible in various cross-sections. That results in a wide variety of possible floor system strengths and stiffnesses. Literature shows that a span of 5 meters, according to the orientation of Figure 6-1, is possible for an FRP panel (Gao et al., 2013). However, the corresponding width is limited compared to a prefab concrete slab due to FRP's lower stiffness and limiting dimensions from the production process, as mentioned in 6.2.1.4. In addition, FRP has limited fire resistance compared to concrete. A prefab concrete slab will be applied in the same orientation shown in Figures 6-1 and 6-2. So, a prefab concrete floor element is more suitable to assess in the preliminary design than the FRP floor. Investigation into the use of FRP floors is an interesting topic for further research.

Finally, a prefabricated closed rib floor plus concrete layer is more favourable than a prefabricated CLT plate plus concrete. Because of the higher structural performance of a rib floor compared to the CLT plate, larger element spans are possible. So, the stiffness criteria will be more governing. Therefore, the beneficial stiffness increment of a concrete top layer is larger for a rib floor than for a CLT floor. Next, the main advantage of a pure CLT panel floor system is its lightweight character and small height. However, this will be increased by applying a concrete top layer with a minimum thickness of 50 mm (NVN-CEN/TS 19103, 2021).

E: Structural calculations preliminary design

Appendix E presents the structural calculations of the preliminary design.
E.1 presents the determination of the most severe position and type of car park point loads. Then, E.2.1 to E.2.4 cover the iterations steps of the structural calculations per floor design. Finally, E.3.1 to E.3.4 calculate the supporting beam dimensions per floor design.

E.1: Determination most severe position point loads and type of loading

Determination most severe position point loads

Figure E-1 presents the influence surface of a 5 meters x 3 meters x 0.1 meters timber plate for a maximal vertical deflection in the centre of the plate.
This figure is created using a multiplication factor of 843000 for the unit load to make the influence surface visible in the graph. Three configurations of the point loads are possible, as indicated in Figure E-1.

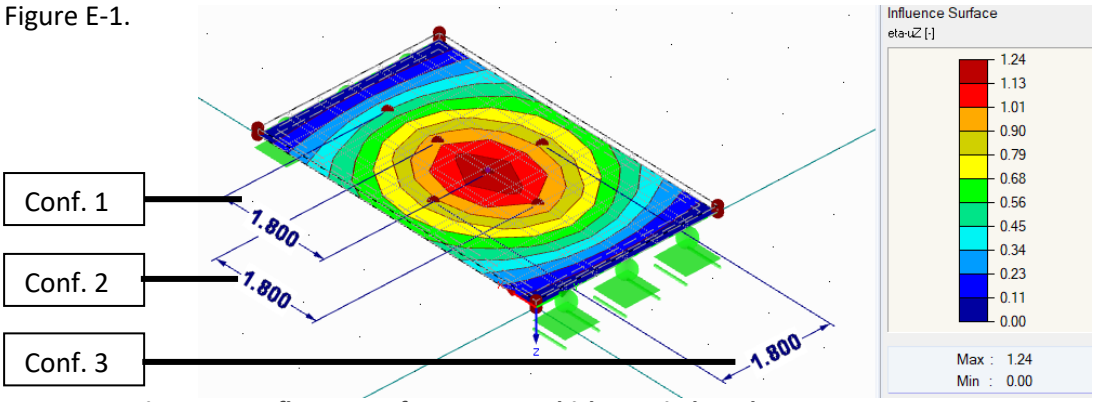

Figure E-1: Influence surface 100 mm thick C30 timber plate

Configuration 1 has one point load in the middle of the plate and one at a 1.8-meter distance. So, at the x-coordinates 2.5 meters and 4.3 meters.
Configuration 2 has both point loads at 0.9 meters distance from the middle of the plate. In this example, the point loads will be located at the x-coordinates 1.6 meters and 3.4 meters.
Configuration 3 has the points loads in the transverse direction at 0.9 meters from the centre at y-coordinates 0.6 meters and 2.4 meters.

Table E-1 shows the calculation of the most severe configuration, in which the factor from the influence surface of both positions is summed up. The configuration with the highest resulting value is the most severe. Concluded, configuration 2 is the most severe one.

Table E-1: Calculations most severe configuration point loads based on influence surface 5 m x 3 m x 0.1 m

Configuration 1		Configuration 2		Configuration 3	
X = 2.5 meters	1.24	X = 1.6 meters	0.96	Y = 0.6 meters	0.87
X = 4.3 meters	0.46	X = 3.4 meters	0.96	Y = 2.4 meters	0.87
Total	1.70	Total	1.82	Total	1.74

However, the larger the span, the less difference in stiffness from the supports can be expected around the centre of the plate. Chapter 6 shows that floor designs 2 and 3 span 16.26 meters. Figure E-2 shows the influence area for a 16.26 meters x 3 meters x 0.5 meters plate, with the same three configurations but changing coordinates, as shown in Table E-2. From that table, it can be concluded that configuration 3 is the most severe one for this plate dimension.

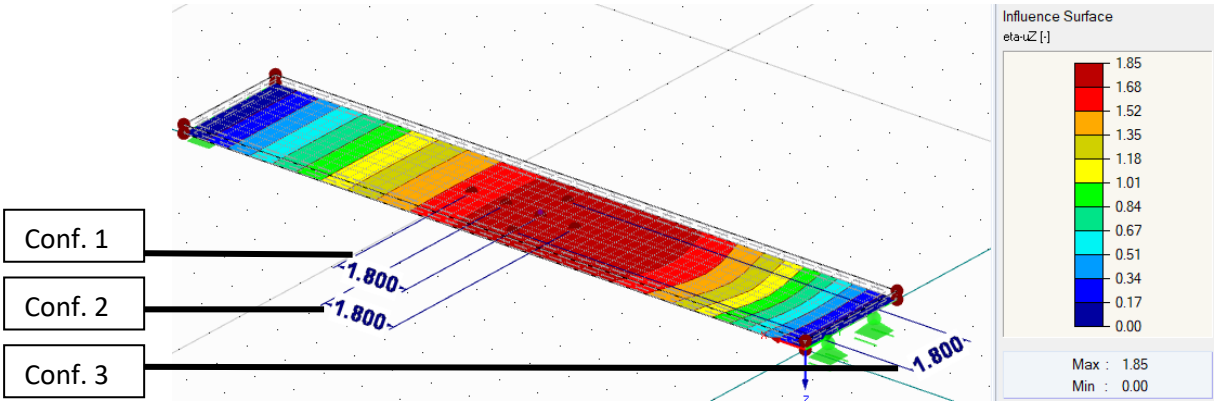

Figure E-2: Influence area 16.26 meters x 2.5 meters plate

Table E-2: Calculations most severe configuration point loads based on influence surface 16.26 m x 3 m x 0.2 m

Configuration 1		Configuration 2		Configuration 3	
X=8.13 meters	1.81	X=7.23 meters	1.85	Y=0.6 meters	1.8
X=9.93 meters	1.58	X=9.03 meters	1.72	Y= 2.4 meters	1.8
Total	3.39	Total	3.57	Total	3.6

<u>Determination most severe type of loading point loads</u>

Figure 5-2 shows that the point load can be divided into a surface load over an area of 0.1 meters x 0.1 meters. Figures E-3 to E-6 determine if there is a difference in the plate behaviour for a point load divided into a surface load or assuming it as a point load.

The figures show that both load types result in the same global deflection and vibrational resistance. So, a point load will be assumed in the models of the floor designs.

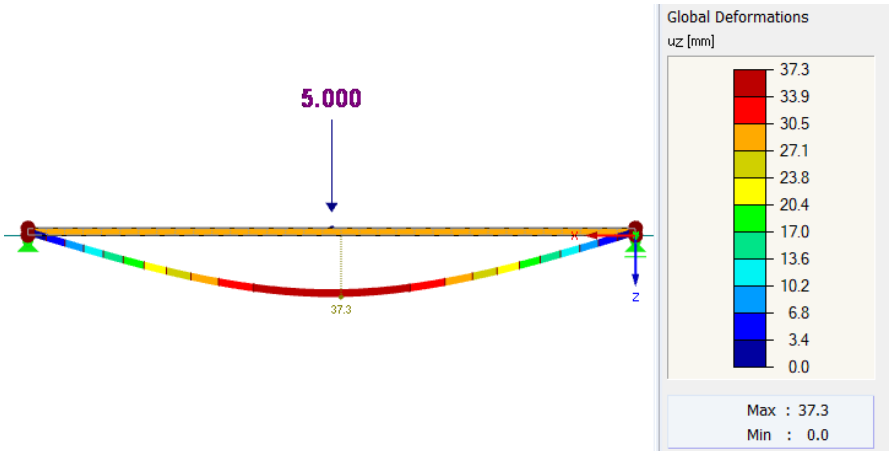

Figure E-3: Global deflection point loads

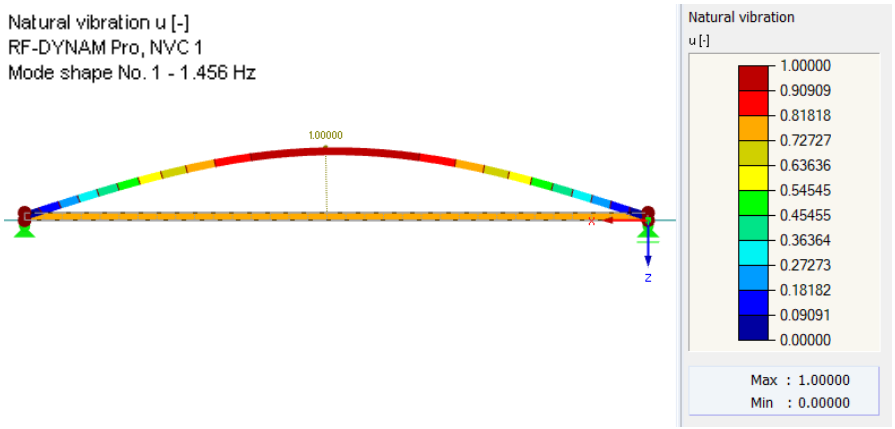

Figure E-4: First eigenfrequency point loads

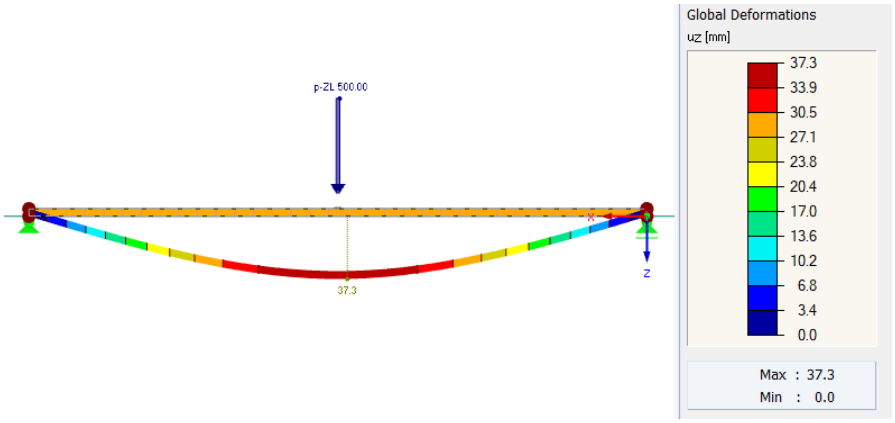

Figure E-5: Global deflection surface loads

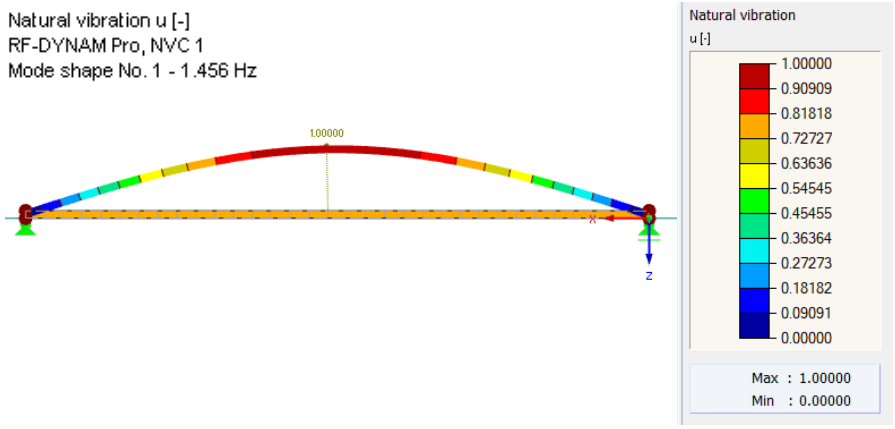

Figure E-6: First eigenfrequency surface loads

E.2: Preliminary floor design dimensioning

Appendix E.2 presents the iteration process for determining the minimum required cross-section of the four remaining floor designs.

E.2.1: Floor design 1 - CLT floor

As stated in sub-paragraph 7.2.2, the floor is made of C30 timber with strength and stiffness values according to Table B-8 of Appendix B.

The global deflection, vibrational resistance, and bending stress will be the criteria checked for the CLT floor, as explained in sub-paragraph 7.2.1. Below, the criteria corresponding to this floor design are determined.

Global deflection

The span is 5 meters, as shown in Figure 7-3. This span results in a maximum final deflection of 15 mm.

Vibrational resistance

As stated in paragraph 5.2 and sub-paragraph 7.2.1, the minimum eigenfrequency of the floor system should be 5 Hz.

Bending stress

Table B-8 of Appendix B shows that the characteristic bending strength of a C30 strength class is 30 N/mm2. Using the indicated parameters in Table 7-5 gives a design bending strength of 19.2 N/mm2.

Iteration 1: 100 mm CLT

In the first iteration, a height of 100 mm is used. Because from Chapter 4, it can be concluded that this is the minimum height used in the reference car parks.
Figures E-7 to E-13 show the results gathered by using the RFEM software.

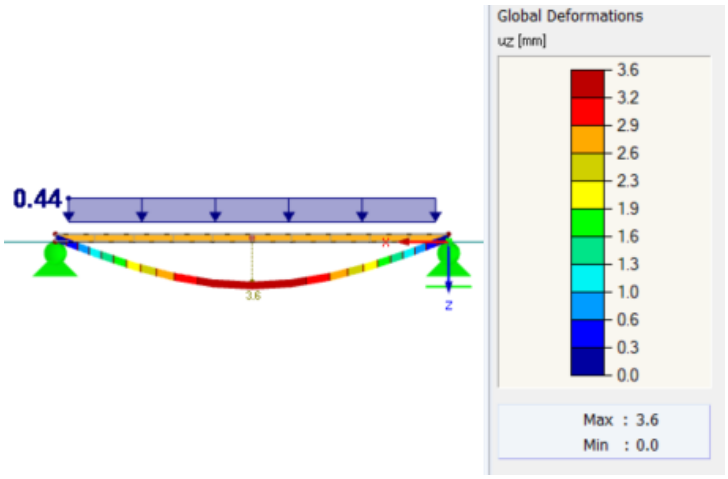

Figure E-7: Initial global deflection iteration 1 floor design 1 by permanent load

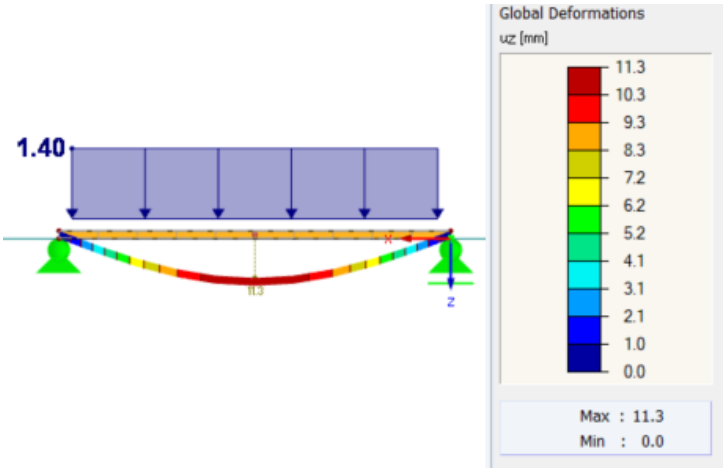

Figure E-8: Initial global deflection iteration 1 floor design 1 by variable surface load

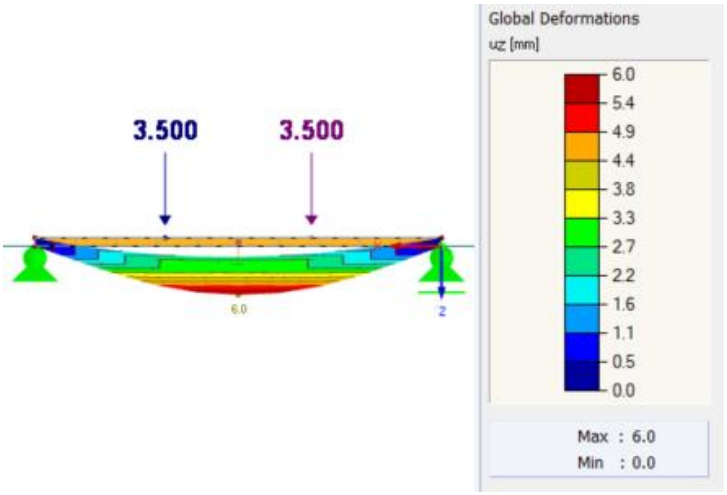

Figure E-9: Initial global deflection iteration 1 floor design 1 by variable point load

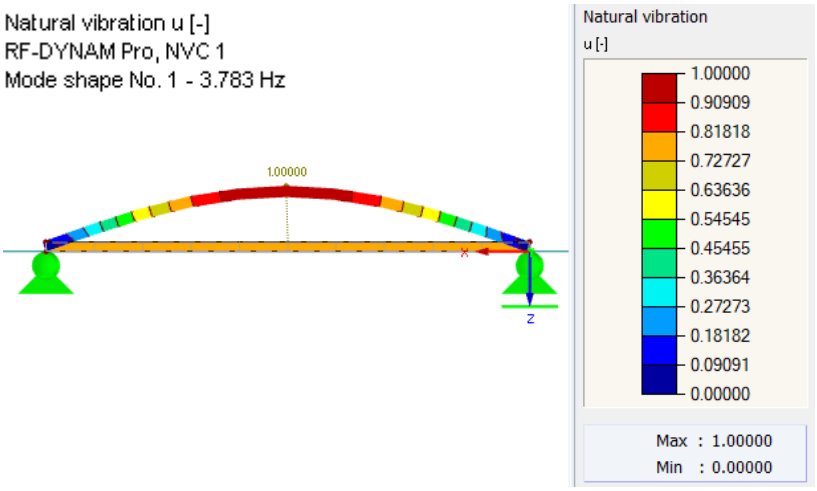

Figure E-10: First eigenfrequency iteration 1 floor design 1 by variable surface load

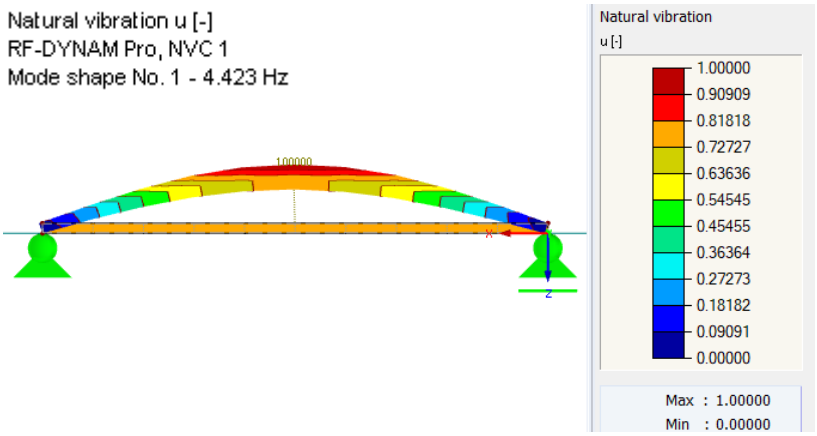

Figure E-11: First eigenfrequency iteration 1 floor design 1 by variable point load

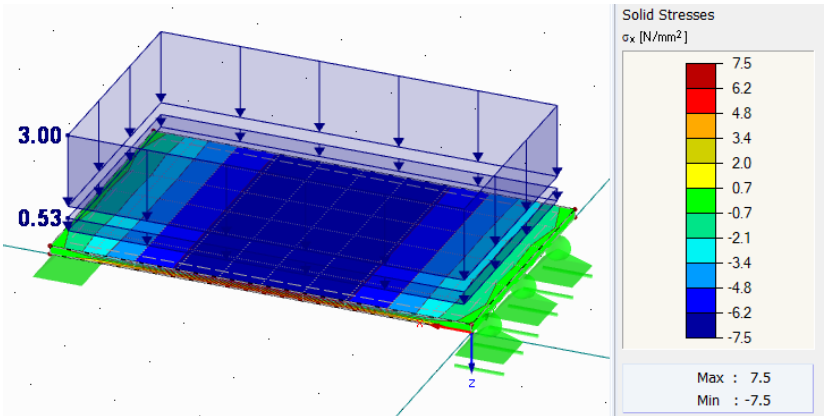

Figure E-12: Bending stress floor design 1 iteration 1 by variable surface load

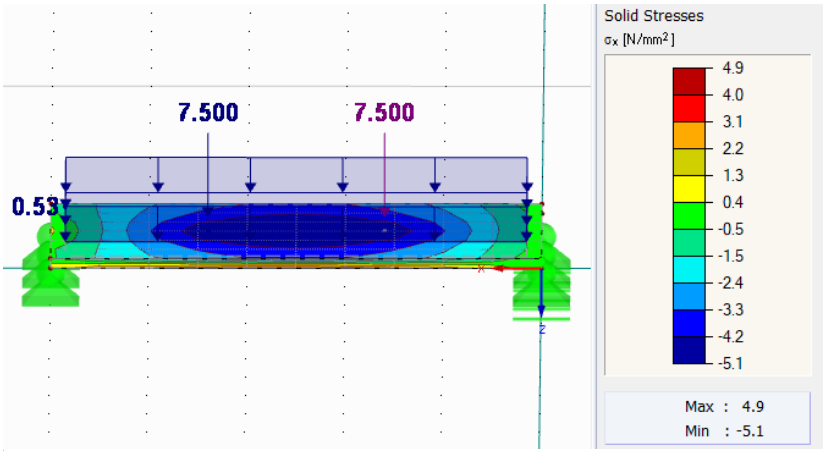

Figure E-13: Bending stress floor design 1 iteration 1 by variable point load

Based on the above results, the unity checks are determined. Table E-3 shows these unity checks for the surface load because this is the most governing type of variable load. It gives more severe values than the variable point load for all global deflection, vibration, and bending stress.
Both SLS unity check values are above 1, so the thickness must be enlarged.

Table E-3: Unity checks floor design 1 iteration 1

Global deflection			**Vibrational resistance**			**Bending stress**		
u_{fin}	23.2	mm	F	3.78	Hz	σ_x	7.5	MPa
u_{lim}	15	mm	f_{min}	5	Hz	$f_{m,d}$	19.2	MPa
UC	1.55		UC	1.32		UC	0.39	

Iteration 2: 120 mm CLT

As stated above, the thickness must be larger. That is done in this second iteration step using a thickness of 120 mm instead of 100 mm because the enlargement of CLT plates goes per 20 mm (*Cross-Laminated Timber (CLT)*, n.d.).

Only the results from the governing variable surface load are considered from now on in this iteration process.

Figures E-14 to E-17 present the results from RFEM of this thickness for the three criteria.

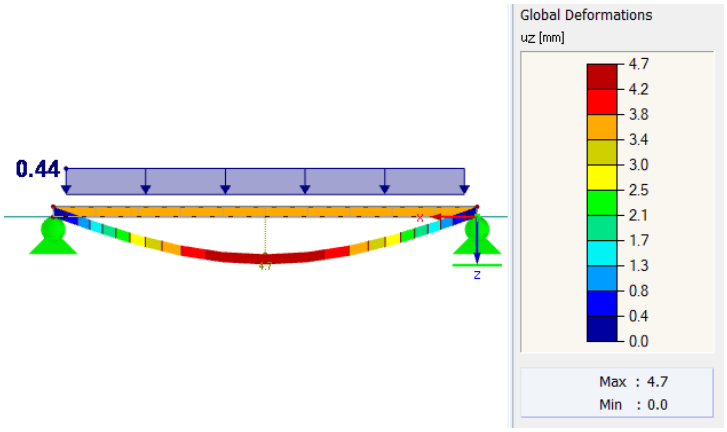

Figure E-14: Initial global deflection iteration 2 floor design 1 by permanent load

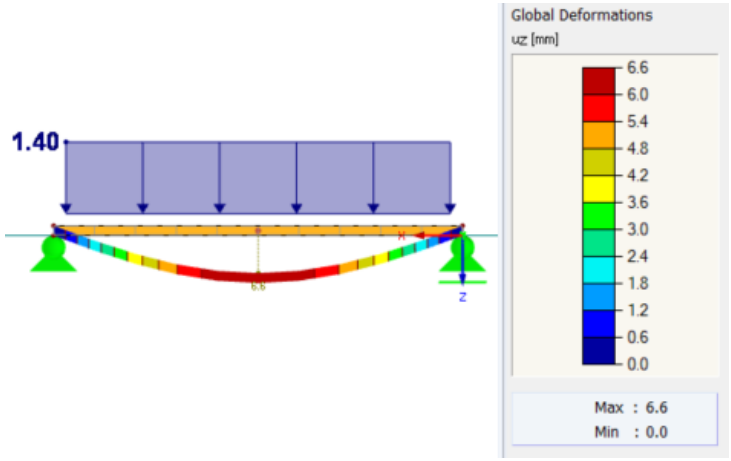

Figure E-15: Initial global deflection iteration 2 floor design 1 by variable surface load

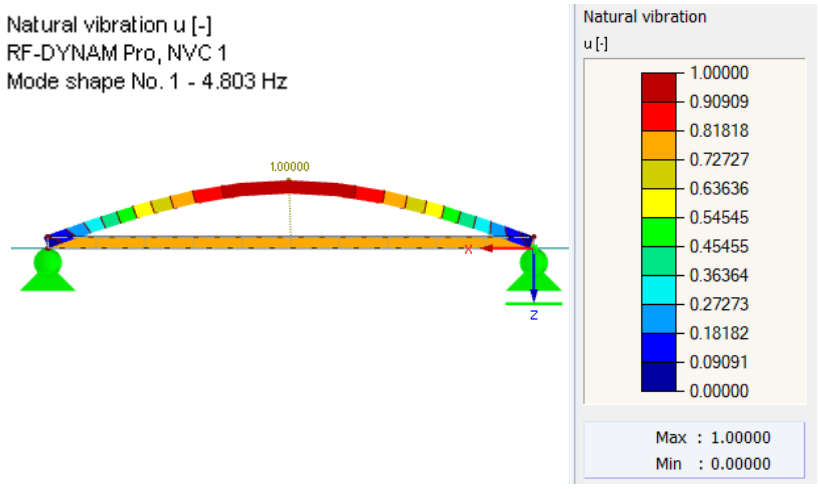

Figure E-16: First eigenfrequency iteration 2 floor design 1

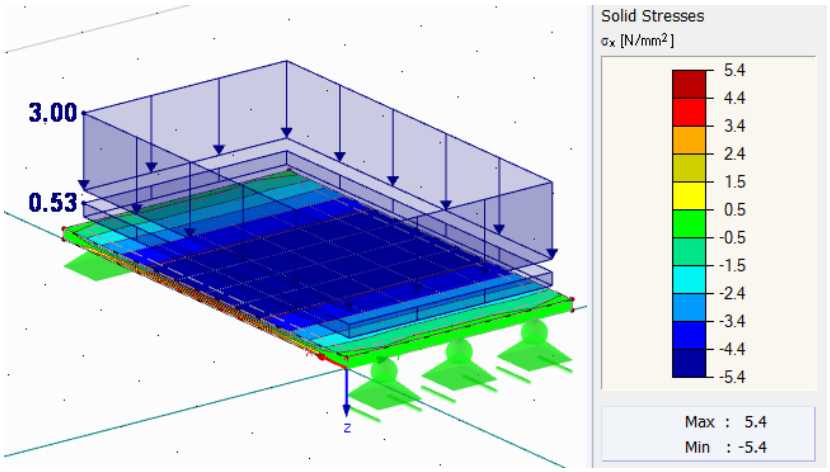

Figure E-17: Bending stress iteration 2 floor design 1

Table E-4 presents the resulting unity checks for this second iteration. Again, both SLS unity checks are above 1, and the bending stress unity check is far below 1. That means the thickness should be larger.

Table E-4: Unity checks floor design 1 iteration 2

Global deflection			**Vibrational resistance**			**Bending stress**		
u_{fin}	18.23	mm	f	4.80	Hz	σ_x	5.4	MPa
u_{lim}	15	mm	f_{min}	5	Hz	$f_{m,d}$	19.2	MPa
UC	1.22		UC	1.04		UC	0.28	

Iteration 3: 140 mm CLT

The thickness of the floor will be enlarged by 20 mm to a total thickness of 140 mm.
Figures E-18 to E-21 are the results from RFEM on the three criteria shown.

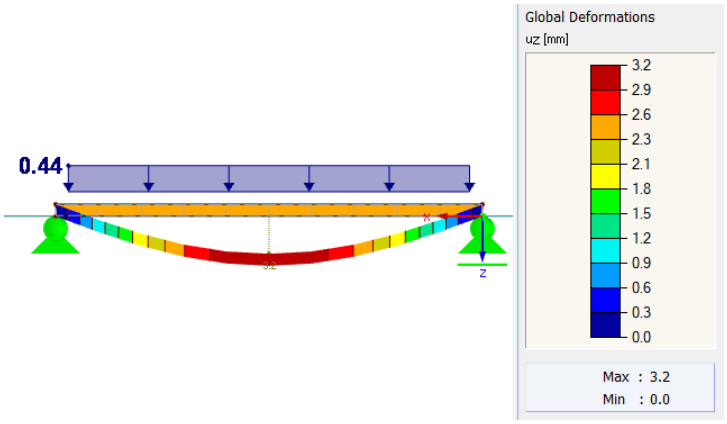

Figure E-18: Initial global deflection iteration 3 floor design 1 by permanent load

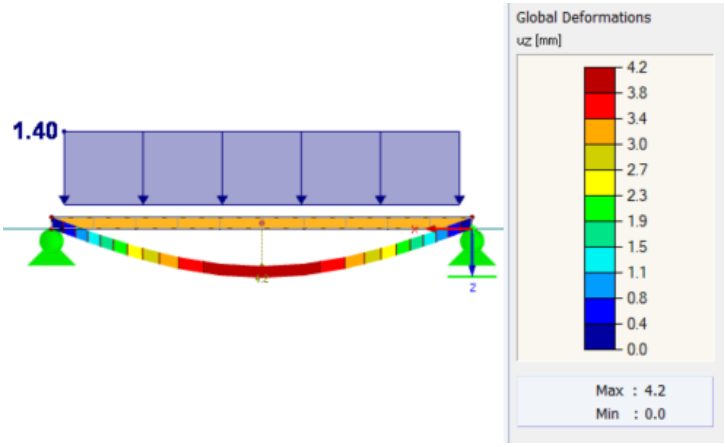

Figure E-19: Initial global deflection iteration 3 floor design 1 by variable load

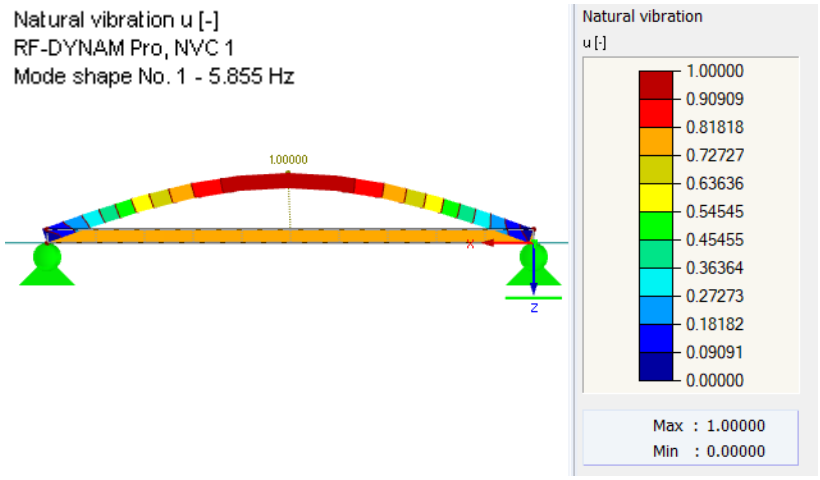

Figure E-20: First eigenfrequency iteration 3 floor design 1

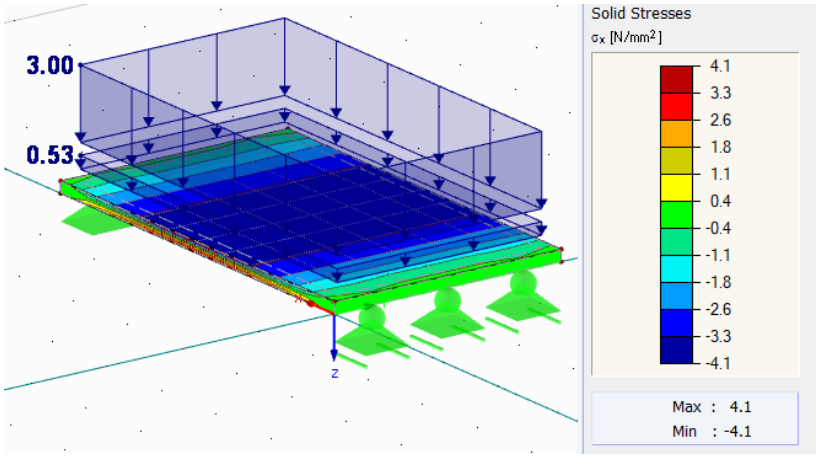

Figure E-21: Bending stress iteration 3 floor design 1

Table E-5 presents the results of the unity checks per criteria from the RFEM calculations. All unity checks are below 1. So, 140 mm is the most optimal thickness of the CLT floor.

Table E-5: Unity checks floor design 1 iteration 3

Global deflection			**Vibrational resistance**			**Bending stress**		
u_{fin}	11.98	mm	f	5.86	Hz	σ_x	4.1	MPa
u_{lim}	15	mm	f_{min}	5	Hz	$f_{m,d}$	19.2	MPa
UC	0.8		UC	0.85		UC	0.21	

E.2.2: Floor design 2 - Closed CLT plus glulam rib floor

As stated in sub-paragraph 7.2.3, the floor is made of C30 for the CLT sheathings and GL32h for the glulam ribs. Strength and stiffness properties are according to Tables B-7 and B-8 of Appendix B. Furthermore, the global deflection and vibrational resistance will be the criteria checked for the closed CLT plus glulam rib floor over 16.26 meters. The requirements of both criteria are summarized below.

Global deflection

The span is 16.26 meters, shown in Figure 7-6. This span results in a maximum final deflection of 48.78 mm.

Vibrational resistance

As stated in paragraph 5.2 and sub-paragraph 7.2.1, the minimum eigenfrequency of the floor system should be 5 Hz.

Iteration 1: 100 mm CLT sheathings plus 4 times a 100x200mm glulam rib

A total height of 400 mm is assumed as a starting point, as indicated in sub-paragraph 7.2.3, including a sheathing thickness of 100 mm and a rib height of 200 mm.
The RFEM results of this first iteration are shown in Figures E-22 to E-26.

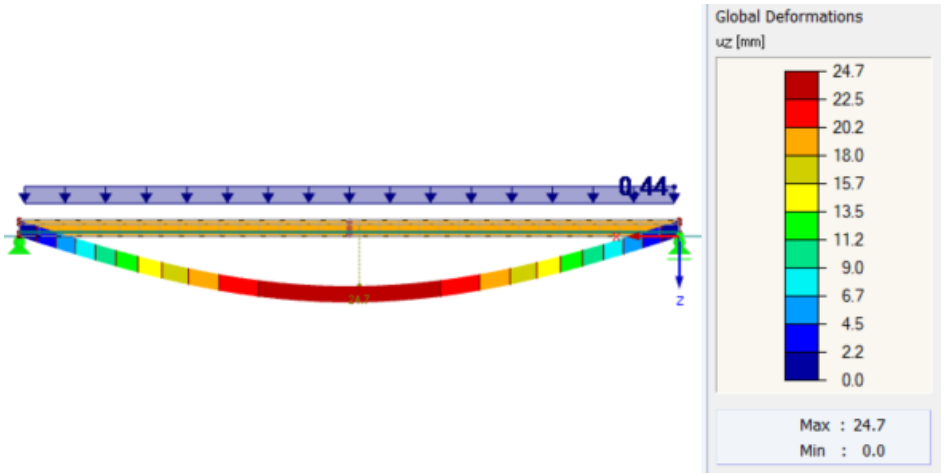

Figure E-22: Initial global deflection iteration 1 floor design 2 by permanent load

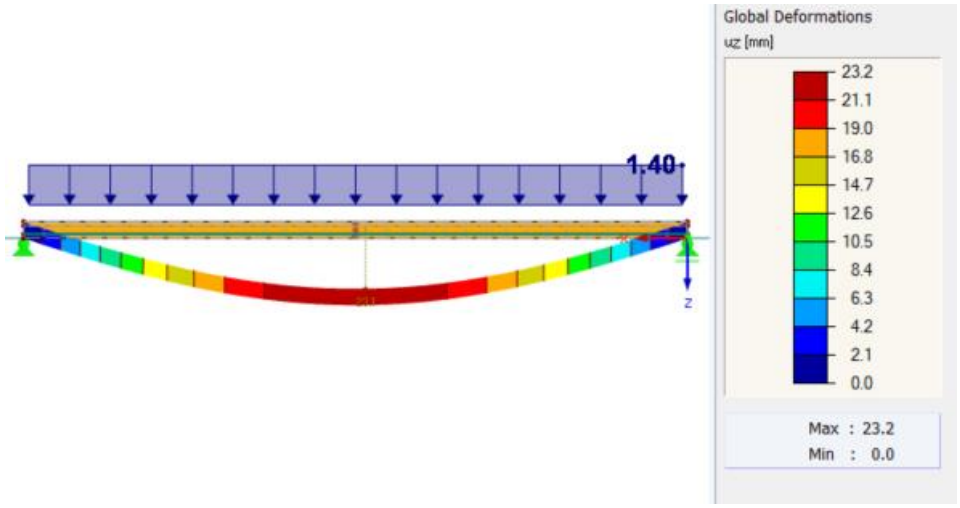

Figure E-23: Initial global deflection iteration 1 floor design 2 by variable surface load

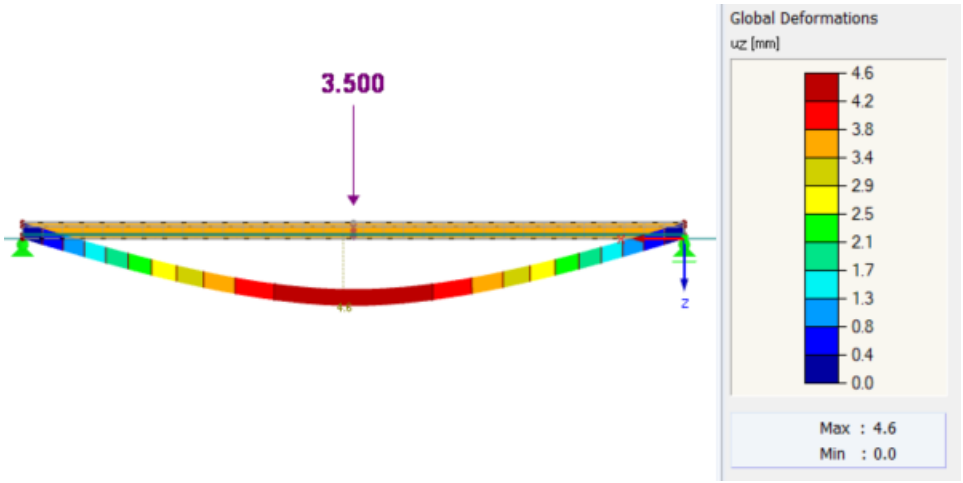

Figure E-24: Initial global deflection iteration 1 floor design 2 by variable point loads

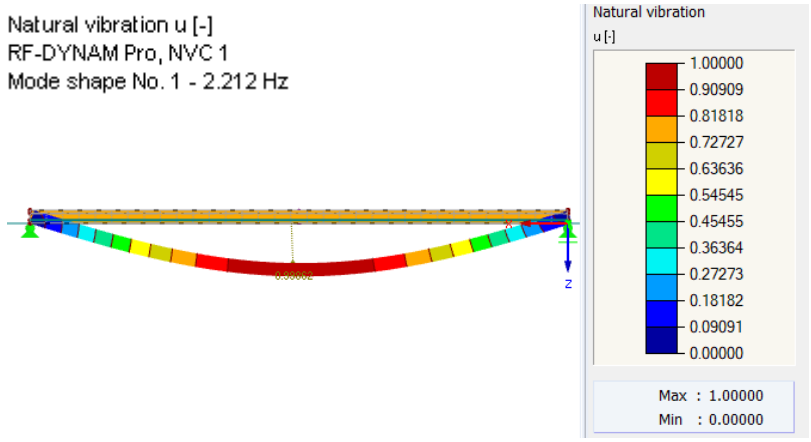

Figure E-25: First eigenfrequency iteration 1 floor design 2 by permanent and variable surface load

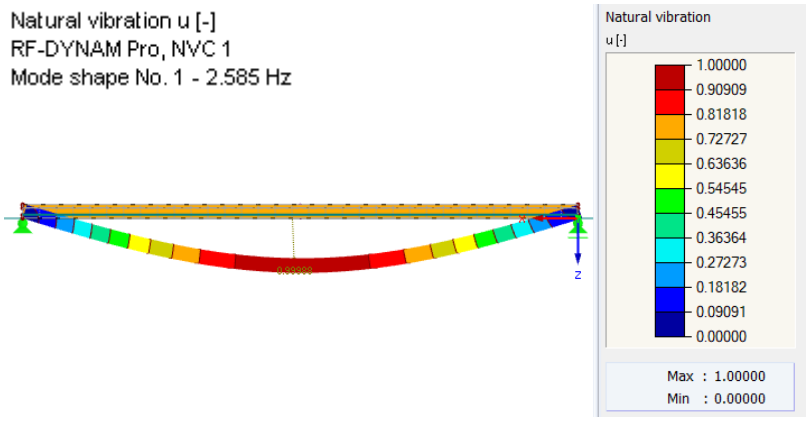

Figure E-26: First eigenfrequency iteration 1 floor design 2 by permanent and variable point loads

From the above figures, the surface load results in more severe values than the point loads. So, the largest values from the surface load will be used to calculate the unity checks.
The final deflection, including creep, is calculated from the initial deflections of Figures E-22 and E-23. This result is shown in the first column of Table E-6 and the eigenfrequency in the second column of the table. Both unity checks are above 1, so the cross-sectional dimensions must increase.

Table E-6: Unity check values floor design 2 iteration 1

Global deflection			Vibrational resistance		
u_{fin}	78.80	mm	F	2.21	Hz
u_{lim}	48.78	mm	f_{min}	5	Hz
UC	1.62		UC	2.27	

Iteration 2: 140 mm CLT sheathing plus 4 times 100x320 mm glulam rib

In this second iteration, the cross-section is heavily enlarged because of the high unity check for vibrational resistance of iteration 1. The thickness of the CLT sheathings is enlarged from 100 mm to a thickness of 140 mm. The height of the glulam ribs is enlarged from 200 mm to a total height of 320 mm. As done for the CLT floor in E.2.1, the deflection and vibration due to the point loads will not be considered because iteration 1 shows that the surface load is governing.

Figures E-27 to E-29 show the RFEM results of this second iteration.

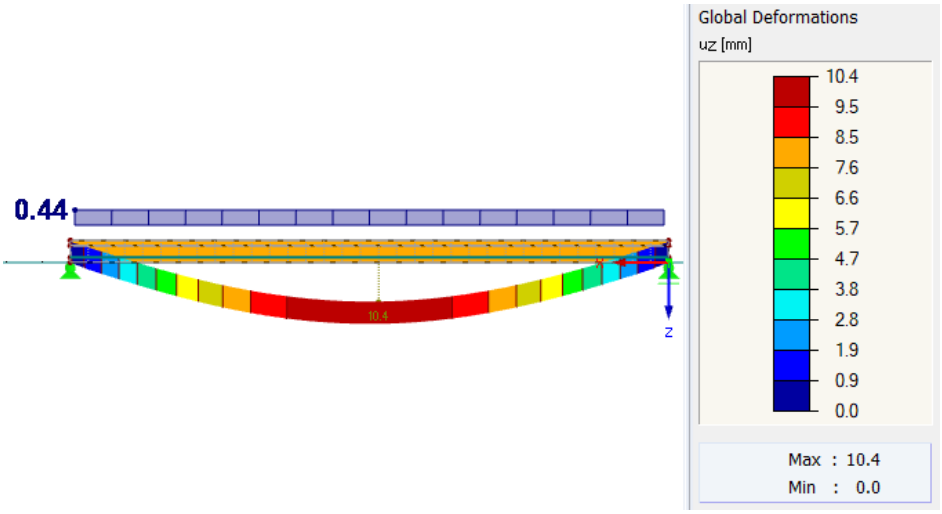

Figure E-27: Initial global deflection iteration 2 floor design 2 by permanent load

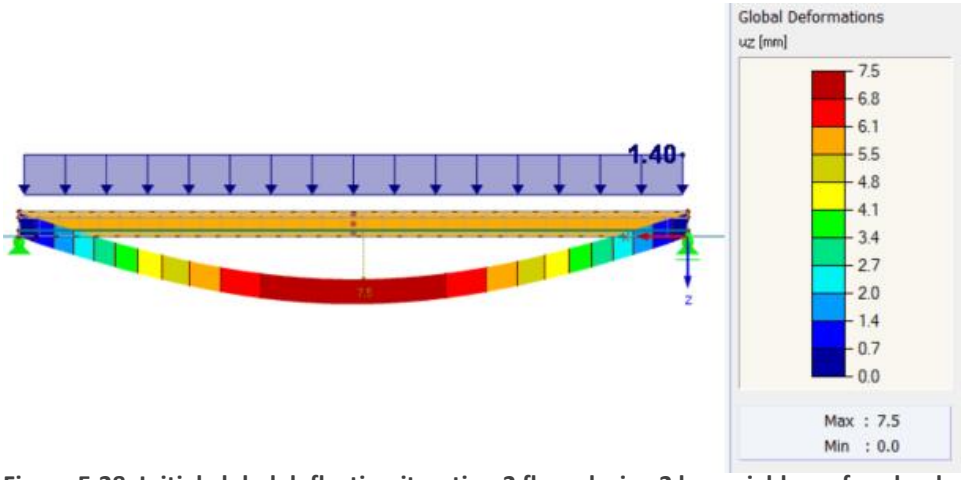

Figure E-28: Initial global deflection iteration 2 floor design 2 by variable surface load

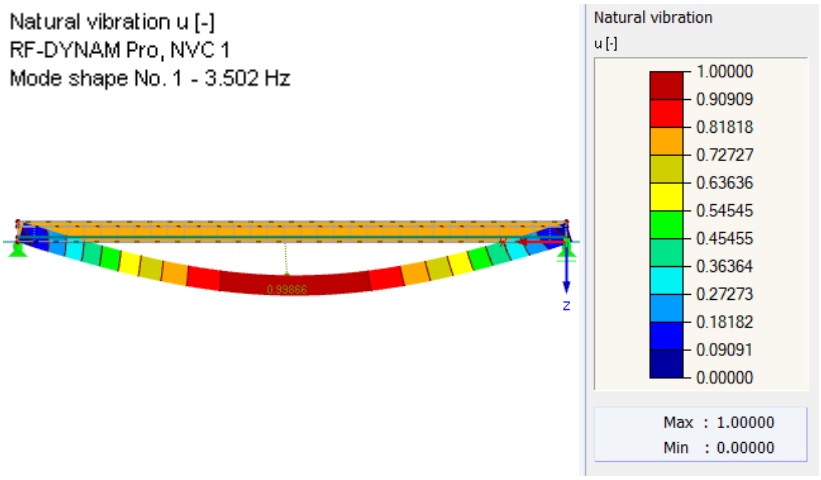

Figure E-29: First eigenfrequency iteration 2 floor design 2

Table E-7 presents the unity checks of this second iteration based on the results of the RFEM calculations. It shows that only the vibrational resistance is not sufficient. So, the cross-section should be larger in the next iteration step.

Table E-7: Unity check values floor design 2 iteration 2

Global deflection			**Vibrational resistance**		
u_{fin}	29.82	mm	f	3.5	Hz
u_{lim}	48.78	mm	f_{min}	5	Hz
UC	0.61		UC	1.43	

Iteration 3: 180 mm CLT plus 4 times 100x340 mm glulam ribs

Again, the thickness of both the sheathing and ribs is increased. The sheathings go from 140 to 180 mm, and the rib from 320 mm to 340 mm.

The corresponding RFEM results of this iteration are shown in Figures E-30 to E-32.

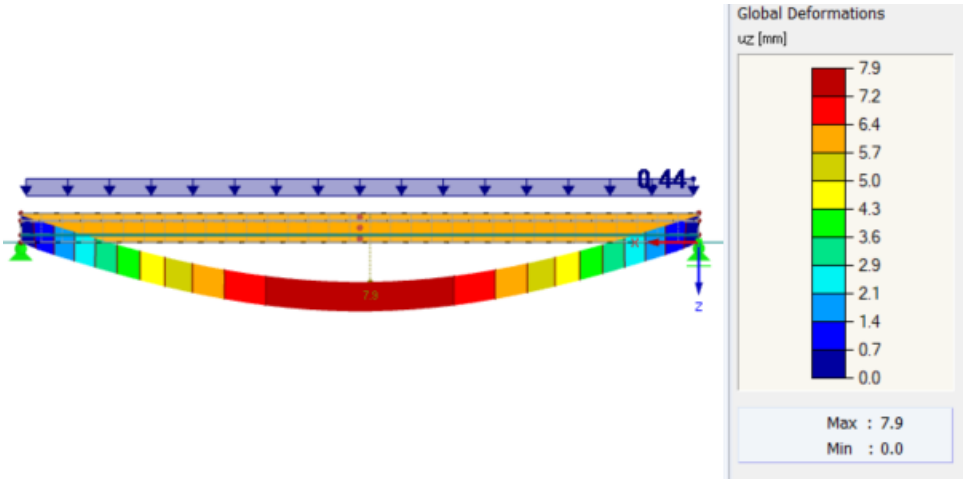

Figure E-30: Initial global deflection iteration 3 floor design 2 by permanent load

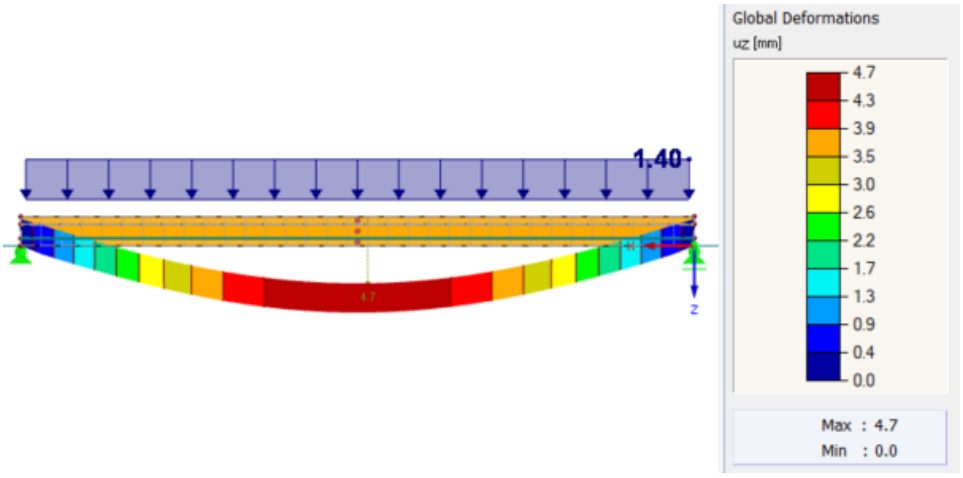

Figure E-31: Initial global deflection iteration 3 floor design 2 by variable surface load

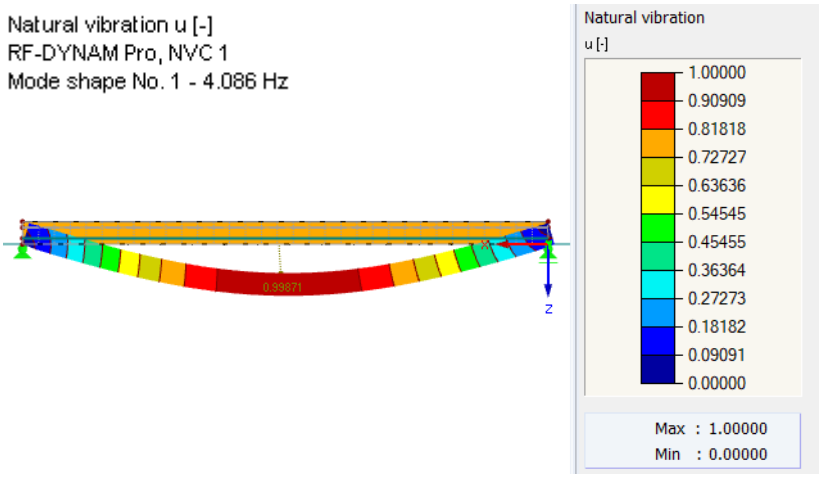

Figure E-32: First eigen frequency iteration 3 floor design 2

The unity check values of the two criteria are provided in Table E-8. Again, the vibrational resistance is not sufficient. Moreover, the global deflection unity check is already far below 1. A subsequent iteration step is required.

Table E-8: Unity check values floor design 2 iteration 3

Global deflection			**Vibrational resistance**		
u_{fin}	21.18	mm	f	4.09	Hz
u_{lim}	48.78	mm	f_{min}	5	Hz
UC	0.43		UC	1.22	

Iteration 4: 180 mm CLT plus 5 times 150x340mm glulam ribs

The goal of this research is to limit the height of the floor system. Therefore, this iteration step increases the rib width by 50 mm and the number by 1 to increase the stiffness of the rib (k in equation 7.1). See the results in Figures E-33 to E-35.

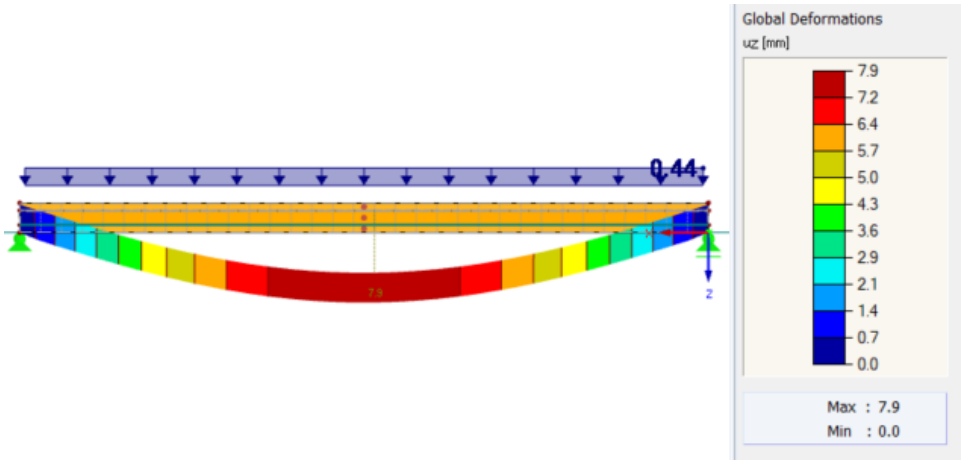

Figure E-33: Initial global deflection iteration 4 floor design 2 by permanent load

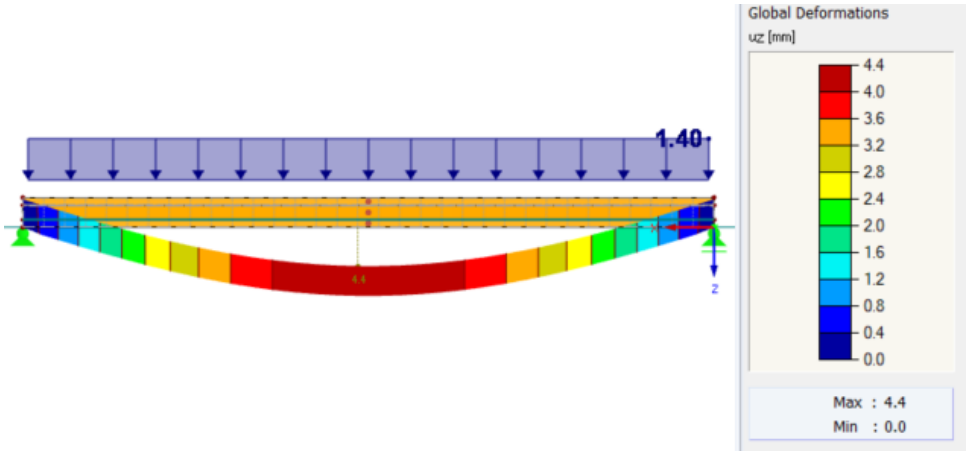

Figure E-34: Initial global deflection iteration 4 floor design 2 by variable surface load

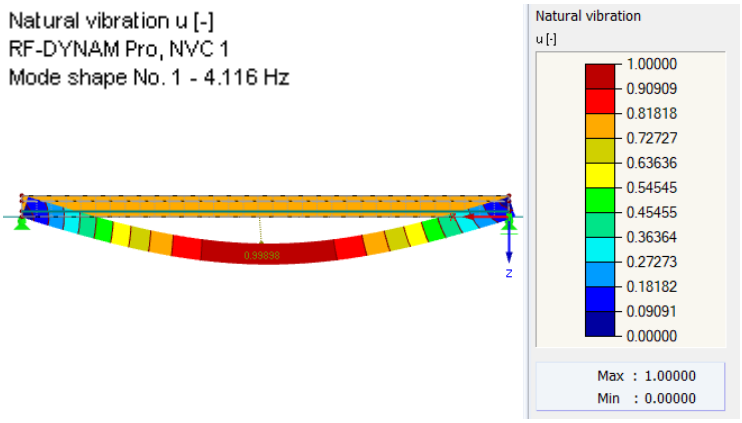

Figure E-35: First eigenfrequency iteration 4 floor design 2

Table E-9 and Figure E-35 show that the vibrational resistance of this cross-section is only slightly increased compared to the previous iteration step. So, increasing the rib width has a minimal effect on stiffness. Therefore, a new iteration step is required to enlarge the height to increase the moment of inertia and resulting stiffness.

Table E-9: Unity check value floor design 2 iteration 4

Global deflection			Vibrational resistance		
u_{fin}	20.73	mm	f	4.12	Hz
u_{lim}	48.78	mm	f_{min}	5	Hz
UC	0.43		UC	1.21	

Iteration 5: 200 mm CLT plus 4 times 100x400 mm glulam ribs

The CLT sheathings and the glulam will be enlarged, as mentioned after iteration 4. Their thickness is now 200 mm, the maximum thickness possible ("European Technical Assessment ETA-20/0893," 2020). In addition, the rib height is enlarged by 60 mm to 400 mm.

Figures E-36 to E-38 show the results of this cross-section calculated in RFEM.

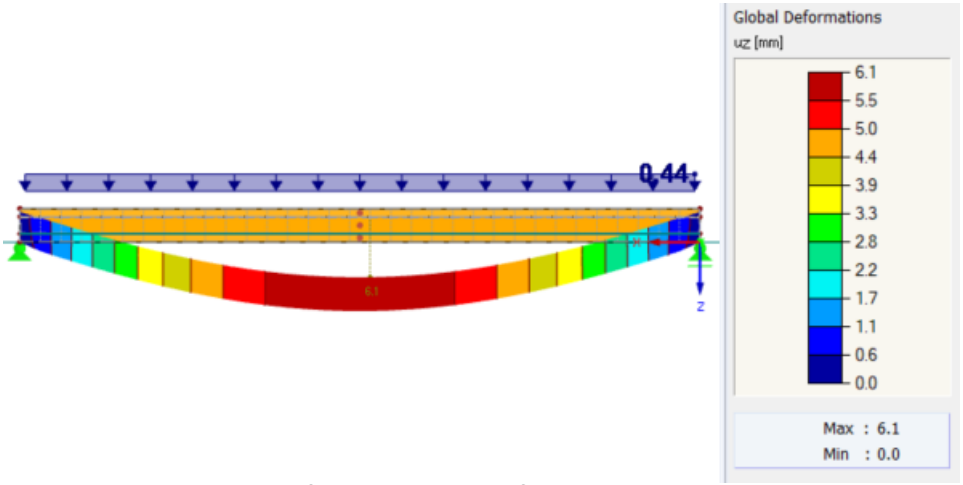

Figure E-36: Initial global deflection iteration 5 floor design 2 by permanent load

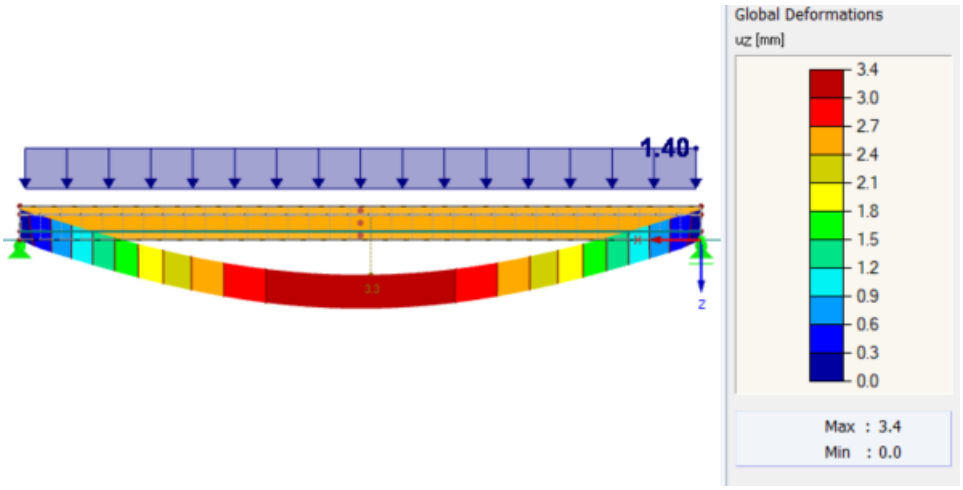

Figure E-37: Initial global deflection iteration 5 floor design 2 by variable surface load

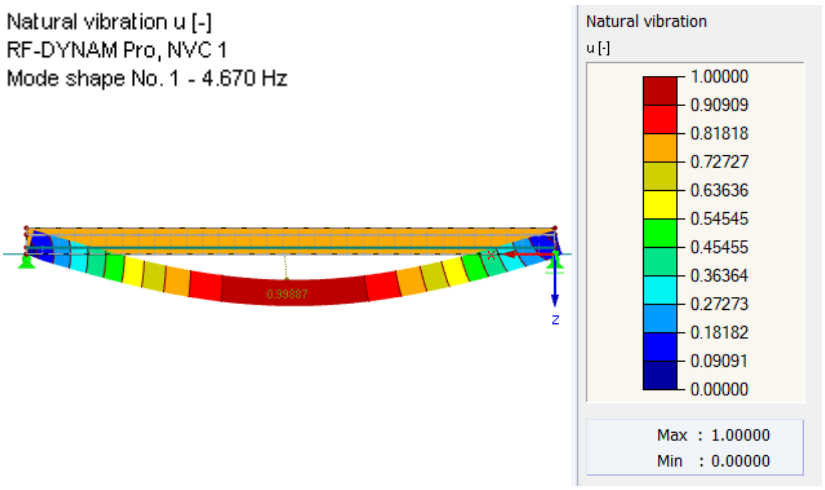

Figure E-38: First eigenfrequency iteration 5 floor design 2

The vibrational resistance is still above 1, shown in Table E-10. Therefore, the cross-section must increase to satisfy the requirement.

Table E-10: Unity check value floor design 2 iteration 5

Global deflection			**Vibrational resistance**		
u_{fin}	16.01	mm	f	4.67	Hz
u_{lim}	48.78	mm	f_{min}	5	Hz
UC	0.33		UC	1.07	

Iteration 6: 200 mm CLT plus 4 times 100x500 mm glulam ribs

Because the thickness of the sheathings cannot increase and increasing the rib width has very limited influence, the rib height is enlarged from 400 to 500 mm.

The resulting deflection and first eigenfrequency are presented in Figures E-39 to E-41.

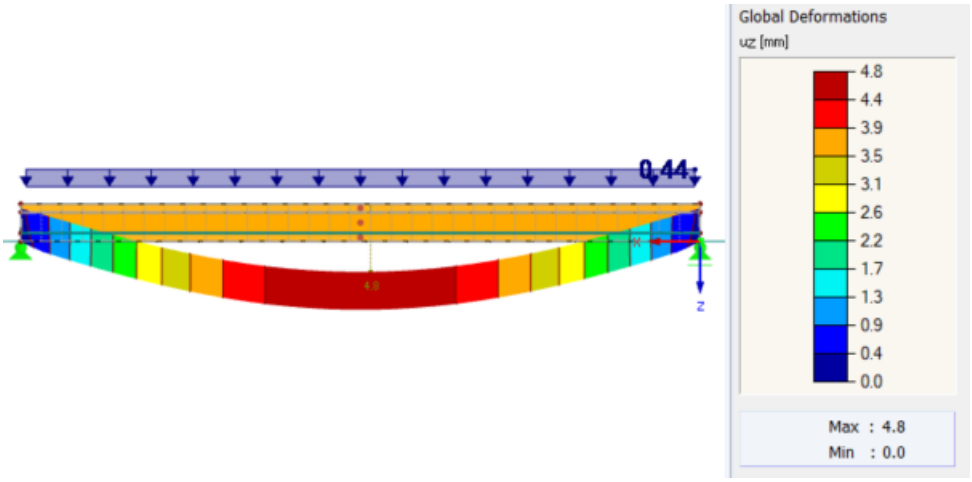

Figure E-39: Initial global deflection iteration 6 floor design 2 by permanent load

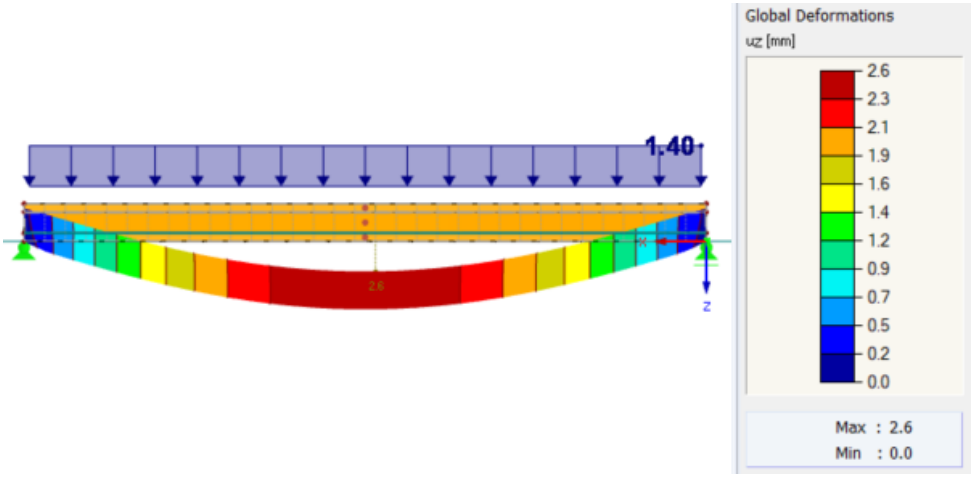

Figure E-40: Initial global deflection iteration 6 floor design 2 by variable surface load

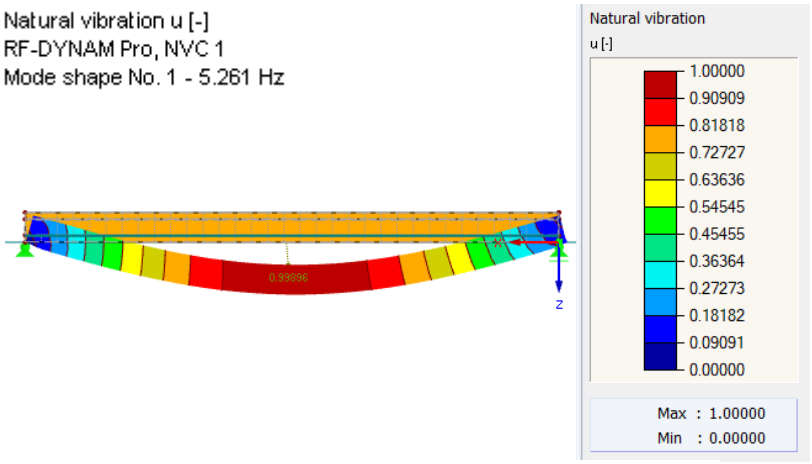

Figure E-41: First eigenfrequency iteration 6 floor design 2

Table E-11 shows that both unity check values are below or equal to 1, so this cross-section satisfies the requirements.

Table E-11: Unity check values floor design 2 iteration 6

Global deflection			**Vibrational resistance**		
u_{fin}	12.49	mm	f	5.26	Hz
u_{lim}	48.78	mm	f_{min}	5	Hz
UC	0.26		UC	0.95	

E.2.3: Floor design 3 - Prefab closed CLT plus glulam rib floor with concrete top layer

As stated in sub-paragraph 7.2.4, the floor is made of C30 for the CLT sheathings and GL32h for the glulam ribs. Tables B-7 and B-8 of Appendix B show strength and stiffness properties. Based on sub-paragraph 7.2.3, the global deflection and vibrational resistance will be the criteria checked for the closed CLT plus glulam rib floor over 16.26 meters. However, for the vibrational resistance, sub-paragraph 7.2.1. states the same resulting height as for floor design 2 will be assumed indicated. Figure E-42 shows that applying the same height with 50 mm of the height translated to concrete results in a minimum eigenfrequency of 4.97 Hz.

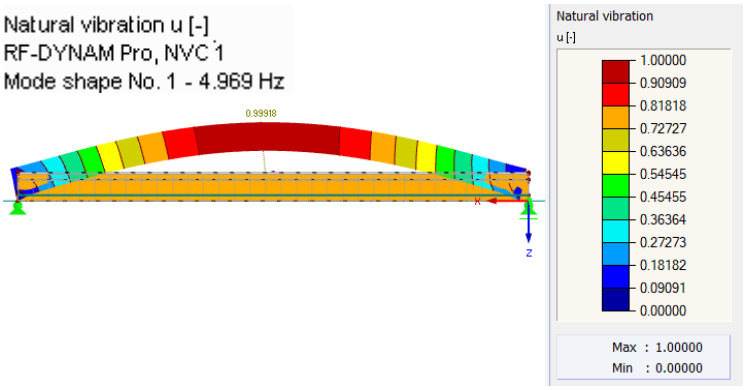

Figure E-42: First eigenfrequency floor design 3 h=900 mm

The minimum required reinforcement for a concrete layer with a thickness of 50 mm and strength class C50/60 is 0.82 cm^2/m, applying both directions with bars Ø5/150 (NVN-CEN/TS 19103, 2021). When this reinforcement is applied, the requirements about crack width are satisfied. This layout can be achieved for the applicable environmental classes. The floor can be variable wet and dry with de-icing salt, resulting in the following classes: XC4, XD3, and XF4. That gives a minimum cover of 25 mm for the applicable construction class S1 (NEN-EN 1992-1-1+C2/NB+A1, 2020).

For determining the lower bound of the floor design 3 height, the global deflection criterion will be checked.

Global deflection

According to Eurocode 1990, the limits should be applied for a timber-composite floor (NVN-CEN/TS 19103, 2021). That means the span of 16.26 meters, shown in Figure 7-9, results in a maximum final deflection of 48.78 mm.

Iteration 1: 100 mm CLT sheathings plus 4 times a 100x200mm glulam rib and 50 mm concrete layer

The dimensions of this iteration step will be used as a starting point in the iteration procedure because these dimensions were the largest for which floor design 2 does not satisfy the global deflection criterion. They have a sheathing thickness of 100 mm and a glulam rib height of 200 mm. Only the variable surface load will be considered because iteration 1 in E.2 shows that this load governs this floor layout.

The RFEM results of this first iteration are shown in Figures E-43 and E-44.

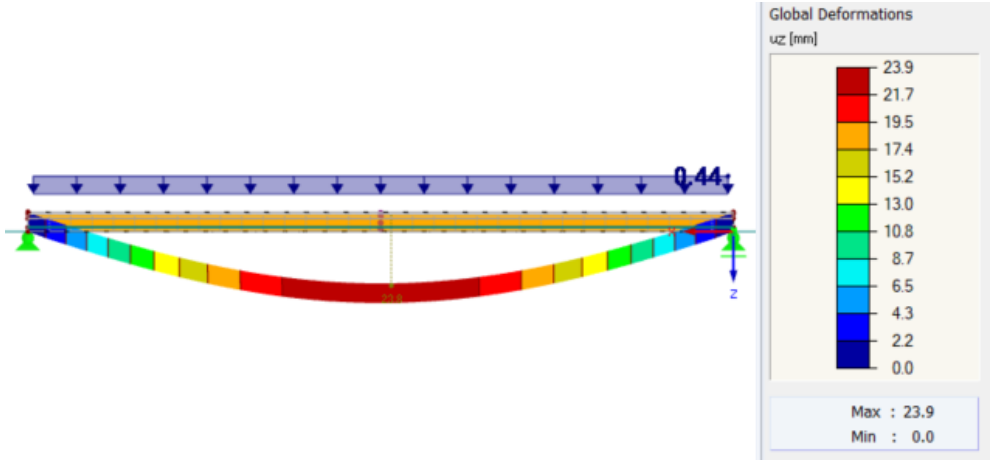

Figure E-43: Initial global deflection iteration 1 floor design 3 by permanent load

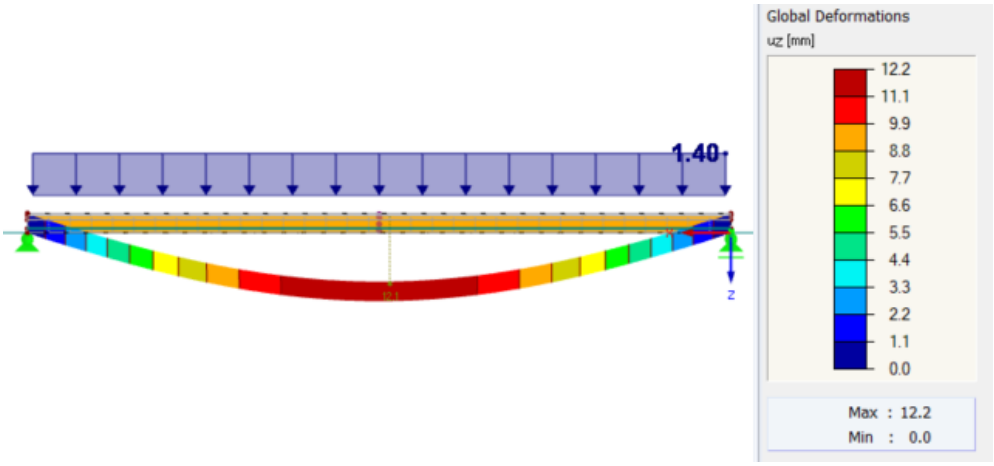

Figure E-44: Initial global deflection iteration 1 floor design 3 by variable surface load

Table E-12 shows that the unity check is above 1, so the cross-section should increase to satisfy the requirement of global deflection.

Table E-12: Unity check values floor design 3 iteration 1

Global deflection		
u_{fin}	61.08	mm
u_{lim}	48.78	mm
UC	1.25	

Iteration 2: 140 mm CLT sheathings plus 4 times a 100x220mm glulam rib and 50 mm concrete layer

The thickness of the sheathings is increased by 40 mm to 140 mm compared to iteration 1. The rib height is increased by 20 mm to 220 mm. Figures E-45 and E-46 present the deflections for this cross-section.

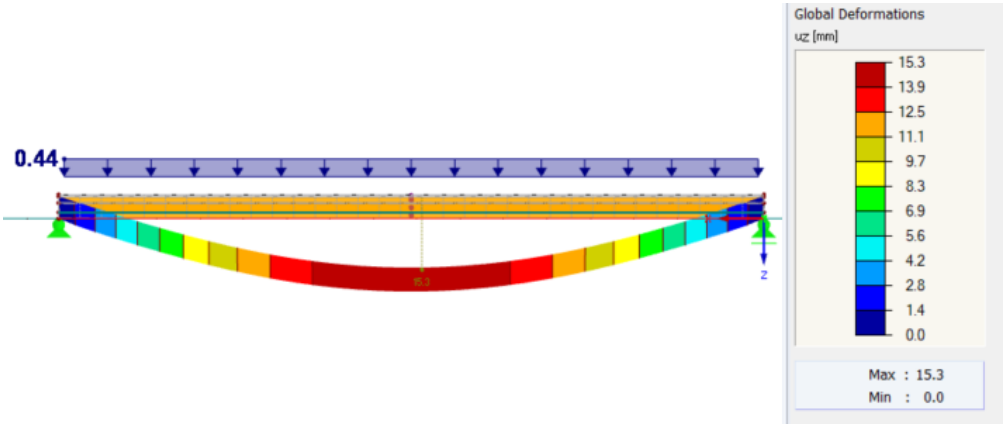

Figure E-45: Initial global deflection iteration 2 floor design 3 by permanent load

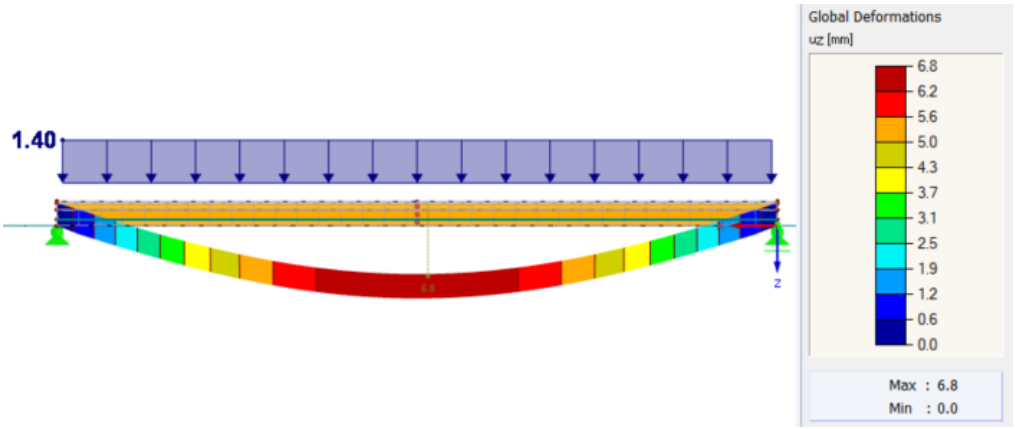

Figure E-46: Initial global deflection iteration 2 floor design 3 by variable surface load

The unity check value is presented in Table E-13. It is below, so the cross-sectional dimensions are sufficient. However, the height can probably be optimized because there is space between the unity check value of 0.77 and the limit of 1.

Table E-13: Unity check values floor design 3 iteration 2

Global deflection		
u_{fin}	37.6	mm
u_{lim}	48.78	mm
UC	0.77	

Iteration 3: 120 mm CLT sheathings plus 4 times a 100x220 glulam rib and 50 mm concrete

This third iteration has 20 mm smaller CLT sheathings compared to iteration 2. Figures E-47 and E-48 present the global deflections for this cross-section.

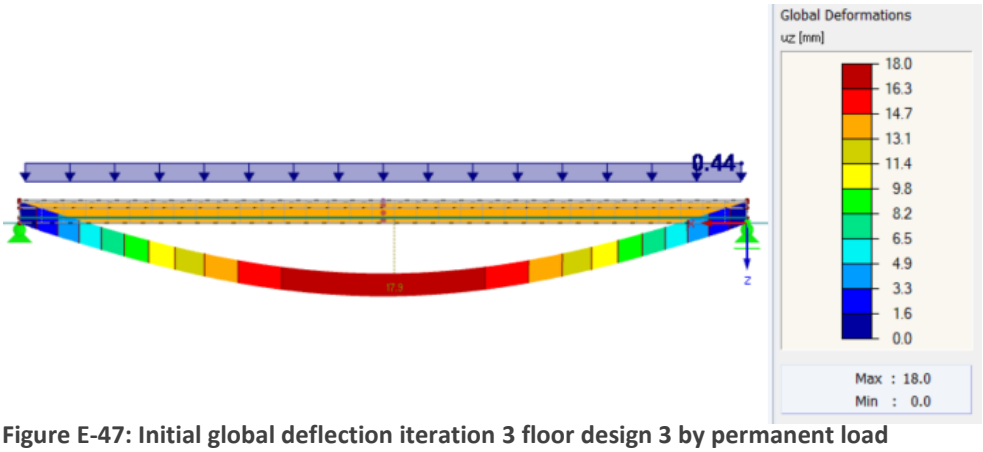

Figure E-47: Initial global deflection iteration 3 floor design 3 by permanent load

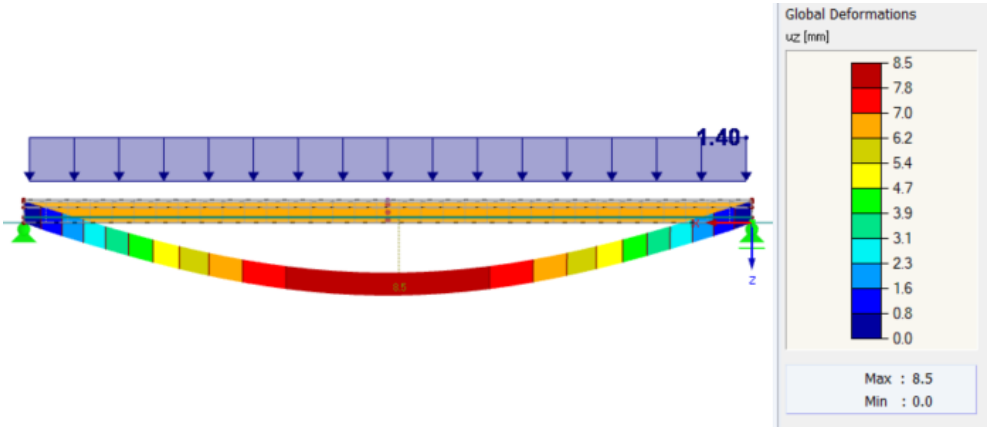

Figure E-48: Initial global deflection iteration 3 floor design 3 by variable surface load

From Table E-14, the unity check value of 0.92 means satisfying the requirement and close to 1. Next, a sheathing reduction is impossible because 100 mm thick sheathings result in a unity check above 1, shown in iteration 1. Therefore, this cross-section will be assumed to be the lower bound.

Table E-14: Unity check values floor design 3 iteration 3

Global deflection		
u_{fin}	44.98	mm
u_{lim}	48.78	mm
UC	0.92	

E.2.4: Floor design 4 - Prefab concrete floor

Sub-paragraph 7.2.5 indicates that the required verifications are global deflection, bending resistance, shear resistance, and crack width. Finally, the vibrational resistance will be checked for the completeness of the design. This chapter also provides the assumptions for the design.

Global deflection

Paragraph 7.2 states that the deflection limit is 0.003L. So, the maximum deflection (w_{max}) is 15 mm for a 5 meters span.

Equations E.1 to E.5 show how to calculate the maximum deflection (NEN-EN 1992-1-1+C2, 2011). Figure 3.1 in Eurocode 1992 provides the creep coefficient. This coefficient depends on multiple parameters. Because this is still a preliminary design, the average value of 3 is assumed because the range is from 0 to 6. Assume a strip of 1 meter, so b = 1000 mm. The prefab slab is a non-continuous member due to the limited element size and the non-monolithic connections that will be made to ensure re-mountability. Because the beam dimensions are still unknown, only the value for the height can be calculated in equation E.4. Because the effect of this assumption is limited to the total span of 5000 mm, this assumption is justified.

$$w[mm] = \frac{5 * q_{SLS}[\frac{N}{mm}] * L_{eff}^4[m^4]}{384 * E_{c,eff}[MPa] * I[mm^4]} \quad \text{(E.1)}$$

$$E_{c,eff}[MPa] = \frac{E_{cm}[MPa]}{1+\varphi_{eff}} \quad \text{(E.2)}$$

$$L_{eff}[m] = l[m] + a_1[m] + a_2[m] \quad \text{(E.3)}$$

$$a_1[m] = a_2[m] = \min\{\frac{1}{2} * h[m]; \frac{1}{2} * t[m]\} \quad \text{(E.4)}$$

$$I[mm^4] = \frac{1}{12} * b[mm] * h^3[mm^3] \quad \text{(E.5)}$$

The minimum required height is the parameter that should be investigated. This investigation is an iterative process because the load depends on the height. From Table E-15, a height of 180 mm is the minimum.

Table E-15: Global deflection verification results

b	1000	mm
h	180	mm
q_g	4.94	kN/m^2
q_q	2	kN/m^2
q_{sls}	6.34	kN/m
ϕ_{eff}	3	
$E_{c,eff}$	9250	MPa
a_1, a_2	90	mm
L_{eff}	5180	mm
w_{max}	15	mm
w	13.22	mm
UC	0.88	

Bending resistance

The first step in the bending resistance calculation is determining the occurring bending moment, given in equation E-6. This bending moment occurs due to the surface load plus the permanent load in Table 7-2.

$$M_{y,ULS}\left[\frac{kNm}{m}\right] = \frac{1}{8} * q_{ULS}\left[\frac{kN}{m^2}\right] * l_{eff}^2[m^2]] \quad \text{(E.6)}$$

The required amount of reinforcement in the primary direction should be calculated by equations E.7 to E.9. Reinforcement of B500 will be assumed with a design yield strength of 435 MPa given in Appendix B.3. For a one-way slab, the amount of reinforcement in the secondary direction is 20% of the main reinforcement. The minimum thickness of the cover depends on multiple parameters, but 30 mm is considered based on the concrete floor design of the ModuPark concept indicated by BNPC.

$$A_{s,x}\left[\frac{mm^2}{m}\right] = \frac{M_{y,ULS}[\frac{kNm}{m}]}{z]mm]*f_{yd}[MPa]} \quad \text{(E.7)}$$

$$z[mm] = 0.9 * d[mm] \quad \text{(E.8)}$$

$$d[mm] = h[mm] - c_{min}[mm] - \frac{\emptyset}{2}[mm] \quad \text{(E.9)}$$

Equation E.10 provides the method to determine the required spacing for the assumed rebar diameter (NEN-EN 1992-1-1+C2, 2011).

$$s[mm] = \frac{1000}{\frac{4*A_s\left[\frac{mm^2}{m}\right]}{\pi*\emptyset^2[mm^2]}} \quad \text{(E.10)}$$

Table E-16 shows that a rebar of 12 mm with a spacing of rounded 212 mm is sufficient. So, the height of h=180 mm can be sufficiently strong in bending.

Table E-16: Bending resistance Ø12 mm h=160 mm

L_{eff}	5180	mm
q_{ULS}	8.93	kN/m^2
$M_{y,ULS}$	29.94	kNm/m
c_{min}	30	mm
Ø	12	mm
d	144	mm
z	129.6	mm
$A_{s,x}$	531.17	mm^2
$A_{s,y}$	106.23	mm^2
s	212.92	mm

Shear resistance

Equation E.11 calculates the acting shear force per cross-sectional area.

$$\upsilon_{ed}\left[\frac{N}{mm^2}\right] = \frac{0.5*q_{ULS}[\frac{N}{mm^2}]*L_{eff}[mm]}{d[mm]} \quad \text{(E.11)}$$

Then, the maximum shear resistance of the concrete without shear reinforcement should be calculated according to equations E.12 to E.15 (NEN-EN 1992-1-1+C2, 2011). The verification is per meter width, so parameter b is 1000 mm.

$$\upsilon_{rd,c}\left[\frac{N}{mm^2}\right] = 0.12 * k * \left(100 * \rho * f_{ck}\left[\frac{N}{mm^2}\right]\right)^{\frac{1}{3}} \quad \text{(E.12)}$$

$$k = 1 + \sqrt{\frac{200[mm]}{d[mm]}} \leq 2 \quad \text{(E.13)}$$

$$\rho = \sqrt{\rho_x * \rho_y} \quad \text{(E.14)}$$

$$\rho_i = \frac{A_{s,i}[mm^2]}{b[mm]*d[mm]} \quad \text{(E.15)}$$

Table E-17 provides the results of the above equations. The concrete shear resistance for a C50/60 strength class is larger than the acting shear for stress. Because it is a prefab concrete floor, high strength classes can be achieved due to the closed production environment.
Concluding, this cross-section is sufficient for shear resistance.

Table E-17: Results shear resistance h=90 mm

υ_{ed}	0.16	N/mm^2
k	2	
ρ_x	0.0037	
ρ_x	0.00074	
ρ	0.0017	
f_{ck}	50	MPa
$\upsilon_{rd,c}$	0.48	N/mm^2
UC	0.33	

Crack width

Third, the crack width limitation is considered according to (NEN-EN 1992-1-1+C2, 2011). The first check is to determine if cracking will occur. That means if the acting bending moment is larger than

the cracking bending moment, as presented in equation E.16. To perform this check, equations E.17 to E.19 should be applied.

$$M_{y,SLS}\left[\frac{kNm}{m}\right] \leq M_{cr}\left[\frac{kNm}{m}\right] \; no\; cracking \tag{E.16}$$

$$M_{y,SLS}\left[\frac{kNm}{m}\right] = \frac{1}{8} * q_{SLS}\left[\frac{kN}{m^2}\right] * l_{eff}^2[m^2] \tag{E.17}$$

$$f_{ctm,fl}[MPa] = \max\left\{\left(1.6 - \frac{h[mm]}{1000}\right) * f_{ctm}[MPa]; f_{ctm}[MPa]\right\} \tag{E.18}$$

$$M_{cr}\left[\frac{Nmm}{m}\right] = \frac{b[mm]*h^2[mm^2]}{6} * f_{ctm,fl}[MPa] \tag{E.19}$$

Table E-18 shows no cracking will occur due to the higher M_{cr} than $M_{y,sls}$. So, the height of 180 mm is also sufficient for crack control in a C50/60 prefab concrete floor.

Table E-18: Check cracking bending moment

L_{eff}	5180	mm
q_{SLS}	6.34	kN/m^2
$M_{y,sls}$	21.23	kNm/m
f_{ctm}	4.1	MPa
$f_{ctm,fl}$	5.82	MPa
M_{cr}	31.44	kNm/m

Vibrational resistance

To check all floor systems for vibrational resistance. Figure E-49 shows the first eigenfrequency of the prefab concrete floor system. With a first eigenfrequency of 8 Hz, this floor system satisfies the requirement of 5 Hz.

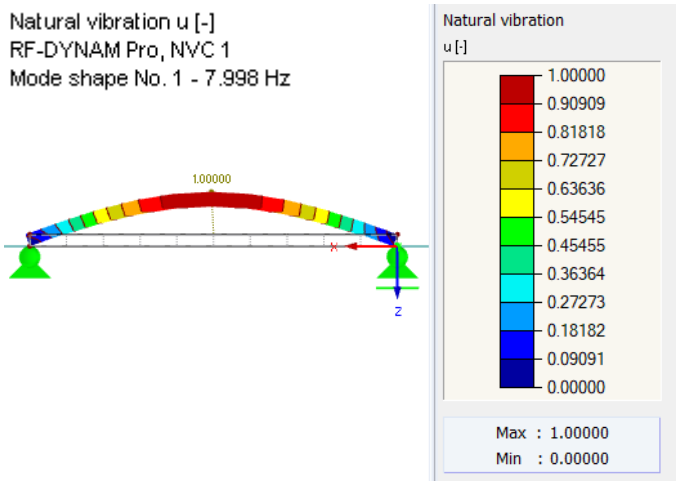

Figure E-49: First eigenfrequency prefab concrete floor

E.3: Preliminary supporting beam dimensioning

From the floor system, a line load is acting on the supporting beam. This load creates bending and deflection. As mentioned in 7.2.1, there are only vertical loads. Therefore, bending stress and global deflection are the only criteria for the supporting beam.

The RFEM models provide the permanent and variable load from the floor. Those surface loads will be multiplied by the full span length to get the line load per beam. In addition, the self-weight of the beam also results in a vertical load. Equations B.1 and B.2 of Appendix B.1 will be used to determine the total ultimate and serviceability limit state.

Table E-19 shows the structural characteristics of a BauBuche beam, and Table B-7 of the glulam beam.

Table E-19: Structural characteristics GL75 (*European Technical Assessment; ETA-14/0354*, 2018)

$F_{m,k}$	75 MPa
$E_{0,mean}$	16800 MPa
$E_{0,05}$	15300 MPa
ρ_{mean}	800 kg/m^3

For optimizing the height, the width of the beams is taken as the maximum. This results in the largest cross-sectional area and moment of inertia possible for that height of the beam.
For a Baubuche beam, the width is maximally 300 mm. In addition, the possible heights range between 80 mm and 1360 mm with steps of 40 mm(*Product Overview, Tolerances and Finishes*, n.d.). Next, the maximum width of a glulam beam is 300 mm (*Gelamineerde Houtconstructies-Toepassing van Het Materiaal Voor Grote Overspanningen*, n.d.). Furthermore, a lamella thickness of 40 mm, comparable with BauBuche, is assumed.

The height factor is required if the beam height exceeds 600 mm for laminated beams. This factor is indicated in equation E.20.

$$k_h = min\begin{cases}\left(\frac{600}{h}\right)^{0.1} \\ 1.1\end{cases} \tag{E.20}$$

Bending stress

Sub-paragraph 7.2.6 states that the bending will only be on the strong axis. Dividing this value by the section modulus gives the required bending stress.
Because it is a simply supported beam, the maximum bending moment can be calculated by equation E.21.

$$M[kNm] = \frac{1}{8} * q[\frac{kN}{m}] * l^2[m^2] \tag{E.21}$$

Global deflection

For a simply supported beam, the maximum deflection should be calculated by equation E.22. As mentioned in 7.2.6, equations B.5 to B.8 from Appendix B must be used to calculate the final deflection.

$$u[mm] = \frac{5}{384} * \frac{q[\frac{N}{mm}]*l^4[mm]}{E[MPa]*I[mm^4]} \tag{E.22}$$

E.3.1: Floor design 1 - CLT floor

The length of the floor is 5 meters. Table E-20 shows the resulting vertical line loads on the supporting beams of 16.26 meters from the RFEM model of the final iteration. Two adjacent grids share one beam, as mentioned in sub-paragraph 7.2.6.

Table E-20: Loads from RFEM model floor design 1

q_g	5.42 kN/m
q_q	10 kN/m

Iteration 1: beams h=960 mm

Based on the reference project of Studen with a comparable floor system (Appendix A.3). The same beam height of 960 mm is taken as the starting point. This height can also be achieved with a lamella thickness of 40 mm.

Table E-21 shows this case's loads, deflections, bending moments and unity checks for both beams. The unity checks of the glulam and BauBuche beams are above 1. Therefore, the cross-sections should be enlarged.

Table E-21: Loads and unity check values beams iteration 1 floor design

BauBuche beam 300x960								
loads			Bending stress			Global deflection		
$q_{g,floor}$	5.42	kN/m	M_{ed}	802.05	kNm	$u_{inst,g}$	18.92	mm
$q_{g,beam}$	2.30	kN/m	$\sigma_{m,y,d}$	17.41	MPa	$u_{inst,q}$	17.15	mm
$q_{g,tot}$	7.72	kN/m	$f_{m,d}$	45.80	MPa	$u_{fin,g}$	34.05	mm
$q_{q,f}$	10	kN/m	UC	0.38		$u_{fin,q}$	25.38	mm
$q_{tot,SLS}$	14.72	kN/m				$u_{fin,tot}$	59.43	mm
$q_{tot,ULS}$	24.27	kN/m				u_{lim}	48.78	mm
						UC	1.22	
Glulam beam 300x960								
Loads			Bending stress			Global deflection		
$q_{g,floor}$	5.42	kN/m	M_{ed}	766.64	kNm	$u_{inst,g}$	19.80	mm
$q_{g,beam}$	1.41	kN/m	$\sigma_{m,y,d}$	16.64	MPa	$u_{inst,q}$	20.29	mm
$q_{g,tot}$	6.83	kN/m	$f_{m,d}$	19.54	MPa	$u_{fin,g}$	35.63	mm
$q_{q,f}$	10	kN/m	UC	0.85		$u_{fin,q}$	30.02	mm
$q_{tot,SLS}$	13.83	kN/m				$u_{fin,tot}$	65.65	mm
$q_{tot,ULS}$	23.20	kN/m				u_{lim}	48.78	mm
						UC	1.35	

Iteration 2: beams h=1040 mm

The height of the beams is increased by 80 to a total value of 1040 mm.

Concluding from the unity check values of Table E-22, the glulam beam resistance is insufficient, with a unity check value of 1.07. The BauBuche beam height is optimal because of the governing unity check of 0.97.

Table E-22: Loads and unity check values beams iteration 2 floor design 1

BauBuche beam 300x1040								
loads			Bending stress			Global deflection		
$q_{g,floor}$	5.42	kN/m	M_{ed}	809.66	kNm	$u_{inst,g}$	15.25	mm
$q_{g,beam}$	2.50	kN/m	$\sigma_{m,y,d}$	14.97	MPa	$u_{inst,q}$	13.49	mm
$q_{g,tot}$	7.92	kN/m	$f_{m,d}$	45.43	MPa	$u_{fin,g}$	27.45	mm
$q_{q,f}$	10	kN/m	UC	0.33		$u_{fin,q}$	19.96	mm
$q_{tot,SLS}$	14.92	kN/m				$u_{fin,tot}$	47.41	mm
$q_{tot,ULS}$	24.50	kN/m				u_{lim}	48.78	mm
						UC	0.97	
Glulam beam 300x1040								
Loads			Bending stress			Global deflection		
$q_{g,floor}$	5.42	kN/m	M_{ed}	771.30	kNm	$u_{inst,g}$	15.84	mm
$q_{g,beam}$	1.53	kN/m	$\sigma_{m,y,d}$	14.26	MPa	$u_{inst,q}$	15.95	mm
$q_{g,tot}$	6.95	kN/m	$f_{m,d}$	19.38	MPa	$u_{fin,g}$	28.51	mm
$q_{q,f}$	10	kN/m	UC	0.74		$u_{fin,q}$	23.61	mm
$q_{tot,SLS}$	13.95	kN/m				$u_{fin,tot}$	52.12	mm
$q_{tot,ULS}$	23.34	kN/m				u_{lim}	48.78	mm
						UC	1.07	

Iteration 3: Glulam beam h= 1080 mm

Iteration 3 uses a height of 1080 mm for the glulam beam. This height results in the loads, global deflection, bending moments and resulting unity checks of Table E-23. The cross-section is most suitable because the unity check of global deflection is 0.96.

Table E-23: Loads and unity check values glulam beam iteration 3 floor design 1

Glulam beam 300x1080								
Loads			Bending stress			Global deflection		
$q_{g,floor}$	5.42	kN/m	M_{ed}	773.64	kNm	$u_{inst,g}$	14.26	mm
$q_{g,beam}$	1.59	kN/m	$\sigma_{m,y,d}$	13.27	MPa	$u_{inst,q}$	14.25	mm
$q_{g,tot}$	7.01	kN/m	$f_{m,d}$	19.31	MPa	$u_{fin,g}$	25.67	mm
$q_{q,f}$	10	kN/m	UC	0.69		$u_{fin,q}$	21.09	mm
$q_{tot,SLS}$	14.01	kN/m				$u_{fin,tot}$	46.76	mm
$q_{tot,ULS}$	23.41	kN/m				u_{lim}	48.78	mm
						UC	0.96	

E.3.2: Floor design 2 - Closed CLT plus glulam rib floor

The length of the floor is 16.26 meters. Table E-24 shows the resulting vertical line loads on the supporting beam of 5 meters from the RFEM model of the final iteration.

Table E-24: Loads from RFEM model floor design 2

q_g	42.56 kN/m
q_q	32.52 kN/m

Iteration 1: beams h= 520mm

A height of 520 mm is assumed because a lower height compared to floor design 1 is most logical due to the lower span of the beam. This height is dividable by a lamella thickness of 40 mm, as stated in E.6.1.

Table E-25 presents the loads, global deflections, bending moment, and unity check values. Concluding, both governing unity checks are above 1. So, the cross-sectional heights should be enlarged.

Table E-25: Loads and unity check values beams iteration 1 floor design 2

BauBuche beam 300x520								
loads			Bending stress			Global deflection		
$q_{g,floor}$	42.56	kN/m	M_{ed}	316.72	kNm	$u_{inst,g}$	6.04	mm
$q_{g,beam}$	1.25	kN/m	$\sigma_{m,y,d}$	23.43	MPa	$u_{inst,q}$	3.14	mm
$q_{g,tot}$	43.81	kN/m	$f_{m,d}$	48.00	MPa	$u_{fin,g}$	10.87	mm
$q_{q,f}$	32.52	kN/m	UC	0.49		$u_{fin,q}$	4.64	mm
$q_{tot,SLS}$	66.57	kN/m				$u_{fin,tot}$	15.51	mm
$q_{tot,ULS}$	101.35	kN/m				u_{lim}	15	mm
						UC	1.03	
Glulam beam 300x520								
Loads			Bending stress			Global deflection		
$q_{g,floor}$	42.56	kN/m	M_{ed}	314.90	kNm	$u_{inst,g}$	7.06	mm
$q_{g,beam}$	0.76	kN/m	$\sigma_{m,y,d}$	23.29	MPa	$u_{inst,q}$	3.71	mm
$q_{g,tot}$	43.32	kN/m	$f_{m,d}$	20.48	MPa	$u_{fin,g}$	12.71	mm
$q_{q,f}$	32.52	kN/m	UC	1.14		$u_{fin,q}$	5.49	mm
$q_{tot,SLS}$	66.09	kN/m				$u_{fin,tot}$	18.21	mm
$q_{tot,ULS}$	100.77	kN/m				u_{lim}	15	mm
						UC	1.21	

Iteration 2: beams h= 560 mm

Compared to iteration 1, the height is increased to 560 mm. This new cross-section leads to the global deflection lines and the bending moments of Table E-26. The resulting unity check values are also provided in Table E-26. Both types of beams have sufficient resistance, so a height of 560 mm is most optimal for both alternatives.

Table E-26: Loads and unity check values beams iteration 2 floor design 2

BauBuche beam 300x560								
loads			Bending stress			Global deflection		
$q_{g,floor}$	42.56	kN/m	M_{ed}	317.08	kNm	$u_{inst,g}$	4.84	mm
$q_{g,beam}$	1.34	kN/m	$\sigma_{m,y,d}$	20.22	MPa	$u_{inst,q}$	2.51	mm
$q_{g,tot}$	43.90	kN/m	$f_{m,d}$	48.00	MPa	$u_{fin,g}$	8.72	mm
$q_{q,f}$	32.52	kN/m	UC	0.42		$u_{fin,q}$	3.72	mm
$q_{tot,SLS}$	66.67	kN/m				$u_{fin,tot}$	12.44	mm
$q_{tot,ULS}$	101.46	kN/m				u_{lim}	15	mm
						UC	0.83	
Glulam beam 300x560								
Loads			Bending stress			Global deflection		
$q_{g,floor}$	42.56	kN/m	M_{ed}	315.12	kNm	$u_{inst,g}$	5.66	mm
$q_{g,beam}$	0.82	kN/m	$\sigma_{m,y,d}$	20.10	MPa	$u_{inst,q}$	2.97	mm
$q_{g,tot}$	43.38	kN/m	$f_{m,d}$	20.48	MPa	$u_{fin,g}$	10.19	mm
$q_{q,f}$	32.52	kN/m	UC	0.98		$u_{fin,q}$	4.40	mm
$q_{tot,SLS}$	66.15	kN/m				$u_{fin,tot}$	14.59	mm
$q_{tot,ULS}$	100.84	kN/m				u_{lim}	15	mm
						UC	0.97	

E.3.3: Floor design 3 - Closed CLT plus glulam rib floor with concrete top layer

The length of the floor is 16.26 meters. Table E-27 shows the resulting vertical line loads on the supporting beam of 5 meters from the final cross-section of E.2.3.
Table E-28 gives the line loads for the adjusted timber rib floor, as indicated in 7.2.4.
Sub-paragraph 7.2.4 shows that this floor system's height is between 510 and 900 mm.
So, the resulting beam height for the maximum and minimum floor height will be determined, which allows combining the maximum and minimum floor height and beam height.

Table E-27: Loads from RFEM model floor design 3 height 510 mm

q_g	48.30 kN/m
q_q	32.52 kN/m

Table E-28: Loads from RFEM model floor design 3 height 900 mm

q_g	60.70 kN/m
q_q	32.52 kN/m

First, the beam for a height of 510 mm will be calculated. Afterwards, the dimensions of the beam for a floor height of 900 mm.

Iteration 1 h=510 mm: beams h= 560 mm

The resulting glulam beam height of floor design 2, see Appendix E.3.2, is applied as a starting point. It results in a most optimal unity check of 0.91 for the BauBuche beam, shown in Table E-29. On the other hand, the glulam beam is insufficient for this beam height. Therefore, an increase in height will be applied in the next iteration step for the glulam beam.

Table E-29: Loads and unity check values beams iteration 1 floor design 3 height 510 mm

BauBuche beam 300x560								
loads			Bending stress			Global deflection		
$q_{g,floor}$	48.30	kN/m	M_{ed}	338.69	kNm	$u_{inst,g}$	5.48	mm
$q_{g,beam}$	1.34	kN/m	$\sigma_{m,y,d}$	21.59	MPa	$u_{inst,q}$	2.51	mm
$q_{g,tot}$	49.64	kN/m	$f_{m,d}$	48.00	MPa	$u_{fin,g}$	9.86	mm
$q_{q,f}$	32.52	kN/m	UC	0.45		$u_{fin,q}$	3.72	mm
$q_{tot,SLS}$	72.14	kN/m				$u_{fin,tot}$	13.58	mm
$q_{tot,ULS}$	108.35	kN/m				u_{lim}	15	mm
						UC	0.91	
Glulam beam 300x560								
Loads			Bending stress			Global deflection		
$q_{g,floor}$	48.30	kN/m	M_{ed}	336.65	kNm	$u_{inst,g}$	6.41	mm
$q_{g,beam}$	0.82	kN/m	$\sigma_{m,y,d}$	21.47	MPa	$u_{inst,q}$	2.97	mm
$q_{g,tot}$	49.12	kN/m	$f_{m,d}$	20.48	MPa	$u_{fin,g}$	11.54	mm
$q_{q,f}$	32.52	kN/m	UC	1.05		$u_{fin,q}$	4.40	mm
$q_{tot,SLS}$	71.89	kN/m				$u_{fin,tot}$	15.94	mm
$q_{tot,ULS}$	107.73	kN/m				u_{lim}	15	mm
						UC	1.06	

Iteration 2 h= 510 mm: glulam beam h= 600 mm

As mentioned in iteration 1, a larger height of the glulam beam should be checked. This minimal increase results in a height of 600 mm. The loads and unity checks are given in Table E-30. The governing unity check is below 1 for the glulam beam, so this is the optimal height for the glulam beam.

Table E-30: Loads and unity check values glulam beam iteration 2 floor design 3 height 510 mm

Glulam beam 300x600								
Loads			Bending stress			Global deflection		
$q_{g,floor}$	48.03	kN/m	M_{ed}	336.87	kNm	$u_{inst,g}$	5.22	mm
$q_{g,beam}$	0.88	kN/m	$\sigma_{m,y,d}$	18.72	MPa	$u_{inst,q}$	2.42	mm
$q_{g,tot}$	49.18	kN/m	$f_{m,d}$	20.48	MPa	$u_{fin,g}$	9.40	mm
$q_{q,f}$	32.56	kN/m	UC	0.91		$u_{fin,q}$	3.58	mm
$q_{tot,SLS}$	71.95	kN/m				$u_{fin,tot}$	12.97	mm
$q_{tot,ULS}$	107.80	kN/m				u_{lim}	15	mm
						UC	0.86	

Now, the beam of the maximum floor design 3 is determined.

Iteration 1 h=900 mm: beams h= 600 mm

From Tables E-27 and E-28, the weight for the 900 mm floor is larger than for a 510 mm floor element. So, a height of 600 mm is assumed as a starting point in this iteration process.

Table E-31 shows that only the unity check of the BauBuche beam is below and close to 1. So, only the height of the glulam beam should be improved. The governing unity check is 1.04 for the glulam beam.

Table E-31: Loads and unity check values beam iteration 1 floor design 3 height 900 mm

BauBuche beam 300x600								
loads			Bending stress			Global deflection		
$q_{g,floor}$	60.70	kN/m	M_{ed}	385.46	kNm	$u_{inst,g}$	5.57	mm
$q_{g,beam}$	1.44	kN/m	$\sigma_{m,y,d}$	21.41	MPa	$u_{inst,q}$	2.04	mm
$q_{g,tot}$	62.14	kN/m	$f_{m,d}$	48.00	MPa	$u_{fin,g}$	10.03	mm
$q_{q,f}$	32.52	kN/m	UC	0.45		$u_{fin,q}$	3.02	mm
$q_{tot,SLS}$	84.90	kN/m				$u_{fin,tot}$	13.06	mm
$q_{tot,ULS}$	123.35	kN/m				u_{lim}	15	mm
						UC	0.87	
Glulam beam 300x600								
Loads			Bending stress			Global deflection		
$q_{g,floor}$	60.70	kN/m	M_{ed}	383.37	kNm	$u_{inst,g}$	6.54	mm
$q_{g,beam}$	0.88	kN/m	$\sigma_{m,y,d}$	21.30	MPa	$u_{inst,q}$	2.42	mm
$q_{g,tot}$	61.58	kN/m	$f_{m,d}$	20.48	MPa	$u_{fin,g}$	11.76	mm
$q_{q,f}$	32.52	kN/m	UC	1.04		$u_{fin,q}$	3.58	mm
$q_{tot,SLS}$	84.35	kN/m				$u_{fin,tot}$	15.34	mm
$q_{tot,ULS}$	122.68	kN/m				u_{lim}	15	mm
						UC	1.02	

Iteration 2 h=900 mm: Glulam h= 640 mm

The height is increased by a minimum of 40 mm for the glulam compared to iteration 1, resulting in 6400 mm. The unity checks of Table E-32 are above 1 for the BauBuche beam. That makes this cross-most optimal.

Table E-32: Loads and unity check values beams iteration 2 floor design 3 height 900 mm

Glulam beam 300x640								
loads			Bending stress			Global deflection		
$q_{g,floor}$	60.70	kN/m	M_{ed}	383.59	kNm	$u_{inst,g}$	5.39	mm
$q_{g,beam}$	0.94	kN/m	$\sigma_{m,y,d}$	18.73	MPa	$u_{inst,q}$	1.99	mm
$q_{g,tot}$	61.64	kN/m	$f_{m,d}$	20.35	MPa	$u_{fin,g}$	9.70	mm
$q_{q,f}$	32.52	kN/m	UC	0.92		$u_{fin,q}$	2.95	mm
$q_{tot,SLS}$	84.40	kN/m				$u_{fin,tot}$	12.65	mm
$q_{tot,ULS}$	122.75	kN/m				u_{lim}	15	mm
						UC	0.84	

E.3.4: Floor design 4 - Prefab concrete floor

The length of the floor is 5 meters. Table E-33 shows the resulting vertical line loads on the supporting beam of 16.26 meters. Table E-15 shows the permanent load of the slab and variable load for the resulting height of 180 mm, including the indicated permanent load in Table 7-2.

Table E-33: Loads from floor design 4

q_g	24.7 kN/m
q_q	10 kN/m

Iteration 1: beams h= 1320 mm

This floor design has the same global layout as floor design 1. However, the load from self-weight is about five times larger compared to floor design 1 due to the use of concrete. The optimal cross-section of floor design 1 is 300x1000 mm and 300x1040. Due to the four times larger self-weight, the first assumption of this iteration procedure is 300x13200 mm.

Table E-34 presents this iteration step's loads, global deflection, bending moment, and unity check values. The governing unity check of both beams is above 1, so both beams are taken into iteration 2 for applying increased cross-sections.

Table E-34: Loads and unity check values beams iteration 1 floor design 4

BauBuche beam 300x1320								
loads			Bending stress			Global deflection		
$q_{g,floor}$	24.70	kN/m	M_{ed}	1600.92	kNm	$u_{inst,g}$	26.26	mm
$q_{g,beam}$	3.17	kN/m	$\sigma_{m,y,d}$	18.38	MPa	$u_{inst,g}$	6.60	mm
$q_{g,tot}$	27.87	kN/m	$f_{m,d}$	44.36	MPa	$u_{fin,g}$	47.26	mm
$q_{q,f}$	10	kN/m	UC	0.41		$u_{fin,q}$	9.76	mm
$q_{tot,SLS}$	34.87	kN/m				$u_{fin,tot}$	57.03	mm
$q_{tot,ULS}$	48.44	kN/m				u_{lim}	48.78	mm
						UC	1.17	
Glulam beam 300x1320								
Loads			Bending stress			Global deflection		
$q_{g,floor}$	24.70	kN/m	M_{ed}	1552.25	kNm	$u_{inst,g}$	29.70	mm
$q_{g,beam}$	1.91	kN/m	$\sigma_{m,y,d}$	17.82	MPa	$u_{inst,g}$	7.80	mm
$q_{g,tot}$	26.64	kN/m	$f_{m,d}$	18.93	MPa	$u_{fin,g}$	53.45	mm
$q_{q,f}$	10	kN/m	UC	0.94		$u_{fin,q}$	11.55	mm
$q_{tot,SLS}$	33.64	kN/m				$u_{fin,tot}$	65.00	mm
$q_{tot,ULS}$	46.97	kN/m				u_{lim}	48.78	mm
						UC	1.33	

Iteration 2: beams h=1400 mm

The height for the beams is improved by changing the height from 1200 to 14000 mm. Table E-35 presents the loads, deflections, bending moments, and resulting unity checks. The governing unity check is 0.99 for the BauBuche beam, meaning this cross-section is the most optimal. For the glulam beam, the governing unity check is 1.12. So, a further height increase is necessary.

Table E-35: Loads and unity check values beams iteration 2 floor design 4

BauBuche beam 300x1400								
loads			Bending stress			Global deflection		
$q_{g,floor}$	24.70	kN/m	M_{ed}	1608.53	kNm	$u_{inst,g}$	22.16	mm
$q_{g,beam}$	3.36	kN/m	$\sigma_{m,y,d}$	16.41	MPa	$u_{inst,g}$	5.53	mm
$q_{g,tot}$	28.06	kN/m	$f_{m,d}$	44.10	MPa	$u_{fin,g}$	39.89	mm
$q_{q,f}$	10	kN/m	UC	0.37		$u_{fin,q}$	8.18	mm
$q_{tot,SLS}$	35.06	kN/m				$u_{fin,tot}$	48.07	mm
$q_{tot,ULS}$	48.67	kN/m				u_{lim}	48.78	mm
						UC	0.99	

Glulam beam 300x1400								
Loads			Bending stress			Global deflection		
$q_{g,floor}$	24.70	kN/m	M_{ed}	1556.90	kNm	$u_{inst,g}$	25.00	mm
$q_{g,beam}$	2.06	kN/m	$\sigma_{m,y,d}$	15.89	MPa	$u_{inst,g}$	6.54	mm
$q_{g,tot}$	26.76	kN/m	$f_{m,d}$	18.82	MPa	$u_{fin,g}$	45.00	mm
$q_{q,f}$	10	kN/m	UC	0.84		$u_{fin,q}$	9.68	mm
$q_{tot,SLS}$	33.76	kN/m				$u_{fin,tot}$	54.68	mm
$q_{tot,ULS}$	47.11	kN/m				u_{lim}	48.78	mm
						UC	1.12	

Iteration 3: Glulam beam h=1480 mm

As mentioned in iteration 2, further improvement in resistance should be applied for the glulam. The increased height in iteration 3 is 1480 mm.

Table E-36 presents the loads, global deflections, bending moment, and unity checks. Concluding, the governing unity check is below 1 for the glulam beam, which means this height is minimally required.

Table E-36: Loads and unity check values glulam beam iteration 3 floor design 4

Glulam beam 300x1480								
Loads			Bending stress			Global deflection		
$q_{g,floor}$	24.70	kN/m	M_{ed}	1561.56	kNm	$u_{inst,g}$	21.26	mm
$q_{g,beam}$	2.18	kN/m	$\sigma_{m,y,d}$	14.26	MPa	$u_{inst,g}$	5.54	mm
$q_{g,tot}$	26.88	kN/m	$f_{m,d}$	18.71	MPa	$u_{fin,g}$	38.26	mm
$q_{q,f}$	10	kN/m	UC	0.76		$u_{fin,q}$	8.19	mm
$q_{tot,SLS}$	33.88	kN/m				$u_{fin,tot}$	46.45	mm
$q_{tot,ULS}$	47.25	kN/m				u_{lim}	48.78	mm
						UC	0.95	

E.4: Visualizations floor designs after preliminary design

Figures E-50 to E-73 below present the preliminary design of floor design 1 to floor design 4.

- **Floor design 1: CLT floor**

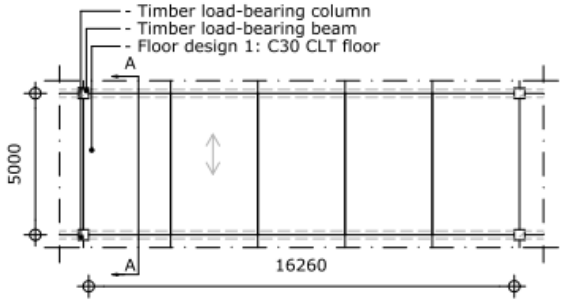

Figure E-50: Top view floor design 1 in mm

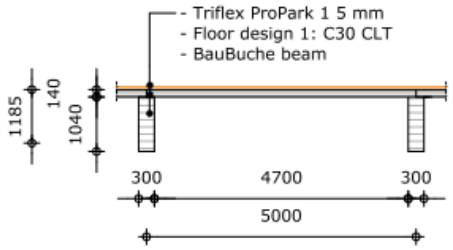

Figure E-51: Cross-section A-A BauBuche beam in mm

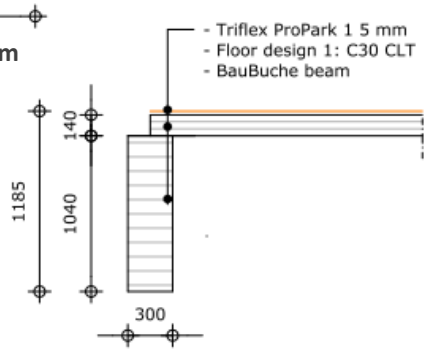

Figure E-52: Floor design 1 BauBuche beam detail cross-section A-A in mm

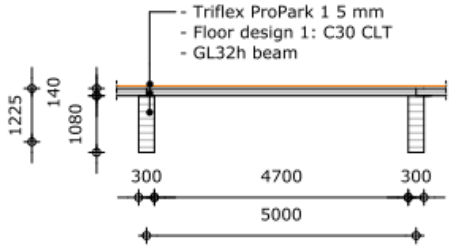

Figure E-53: Cross-section A-A glulam beam in mm

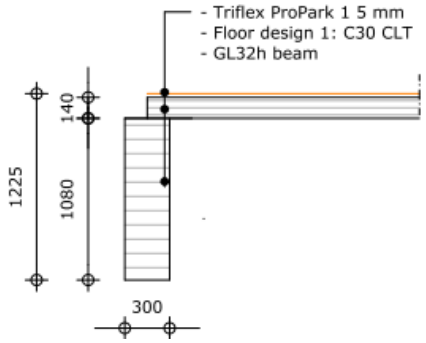

Figure E-54: Floor design 1 glulam beam detail cross-section A-A in mm

- **Floor design 2: Closed CLT plus glulam rib floor**

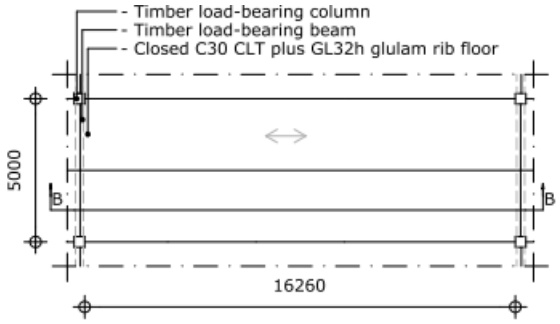

Figure E-55: Top view floor design 2 in mm

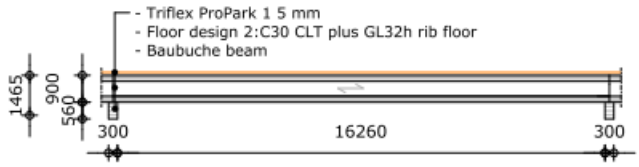

Figure E-56: Cross-section B-B BauBuche beam in mm

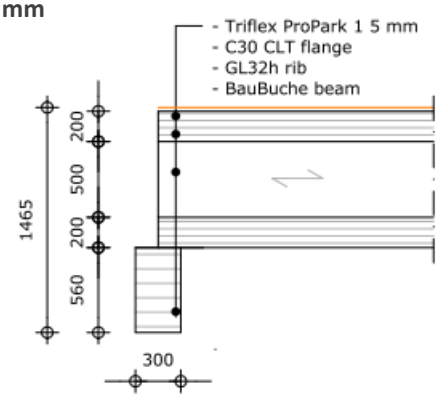

Figure E-57: Floor design 2 BauBuche beam detail cross-section B-B in mm

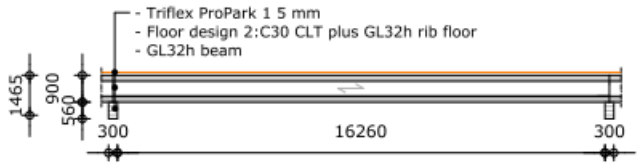

Figure E-58: Cross-section B-B glulam beam in mm

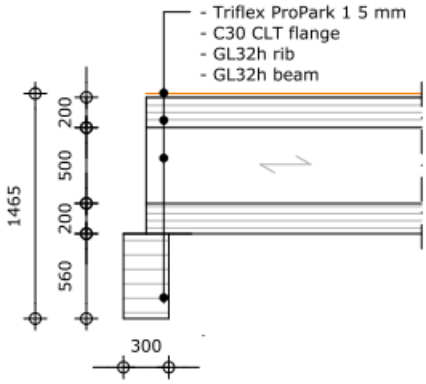

Figure E-59: Floor design 2 glulam beam detail cross-section B-B in mm

- **Floor design 3: Prefab closed CLT plus glulam rib floor with concrete top layer**

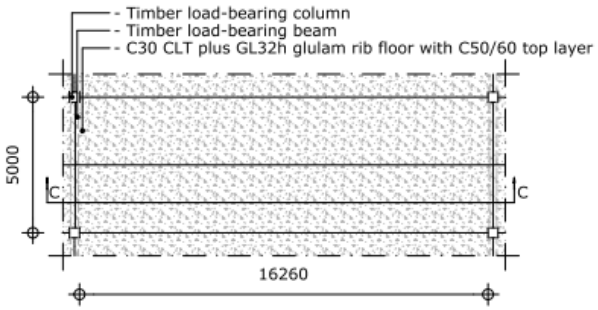

Figure E-60: Top view floor design 3

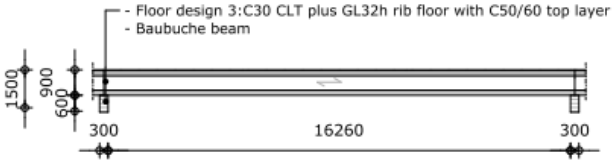

Figure E-61: Cross-section C-C BauBuche beam in mm maximum height

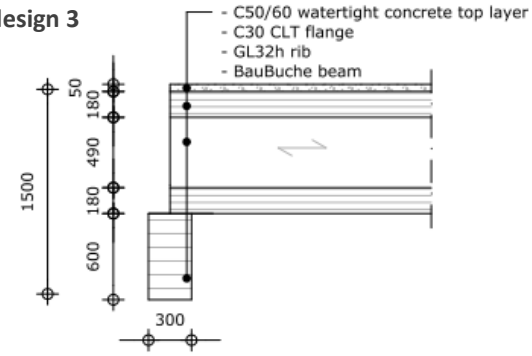

Figure E-62: Floor design 3 BauBuche beam detail cross-section C-C maximum height in mm

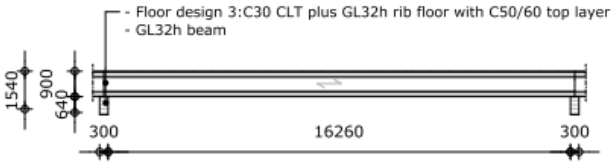

Figure E-63: Cross-section C-C glulam beam in mm maximum height

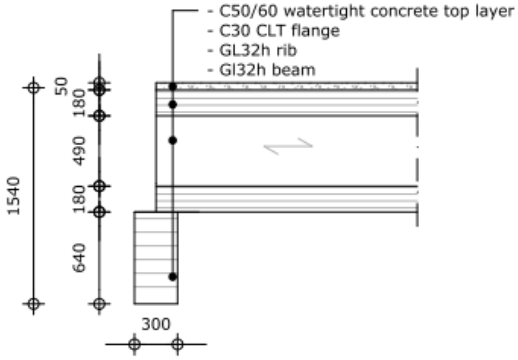

Figure E-64: Floor design 3 glulam beam detail cross-section C-C maximum height in mm

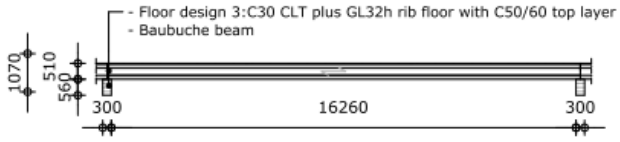

Figure E-65: Cross-section C-C BauBuche beam in mm minimum height

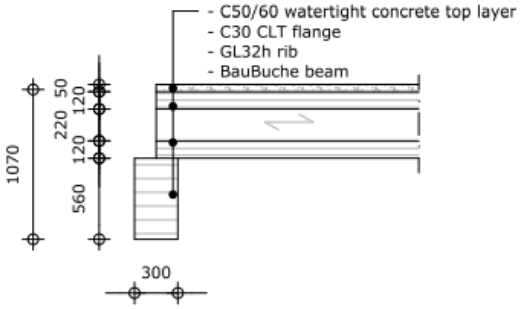

Figure E-66: Floor design 3 BauBuche beam detail cross-section C-C minimum height in mm

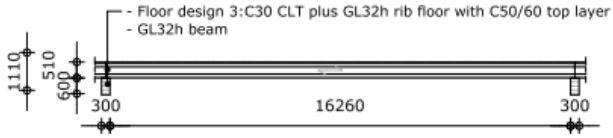

Figure E-67: Cross-section C-C glulam beam in mm minimum height

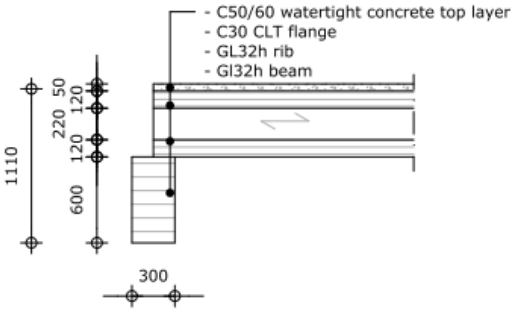

Figure E-68: Floor design 3 glulam beam detail cross-section C-C minimum height in mm

- **Floor design 4: Prefab concrete floor**

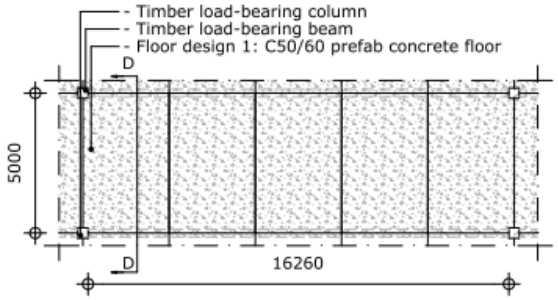

Figure E-69: Top view floor design 4 in mm

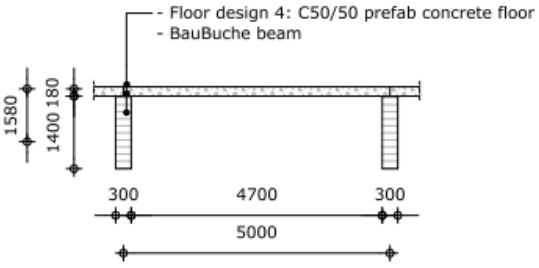

Figure E-70: Cross-section D-D BauBuche beam in mm

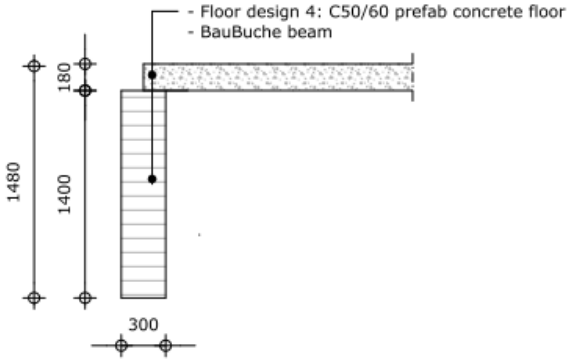

Figure E-71: Floor design 4 BauBuche beam detail cross-section D-D in mm

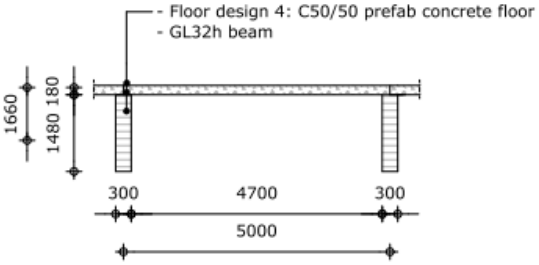

Figure E-72: Cross-section D-D glulam beam in mm

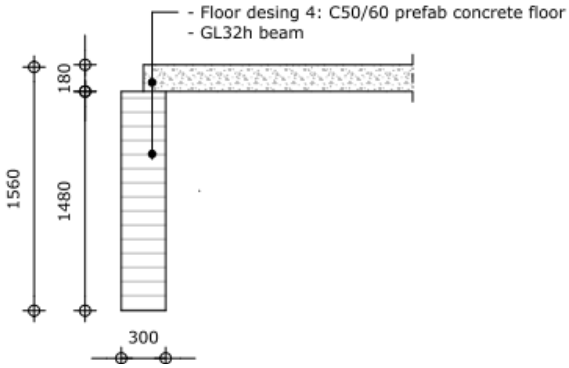

Figure E-73: Floor design 4 glulam beam detail cross-section D-D in mm

F: Fire resistance calculations preliminary design

Appendix F presents the calculations of the preliminary fire design for floor designs 1 to 3. Appendix F.1.1 to F.1.3 presents the floor fire resistance assessment, and Appendix F.2.1 to F.2.4 the beam fire resistance assessment.

F.1: Preliminary fire resistance assessment floor system

This paragraph presents the assessment of the floor system for floor designs 1 to 3 in respectively F.1.1, F.1.2, and F.1.3.

F.1.1: Floor design 1 - preliminary fire resistance assessment

The CLT floor has a thickness of 140 mm, concluded in 7.2.2. Figure F-1 shows that the charring depth is 76.7 mm.

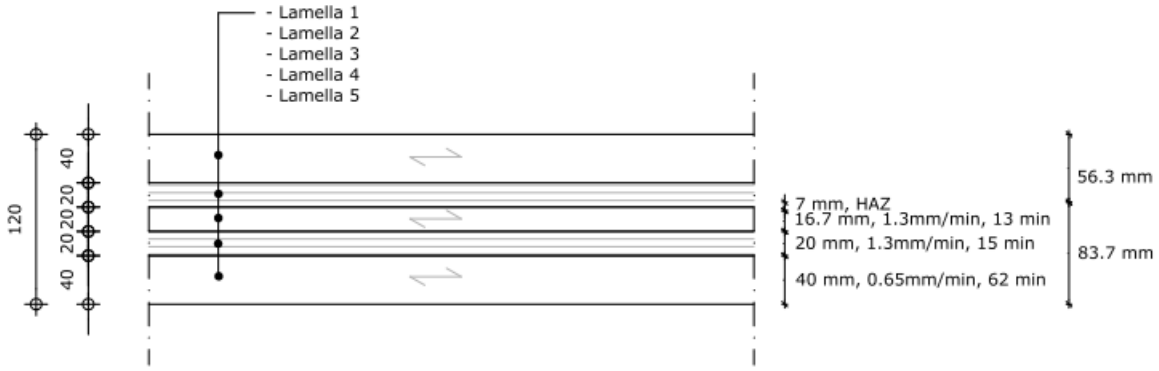

Figure F-1: Charring thickness floor design 1 in mm

Combining the charring thickness with the heat-affected zone results in a total thickness reduction of 83.7, calculated in equation F.1. Resulting in a reduced cross-section of 56.3 mm thickness.

$$d_{ef}[mm] = d_{char}[mm] + k_0[-] * d_0[mm] = 76.7 + 1 * 7 = 83.7\ mm \quad \text{(F.1)}$$

Next, the strength should be adjusted. See equations B.8 and B.10 plus Tables B-14 and B-15 of Appendix B. The adjusted bending strength is 34.5 MPa for a C30 strength class calculated in equations F.2 and F.3.

$$f_{20}[MPa] = k_{fi}[-] * f_{m,k}[MPa] = 1.15 * 30 = 34.5\ MPa \quad \text{(F.2)}$$

$$f_{d,fi}[MPa] = k_{mod,fi}[-] * \frac{f_{20}[MPa]}{\gamma_{m,fi}[MPa]} = 1 * \frac{34.5}{1} = 34.5\ MPa \quad \text{(F.3)}$$

Figures F-2 and F-3 show the bending stress for the two types of variable loads.
The loads are translated to an accidental fire situation by applying equation B.12. Those figures conclude that the variable surface load gives the governing bending stress corresponding to 11 MPa. This stress is below the resistance calculated in equation F.3, so the CLT element satisfies the requirement.

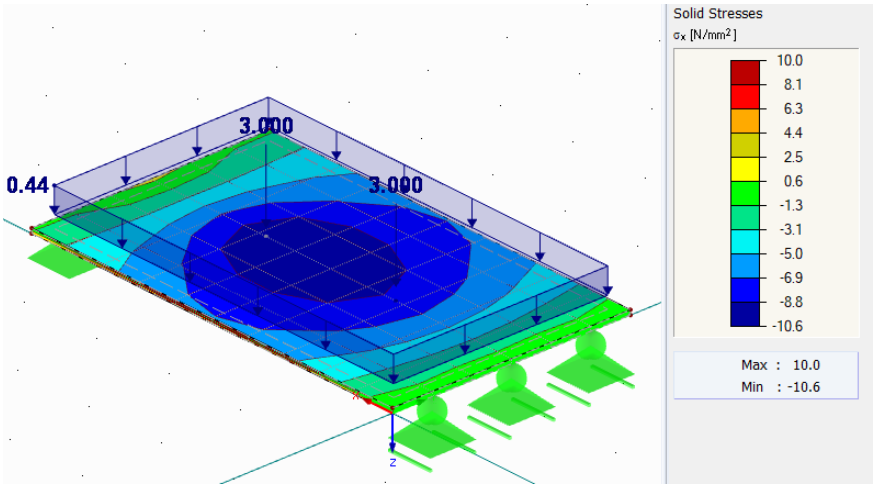

Figure F-2: Bending stress variable point loads reduced thickness CLT floor

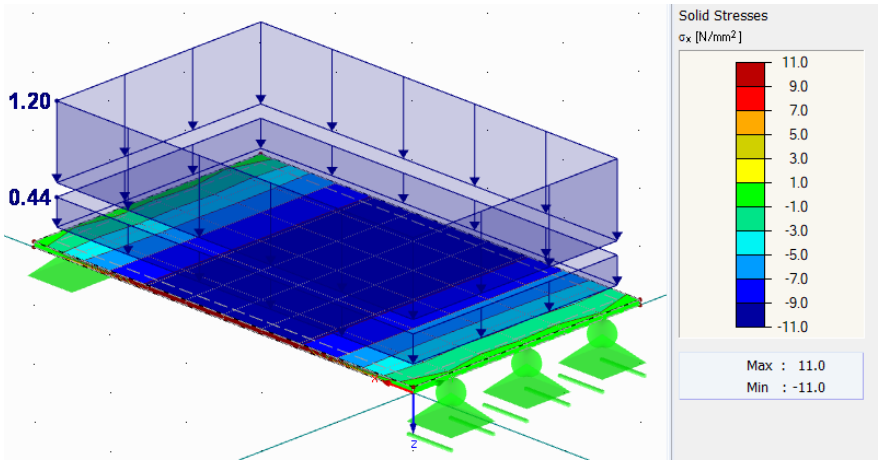

Figure F-3: Bending stress variable surface load reduced thickness CLT floor

F.1.2: Floor design 2 - preliminary fire resistance assessment

Figure F-4 shows the charring procedure of the floor element of floor design 2 CLT sheathing based on the layout determined in sub-paragraph 7.3.2.

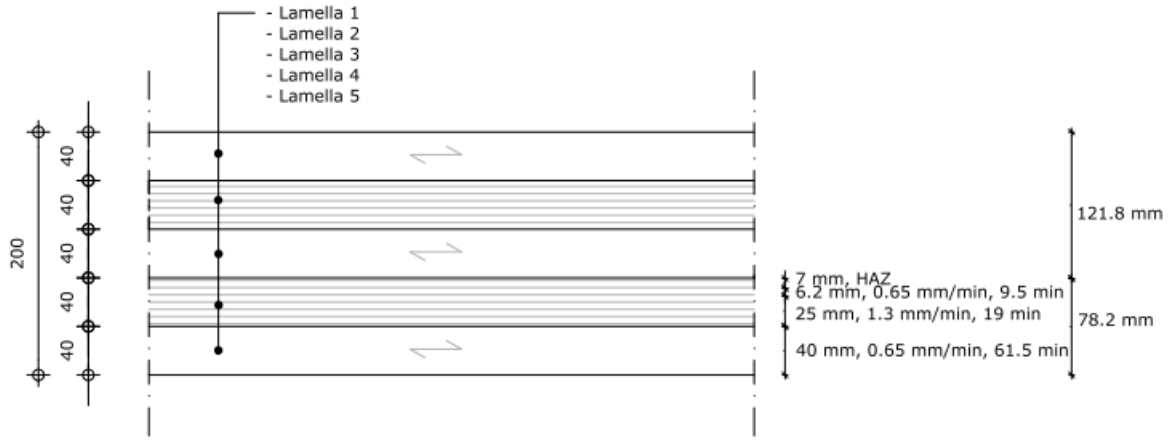

Figure F-4: Charring thickness floor design 2 in mm

The resulting thickness reduction is calculated in equation F.4. Resulting in a remaining bottom sheathing thickness of 121.8 mm instead of 200 mm initially.

$$d_{ef}[mm] = d_{char}[mm] + k_0[-] * d_0[mm] = 71.2 + 1 * 7 = 78.2\ mm \qquad \text{(F.4)}$$

The sheathings of the rib have strength class C30, like the floor design of 7.3.1. So, the resistance bending resistance during a fire is 34.5 MPa.

Figures F-5 and F-6 show the resulting bending moment in the rib floor for the reduced thickness of the bottom sheathing. The highest stresses are most logical in the sheathings. Both stress values are far below the limit of 34.5 MPa, so the reduced cross-section satisfies the 90 minutes fire resistance.

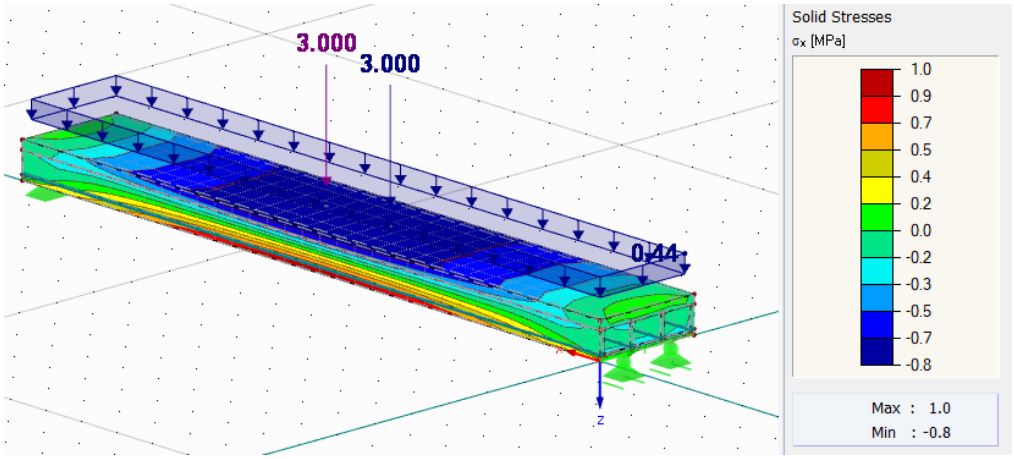

Figure F-5: Bending stress variable point loads reduced thickness CLT plus glulam rib floor

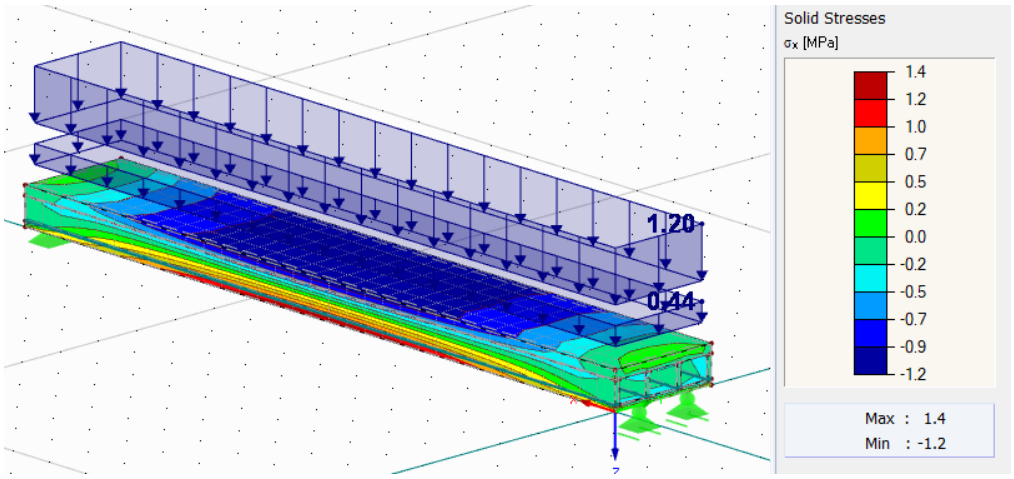

Figure F-6: Bending stress variable surface load reduced thickness CLT plus glulam rib floor

F.1.3: Floor design 3 - preliminary fire resistance assessment

Equation F-5 calculates the total thickness reduction of the 180 mm sheathing, which is 78.3 mm based on the charring layer steps of Figure F-7. So, the remaining bottom sheathing thickness is 101.7 mm instead of the initial 180 mm.

$$d_{ef}[mm] = d_{char}[mm] + k_0[-] * d_0[mm] = 71.3 + 1 * 7 = 78.3\ mm \qquad \text{(F.5)}$$

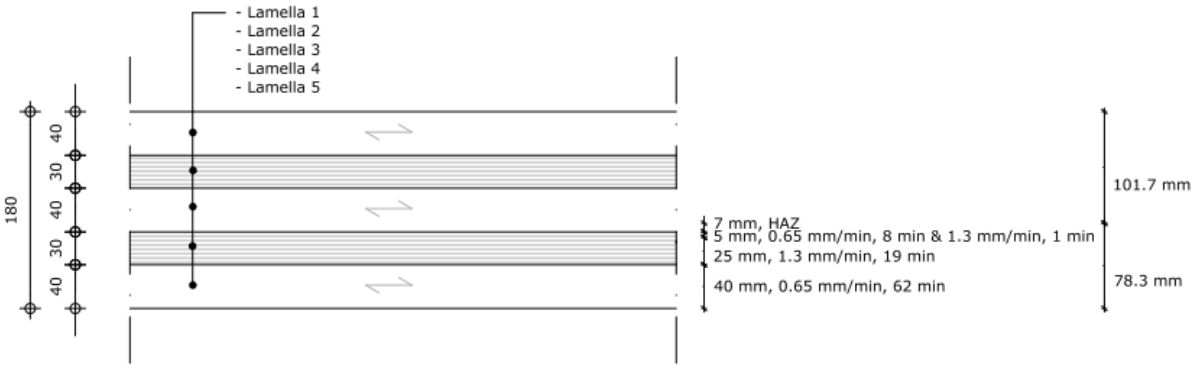

Figure F-7: Charring thickness floor design 3 maximum cross-section in mm

For the 120 mm sheathing, the total thickness reduction is 77.9. That gives a remaining bottom sheathing thickness of 42.1 mm, shown in equation F.6 and Figure F-8.

$$d_{ef}[mm] = d_{char}[mm] + k_0[-] * d_0[mm] = 70.9 + 1 * 7 = 77.9\ mm \qquad \text{(F.6)}$$

Figure F-8: Charring thickness floor design 3 minimum cross-section in mm

The sheathings of the rib panel have strength class C30, like the floor design of 7.1.3. So, the resistance bending resistance during a fire is 34.5 MPa.

Figure F-9 shows the resulting bending moment in the timber-concrete composite rib floor for the reduced thickness of the 180 mm bottom sheathing. Appendix F.1.2 indicates that the surface load governs a 16.26 meters span. The highest bending stress in the timber is in the sheathings, with a maximum value of about 2 MPa. This value is much lower than the limit of 34.5 MPa. In conclusion, the reduced cross-section satisfies the 90 minutes fire resistance.

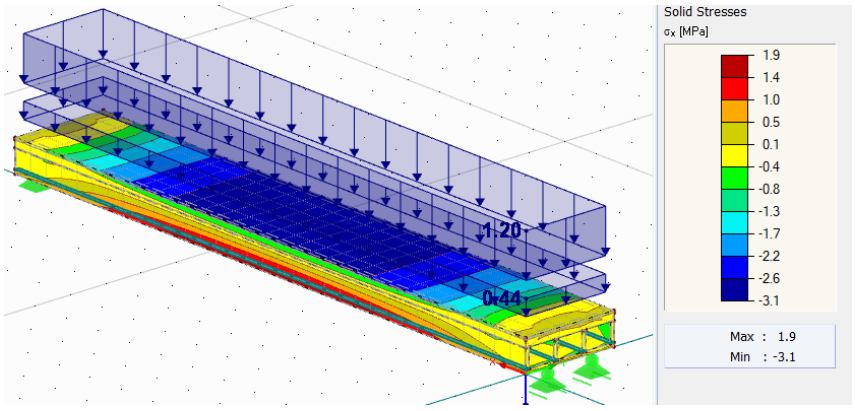

Figure F-9: Bending stress variable surface load reduced thickness 180 mm CLT plus glulam rib floor with concrete top layer

From Figure F-10, the 120 mm thick sheathing has sufficient resistance for bending. The bending stress value of 6 MPa is much lower than the resistance of 34.5 MPa.

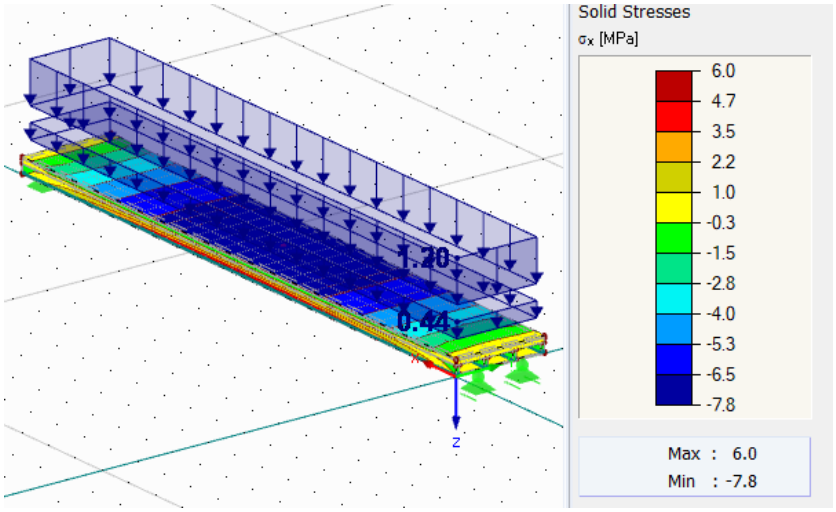

Figure F-10: Bending stress variable surface load reduced thickness 120 mm CLT plus glulam rib floor with concrete top layer

F.2: Preliminary fire resistance assessment beam

Appendix F.2 presents the beam resistance check on fire using the preliminary beam cross-sections of sub-paragraph 7.2.6.

The beam will be exposed to fire on all surfaces in the governing situation except the top surface on which the CLT panel is located. The charring rate of glulam and BauBuche is 0.7 mm/min based on Table B-16 and the technical assessment of BauBuche (*European Technical Assessment; ETA-14/0354*, 2018)uation except the top surface on which the CLT panel is located. The charring rate of glulam and BauBuche is 0.7 mm/min based on Table B-16 and the technical assessment of BauBuche (*European Technical Assessment; ETA-14/0354*, 2018).
That means a cross-section reduction of 63 mm, so 126 mm in total for both cross-sectional directions.

A strength class GL32h is assumed for the glulam beam in sub-paragraph 7.2.6, and Table E-19 presents a bending strength of 75 MPa for the BauBuche beam.
Equations F.7 and F.8 show the glulam beam's bending resistance during a fire is 36.8 MPa. Next, 82.5 MPa is the resistance for the BauBuche beam in fire, as calculated in equations F.9 and F.10. These calculations are based on the factors of Tables B-14 and B-15.

$$f_{20}[MPa] = k_{fi}[-] * f_{m,k}[MPa] = 1.15 * 32 = 36.8\ MPa \quad \text{(F.7)}$$

$$f_{d,fi}[MPa] = k_{mod,fi}[-] * \frac{f_{20}[MPa]}{\gamma_{m,fi}[MPa]} = 1 * \frac{36.8}{1} = 36.8\ MPa \quad \text{(F.8)}$$

$$f_{20}[MPa] = k_{fi}[-] * f_{m,k}[MPa] = 1.1 * 75 = 82.5\ MPa \quad \text{(F.9)}$$

$$f_{d,fi}[MPa] = k_{mod,fi}[-] * \frac{f_{20}[MPa]}{\gamma_{m,fi}[MPa]} = 1 * \frac{82.5}{1} = 82.5\ MPa \quad \text{(F.10)}$$

Equation B-12 of Appendix B.2 shows that the load should be adjusted to a fire situation. Using the governing factors ψ_1 and ψ_2 given in Appendix B.1 results in a governing reduction factor of 0.6 corresponding to ψ_2.

F.2.1: Beam floor design 1 - preliminary fire resistance assessment

Table F-1 presents the preliminary beam dimensions of floor design 1, including the 90 minutes charring time, combined with the resistance in a fire situation and the adjusted loads based on equation B.12. Appendix E.3.1 gives the concluding preliminary beam designs.
Only the ultimate limit state resistance should be checked in a fire situation. Both unity checks are below 1, so the beams have sufficient fire resistance.

Table F-1: Preliminary fire resistance calculations beams floor design 1

Fire BauBuche beam 300x1040 →174x977					
loads			Bending stress		
$q_{g,floor}$	5.42	kN/m	M_{ed}	422.36	kNm
$q_{g,beam}$	1.36	kN/m	$\sigma_{m,y,d}$	15.26	MPa
$q_{g,tot}$	6.78	kN/m	$f_{m,d}$	78.57	MPa
$q_{q,f}$	10	kN/m	UC	0.19	
$q_{tot,fire}$	12.78	kN/m			
Fire Glulam beam 300x1080→174x1017					
Loads			Bending stress		
$q_{g,floor}$	5.42	kN/m	M_{ed}	406.07	kNm
$q_{g,beam}$	0.87	kN/m	$\sigma_{m,y,d}$	13.54	MPa
$q_{g,tot}$	6.29	kN/m	$f_{m,d}$	34.91	MPa
$q_{q,f}$	10	kN/m	UC	0.39	
$q_{tot,fire}$	12.29	kN/m			

F.2.2: Beam floor design 2 - preliminary fire resistance assessment

Again, the corresponding beam design should also be checked on its fire resistance. Table F-2 presents the fire design of the concluding preliminary beams corresponding to floor design 2, based on Appendix E.3.2.
Based on Table F-2, both unity checks are sufficient.

Table F-2: Preliminary fire resistance calculations beams floor design 2

Fire BauBuche beam 300x560 →174x497					
loads			Bending stress		
$q_{g,floor}$	42.56	kN/m	M_{ed}	196.14	kNm
$q_{g,beam}$	0.69	kN/m	$\sigma_{m,y,d}$	27.38	MPa
$q_{g,tot}$	43.25	kN/m	$f_{m,d}$	82.50	MPa
$q_{q,f}$	32.52	kN/m	UC	0.33	
$q_{tot,fire}$	62.76	kN/m			
Fire Glulam beam 300x560→174x497					
Loads			Bending stress		
$q_{g,floor}$	42.56	kN/m	M_{ed}	195.30	kNm
$q_{g,beam}$	0.42	kN/m	$\sigma_{m,y,d}$	27.26	MPa
$q_{g,tot}$	42.98	kN/m	$f_{m,d}$	36.80	MPa
$q_{q,f}$	32.52	kN/m	UC	0.74	
$q_{tot,fire}$	62.50	kN/m			

F.2.3: Beam floor design 3 - preliminary fire resistance assessment

Table F-3 gives the preliminary fire design of the concluding beams corresponding to the maximum floor design 3, as calculated in Appendix E.3.3. Like Appendix F.2.1 and F.2.2, both beams have a sufficient cross-section to satisfy a 90 minutes fire resistance.

Also, the minimum floor design 3 cross-section has sufficient resistance, as concluded in Table F-4.

Table F-3: Preliminary fire resistance calculations beams floor design 3 maximum

Fire BauBuche beam 300x600 →174x537					
loads			Bending stress		
$q_{g,floor}$	60.70	kN/m	M_{ed}	253.00	kNm
$q_{g,beam}$	0.75	kN/m	$\sigma_{m,y,d}$	30.25	MPa
$q_{g,tot}$	61.45	kN/m	$f_{m,d}$	82.50	MPa
$q_{q,f}$	32.52	kN/m	UC	0.37	
$q_{tot,fire}$	80.96	kN/m			
Fire Glulam beam 300x640→174x577					
Loads			Bending stress		
$q_{g,floor}$	60.70	kN/m	M_{ed}	252.20	kNm
$q_{g,beam}$	0.49	kN/m	$\sigma_{m,y,d}$	26.12	MPa
$q_{g,tot}$	61.19	kN/m	$f_{m,d}$	36.80	MPa
$q_{q,f}$	32.52	kN/m	UC	0.71	
$q_{tot,fire}$	80.70	kN/m			

Table F-4: Preliminary fire resistance calculations beams floor design 3 minimum

Fire BauBuche beam 300x560 →174x497					
loads			Bending stress		
$q_{g,floor}$	48.30	kN/m	M_{ed}	214.07	kNm
$q_{g,beam}$	0.69	kN/m	$\sigma_{m,y,d}$	29.89	MPa
$q_{g,tot}$	48.99	kN/m	$f_{m,d}$	82.50	MPa
$q_{q,f}$	32.52	kN/m	UC	0.36	
$q_{tot,fire}$	68.50	kN/m			
Fire Glulam beam 300x600→174x537					
Loads			Bending stress		
$q_{g,floor}$	48.30	kN/m	M_{ed}	213.34	kNm
$q_{g,beam}$	0.46	kN/m	$\sigma_{m,y,d}$	25.51	MPa
$q_{g,tot}$	48.76	kN/m	$f_{m,d}$	36.8	MPa
$q_{q,f}$	32.52	kN/m	UC	0.69	
$q_{tot,fire}$	68.27	kN/m			

F.2.4: Beam floor design 4 - preliminary fire resistance assessment

Appendix E.3.4 shows the preliminary beam design of floor design 4. Table F-5 presents the fire resistance check of those beams using the adjusted strength and charring depth.
Both unity checks are below 1, so the preliminary beam designs satisfy the fire resistance requirement.

Table F-5: Preliminary fire resistance calculations beams floor design 4

Fire BauBuche beam 300x1400 →174x1337					
loads			Bending stress		
$q_{g,floor}$	24.70	kN/m	M_{ed}	1076.09	kNm
$q_{g,beam}$	1.86	kN/m	$\sigma_{m,y,d}$	20.76	MPa
$q_{g,tot}$	26.56	kN/m	$f_{m,d}$	76.15	MPa
$q_{q,f}$	10	kN/m	UC	0.27	
$q_{tot,fire}$	32.56	kN/m			
Fire Glulam beam 300x1480→174x1417					
Loads			Bending stress		
$q_{g,floor}$	24.70	kN/m	M_{ed}	1054.51	kNm
$q_{g,beam}$	1.21	kN/m	$\sigma_{m,y,d}$	18.11	MPa
$q_{g,tot}$	25.91	kN/m	$f_{m,d}$	33.77	MPa
$q_{q,f}$	10	kN/m	UC	0.54	
$q_{tot,fire}$	31.91	kN/m			

G: Background information and results multi-criteria analysis

Appendix G covers additional information for the multi-criteria analysis of Chapter 8. In G.1, the criteria will be explained. Then, the assessment per supporting beam and floor design on each criterion will be given in G.2. It is divided into two parts. G.2.1 covers the assessment of the supporting beam and G.2.2 for the floor systems. Appendix G.3.1 shows the results of the multi-criteria analysis for the assumed ranking of main criteria, followed by a sensitivity analysis and secondary ranking results in G.3.2.

G.1: Explanation criteria floor system

The eight main criteria with their sub-criteria of Table 8-1 are explained below, and weight factors are linked to the sub-criteria. Table 8-4 presents the weight factors corresponding to the number of criteria.

- Criterion: 1: Construction time

  This first criterion covers the comparison in construction time per floor design. Construction time is indicated as the time from the start of production to the moment that the erection of the car park is finished.

  A short construction time reduces, for example, the hindrance for the surrounding, nitrogen emission, and costs. Because of the re-mountable potential, the construction time is essential for both the mounting and demounting phases. The number of elements should be minimal to achieve a favourable construction time. Fewer seams are present, and connections are required. This results in less risk of human errors during execution and a more efficient and straightforward logistics plan. Secondly, limiting the necessary on-site actions increases the erection process speed. The number of actions increases for a higher number of elements. So, it gets a higher weight than the number of actions on-site. Possible damage to the elements during execution also results in a longer construction time. Sub-criterion quality control covers this aspect, which gets the second-highest weight factor because it negatively affects the necessary on-site handlings.

  Table G.1 summarizes the sub-criteria and weight factors.

  Table G-1: Sub-criteria with weight factors main criterion construction time

Sub-criteria	Aspects to compare	Weight factor
Number of elements	- Number of floor and beam elements	0.61
Quality control	- Executional damage risk - Necessary temporary measures	0.28
On-site handlings	- Time for installation of the moisture resistance measure	0.11

- Criterion 2: MEP installations

  Normally, a prefab floor element that comes on-site is only prefabricated in a way that it can achieve its structural performance. However, adding MEP installations already in the factory to the floor results in an even higher prefabrication level. As indicated by the supervisors of BNPC, placing installations inside is possible to a certain level. Because the cables and ducts can, for example, only be placed in the longitudinal direction, not crossing the ribs.

Next, this prefabrication aspect is linked to the possibility of making recesses and holes in the floors, which is called machineability. A second aspect of machineability is accessibility, which gives the potential to adjust the element. If this machineability potential is low, the potential for integration of the MEP installations is also low. Therefore, machineability is assumed to be the most important criterion. The summary of the sub-criteria is given in Table G-2.

Table G-2: Sub-criteria with weight factors main criterion MEP installations

Sub-criteria	Aspects to compare	Weight factor
Machineability	- Machineability potential materials	0.75
Integration of installations	- Potential for MEP installations inside the floor	0.25

- Criterion 3: Future-proof

  As mentioned in the research goal and question (Chapter 1), the design should be re-mountable. For arranging this characteristic, the car park should be future-proof. The main sub-criteria is the level of re-mountability. Next, the technical service life of the materials should give time for a second application. So, this becomes the second most important sub-criterion. In addition, demounting and re-mounting require transportation. The layout of the floor systems affects the ease of transportation and the risks of getting damaged. The third-highest weight factors will be applied to this aspect.
  New applications can require a different element size. The fourth sub-criterion, adjustability, covers this aspect per floor design. This is not always necessary for the new application, so it is less important than the other three sub-criteria. Finally, the amount of waste affects the re-mounting process negatively. Because all the floor designs are re-mountable, only a small part of the structure is waste. Therefore, this sub-criterion is the least important of the future-proof main criteria. The summary of the main criterion future-proof is given in Table G-3.

Table G-3: Sub-criteria with weight factors main criterion future-proof

Sub-criteria	Aspects to compare	Weight factor
Re-mountability	- Re-mountability potential structural joint - Re-mountability potential water-resistant seam	0.46
Technical service life	- Governing technical service life	0.26
Re-mounting damage	- Positioning of vulnerable details	0.16
Adjustability	- Effects of change in cross-section on dimensions and layout	0.09
Waste	- Amount of waste during demounting	0.04

- Criterion 4: Structural height

  As the problem statement (paragraph 1.1) indicates, limiting the floor height results in shorter ramps and more parking levels for a certain total car park height. The resulting floor heights of Chapter 7 are compared in this third criterion. So, the only sub-criterion is floor height, as shown in Table G-4.

  Table G-4: Sub-criterion with weight factor main criterion structural height

Sub-criteria	Aspects to compare	Weight factor
Floor height	- Height of the floor	1

- Criterion 5: Structural weight

  A lower floor weight reduces the thickness of the columns and dimensions of the foundation, which is beneficial for the design in terms of material costs and the potential number of parking lots. Next, it makes the execution simpler because less heavy equipment is necessary. The performance of the floor designs on weight will be compared for criterion 4. It consists of only one sub-criterion called floor weight. See Table G.5 below.

  Table G-5: Sub-criterion with weight factor main criterion structural weight

Sub-criteria	Aspects to compare	Weight factor
Floor weight	- Weight of the floor	1

- Criterion 6: Environmental impact

  Like criterion 2 for the MCA of the supporting beams, comparing the floor designs' EPD declares the floor designs' relative sustainability. Criterion 5 covers only this material sustainability sub-criterion, as shown in Table G-6 below.

  Table G-6: Sub-criterion with weight factor main criterion environmental impact

Sub-criteria	Aspects to compare	Weight factor
Material sustainability	- Environmental Product Declaration	1

- Criterion 7: Moisture resistance

  All floor designs are water-resistant, but some designs perform better in moisture resistance or require more measures to make them water-resistant. Also, the water-resistant measure's performance can differ between the floor designs, making it important to investigate in this multi-criteria analysis. The measures are more important than the layout because the measures prevent direct wetting from rain or cars, while a disadvantageous layout will not directly result in deterioration. Table G-7 shows the sub-criteria with weight factors for the main criterion moisture resistance.

  Table G-7: Sub-criteria with weight factors main criterion moisture resistance

Sub-criteria	Aspects to compare	Weight factor
Protection performance	- Performance moisture resistance measure	0.75
Design influence	- Moisture resistance influence cross-sectional shape and materials	0.25

- Criterion 8: production cost
  Knowing the production cost of the floor systems is important to determine the competitiveness of the floor design. The production cost is one of the main parts of the total cost next to the erection cost included in the criterion construction time.
  The costs of materials are arbitrary. They are affected by worldwide politics, economics, and trends in the construction industry. So, comparing the floor system's real production values is impossible, and it has a low value due to the price changes over time.
  But the handlings to produce can be used to assess the product cost values. The number of handlings required also affects the necessary logistics, like producing a concrete-timber composite in two factories or a pure timber system in one factory. Both aspects together correspond to the sub-criterion handlings and coordination.

  Next, the necessary material amount can also be compared per floor design. A higher volume of materials necessary per floor module grid negatively influences the minimum required number of transportation from the factory to the construction site. In addition, the total material cost is higher for a floor design with a larger total material volume necessary because BNPC indicates that the unit price of prefab concrete and engineered timber like GLT and CLT is comparable.

  The difference in the number of handlings and possible problems regarding the coordination has more effect on the production cost than the difference in the volume of material applied due to the almost equal unit price. So, the sub-criterion covering handlings and coordination is assumed to be more important than material cost, as concluded in Table G-8.

Table G-8: Sub-criteria with weight factors main criterion production cost

Sub-criteria	Aspects to compare	Weight factor
Handlings and coordination	- Required handlings to produce floor system - Required coordination between factories	0.75
Material cost	- Amount of material necessary per floor design	0.25

G.2: Ranking of the floor designs

This paragraph explains the assessment of the floor designs on the listed criteria. First, the two types of beams will be assessed on the criteria in G.2.1. Then, G.2.2 shows the resulting floor systems assessed on all stated criteria.

G.2.1: Ranking of the supporting beams

There are two types of beams mentioned in sub-paragraph 7.2.6. A multi-criteria assessment will determine the most favourable type of beam using the criteria of Table 8-1.
The two types of beams are timber and have the same cross-sectional shape, so they do not differ on the main criteria of construction time, MEP installations, future-proof, and moisture resistance.
Tables G-9 to G-13 present the ranking positions of both beams per criterion.

For the remaining four criteria, the difference between the types of beams is determined below.

- **Structural height**

The resulting beam heights per floor design are given in sub-paragraph 7.2.6. It shows that the height of a BauBuche beam is between 0 mm for floor design 2 to 80 mm for floor design 4, smaller than that of a glulam beam. Therefore, the BauBuche beam gets the highest ranking position on this first criterion given in Table G-9.

Table G-9: Ranking supporting beam criterion beam height

	BauBuche beam	Glulam beam
Height	1	2

- **Structural weight**

Table E-19 presents a Baubuche beam's density of 800 kg/m3. GL32h has a 490 kg/m3 density, given in Table B-7. This value is much lower than the weight of the BauBuche beam. However, due to the higher strength of BauBuche, less material is required compared to glulam. So, Table G-10 below presents the self-weight per meter length of both types of beams for the governing floor designs, as given in Table 7-6. The most right column presents the difference in the weights of the BauBuche beam and the glulam beam.

Table G-10: Beam weights per floor design

Floor design	**BauBuche beam weight [kN/m]**	**Glulam beam weight [kN/m]**	**BauBuche – glulam [kN/m]**
1	2.49	1.59	0.90
2	1.34	0.88	0.46
3 maximum	1.44	1.00	0.44
3 minimum	1.34	0.94	0.40
4	3.36	2.18	1.18

Concluding, the weight difference between the two types of timber is about 0.4 kN/m for the beams over 5 meters and 1 kN/m for the beams over 16.26 meters. Those differences are in favour of the glulam beam for all four floor designs. So, the glulam beam gets a higher score on this criterion than the Baubuche beam, as shown in Table G-11.

Table G-11: Ranking supporting beam criterion beam weight

	BauBuche beam	Glulam beam
Weight	2	1

- **Material environmental impact**

No EPD is available specifically for BauBuche, as indicated by the company Pollmeier. However, there is an EPD of beech laminated veneer lumber in the database of the German Federal Ministry for Housing, Urban Development and Building (*Sustainable Construction Information Portal*, n.d.). This type of timber element is approximately the same as BauBuche (*European Technical Assessment; ETA-14/0354*, 2018). An EPD for glulam is also provided in the same database for an accurate comparison.

The EPD of Beech LVL consists of only life cycle stages A1 to A3. So, the values for those three stages will be compared. The limited number of included stages is not a real problem because the comparison is between two timber materials, which means the recyclability advantage of timber compared to other materials is equal for both alternatives.

The resulting values of the environmental impact indicators of the glulam and beech laminated veneer lumber are given in Table G-12 (*Process Data Set: Glued Laminated Timber*, 2022; *Process Data Set: Laminated Veneer Board*, 2018). The fifth column indicates the best-performing type of beam on that indicator. The most right column in Table G-12 gives the absolute difference in results.

Table G-12: EPD beech laminated veneer lumber and glulam (*Process Data Set: Glued Laminated Timber*, 2022; *Process Data Set: Laminated Veneer Board*, 2018)

Environmental Impact Indicator abbreviations	Unity	A1-A3 beech laminated veneer lumber	A1-A3 glulam	Best type of beam	Absolute difference in results
GWP	kg CO_2 eq.	-4.69E+2	-6.37E+2	Glulam	1.67E+2
ODP	kg R11 eq.	4.32E-10	2,33E-12	Glulam	4.29E-10
POCP	kg ethene eq.	2.74E-2	1,19E-1	Beech LVL	4.28E-2
AP	kg $S0_2$ eq.	1.19E+0	4,8E-1	Glulam	7.14E-1
EP	kg Phosphate eq.	2.48E-1	1,19E-1	Glulam	1.29E-1
ADPE	kg Sb eq.	1.79E-4	5,69E-5	Glulam	1.22E-4
ADPF	MJ	6.41E+3	1,72E-3	Glualm	4.68E+3

In conclusion, the glulam beam is the best-performing beam for six indicators. And the effect of the remaining seventh indicator is the smallest of all seven. That makes the glulam beam EPD more favourable than the EPD of beech laminated veneer lumber.

The outcome of the assessment on material environmental impact is summarized in Table G-13.

Table G-13: Ranking supporting beam criterion material environmental impact

	BauBuche beam	Glulam beam
Material environmental impact	2	1

- **Production cost**

LVL and glulam are engineered timber products with different layups. LVL use veneers, as the name already mentions. The veneers have a thickness of about 3 mm (Purba et al., 2019), compared to a glulam lamellae thickness of about 20 mm (*CLT by Stora Enso; Technical Brochure*, 2017). A smaller lamellae thickness results in a higher number of layers, with correspondingly a higher number of glue surfaces present in laminated veneer lumber compared to glulam. So, more handlings are required in the total production process, increasing the production cost. And a higher amount of glue is required, also increasing the production cost by a higher amount of material required.

Table 6.1 of the book Timber Engineering; Design for Principles (Blaß & Sandhaas, 2017) also states that the manufacturing cost for laminated veneer lumber is higher than for glulam due to the smaller timber element size.

Based on the above production cost analysis, the BauBuche beam is less favourable than the glulam beam, as summarized in Table G-14.

Table G-14: Ranking supporting beams criterion production cost

	BauBuche beam	Glulam beam
Production cost	2	1

G.2.2: Ranking of the floor systems

The ranking positions of the four floor designs per criterion are determined in this paragraph. A value of 1 corresponds to the most favourable ranking position, and 4 indicates the least favourable floor design. If multiple alternatives perform similarly, equal ranking positions are given.

- **Construction time**

Below, criterion construction time will be discussed for each floor design, resulting in a summary of ranking positions in Tables G-15 to G-17. First, the sub-criterion number of elements is investigated. Second, the number of on-site handlings and quality control third.

Number of elements

The number of elements can be divided into the number of beams and floor elements.

Number of floor elements

Paragraph 7.2 states that floor designs 1 and 4 have elements with an area of 3 meters by 5 meters, and floor designs 2 and 3 of 2.5 meters by 16.26 meters. For all four floor designs, one module has an area of 5 meters by 16.26 meters, shown in the top view figures in Appendix E. That results in 5 to 6 required elements for floor designs 1 and 4. Next, two elements are necessary per module for floor designs 2 and 3 (*Grote Voertuigen*, n.d.). That means the beams of floor designs 2 and 3 with a module length of 5 meters, indicated in Figures E-55 and E-60, can be designed continuously to a maximum of four modules, see Figure G-2. Continuous beams limit the total number of elements. However, the beams of floor designs 1 and 4 have a module length of 16.26 meters, as shown in Figures E-50 and E-69. Making them continuous over two spans results in a length above the limit of 22 meters. Therefore, the beams of floor designs 1 and 4 cannot be continuous. See Figure G-1. Next, a continuous make sure they only carry half the span of one grid so that they can be smaller than the configuration with a sharing beam.

In conclusion, floor designs 2 and 3 could have a more efficient number of beams.

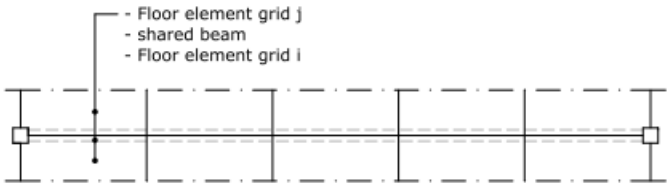

Figure G-1: Supporting beam used for two adjacent modules in mm

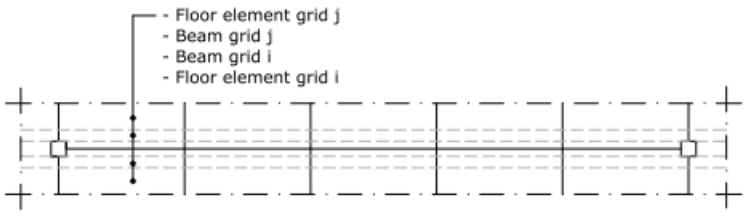

Figure G-2: Continuous beam per grid edge in mm

Total number of elements

Combining the number of floor elements and the number of beams presents that floor design 2 and 3 requires less number of elements and, therefore, fewer seams with resulting required actions than floor design 1 and 4. This statement can be made even if they do not use continuous beams. So, floor

designs 1 and 4 are the least favourable alternatives, and floor designs 2 and 3 are the most favourable on this sub-criterion, as shown in Table G-15.

Table G-15: Ranking positions sub-criterion number of elements

Sub-criterion	Floor design 1	Floor design 2	Floor design 3	Floor design 4
Number of elements	3-4	1-2	1-2	3-4

On-site handlings

The main difference between the floor designs is the type of material applied. Floor designs 1 and 2 consist only of timber, and floor designs 3 and 4 are partly or entirely made of prefab concrete. Only timber elements should be protected from long-term wetting during the transportation, erection, and use phases. These handlings require more actions and corresponding construction time. Therefore, floor designs 3 and 4 with a concrete top surface rank higher than floor designs 1 and 2 with a timber top surface.

The resulting ranking on the sub-criterion actions on-site is given in Table G-16.

Table G-16: Ranking positions sub-criterion actions on-site handlings

Sub-criterion	Floor design 1	Floor design 2	Floor design 3	Floor design 4
On-site handlings	3-4	3-4	1-2	1-2

Quality control

Floor design 3 consists of timber and concrete with different properties. Possible swelling or shrinkage during erection is more hazardous for floor design 3 because the concrete layer should follow the deformation of the timber. For the same reason, lifting the timber-concrete composite floor makes floor design 3 more prone to cracks than floor design 2, as indicated by the supervisors of BNPC. These risks of applying different materials are absent in the complete timber floor designs 1, 2, and 3. The disadvantage of floor design 4 is the higher brittleness compared to timber with the more complex reinforcement and corresponding minimum cover. That makes floor design 4 more prone to failure during the erection process.
Table G-17 presents the ranking positions corresponding to this sub-criterion.

Table G-17: Ranking positions sub-criterion quality control

Sub-criterion	Floor design 1	Floor design 2	Floor design 3	Floor design 4
Quality control	1-2	1-2	4	3

- **MEP installations**

The two sub-criteria corresponding to the MEP installations are scored below. The integration of installations comes first and the machineability second.

Integration of installations

The timber rib floors of floor designs 2 and 3 have holes between the ribs. Those holes can be used for some of the MEP installations, which are otherwise below the bottom surface of the floor. Applying the installations inside the holes makes transporting the floors, including installations, from the factory to the construction site less prone to damage. However, not all installations can be placed inside, as indicated by the supervisors of BNPC. Cables and ducts perpendicular to the ribs of the cassette cannot be placed inside due to the presence of the ribs.

The resulting ranking positions for the sub-criterion integration of installations are given in Table G-18.

Table G-18: Ranking positions sub-criterion integration of installations

Sub-criterion	Floor design 1	Floor design 2	Floor design 3	Floor design 4
Integration of installations	3-4	1-2	1-2	3-4

Machineability

Sawing recesses and holes are easier and more accurate in timber than in concrete. For example, timber tenon-mortise joints can be sawn in the factory with very small tolerances.
Concrete has a higher hardness than timber, so cutting concrete requires heavier equipment. Therefore, it is more complex and expensive than sawing in timber. Next, concrete has reinforcement inside that hinders the possible positions of the recesses or holes. Third, the reinforcement requires a minimum cover, which will be removed by making recesses. This statement is also in line with the opinion of the BNPC supervisors. Next, a rib floor's machineability is lower than a solid floor. The layout of different elements glued together with holes inside the rib floor reduces the ease of detailing the floor element.

In conclusion, floor design 1 consists only of timber and has a solid shape, making it the most favourable design on this sub-criterion. Floor designs 2 and 3 are rib floors made completely or largely of timber, but they have reduced machinability due to the rib design compared to a solid design. Resulting in an equally second favourable ranking position. Floor design 4 is completely made of concrete, resulting in ranking position 4. Table G-19 gives a summary of the ranking positions.

Table G-19: Ranking positions sub-criterion machineability

Sub-criterion	Floor design 1	Floor design 2	Floor design 3	Floor design 4
Machineability	1	2-3	2-3	4

- **<u>Future-proof</u>**

The five sub-criteria of the future-proof potential will be considered for the four floor designs in this part of Appendix G.2.2. First, the sub-criteria re-mountability potential. Second, the adjustability potential, followed by the re-mounting damage. Fourth, the alternatives' technical service life is compared and fifth, the amount of waste.

Re-mountability

Re-mountability of the connection is key for getting a high future-proof potential. Metal fasteners like dowels, bolts, and probably screws can be easily demounted using small hand tools. Next, timber joints can be made with carpentry joints, which also have a high re-mountability potential.
In the case of concrete, those connections are mostly impossible because the hardness and brittleness of concrete make bonding by the fastener thread less suitable. So, a re-mountable joint in timber is more common, resulting in an already higher experience and knowledge of the erection process. That gives the alternatives with more timber a higher favour on the re-mountability potential.
Next, a solid floor element like floor designs 1 and 4 allows simpler connections than a rib floor. So, floor designs 1 and 4 rank higher in the re-mountability sub-criterion. Because floor design 1 is made of timber, it performs better than floor design 4. Due to the small concrete layer of floor design 3, the influence on the re-mountability of the connections applied is most probably very limited.

Applying a fastener from the top of the floor element is not possible to ensure good driveability of the floor without damaging the connection. Summarizing the above comparison, the ranking positions of Table G-20 present the performance of the floor designs on this sub-criterion.

Table G-20: Ranking positions sub-criterion re-mountability

Sub-criterion	Floor design 1	Floor design 2	Floor design 3	Floor design 4
Re-mountability	1	3-4	3-4	2

Adjustability

All timber floors have good characteristics in adjustability of the dimensions because timber elements can be sawn in multiple forms, as indicated for criterion construction time. Next, adjusting the dimensions does not directly affect the element's strength and stiffness properties. These adjustments are more difficult for a pure concrete floor element like floor design 4 because the reinforcement is designed for a certain internal force transfer, and adjusting the length means redesigning the internal reinforcement. New element dimensions can also damage the connection. This principle applies to all floor systems. Because if the connection between the elements is cut off, then the future-proof potential is strongly reduced. A timber rib floor cross-section changes over its width due to the possible presence of ribs, holes, and end-blocking beams of the holes ("European Technical Assessment ETA-20/0893," 2020). On the other hand, floor design 1 has the same cross-section over the entire floor element area. Therefore, the adjustability of a rib floor is lower than for a CLT floor. Next, the presence of a top concrete surface with a corresponding connection in floor design 3 reduces the dimensional freedom more critically than floor design 2 without a concrete top surface. An example can be the presence of shear fastening between the two materials. The resulting ranking positions are given in Table G-21.

Table G-21: Ranking positions sub-criterion adjustability

Sub-criterion	Floor design 1	Floor design 2	Floor design 3	Floor design 4
Adjustability	1	2	3	4

Re-mounting damage

In terms of re-mountability, for all floor systems, the bottom surface is flat. So, the services like lights and ducts below the floor should be removed during transportation from the old to the new location. Next, the re-mountable types of connection for timber require small tolerances, so any damage during transportation will result in a high drop in performance. In addition, re-mounting the timber water resistance measures requires more actions than the concrete sealant. Namely, polishing the wearing layer and cutting the water-resistant layer, while the concrete sealant only requires cutting. And the coating should be removed over a width of about 200 mm, as mentioned in sub-paragraph 5.4.2, compared to a sealant only in the seam.
Table G-22 presents the ranking positions on this sub-criterion.

Table G-22: Ranking positions sub-criterion re-mounting damage

Sub-criterion	Floor design 1	Floor design 2	Floor design 3	Floor design 4
Re-mounting damage	3-4	3-4	1-2	1-2

Technical service life

Floor elements with a long technical service life also have a higher future-proof potential, as indicated in paragraph 3.1 by the layering principle of Brand. Knowing a floor system's technical service life and its influence on the other components is important to ensure the most beneficial service life of the whole structure.

The Triflex coating for the top timber surfaces can perform for 25 years, as indicated by the supervisors of BNPC and Triflex. Concrete has a higher hardness than the coating, so it will wear less rapidly than the coating. The other components of the floors have a long service life if sufficiently protected and maintained. So, the technical service life of the Triflex is the governing one.

Next, recycling the rib floor is easier than for a solid floor in case of damage to the floor system. For example, the closed rib floor can be used as an open rib floor in another type of application when the bottom sheathing is damaged. The concluding ranking positions are given in Table G-23.

Table G-23: Ranking positions sub-criterion technical service life

Sub-criterion	Floor design 1	Floor design 2	Floor design 3	Floor design 4
Technical service life	4	3	1	2

Waste

The waste produced during the re-mounting process is mainly produced by removing the water-resistant material at the seams. Sub-paragraph 5.4.2 states that a width of 200 mm at the seam should be removed to ensure sufficient attachment length for the coating in the new application. In the case of concrete, only the sealant in the seam should be removed. This results in less waste than for a coating. So, floor designs 3 and 4 get a higher ranking on this sub-criterion than floor designs 1 and 2, as summarized in Table G-24.

Table G-24: Ranking positions sub-criterion waste

Sub-criterion	Floor design 1	Floor design 2	Floor design 3	Floor design 4
Waste	3-4	3-4	1-2	1-2

- **Structural height**

The only sub-criterion of the structural height is the investigation of the floor heights. The total heights per floor design are listed in Table 7-7. This table shows that floor design 1 has the lowest total height and floor design 4 has the highest total height. Floor design 3 will always be thinner than floor design 2 due to the favourable performance on the governing criterion vibrational resistance compared to floor design 2. However, the higher weight of the concrete top layer results in a higher floor height. So, the ultimate height will be assumed to be equal.

In conclusion, Table G-25 gives the ranking per floor design on the sub-criterion floor height.

Table G-25: Ranking positions sub-criterion floor height

Sub-criterion	Floor design 1	Floor design 2	Floor design 3	Floor design 4
Floor height	1	2-3	2-3	4

- **Structural weight**

This main criterion has only one sub-criterion called floor weight.
The resulting weights of the floor designs, including the beam, are given in appendices E.3.1 to E.3.4. For the most accurate comparison, the weights of the most optimal iteration step should be considered. The total SLS load ($q_{tot,SLS}$) will be compared because this parameter includes self-weight and variable load but no additional load factors. This parameter is indicated per meter beam length. For floor designs 1 and 4, the line load should be multiplied by 16.26 meters to get the total weight according to floor orientation shown in Figures E-50 and E-69 with the shared beams of two modules. For floor designs 2 and 3, the line load should be multiplied by 5 meters to get the total weight, as indicated in Figures E-55 and E-60.

Table G-26 shows the resulting line load for the most favourable glulam beam, the corresponding total beam length, and the resulting total weight.

Table G-26: Resulting weights floor designs

	$q_{tot,SLS}$ [kN/m]	L [m]	$Q_{tot,SLS}$ [kN]
Floor design 1	14.01	16.26	227.80
Floor design 2	66.15	5	330.75
Floor design 3 maximum	84.40	5	422.00
Floor design 3 minimum	71.95	5	359.75
Floor design 4	33.88	16.26	550.89

The ranking positions of the sub-criterion floor weight are given in Table G-27 based on the results of Table G-26.

Table G-27: Ranking positions sub-criterion floor weight

Sub-criterion	Floor design 1	Floor design 2	Floor design 3	Floor design 4
Floor weight	1	2	3	4

- **Environmental impact**

The corresponding sub-criterion to the main criterion environmental impact is material sustainability. Comparing the difference in the material sustainability is done using the MPG scores for the different elements of the floor designs, calculated by "GPR gebouw" software. The cost per m^3 material per year of Table G-28 is determined from the values of Figure G-3 provided by BNPC. The least favourable timber category 3 gets the most conservative results, which is applied in this research.

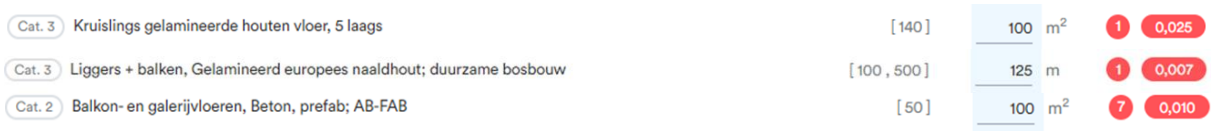

Figure G-3: MPG scores from GPR gebouw software

Table G-28: MPG scores per m^3

Material	Score €/m^3/year
CLT	0.0018
GLT	0.0011
Beton	0.02

Applying the resulting dimensions of the floor designs of paragraph 7.4 combined with the values of Table G-28 gives the total value per floor design. These resulting values are given in Table G-29, corresponding to one module of 5 meters by 16.26 meters.

Table G-29: Outcome MPG score per floor design

Floor design	Score €/year/module
1	0.032
2	0.063
3	0.113-0.102
4	0.277

Based on Table G-29, the resulting ranking positions are given in Table G-30.

Table G-30: Ranking positions sub-criterion material sustainability

Sub-criterion	Floor design 1	Floor design 2	Floor design 3	Floor design 4
Material sustainability	1	2	3	4

- **Moisture resistance**

There are two sub-criteria for the main criterion moisture resistance. First, the sub-criterion layout resistance is discussed. Afterwards, the alternatives are compared on their performance of the protection measures applied.

Design influence

The prefab concrete slab of floor design 4 is the only floor design consisting of no biobased materials, so this floor design faces the least problems with moisture resistance. Therefore, this floor design gets the highest ranking given in Table G-31.

The difference between floor design 1 and floor designs 2 and 3 is the presence of holes in the longitudinal direction. Moisture can enter the rib floors from the environment via the recesses and holes for the installations or possibly via the open longitudinal ends. Because almost no ventilation is available inside the hole, it means creating a favourable environment for the biodegradation mechanisms like fungi. See paragraph 3.4 for the living conditions of, for example, fungi. Concluding, floor design 1 is more favourable than floor designs 2 and 3, resulting in the ranking of Table G-31.

Table G-31: Ranking positions sub-criterion design influence

Sub-criterion	Floor design 1	Floor design 2	Floor design 3	Floor design 4
Design influence	2	3-4	3-4	1

Protection performance

Sub-paragraph 5.4.2 describes both water-resistance measures. The main difference between those measures is that a PMMA coating is elastic compared to more brittle concrete. Next, timber is hygroscopic, and concrete is not, so timber has a lower dimensional stability than concrete. The coating and the water-resistant concrete top layer should follow the dimensional changes of the timber floor. For the elastic PMMA, this is easier than for brittle concrete. Therefore, the possibility of damage and reduced performance of the water-resistance layer is higher for concrete. That means floor designs 1 and 2 are more favourable for this criterion than floor design 3.

In addition, floor design 4 requires only a watertight sealant, but cracking of the concrete element can also lead to reinforcement corrosion. Finally, BNPC indicates that the water resistance performance of a sealant is lower than that of a coating. So, the timber supporting beam below the floor panel with a concrete top surface faces a higher risk of becoming wet during its lifetime.

Table G-32 presents the ranking positions of the floor designs on this criterion.

Table G-32: Ranking positions sub-criterion protection performance

Sub-criterion	Floor design 1	Floor design 2	Floor design 3	Floor design 4
Protection performance	1-2	1-2	3-4	3-4

- **Production costs**

The two sub-criteria of production cost are discussed below.

Handlings and coordination
The number of handlings required to produce the floor elements is investigated in this sub-criterion and combined with the required coordination between companies.

Floor design 1 consists only of a CLT panel and a glulam beam. Compared with floor design 2, the beam production requires the same actions, but floor design 2 has a rib floor. So, the CLT top and bottom sheathings should be glued to the glulam ribs. So, a higher number of handlings should be done in the factory to produce the floor system compared to one CLT panel of floor design 1. Therefore, the production cost of floor design 1 will be lower than for floor design 2.

Floor design 2 requires fewer actions than floor design 3 because both designs use a timber rib floor. But floor design 3 also requires producing the concrete top layer with the associated connection between the timber rib floor and the concrete top layer. As mentioned in paragraph 7.1, both systems require a water-resistant layer, Triflex for timber and a vapour retarder for concrete. That means the moisture resistance design gives no clear difference in production cost for those two floor designs.

Floor design 4 requires only the installation of the reinforcement and casting of the concrete. However, the hardening time of concrete results in a longer production time, which is less favourable for the production cost. So, it probably requires fewer handlings than floor designs 1 and 2, but the overall ease of production is comparable or slightly disadvantageous compared to floor designs 1 and 2 due to the longer production time.

Floor designs 1 and 2 are only made of timber, so one company can deliver all the floor elements parts. Two companies are required for floor design 4: a concrete company for the floor element and a timber company for the beams. This higher number of companies requires more coordination, so less efficient process and with a possible higher risk of errors and resulting costs.
Floor design 3 requires two companies to design the floor. A timber and concrete company for the rib floor and this timber company for the beams. So, the timber and concrete company should work together on the floor design and second to ensure a sufficient beam-to-floor connection.

To summarize, floor design 1 requires less handling and coordination. So, this is the most favourable design. Next, floor design 2 requires more handlings than floor design 1 but fewer coordination costs and risks than floor designs 3 and 4. Third, floor design 4 requires fewer handlings than floor design 3 but an equal or longer production time than floor design 2 and more coordination.

So, floor design 4 is less favourable than floor design 2. Finally, floor design 3 is the least favourable one due to the high number of handling and high level of coordination required. This ranking is given in Table G-33.

Table G-33: Ranking positions sub-criterion handlings and coordination

Sub-criterion	Floor design 1	Floor design 2	Floor design 3	Floor design 4
Handlings and coordination	1	2	4	3

Material cost

The amount of material necessary also indicates the total production cost. BNPC indicates that the price per m^3 of prefab concrete and engineered timber elements like CLT and GLT is almost the same. Table G-34 shows the total required material in m^3 per alternative based on the preliminary floor design in sub-paragraphs 7.2.2 to 7.2.5 and the preliminary glulam beam designs in sub-paragraph 7.2.6. The results are based on a grid of 16.26 meters by 5 meters.

Table G-34: Material volumes per floor design

	Floor design 1	Floor design 2	Floor design 3 maximum	Floor design 3 minimum	Floor design 4
Floor material [m^3]	11.38	39.74	39.71	26.44	14.63
Beam material [m^3]	5.27	0.84	0.96	0.9	7.22
Total volume	16.65	40.58	40.67	26.34	21.85

Table G-35 presents the resulting ranking of the floor designs. Floor design 1 requires the least material, so it gets the highest ranking position. This design is followed by floor design 4 with the second-lowest material amount. Floor designs 2 and 3 are comparable in the amount of material, as also mentioned for the structural height criterion. However, floor design 3 requires a connection between timber and concrete to ensure composite action. This connection requires steel parts, as indicated in Appendix D.1 for KLH's timber concrete composite. Those steel connectors will increase the cost of floor design 3. So, this floor design is assumed to be at ranking position 4.

Table G-35: Ranking positions sub-criterion material cost

Sub-criterion	Floor design 1	Floor design 2	Floor design 3	Floor design 4
Material cost	1	3	4	2

Summarizing all the criterion scores is done in Table G-36 below.

Table G-36: Summary criterion ranking positions per floor design

Main criterion	Sub-criterion	Floor design 1	Floor design 2	Floor design 3	Floor design 4
Construction time	Number of elements	3-4	1-2	1-2	3-4
	On-site handlings	3-4	3-4	1-2	1-2
	Quality control	1-2	1-2	4	3
MEP installations	Integration of installations	3-4	1-2	1-2	3-4
	Machineability	1	2-3	2-3	4
Future-proof	Adjustability	1	2	3	4
	Re-mountability	1	3-4	3-4	2
	Re-mounting damage	3-4	3-4	1-2	1-2
	Technical service life	4	3	1	2
	Waste	3-4	3-4	1-2	1-2
Structural height	Floor height	1	2-3	2-3	4
Structural weight	Floor weight	1	2	3	4
Environmental impact	Material sustainability	1	2	3	4
Moisture resistance	Protection performance	1-2	1-2	3-4	3-4
	Design influence	2	3-4	3-4	1
Production cost	Material cost	1	3	4	2
	Handlings and coordination	1	2	4	3

G.3: Results multi-criteria analyses and sensitivity analysis

G.3.1 shows the results of the multi-criteria analysis for the primary ranking of Table 8-10. Then, G.3.2. presents the sensitivity analysis results and the secondary rankings discussed in 8.3.3.

G.3.1: Resulting scores for the primary ranking

Table G-37 presents the weighted scores per criterion for the four floor designs, and the bottom row shows the resulting scores based on the ranking of importance given in Table 8-10. The bold value is the resulting score, including both the weight factor for the sub-criteria and the main criteria.

Table G-37: MCA results primary ranking main criteria

Position	Main criterion	Main weight factor	Sub-criterion	Sub weight factor	Floor design 1			Floor design 2			Floor design 3			Floor design 4		
					Score	Sub-criterion weighted score	Total weighted score	Score	Sub-criterion weighted score	Total weighted score	Score	Sub-criterion weighted score	Total weighted score	score	Sub-criterion weighted score	Total weighted score
1	Structural height	W1= 0,34	Floor height	W1= 1,00	1	1,000	0,340	0,87	0,870	0,296	0,87	0,870	0,296	0,52	0,520	0,177
2	Structural weight	W2= 0,21	Floor weight	W1= 1,00	1	1,000	0,210	0,94	0,940	0,197	0,79	0,790	0,166	0,52	0,520	0,109
3	Construction time	W3= 0,15	Number of elements	W1= 0,61	0,65	0,397	0,059	0,97	0,592	0,089	0,97	0,592	0,089	0,65	0,397	0,059
			Quality control	W2= 0,28	0,97	0,272	0,041	0,97	0,272	0,041	0,52	0,146	0,022	0,79	0,221	0,033
			On-site handlings	W3= 0,11	0,65	0,072	0,011	0,65	0,072	0,011	0,97	0,107	0,016	0,97	0,107	0,016
4	MEP installations	W4= 0,11	Machineability	W1= 0,75	1	0,750	0,083	0,87	0,653	0,072	0,87	0,653	0,072	0,52	0,390	0,043
			Integration of installations	W2= 0,25	0,65	0,163	0,018	0,97	0,243	0,027	0,97	0,243	0,027	0,65	0,163	0,018
5	Future-proof	W5= 0,08	Re-mountability	W1= 0,46	1	0,460	0,037	0,65	0,299	0,024	0,65	0,299	0,024	0,94	0,432	0,035
			Technical service life	W2= 0,26	0,52	0,135	0,011	0,79	0,205	0,016	1	0,260	0,021	0,94	0,244	0,020
			Re-mounting damage	W3= 0,16	0,65	0,104	0,008	0,65	0,104	0,008	0,97	0,155	0,012	0,97	0,155	0,012
			Adjustability	W4= 0,09	1	0,090	0,007	0,94	0,085	0,007	0,79	0,071	0,006	0,52	0,047	0,004
			Waste	W5= 0,04	0,65	0,026	0,002	0,65	0,026	0,002	0,97	0,039	0,003	0,97	0,039	0,003
6	Moisture resistance	W6= 0,05	Protection performance	W1= 0,75	0,97	0,728	0,036	0,97	0,728	0,036	0,65	0,488	0,024	0,65	0,488	0,024
			Design influence	W2= 0,25	0,94	0,235	0,012	0,65	0,163	0,008	0,65	0,163	0,008	1	0,250	0,013
7	Environmental impact	W7= 0,03	Material sustainability	W1= 1,00	1	1,000	0,030	0,94	0,940	0,028	0,79	0,790	0,024	0,52	0,520	0,016
8	Production cost	W8= 0,02	Handlings and coordination	W1= 0,75	1	0,750	0,015	0,94	0,705	0,014	0,52	0,390	0,008	0,79	0,593	0,012
			Material cost	W2= 0,25	1	0,250	0,005	0,79	0,198	0,004	0,52	0,130	0,003	0,94	0,235	0,005
Total value					14,65	7,430	**0,925**	14,21	7,091	**0,880**	13,47	6,183	**0,819**	12,86	5,320	**0,598**

Figures G-4 to G-9 present the radar plots for each pair of floor designs.

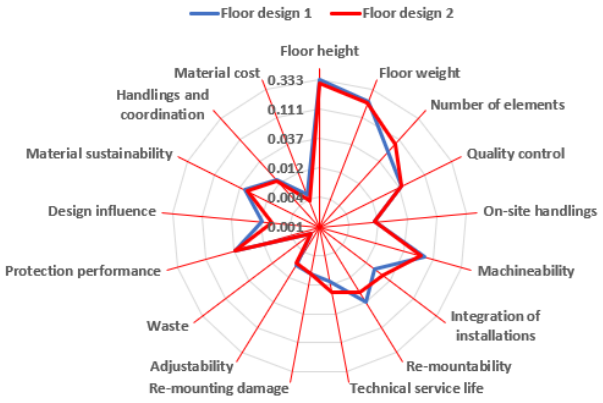

Figure G-4: Weighted scores floor designs 1 vs 2

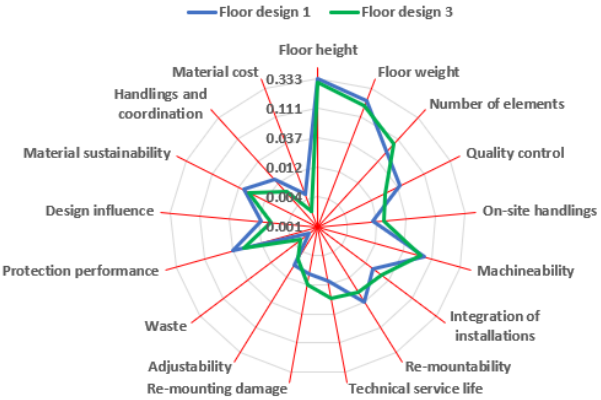

Figure G-5: Weighted scores floor designs 1 vs 3

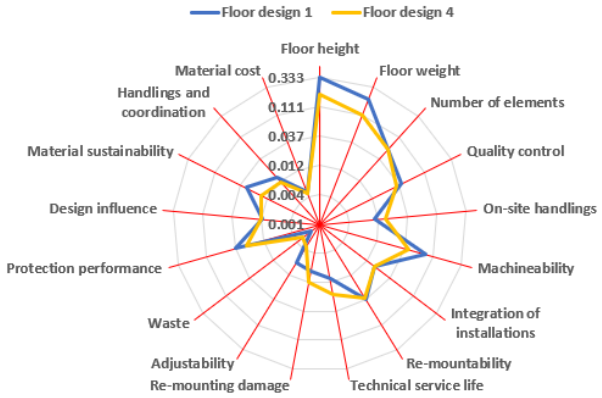

Figure G-6: Weighted scores floor designs 1 vs 4

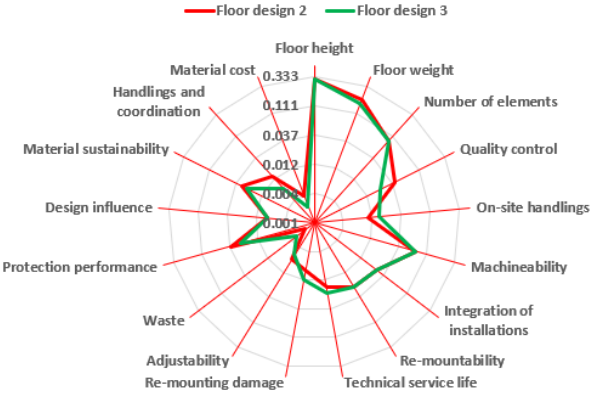

Figure G-7: Weighted scores floor designs 2 vs 3

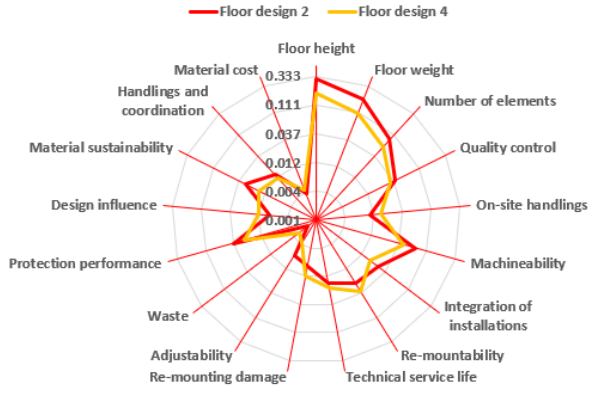

Figure G-8: Weighted scores floor designs 2 vs 4

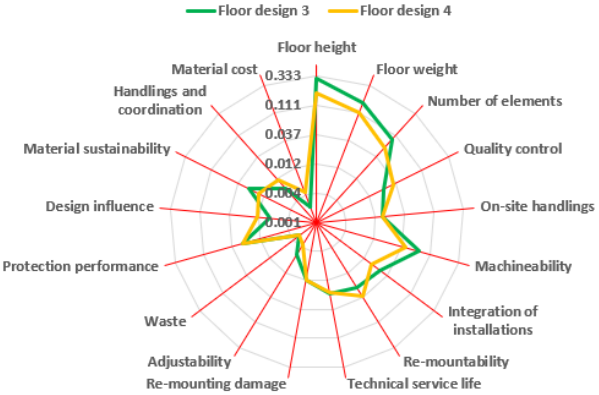

Figure G-9: Weighted scores floor designs 3 vs 4

G.3.2: Resulting scores for the sensitivity analysis and secondary rankings

In this paragraph, the influence of changing the position of the criteria on the ranking list is determined. If there are limited changes in the ultimate ranking positions of the floor designs, then the conclusion has low uncertainty. When the outcome of the MCA is volatile, the conclusion has high uncertainty and is less valuable.

<u>Changing structural performance and feasibility in order of importance</u>

In this first sensitivity analysis, the sub-criteria floor height and floor weight correspond to structural performance and are changed from positions 1 and 2 to positions 4 and 5. Because Table 8-7 shows that floor weight also corresponds to the feasibility topic, this main criterion is assumed to be more

important than structural height. Therefore, it is positioned as fourth. Table G-38 shows the results of this sensitivity analysis.

Table G-38: Sensitivity analysis structural performance vs feasibility

Position	Main criterion	Main weight factor	Sub-criterion	Sub weight factor	Floor design 1			Floor design 2			Floor design 3			Floor design 4		
					Score	Sub-criterion weighted score	Total weighted score	Score	Sub-criterion weighted score	Total weighted score	Score	Sub-criterion weighted score	Total weighted score	score	Sub-criterion weighted score	Total weighted score
1	Construction time	W1= 0.34	Number of elements	W1= 0.61	0.65	0.397	0.135	0.97	0.592	0.201	0.97	0.592	0.201	0.65	0.397	0.135
			Quality control	W2= 0.28	0.97	0.272	0.092	0.97	0.272	0.092	0.52	0.146	0.050	0.79	0.221	0.075
			On-site handlings	W3= 0.11	0.65	0.072	0.024	0.65	0.072	0.024	0.97	0.107	0.036	0.97	0.107	0.036
2	MEP installations	W2= 0.21	Machineability	W1= 0.75	1	0.750	0.158	0.87	0.653	0.137	0.87	0.653	0.137	0.52	0.390	0.082
			Integration of installations	W2= 0.25	0.65	0.163	0.034	0.97	0.243	0.051	0.97	0.243	0.051	0.65	0.163	0.034
3	Future-proof	W3= 0.15	Re-mountability	W1= 0.46	1	0.460	0.069	0.65	0.299	0.045	0.65	0.299	0.045	0.94	0.432	0.065
			Technical service life	W2= 0.26	0.52	0.135	0.020	0.79	0.205	0.031	1	0.260	0.039	0.94	0.244	0.037
			Re-mounting damage	W3= 0.16	0.65	0.104	0.016	0.65	0.104	0.016	0.97	0.155	0.023	0.97	0.155	0.023
			Adjustability	W4= 0.09	1	0.090	0.014	0.94	0.085	0.013	0.79	0.071	0.011	0.52	0.047	0.007
			Waste	W5= 0.04	0.65	0.026	0.004	0.65	0.026	0.004	0.97	0.039	0.006	0.97	0.039	0.006
4	Structural weight	W5= 0.08	Floor weight	W1= 1.00	1	1.000	0.080	0.94	0.940	0.075	0.79	0.790	0.063	0.52	0.520	0.042
5	Structural height	W4= 0.11	Floor height	W1= 1.00	1	1.000	0.110	0.87	0.870	0.096	0.87	0.870	0.096	0.52	0.520	0.057
6	Moisture resistance	W6= 0.05	Protection performance	W1= 0.75	0.97	0.728	0.036	0.97	0.728	0.036	0.65	0.488	0.024	0.65	0.488	0.024
			Design influence	W2= 0.25	0.94	0.235	0.012	0.65	0.163	0.008	0.65	0.163	0.008	1	0.250	0.013
7	Environmental impact	W7= 0.03	Material sustainability	W1= 1.00	1	1.000	0.030	0.94	0.940	0.028	0.79	0.790	0.024	0.52	0.520	0.016
8	Production cost	W8= 0.02	Handlings and coordination	W1= 0.75	1	0.750	0.015	0.94	0.705	0.014	0.52	0.390	0.008	0.79	0.593	0.012
			Material cost	W2= 0.25	1	0.250	0.005	0.52	0.130	0.003	0.79	0.198	0.004	0.94	0.235	0.005
Total value					14.65	7.430	**0.853**	13.94	7.024	**0.874**	13.74	6.251	**0.825**	12.86	5.320	**0.668**

Rank the most favourable structural performance criterion as the least favourable criterion of feasibility and structural performance

This sensitivity analysis changes the position of the most favourable and least favourable criterion corresponding to the most important sub-criteria corresponding to the research question. Table G-39 presents the results of this sensitivity analysis.

Table G-39: Sensitivity analysis structural performance and feasibility part 2

Position	Main criterion	Main weight factor	Sub-criterion	Sub weight factor	Floor design 1			Floor design 2			Floor design 3			Floor design 4		
					Score	Sub-criterion weighted score	Total weighted score	Score	Sub-criterion weighted score	Total weighted score	Score	Sub-criterion weighted score	Total weighted score	score	Sub-criterion weighted score	Total weighted score
1	Structural weight	W1= 0.34	Floor weight	W1= 1.00	1	1.000	0.340	0.94	0.940	0.320	0.79	0.790	0.269	0.52	0.520	0.177
2	Construction time	W2= 0.21	Number of elements	W1= 0.61	0.65	0.397	0.083	0.97	0.592	0.124	0.97	0.592	0.124	0.65	0.397	0.083
			Quality control	W2= 0.28	0.97	0.272	0.057	0.97	0.272	0.057	0.52	0.146	0.031	0.79	0.221	0.046
			On-site handlings	W3= 0.11	0.65	0.072	0.015	0.65	0.072	0.015	0.97	0.107	0.022	0.97	0.107	0.022
3	MEP installations	W3= 0.15	Machineability	W1= 0.75	1	0.750	0.113	0.87	0.653	0.098	0.87	0.653	0.098	0.52	0.390	0.059
			Integration of installations	W2= 0.25	0.65	0.163	0.024	0.97	0.243	0.036	0.97	0.243	0.036	0.65	0.163	0.024
4	Future-proof	W4= 0.11	Re-mountability	W1= 0.46	1	0.460	0.051	0.65	0.299	0.033	0.65	0.299	0.033	0.94	0.432	0.048
			Technical service life	W2= 0.26	0.52	0.135	0.015	0.79	0.205	0.023	1	0.260	0.029	0.94	0.244	0.027
			Re-mounting damage	W3= 0.16	0.65	0.104	0.011	0.65	0.104	0.011	0.97	0.155	0.017	0.97	0.155	0.017
			Adjustability	W4= 0.09	1	0.090	0.010	0.94	0.085	0.009	0.79	0.071	0.008	0.52	0.047	0.005
			Waste	W5= 0.04	0.65	0.026	0.003	0.65	0.026	0.003	0.97	0.039	0.004	0.97	0.039	0.004
5	Structural height	W5= 0.08	Floor height	W1= 1.00	1	1.000	0.080	0.87	0.870	0.070	0.87	0.870	0.070	0.52	0.520	0.042
6	Moisture resistance	W6= 0.05	Protection performance	W1= 0.75	0.97	0.728	0.036	0.97	0.728	0.036	0.65	0.488	0.024	0.65	0.488	0.024
			Design influence	W2= 0.25	0.94	0.235	0.012	0.65	0.163	0.008	0.65	0.163	0.008	1	0.250	0.013
7	Environmental impact	W7= 0.03	Material sustainability	W1= 1.00	1	1.000	0.030	0.94	0.940	0.028	0.79	0.790	0.024	0.52	0.520	0.016
			Handlings and coordination	W1= 0.75	1	0.750	0.015	0.94	0.705	0.014	0.52	0.390	0.008	0.79	0.593	0.012
8	Production cost	W8= 0.02	Material cost	W2= 0.25	1	0.250	0.005	0.52	0.130	0.003	0.79	0.198	0.004	0.94	0.235	0.005
Total value					14.65	7.430	**0.900**	13.94	7.024	**0.888**	13.74	6.251	**0.808**	12.86	5.320	**0.623**

Exchange the best and second-best main criteria

Exchanging the ranking positions of main criteria 1 and 2 gives the resulting values of Table G-40.

Table G-40: Sensitivity analysis exchange position 1 and 2

Position	Main criterion	Main weight factor	Sub-criterion	Sub weight factor	Floor design 1			Floor design 2			Floor design 3			Floor design 4		
					Score	Sub-criterion weighted score	Total weighted score	Score	Sub-criterion weighted score	Total weighted score	Score	Sub-criterion weighted score	Total weighted score	score	Sub-criterion weighted score	Total weighted score
1	Structural weight	W1= 0.34	Floor weight	W1= 1.00	1	1.000	0.340	0.94	0.940	0.320	0.79	0.790	0.269	0.52	0.520	0.177
2	Structural height	W2= 0.21	Floor height	W1= 1.00	1	1.000	0.210	0.87	0.870	0.183	0.87	0.870	0.183	0.52	0.520	0.109
3	Construction time	W3= 0.15	Number of elements	W1= 0.61	0.65	0.397	0.059	0.97	0.592	0.089	0.97	0.592	0.089	0.65	0.397	0.059
			Quality control	W2= 0.28	0.97	0.272	0.041	0.97	0.272	0.041	0.52	0.146	0.022	0.79	0.221	0.033
			On-site handlings	W3= 0.11	0.65	0.072	0.011	0.65	0.072	0.011	0.97	0.107	0.016	0.97	0.107	0.016
4	MEP installations	W4= 0.11	Machineability	W1= 0.75	1	0.750	0.083	0.87	0.653	0.072	0.87	0.653	0.072	0.52	0.390	0.043
			Integration of installations	W2= 0.25	0.65	0.163	0.018	0.97	0.243	0.027	0.97	0.243	0.027	0.65	0.163	0.018
5	Future-proof	W5= 0.08	Re-mountability	W1= 0.46	1	0.460	0.037	0.65	0.299	0.024	0.65	0.299	0.024	0.94	0.432	0.035
			Technical service life	W2= 0.26	0.52	0.135	0.011	0.79	0.205	0.016	1	0.260	0.021	0.94	0.244	0.020
			Re-mounting damage	W3= 0.16	0.65	0.104	0.008	0.65	0.104	0.008	0.97	0.155	0.012	0.97	0.155	0.012
			Adjustability	W4= 0.09	1	0.090	0.007	0.94	0.085	0.007	0.79	0.071	0.006	0.52	0.047	0.004
			Waste	W5= 0.04	0.65	0.026	0.002	0.65	0.026	0.002	0.97	0.039	0.003	0.97	0.039	0.003
6	Moisture resistance	W6= 0.05	Protection performance	W1= 0.75	0.97	0.728	0.036	0.97	0.728	0.036	0.65	0.488	0.024	0.65	0.488	0.024
			Design influence	W2= 0.25	0.94	0.235	0.012	0.65	0.163	0.008	0.65	0.163	0.008	1	0.250	0.013
7	Environmental impact	W7= 0.03	Material sustainability	W1= 1.00	1	1.000	0.030	0.94	0.940	0.028	0.79	0.790	0.024	0.52	0.520	0.016
8	Production cost	W8= 0.02	Handlings and coordination	W1= 0.75	1	0.750	0.015	0.94	0.705	0.014	0.52	0.390	0.008	0.79	0.593	0.012
			Material cost	W2= 0.25	1	0.250	0.005	0.52	0.130	0.003	0.79	0.198	0.004	0.94	0.235	0.005
Total value					14.65	7.430	**0.925**	13.94	7.024	**0.888**	13.74	6.251	**0.810**	12.86	5.320	**0.598**

Exchange the maximum and minimum feasibility criteria

Exchanging the most important and least important pure feasibility main criterion means the future-proof potential and construction time are changed in position. This results in the values of G-41.

Table G-41: Sensitivity analysis exchange feasibility main criteria

Position	Main criterion	Main weight factor	Sub-criterion	Sub weight factor	Floor design 1			Floor design 2			Floor design 3			Floor design 4		
					Score	Sub-criterion weighted score	Total weighted score	Score	Sub-criterion weighted score	Total weighted score	Score	Sub-criterion weighted score	Total weighted score	score	Sub-criterion weighted score	Total weighted score
1	Structural height	W1= 0.34	Floor height	W1= 1.00	1	1.000	0.340	0.87	0.870	0.296	0.87	0.870	0.296	0.52	0.520	0.177
2	Structural weight	W2= 0.21	Floor weight	W1= 1.00	1	1.000	0.210	0.94	0.940	0.197	0.79	0.790	0.166	0.52	0.520	0.109
3	Future-proof	W3= 0.15	Re-mountability	W1= 0.46	1	0.460	0.069	0.65	0.299	0.045	0.65	0.299	0.045	0.94	0.432	0.065
			Technical service life	W2= 0.26	0.52	0.135	0.020	0.79	0.205	0.031	1	0.260	0.039	0.94	0.244	0.037
			Re-mounting damage	W3= 0.16	0.65	0.104	0.016	0.65	0.104	0.016	0.97	0.155	0.023	0.97	0.155	0.023
			Adjustability	W4= 0.09	1	0.090	0.014	0.94	0.085	0.013	0.79	0.071	0.011	0.52	0.047	0.007
			Waste	W5= 0.04	0.65	0.026	0.004	0.65	0.026	0.004	0.97	0.039	0.006	0.97	0.039	0.006
4	MEP installations	W4= 0.11	Machineability	W1= 0.75	1	0.750	0.083	0.87	0.653	0.072	0.87	0.653	0.072	0.52	0.390	0.043
			Integration of installations	W2= 0.25	0.65	0.163	0.018	0.97	0.243	0.027	0.97	0.243	0.027	0.65	0.163	0.018
			Number of elements	W1= 0.61	0.65	0.397	0.032	0.97	0.592	0.047	0.97	0.592	0.047	0.65	0.397	0.032
5	Construction time	W5= 0.08	Quality control	W2= 0.28	0.97	0.272	0.022	0.97	0.272	0.022	0.52	0.146	0.012	0.79	0.221	0.018
			On-site handlings	W3= 0.11	0.65	0.072	0.006	0.65	0.072	0.006	0.97	0.107	0.009	0.97	0.107	0.009
6	Moisture resistance	W6= 0.05	Protection performance	W1= 0.75	0.97	0.728	0.036	0.97	0.728	0.036	0.65	0.488	0.024	0.65	0.488	0.024
			Design influence	W2= 0.25	0.94	0.235	0.012	0.65	0.163	0.008	0.65	0.163	0.008	1	0.250	0.013
7	Environmental impact	W7= 0.03	Material sustainability	W1= 1.00	1	1.000	0.030	0.94	0.940	0.028	0.79	0.790	0.024	0.52	0.520	0.016
8	Production cost	W8= 0.02	Handlings and coordination	W1= 0.75	1	0.750	0.015	0.94	0.705	0.014	0.52	0.390	0.008	0.79	0.593	0.012
			Material cost	W2= 0.25	1	0.250	0.005	0.52	0.130	0.003	0.79	0.198	0.004	0.94	0.235	0.005
Total value					14.65	7.430	**0.930**	13.94	7.024	**0.864**	13.74	6.251	**0.819**	12.86	5.320	**0.611**

Below, the two resulting tables for the secondary rankings are provided in Tables G-42 to G-44.

Table G-42: Resulting scores secondary ranking on costs

Position	Main criterion	Main weight factor	Sub-criterion	Sub weight factor	Floor design 1			Floor design 2			Floor design 3			Floor design 4		
					Score	Sub-criterion weighted score	Total weighted score	Score	Sub-criterion weighted score	Total weighted score	Score	Sub-criterion weighted score	Total weighted score	score	Sub-criterion weighted score	Total weighted score
1	Production cost	W1= 0.34	Handlings and coordination	W1= 0.75	1	0.750	0.255	0.94	0.705	0.240	0.52	0.390	0.133	0.79	0.593	0.201
			Material cost	W2= 0.25	1	0.250	0.085	0.52	0.130	0.044	0.79	0.198	0.067	0.94	0.235	0.080
2	Structural weight	W2= 0.21	Floor weight	W1= 1.00	1	1.000	0.210	0.94	0.940	0.197	0.79	0.790	0.166	0.52	0.520	0.109
3	Construction time	W3= 0.15	Number of elements	W1= 0.61	0.65	0.397	0.059	0.97	0.592	0.089	0.97	0.592	0.089	0.65	0.397	0.059
			Quality control	W2= 0.28	0.97	0.272	0.041	0.97	0.272	0.041	0.52	0.146	0.022	0.79	0.221	0.033
			On-site handlings	W3= 0.11	0.65	0.072	0.011	0.65	0.072	0.011	0.97	0.107	0.016	0.97	0.107	0.016
4	Structural height	W4= 0.11	Floor height	W1= 1.00	1	1.000	0.110	0.87	0.870	0.096	0.87	0.870	0.096	0.52	0.520	0.057
5	MEP installations	W5= 0.08	Machineability	W1= 0.75	1	0.750	0.060	0.87	0.653	0.052	0.87	0.653	0.052	0.52	0.390	0.031
			Integration of installations	W2= 0.25	0.65	0.163	0.013	0.97	0.243	0.019	0.97	0.243	0.019	0.65	0.163	0.013
6	Future-proof	W6= 0.05	Re-mountability	W1= 0.46	1	0.460	0.023	0.65	0.299	0.015	0.65	0.299	0.015	0.94	0.432	0.022
			Technical service life	W2= 0.26	0.52	0.135	0.007	0.79	0.205	0.010	1	0.260	0.013	0.94	0.244	0.012
			Re-mounting damage	W3= 0.16	0.65	0.104	0.005	0.65	0.104	0.005	0.97	0.155	0.008	0.97	0.155	0.008
			Adjustability	W4= 0.09	1	0.090	0.005	0.94	0.085	0.004	0.79	0.071	0.004	0.52	0.047	0.002
			Waste	W5= 0.04	0.65	0.026	0.001	0.65	0.026	0.001	0.97	0.039	0.002	0.97	0.039	0.002
7	Moisture resistance	W7= 0.03	Protection performance	W1= 0.75	0.97	0.728	0.022	0.97	0.728	0.022	0.65	0.488	0.015	0.65	0.488	0.015
			Design influence	W2= 0.25	0.94	0.235	0.007	0.65	0.163	0.005	0.65	0.163	0.005	1	0.250	0.008
8	Environmental impact	W8= 0.02	Material sustainability	W1= 1.00	1	1.000	0.020	0.94	0.940	0.019	0.79	0.790	0.016	0.52	0.520	0.010
Total value					14.65	7.430	**0.934**	13.94	7.024	**0.870**	13.74	6.251	**0.736**	12.86	5.320	**0.679**

Table G-43: Resulting values secondary ranking on sustainability

Position	Main criterion	Main weight factor	Sub-criterion	Sub weight factor	Floor design 1				Floor design 2				Floor design 3				Floor design 4			
					Score	Sub-criterion weighted score	Total weighted score		Score	Sub-criterion weighted score	Total weighted score		Score	Sub-criterion weighted score	Total weighted score		Score	Sub-criterion weighted score	Total weighted score	
1	Environmental impact	W1= 0,34	Material sustainability	W1= 1,00	1	1,000	0,340		0,94	0,940	0,320		0,79	0,790	0,269		0,52	0,520	0,177	
2	Future-proof	W2= 0,21	Re-mountability	W1= 0,46	1	0,460	0,097		0,65	0,299	0,063		0,65	0,299	0,063		0,94	0,432	0,091	
			Technical service life	W2= 0,26	0,52	0,135	0,028		0,79	0,205	0,043		1	0,260	0,055		0,94	0,244	0,051	
			Re-mounting damage	W3= 0,16	0,65	0,104	0,022		0,65	0,104	0,022		0,97	0,155	0,033		0,97	0,155	0,033	
			Adjustability	W4= 0,09	1	0,090	0,019		0,94	0,085	0,018		0,79	0,071	0,015		0,52	0,047	0,010	
			Waste	W5= 0,04	0,65	0,026	0,005		0,65	0,026	0,005		0,97	0,039	0,008		0,97	0,039	0,008	
3	Structural height	W3= 0,15	Floor height	W1= 1,00	1	1,000	0,150		0,79	0,790	0,119		0,94	0,940	0,141		0,52	0,520	0,078	
4	Structural weight	W4= 0,11	Floor weight	W1= 1,00	1	1,000	0,110		0,94	0,940	0,103		0,79	0,790	0,087		0,52	0,520	0,057	
5	Construction time	W5= 0,08	Number of elements	W1= 0,61	0,65	0,397	0,032		0,97	0,592	0,047		0,97	0,592	0,047		0,65	0,397	0,032	
			Quality control	W2= 0,28	0,97	0,272	0,022		0,97	0,272	0,022		0,52	0,146	0,012		0,79	0,221	0,018	
			On-site handlings	W3= 0,11	0,65	0,072	0,006		0,65	0,072	0,006		0,97	0,107	0,009		0,97	0,107	0,009	
6	MEP installations	W6= 0,05	Machineability	W1= 0,75	1	0,750	0,038		0,87	0,653	0,033		0,87	0,653	0,033		0,52	0,390	0,020	
			Integration of installations	W2= 0,25	0,65	0,163	0,008		0,97	0,243	0,012		0,97	0,243	0,012		0,65	0,163	0,008	
7	Moisture resistance	W7= 0,03	Protection performance	W1= 0,75	0,97	0,728	0,022		0,97	0,728	0,022		0,65	0,488	0,015		0,65	0,488	0,015	
			Design influence	W2= 0,25	0,94	0,235	0,007		0,65	0,163	0,005		0,65	0,163	0,005		1	0,250	0,008	
8	Production cost	W8= 0,02	Handlings and coordination	W1= 0,75	1	0,750	0,015		0,94	0,705	0,014		0,52	0,390	0,008		0,79	0,593	0,012	
			Material cost	W2= 0,25	1	0,250	0,005		0,52	0,130	0,003		0,79	0,198	0,004		0,94	0,235	0,005	
Total value					14,65	7,430	**0,925**		13,86	6,944	**0,855**		13,81	6,321	**0,813**		12,86	5,320	**0,629**	

Table G-44: Resulting values secondary ranking on durability

Position	Main criterion	Main weight factor	Sub-criterion	Sub weight factor	Floor design 1			Floor design 2			Floor design 3			Floor design 4		
					Score	Sub-criterion weighted score	Total weighted score	Score	Sub-criterion weighted score	Total weighted score	Score	Sub-criterion weighted score	Total weighted score	score	Sub-criterion weighted score	Total weighted score
1	Moisture resistance	W1= 0.34	Protection performance	W1= 0.75	0.97	0.728	0.247	0.97	0.728	0.247	0.65	0.488	0.166	0.65	0.488	0.166
			Design influence	W2= 0.25	0.94	0.235	0.080	0.65	0.163	0.055	0.65	0.163	0.055	1	0.250	0.085
2	Structural height	W2= 0.21	Floor height	W1= 1.00	1	1.000	0.210	0.79	0.790	0.166	0.94	0.940	0.197	0.52	0.520	0.109
3	Structural weight	W3= 0.15	Floor weight	W1= 1.00	1	1.000	0.150	0.94	0.940	0.141	0.79	0.790	0.119	0.52	0.520	0.078
4	Construction time	W4= 0.11	Number of elements	W1= 0.61	0.65	0.397	0.044	0.97	0.592	0.065	0.97	0.592	0.065	0.65	0.397	0.044
			Quality control	W2= 0.28	0.97	0.272	0.030	0.97	0.272	0.030	0.52	0.146	0.016	0.79	0.221	0.024
			On-site handlings	W3= 0.11	0.65	0.072	0.008	0.65	0.072	0.008	0.97	0.107	0.012	0.97	0.107	0.012
5	MEP installations	W5= 0.08	Machineability	W1= 0.75	1	0.750	0.060	0.87	0.653	0.052	0.87	0.653	0.052	0.52	0.390	0.031
			Integration of installations	W2= 0.25	0.65	0.163	0.013	0.97	0.243	0.019	0.97	0.243	0.019	0.65	0.163	0.013
6	Future-proof	W6= 0.05	Re-mountability	W1= 0.46	1	0.460	0.023	0.65	0.299	0.015	0.65	0.299	0.015	0.94	0.432	0.022
			Technical service life	W2= 0.26	0.52	0.135	0.007	0.79	0.205	0.010	1	0.260	0.013	0.94	0.244	0.012
			Re-mounting damage	W3= 0.16	0.65	0.104	0.005	0.65	0.104	0.005	0.97	0.155	0.008	0.97	0.155	0.008
			Adjustability	W4= 0.09	1	0.090	0.005	0.94	0.085	0.004	0.79	0.071	0.004	0.52	0.047	0.002
			Waste	W5= 0.04	0.65	0.026	0.001	0.65	0.026	0.001	0.97	0.039	0.002	0.97	0.039	0.002
7	Environmental impact	W7= 0.03	Material sustainability	W1= 1.00	1	1.000	0.030	0.94	0.940	0.028	0.79	0.790	0.024	0.52	0.520	0.016
8	Production cost	W8= 0.02	Handlings and coordination	W1= 0.75	1	0.750	0.015	0.94	0.705	0.014	0.52	0.390	0.008	0.79	0.593	0.012
			Material cost	W2= 0.25	1	0.250	0.005	0.52	0.130	0.003	0.79	0.198	0.004	0.94	0.235	0.005
Total value					14.65	7.430	**0.932**	13.86	6.944	**0.865**	13.81	6.321	**0.778**	12.86	5.320	**0.640**

H: Final design considerations and calculations

In this Appendix, the final design calculations and visualizations are given. The design calculations and visualizations corresponding to the global layout are given in paragraph H.1.
The wind load calculations are given in H.2. Then, the final design calculations are given in H.3 to H.5. Finally, Appendix H.6 presents the visualizations of the mounting and demounting sequence.

H.1: Calculations and visualizations global layout assessment

First, the drainage system is given in sub-paragraph H.1.1. Followed by the calculation and assessment considerations corresponding to the global layout assessment in H.1.2.

H.1.1: Installation design visualizations

Figures H-1 and H-2 show that an equal number of CLT panels must be arranged because a CLT panel cannot be positioned exactly in the middle of the span. Based on the length of the beam shown in Figure H-2, three panels per side are necessary, and it satisfies the boundary conditions. So, there are six CLT panels per module of 5 meters by 16.26 meters.

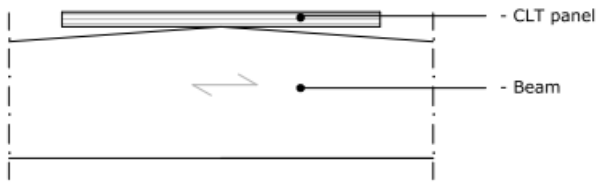

Figure H-1: Detail A CLT panel positioning

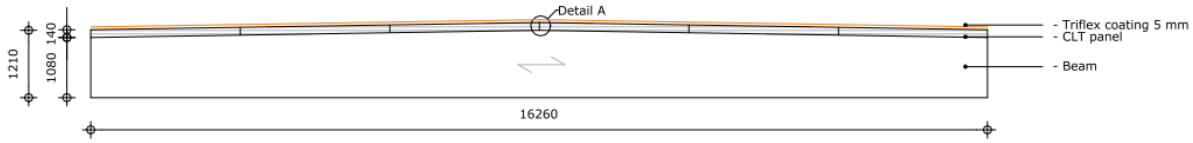

Figure H-2: Taper design in mm

There are two possible collection duct configurations.

1. Two ducts pass through the whole car park per grid, as visualized in Figure H-3
2. One central duct passes through the whole car park per grid, as visualized in Figure H-4.

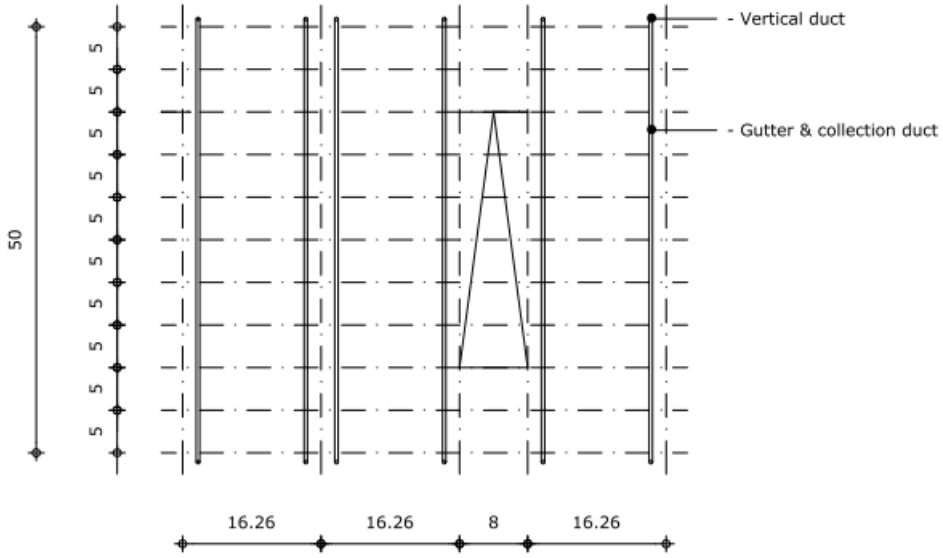

Figure H-3: Collection duct configuration 1 with grid lines in mm

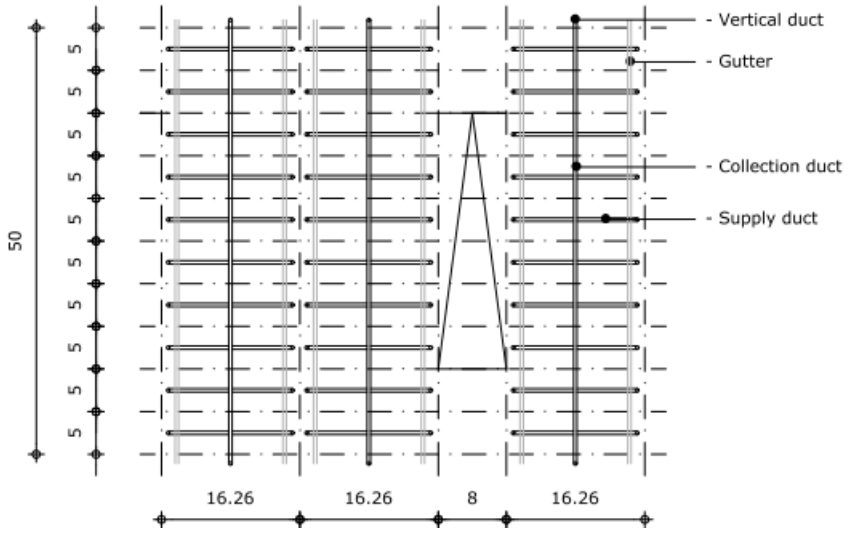

Figure H-4: Collection duct configuration 2 with grid lines in mm

Based on Figures H-3 and H-4, per car park area of 16.26 meters x 50 meters, configuration 1 requires fewer meters of duct. Namely, 156 meters instead of about 238 meters for configuration 2, assuming a car park height of 14 meters. So, configuration 2 has more water transportation, meaning a higher risk of leakage. Next, the ducts become more visible due to the collection duct's lower position to ensure the supply duct's slope.

The only disadvantage is the necessary openings in the beam with an assumed square area of 150 mm x 150 mm, as mentioned in paragraph 9.3. These openings create a change in the stress path. The vertical load should be translated to both sides of the opening, creating a small bending moment and a resulting tensile and compression stress in the grain direction. Table B-7 shows that the tensile resistance is the lowest, with a design value of 16.38 MPa. Applying a distance of 150 mm from the beam's top side to the opening results in a tension stress of 0.1 MPa. So, far below the ultimate resistance.

Next, the shear resistance at this position results in a satisfying unity check of 0.46, as shown in Table H-1. This value is calculated using the ULS line load of Table E-23 and the design shear resistance from Table B-7, and the k_{mod} factor of 0.8 like the preliminary design.

Table H-1: Shear resistance check duct opening beam

Shear resistance beam recess		
b	300	mm
h	1080	mm
h_{eff}	930	mm
k_{cr}	0.67	
b_{eff}	201	mm
V_{ed}	190320	N
τ_{ed}	1.02	MPa
f_{vd}	2.24	MPa
UC	0.46	

Figures H-5 and H-6 present a detailed visualization of the drainage system design. The centre column drainage design is in Figure H-5, and the edge column drainage design is in Figure H-6.

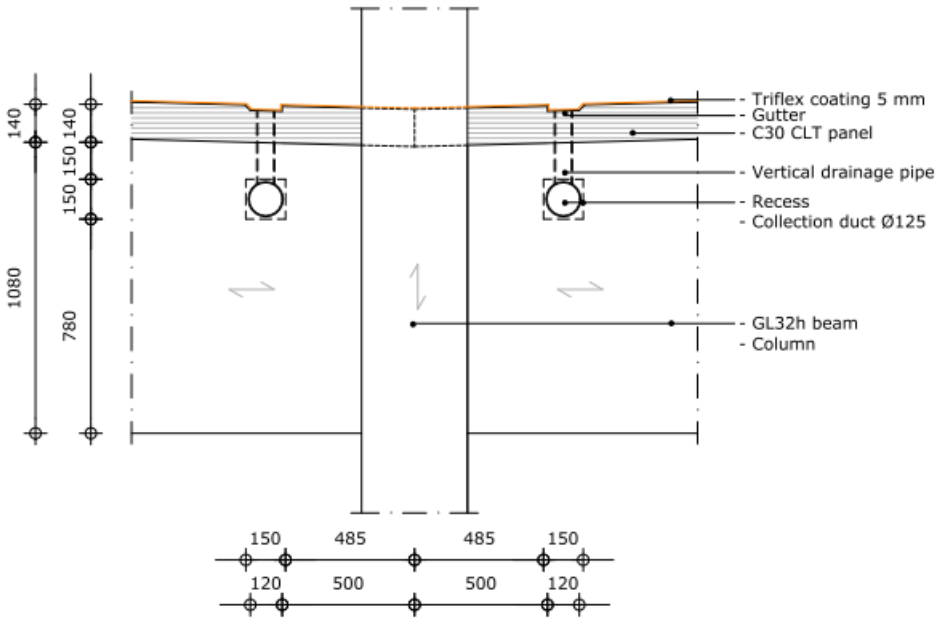

Figure H-5: Detailed drainage system design centre panel in mm

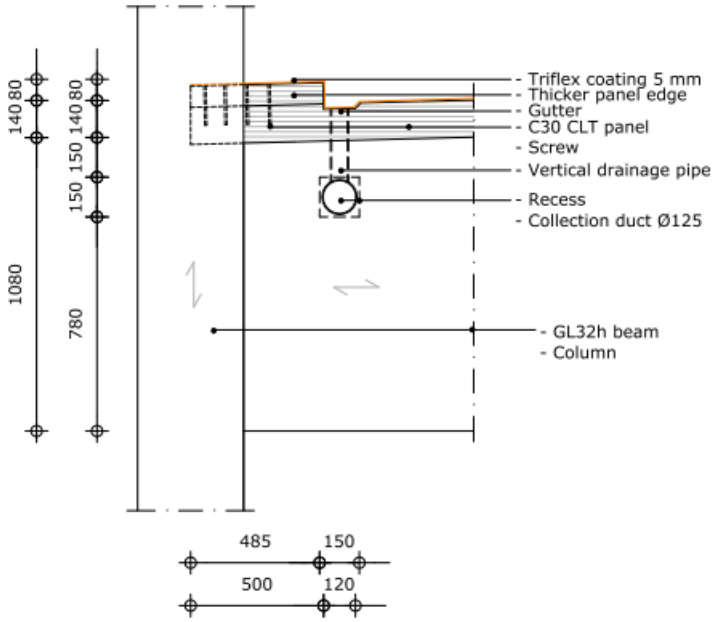

Figure H-6: Detailed drainage system design edge panel in mm

H.1.2: Global layout assessment

The calculation and assessment considerations corresponding to the global layout assessment are given in this paragraph. H.1.2.1 presents the height optimizations and the assessment of global layout optimization 1. For global layout optimization 2, this information is given in sub-paragraph H.1.2.2.

H.1.2.1: Global layout optimization solution 1

The preliminary and the optimized layout require about the same number of elements, based on Figures 9-17 to 9-19, because the CLT panels in the global layout optimization can be placed over 8 meters with a width of 2.5 meters. This results in four CLT panels per 5 meters x 16.26 meters grid instead of six panels.

Advantages:

- A beam height of 300x880 can minimally be applied due to the reduced load per beam. So, a height reduction of 200 mm is possible compared to the preliminary design. This height is calculated in Table H-2. Also, the floor height will be reduce by 70 mm using a non-continuous span of 2.5 meters for a width of 8 meters. See Figure H-7 and Table H-3.

Table H-2: Beam height optimization solution 1

Glulam beam 300x880								
Loads			Bending stress			Global deflection		
$q_{g,floor}$	2.71	kN/m	M_{ed}	406.64	kNm	$u_{inst,g}$	15.06	mm
$q_{g,beam}$	1.29	kN/m	$\sigma_{m,y,d}$	10.5	MPa	$u_{inst,q}$	13.17	mm
$q_{g,tot}$	4.00	kN/m	$f_{m,d}$	19.71	MPa	$u_{fin,g}$	27.11	mm
$q_{q,f}$	5.00	kN/m	UC	0.53		$u_{fin,q}$	19.49	mm
$q_{tot,SLS}$	7.50	kN/m				$u_{fin,tot}$	46.60	mm
$q_{tot,ULS}$	12.30	kN/m				u_{lim}	48.78	mm
						UC	0.96	

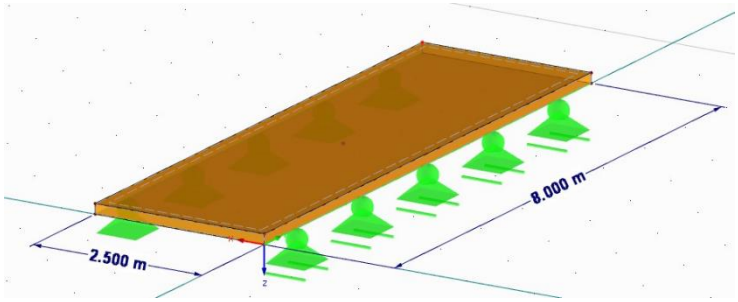

Figure H-7: Floor system design optimization dimensions in m

Table H-3: Floor height optimization solution 1 h=70 mm

Global deflection			**Vibrational resistance**		
u_{fin}	4.79	mm	F	18.42	Hz
u_{lim}	7.50	mm	f_{min}	5	Hz
UC	0.64		UC	0.27	

- Due to the larger CLT panel area, the total seam length reduces per grid by a few meters. So, a smaller part of the Triflex coating should be removed during demounting. And less floor-to-floor connections are necessary.

Disadvantages:

- Because of the extra beam, there should be a support each 2.5 meters instead of 5 meters. This support can be a column or an additional supporting beam. However, both alternatives result in a higher number of connections.

- Using the column support gives the following disadvantages, from which it is concluded that this option is not possible.
    - The view lines in the direction of about 45 degrees to the column are heavier blocked. So, the social safety of the car park is reduced.
    - Second, the vertical drainage pipe from top to bottom of the floor should be positioned at the lowest floor position, including deformation. In the preliminary design, there should be one vertical drainage pipe per edge per grid, as shown in Figure 9-17. Nevertheless, applying a column support in the new layout requires two pipes per side, as shown in Figure 9-18. This aspect further reduces the benefit of this updated layout.
    - At the grids with the driveway in the transverse direction, the top and bottom grids of Figure 1-2, the extra column will block the road.

- Applying a supporting beam on both edges instead of a column also results in an increased number of connections, as mentioned before. The other disadvantages are:
    - The beam support should have a height equal to the grid beams to prevent a recess prone to moisture degradation. Applying this height of the beam results in a large slotted-in steel plate for the column-bracing connection by ensuring no eccentricity to prevent a bending moment is being created. See Figure A-25 for a comparable type of connection.
    - Next, an extra beam results in less natural ventilation and more sharp corners that are prone to moisture degradation.
    - Finally, in terms of installation application, the vertical drainage pipe should be located exactly at the position of the beam when the floor is connected to this secondary beam. If it is not connected, then the centre point is not explicitly the lowest point due to the lower stiffness of the CLT panel compared to the edge beam. Next, using the beam support gives two types of supporting systems for the beams with different deflection lines. This principle is shown in Figure H-8. This means a higher number of vertical drainage pipes is required. Therefore, when the horizontal water collection duct passes through those two types of beams, it becomes not perfectly straight all the time, or the recess should be made larger to allow this height difference.
      Keeping the recess the same reduces the drainage performance and increases the risks of damage in the drainage system with corresponding leakages. Applying an increased recess area requires openings between the duct and beam, which is prone to dust and moisture accumulation.

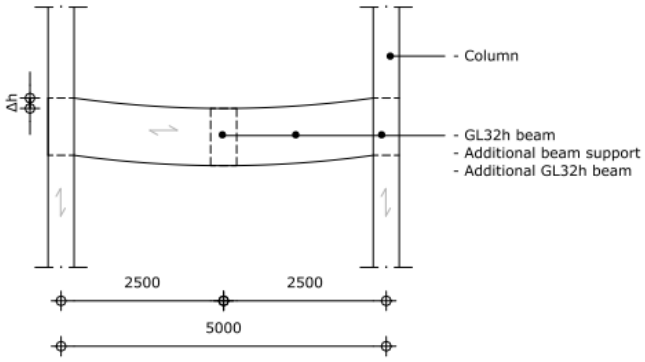

Figure H-8: Beam deflection difference

H.1.2.2: Global layout optimization solution 2

Designing a complete prefabricated grid part of 2.5 meters by 16.26 meters lets some re-mountable connections disappear. However, the horizontal loads should be translated to the adjacent prefabricated grid to ensure the floor acts as a diaphragm. So, there should still be a connection between the prefabricated grids. Figure H-9 indicates a reduction in re-mountable connections with a minus sign and an increase in re-mountable connections with a plus sign. At the floor-to-beam connection position, no positive or negative number sign is given. Because the re-mountable connection between the floor and the beam will be prefabricated, but at this location, the beams of both prefabricated grids should still be connected.

Based on Figure H-9, there is no clear benefit in reducing the number of connections.

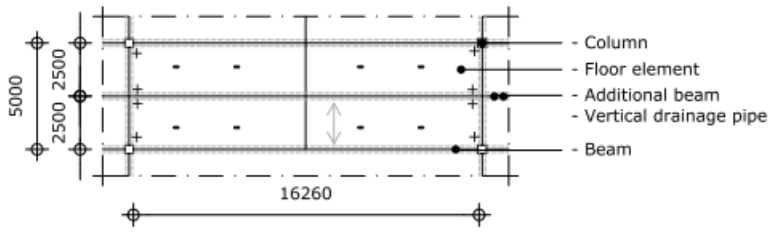

Figure H-9: Assessment benefit number of re-mountable connections in mm

Advantages:

- Due to the prefabricated floor systems like a rib panel, the feasibility is improved compared to the preliminary global layout. For example, installations like lights can stay in place during transportation because there is less damage risk due to the presence of the beams during transport.
- Due to the large prefabricated CLT panel area, the total seam length reduces by about 10 meters. So, a smaller part of the Triflex coating should be removed during demounting.
- Another advantage is that the height per beam can be reduced to 880 mm using a beam width of 150 mm per grid part. See Table H-4 below. This total height is 200 mm smaller than in the preliminary design. The floor panel height can be reduced up to approximately 70 mm for a span of 2.5 meters. Resulting in a total floor height of 950 mm. Table H-3 of Appendix H.1.2.1 presents the floor thickness calculation outcome.

Table H-4: Beam height optimization solution 2

Glulam beam 150x880								
Loads			Bending stress			Global deflection		
$q_{g,floor}$	1.36	kN/m	M_{ed}	203.32	kNm	$u_{inst,g}$	15.06	mm
$q_{g,beam}$	0.65	kN/m	$\sigma_{m,y,d}$	10.50	MPa	$u_{inst,q}$	13.17	mm
$q_{g,tot}$	2.00	kN/m	$f_{m,d}$	19.71	MPa	$u_{fin,g}$	27.11	mm
$q_{q,f}$	2.5	kN/m	UC	0.53		$u_{fin,q}$	19.49	mm
$q_{tot,SLS}$	3.75	kN/m				$u_{fin,tot}$	46.60	mm
$q_{tot,ULS}$	6.15	kN/m				u_{lim}	48.78	mm
						UC	0.96	

Disadvantages:

- The same disadvantages corresponding to the column and beam supports of the new mid-beam are valid for this global layout. Those points are mentioned in the previous global layout of H.1.2.1.
- There are two beams per column. So, by asymmetric loading of the two beams, an eccentricity (e of Figure H-10) will generate a bending moment in the column and the support connection of the beam. Timber acts favourable in compression, but bending lowers this favourable strength characteristic.

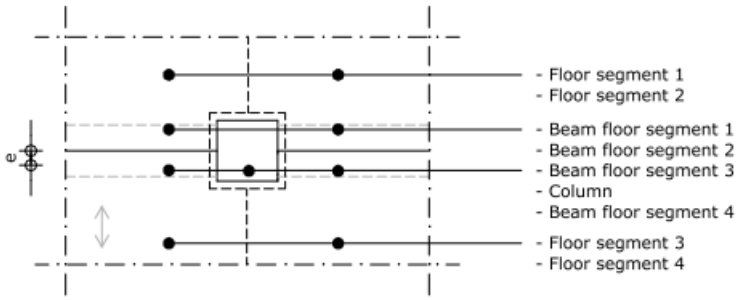

Figure H-10: Eccentricity detail B of Figure 9-20

- Placing the two beams next to each other requires a perfect connection because a small gap between the beams makes it prone to moisture degradation. Preferably, a ventilation space should be present between the beams to reduce the moisture degradation potential. This space results in extra bending in the support connection of the beam and the bolt, fastening the two adjacent beams. Therefore, more connections between the beams should be applied, meaning an unfavourable increase in re-mountable connections.
- The transportation potential of the preliminary design and optimization solution 2 are compared below. Resulting in a higher transportation potential for the preliminary design compared to the optimization solution 2. Namely one grid of 5 meters x 16.26 meters per truck compared to three grids of 5 meters x 16.26 meters per truck.

Comparing the transportation potential of the layouts will be on two aspects: weight and dimensions.
First, the weights of both grids of 5 meters by 16.26 meters will be determined and linked to the total possible weight per truck.

Second, the resulting number of grids per truck based on weight will be checked on maximum dimensions. This aspect becomes governing if the maximum number is lower than the one for the weight. Otherwise, the weight governs the transportation potential.

Weight

The preliminary layout of floor system 1 given in paragraphs 7.2 and 7.6 and Figure 9-1 results in a total weight of 7817.18 kg, determined in equation H.1. In the same way, the weight of the optimization solution 2 is determined by applying the increased number of beams and the reduced cross-sections. This results in a weight of 7717.00 kg, calculated in equation H.2.

$$Q_{prelim}[kg] = Q_{prelim,floor}[kg] + Q_{prelim,beam}[kg] = 5235.72 + 2581.44 = 7817.18\ kg \quad \text{(H.1)}$$

$$Q_{sol,2}\ [kg] = Q_{sol,2,floor}[kg] + Q_{sol,2,beam}[kg] = 2617.86 + 5609.05 = 8226.91\ kg \quad \text{(H.2)}$$

Using the maximum load of 27.3 tonnes per truck results in three grids per truck, as provided in Table H-5.

Table H-5: Weight assessment truck transport

	Weight per grid [kg]	Grids per truck
Preliminary design	7817.18	3.49 → 3
Optimization solution 2	8226.91	3.32 → 3

Dimensions

For the preliminary global layout, the elements can be positioned in multiple ways in the truck because the elements are not connected. One row of beams results in a total height of 1.08 meters, and about six beams can be placed in one row using a truck width of 2.55 meters. There is a 1.62-meter height left. Using this height by floor panels of 0.14 meters gives a total number of panel layers of 11 rounded down. Figures H-11 and H-12 visualize the layout of the elements assuming a fully stacked truck. Most possibly, some extra tolerances should be applied. The panels can be placed in three stacks for a 5 meter panel length. About six panels of 5 meters by 3 meters are necessary per grid, so the truck can carry about five grids based on the dimensional restrictions.

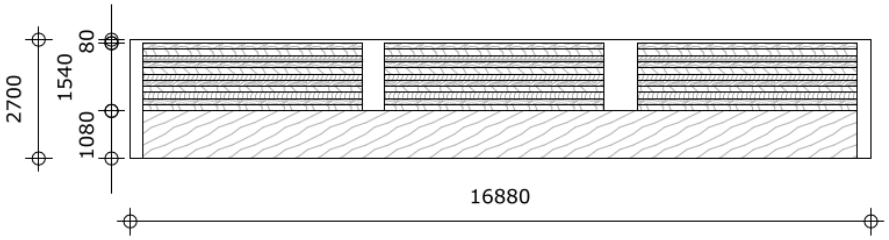

Figure H-11: Side view length direction stacking layout preliminary design in mm

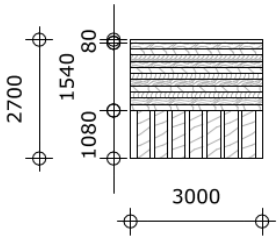

Figure H-12: Side view cross-section direction stacking layout preliminary design in mm

As mentioned in paragraph 9.3, the width and length of optimization solution 2 satisfy the transportation requirements. So, height is the governing dimension. The total floor height is 0.95 m, as calculated in this Appendix H.1.2.2. The total possible number of grid parts of 2.5 meters by 16.26 meters per truck is two, as shown in Figure H-13. This means one complete grid. Stacking the grid parts in the way of Figure H-14 results in possible damage to the installations below the floor. Next, an extra crane is necessary for turning the floor, or manual actions with safety risks are required. It results in maximally four grid parts, which is lower than for the preliminary layout. Concluding, this transportation way is not favourable.

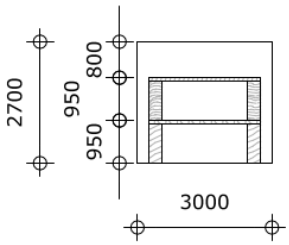

Figure H-13: Stacking layout prefab modules in mm

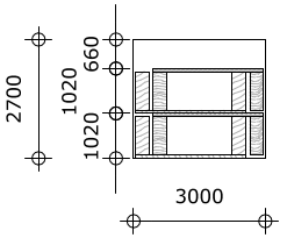

Figure H-14: Optimized stacking layout prefab modules in mm

H.2: Wind load calculations

Equation H.3 presents the calculation procedure for a wind force in a certain direction. Factor c_{pe} corresponds to a certain zone for a certain wind direction. This factor can be $c_{pe,1}$ or $c_{pe,10}$, in which $c_{pe,10}$ should be used for affected areas of about 10 m^2. Factor $c_{pe,1}$ corresponds to affected areas of about 1 m^2, which are not present in this research.

$$Q_{wind}\left[\frac{kN}{m^2}\right] = q_p(z)\left[\frac{kN}{m^2}\right] * c_{pe}[-] \tag{H.3}$$

To determine how the zones with c_{pe} factors of Tables B-3 and B-4 of Appendix B.1 are distributed over the car park, the following limits should be determined e<d, e>6, or e>5d.
Equation H.4 presents how to calculate parameter e.

$$e[m] = \min\left(b[m], 2 * h[m]\right) \tag{H.4}$$

Figure 7.5 of Eurocode 1991-1-4 presents the definition of parameters b and d. Figure 1-1 of Chapter 1 shows that parameters b and d can be 50 meters or about 57 meters.
Next, chapter 1 states that the car park should have four levels above ground.
The free height is 2.2 meters (paragraph 5.1) plus four combined thicknesses of the beam and floor of about 1.2 meters (sub-paragraph 7.2.7), resulting in a total height of about 14 meters.

Based on equations H.5 and H.6, the condition e<d is the case for a horizontal wind acting on the car park.

$$e[m] < d[m] = \min(50, 28\,) < 57\ m\ (valid\ statment) \tag{H.5}$$

$$e[m] < d[m] = \min(57, 28\,) < 50\ m\ (valid\ statemnt) \tag{H.6}$$

Horizontal wind load

The corresponding wind zones for horizontal wind on the façade according to the given condition are shown in Figure H-15.

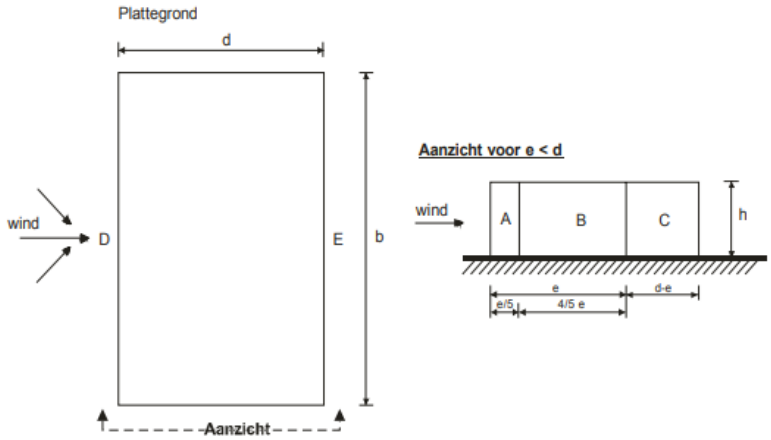

Figure H-15: Windzones on the facade from Figure 7.5 of Eurocode 1991-1-4 (NEN-EN 1991-1-4+A1+C2, 2011)

Table B.3 has two rows of c_{pe} values depending on the ratio h/d. Equation H.7 presents the two possible values of this ratio. In conclusion, both ratios are below 1. That means the bottom row values of Table B-3 should be used.

$$\frac{h[m]}{d[m]}: \frac{14}{50} = 0.28\ and \frac{14}{57} = 0.25 \tag{H.7}$$

Table H-7 present the loads on the façade zones by applying equation H.3 with the loads of Table H-6. The wind force $q_p(z)$ for the assumed heights per level is determined based on interpolating the values in Table B.2 of Appendix B.1.

Table H-6: Horizontal surface wind loads per level

Level	Height [m]	Wind load $q_p(z)$ [kN/m^2]
4	13.6	1.12
3	10.2	1.03
2	6.8	0.88
1	3.4	0.71

Table H-7: Horizontal wind loads of upper floor level façade

Zone	A	B	C	D	E
$c_{pe,10}$ factor	**-1.2**	**-0.8**	**-0.5**	**+0.8**	**-0.5**
$Q_{wind,level\ 4}$ [kN/m^2]	-1.34	-0.90	-0.56	0.90	-0.56
$Q_{wind,level\ 3}$ [kN/m^2]	-1.24	-0.82	-0.52	0.82	-0.52
$Q_{wind,level\ 2}$ [kN/m^2]	-1.06	-0.7	-0.44	0.70	-0.44
$Q_{wind,level\ 1}$ [kN/m^2]	-0.85	-0.57	-0.36	0.57	-0.36

Chapter 5.3 states that at least one-third of the façade per level should be open. The most conservative situation for the wind load is applying the minimum façade openings. So, the closed part of the façade per level has a height of two-thirds of the floor height. This total height is about 3.4 meters, resulting in a closed façade height of about 2.27 meters per level.

Vertical wind load

The vertical wind force on floor elements should be determined as an open roof (NEN-EN 1991-1-4+A1+C2, 2011) because of the opening of one-third of the height.

Table B-4 presents the C_p factors for an open roof situation. Factor c_f should be applied to dimension the load-bearing elements and the $c_{p,net}$ factor for small areas like factor $C_{pe,1}$, which are not included in this research, as mentioned before. The roof angle is assumed to be zero because the taper will be limited to the minimum possible. That gives a c_f factor of 0.2 to -1 for a one-thrid open façade (NEN-EN 1991-1-4+A1+C2, 2011) applicable for the complete roof area. Table H-8 presents the ultimate vertical loads per level by using the loads of Table H-6.

Table H-8: Vertical wind loads of upper floor level façade

c_f factor	**0.2**	**-1**
$Q_{wind,\mathbf{13.6}}$ [kN/m^2]	0.22	-1.12
$Q_{wind,\mathbf{10.2}}$ [kN/m^2]	0.21	-1.03
$Q_{wind,\mathbf{6.8}}$ [kN/m^2]	0.18	-0.88
$Q_{wind,\mathbf{3.4}}$ [kN/m^2]	0.14	-0.71

H.3: Calculations final design floor system

First, the final dimension of the load-bearing floor and beam elements are given in Appendix H.3.1 and H.3.2. Then, the diaphragm action is calculated in Appendix H.3.3. Finally, the re-mountable connections in the floor system are designed. Appendix H.3.4 presents the floor-to-floor connection design, and H.3.5 the floor-to-beam connection design.

H.3.1: Calculations final dimensioning floor system

The upper floor will face the highest vertical wind load due to the highest $q_p(z)$ value, as given in Table H-6. A downward wind load acts in the same direction as the self-weight and car park load, so combining those loads can increase the ultimate vertical load.

Table H-9 presents the combination of the two variable loads and the self-weight. Both variable loads can be assumed as the main load, so two configurations are possible. The Ψ-factors are given in Appendix B.1. Appendix E.2 presents that the serviceability limit state criteria are governing, so the ultimate limit state criteria will not be checked in this final design phase.
The configuration with the car park load is the governing one based on Table H-9. And there is no effect of the wind load, so the same load as in the preliminary design must be used in the final design phase.

Table H-9: Load configurations governing floor element upper level

	Configuration 1: Q_1 wind & Q_2 Cat. F car park	**Configuration 2: Q_1 Cat. F car park & Q_2 wind**
Q_1	0.22 kN/m^2	2 kN/m^2
Ψ_1	0.2	0.7
Q_2	2 kN/m^2	1.98 kN/m^2
Ψ_2	0.6	0
Q_{tot}	1.24 kN/m^2	1.4 kN/m^2

To determine if strength class optimization is possible. Figures H-16 to H-18 present the global deflection and first eigenfrequency of the C24 floor panel. It results in the unity checks of Table H-10. Both values are below 1, so the satisfy the requirements. And the governing unity check is close to one.

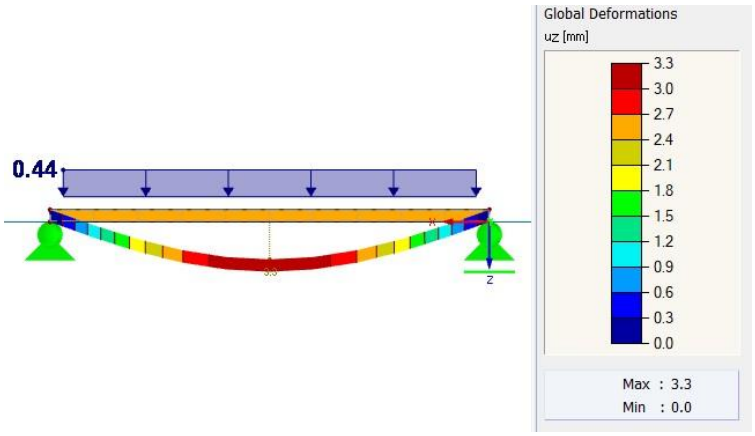

Figure H-16: Initial global deflection line permanent load

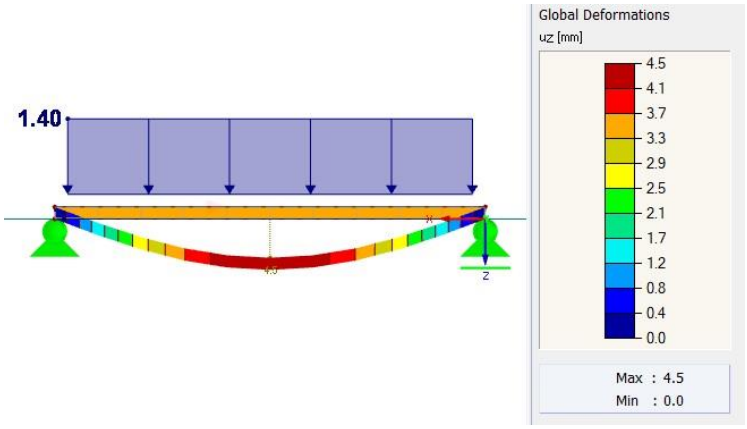

Figure H-17: Initial global deflection line governing variable load

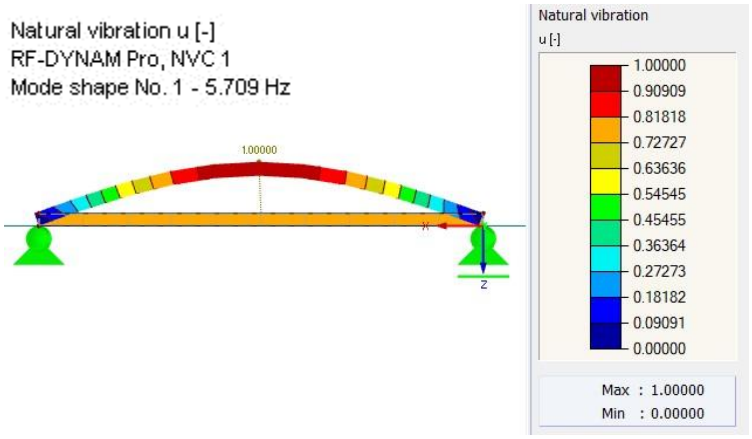

Figure H-18: First eigenfrequency

Table H-10: Unity checks upper floor level 140 mm C24

Global deflection			**Vibrational resistance**		
u_{fin}	12.86	mm	f	5.71	Hz
u_{lim}	15	mm	f_{min}	5	Hz
UC	0.84		UC	0.88	

The reduction in panel width will not result in differences in global deflection or first eigenfrequency, as shown in Figures H-19 to H-21 for a 2 meters x 5 meters plate instead of 3 meters x 5 meters.

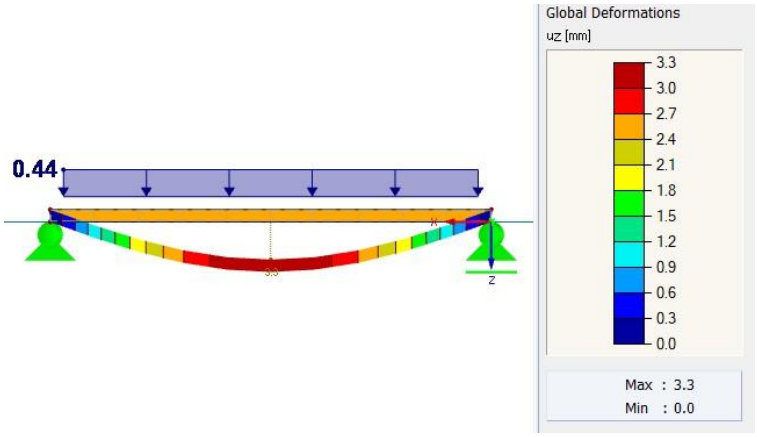

Figure H-19: Initial global deflection line permanent load 2x5 m plate

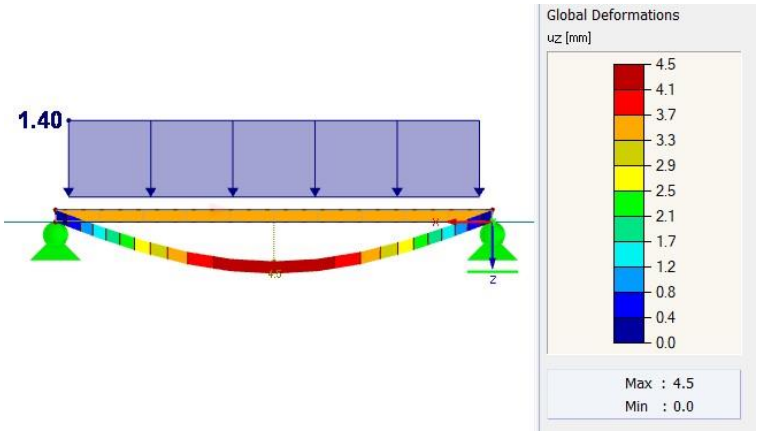

Figure H-20: Initial global deflection line governing variable load 2x5 m plate

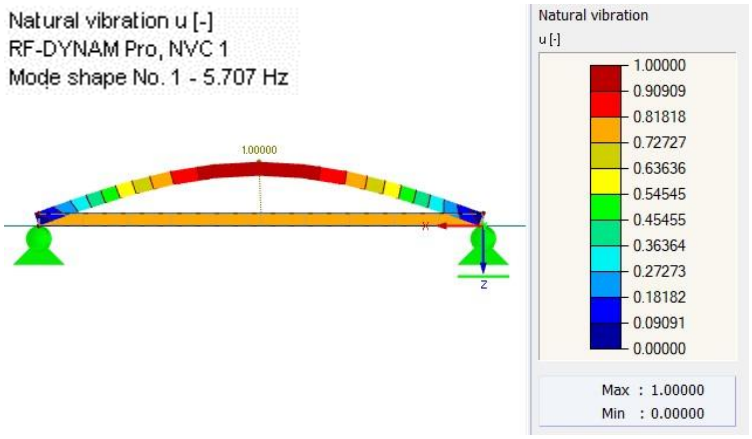

Figure H-21: First eigenfrequency 2x5 m plate

H.3.2: Calculations final dimensioning beam

Equations E.20 to E.22 are still valid for the final beam calculations.

The verification of equation H.8 must be used for the bending resistance check due to applying a taper. The factor $k_{m,\alpha}$ must be determined using equations H.9 and H.10. Equation H.10 is valid because there is compression on the beam's tapered side due to the positive bending moment (NEN-EN 1995-1-2+C2, 2011).

$$\sigma_{m,\alpha,d}[MPa] \leq k_{m,\alpha} * f_{m,d}[MPa] \tag{H.8}$$

$$\sigma_{m,\alpha,d}[MPa] = \sigma_{m,0,d}[MPa] = \frac{M_{ed,y}[Nmm]}{W[mm^3]} \tag{H.9}$$

$$k_{m,\alpha} = \frac{1}{1+\left(\frac{f_{m,d}[MPa]}{1.5*f_{v,d}[MPa]}*\tan(\alpha)\right)^2+\left(\frac{f_{m,d}[MPa]}{f_{c,90,d}[MPa]}*\tan^2(\alpha)\right)^2} \tag{H.10}$$

The comparison of the governing vertical load configuration of Table H-9 is also applicable to the beam design. So, the 1.4 kN/m^2 variable load is the governing one.

Table H-11 presents the governing unity checks for a GL32h beam by applying a taper.

Table H-11: Loads and unity checks final design supporting beam upper level GL32h

Glulam beam 300x1080								
Loads			Bending stress			Global deflection		
$q_{g,floor}$	5.42	kN/m	M_{ed}	773.64	kNm	$u_{inst,g}$	14.26	mm
$q_{g,beam}$	1.59	kN/m	$\sigma_{m,y,d}$	13.27	MPa	$u_{inst,q}$	14.25	mm
$q_{g,tot}$	7.01	kN/m	$f_{m,d}$	19.31	MPa	$u_{fin,g}$	25.67	mm
$q_{q,f}$	10	kN/m	UC	0.69		$u_{fin,q}$	21.09	mm
$q_{tot,SLS}$	14.01	kN/m				$u_{fin,tot}$	46.76	mm
$q_{tot,ULS}$	23.41	kN/m				u_{lim}	48.78	mm
						UC	0.96	

For determining the possible strength class optimization, the minimum required height for strength GL24h is determined in Table H-12.

Table H-12: Loads and unity checks final design supporting beam upper level GL24h

Glulam beam 300x1130								
Loads			Bending stress			Global deflection		
$q_{g,floor}$	5.42	kN/m	M_{ed}	770.50	kNm	$u_{inst,g}$	14.45	mm
$q_{g,beam}$	1.51	kN/m	$\sigma_{m,y,d}$	12.07	MPa	$u_{inst,q}$	14.60	mm
$q_{g,tot}$	6.93	kN/m	$f_{m,d}$	14.27	MPa	$u_{fin,g}$	26.01	mm
$q_{q,f}$	10	kN/m	UC	0.85		$u_{fin,q}$	21.60	mm
$q_{tot,SLS}$	13.93	kN/m				$u_{fin,tot}$	47.61	mm
$q_{tot,ULS}$	23.31	kN/m				u_{lim}	48.78	mm
						UC	0.98	

Finally, only the fire resistance of the GL24h beam should be considered because the dimensions of the GL32h beam do not change compared to the preliminary design. The sufficient preliminary fire resistance is also valid in this final design.
The fire resistance check is done in Table H-13 using the indicated procedure of Appendix B.2 and using the same parameter values as applied in Appendix F.1 for the preliminary design.

Table H-13: Fire resistance check final beam design GL24h

Fire Glulam beam 300x1130→160x1060					
Loads			Bending stress		
$q_{g,floor}$	5.42	kN/m	M_{ed}	435.40	kNm
$q_{g,beam}$	0.75	kN/m	$\sigma_{m,y,d}$	14.53	MPa
$q_{g,tot}$	6.17	kN/m	$f_{m,d}$	16.69	MPa
$q_{q,f}$	10	kN/m	UC	0.87	
$q_{tot,fire}$	13.17	kN/m			

H.3.3: Calculations diaphragm action

The diaphragm action in two directions will be investigated because the area of each diaphragm differs for both directions, and the amount of load slightly differs.

Equations H.11 and H-12 determine the load for both the longitudinal and the transverse direction. Resulting in a longitudinal line load of 3.58 kN/m and a transverse line load of 3.62 kN/m for the governing upper floor level facing the highest wind loads.

$$q_{tot,long}\left[\frac{kN}{m}\right] = q_{comp}\left[\frac{kN}{m}\right] + q_{suc}\left[\frac{kN}{m}\right] + q_{sec}\left[\frac{kN}{m}\right] = 2.03 + 1.27 + 0.28 = 3.58\frac{kN}{m} \quad \text{(H.11)}$$

$$q_{tot,trans}\left[\frac{kN}{m}\right] = q_{comp}\left[\frac{kN}{m}\right] + q_{suc}\left[\frac{kN}{m}\right] + q_{sec}\left[\frac{kN}{m}\right] = 2.03 + 1.27 + 0.32 = 3.62\frac{kN}{m} \quad \text{(H.12)}$$

Below, the forces and bending moments corresponding to the two diaphragm actions are discussed.

Transverse diaphragm action

Figure 10-6 shows the transverse diaphragm action. Each grid of 5 meters x 16.26 meters is assumed to be a simply supported panel because the connection between two floor panels in the different diaphragms cannot ensure a complete bending moment transfer. Next, the connections will be as simple as possible, meaning a moment-fixed connection between the floor panels is unfavourable.

Each grid faces one-tenth of the load because ten grids are in the transverse direction.
The corresponding bending moment, tension force, compression force and shear force are calculated below in equations H-13 to H-15. Figure H-22 presents the position of the loads on one diaphragm.

$$M_{max}[kNm] = \frac{1}{8} * \frac{q_{tot,trans}\left[\frac{kN}{m}\right]}{10} * l^2[m^2] = \frac{1}{8} * \frac{3.62}{10} * 16.26^2 = 11.96\ kNm \quad \text{(H.13)}$$

$$F_c[kN] = F_t[kN] = \frac{M_{max}[kNm]}{b\ [m]} = \frac{11.96}{5} = 2.39\ kN \quad \text{(H.14)}$$

$$V[kN] = \frac{1}{2} * \frac{q_{tot,trans}\left[\frac{kN}{m}\right]}{10} * l[m] = \frac{1}{2} * \frac{3.62}{10} * 16.26 = 2.94\ kN \quad \text{(H.15)}$$

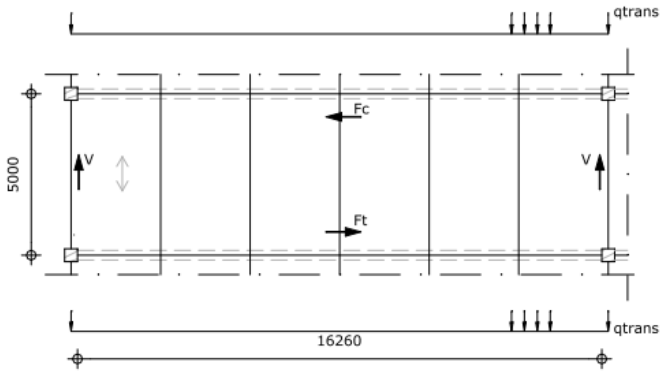

Figure H-22: Transverse diaphragm in mm

The CLT panel should resist bending stress. Table B-8 presents that the tensile resistance perpendicular to the grain is the governing one. The design value of this resistance is 0.26 MPa for a k_{mod} of 0.8 and γ_m of 1.25 for CLT.
Equation H-16 presents that the tension stress is 0.02 MPa, below the ultimate resistance.

$$\sigma_t[MPa] = \frac{M[Nmm]}{\frac{1}{6} * b[mm] * h^2[mm^2]} = \frac{11.96E6}{\frac{1}{6} * 140 * 5000^2} = 0.02\ MPa \quad \text{(H.16)}$$

Also, the shear stress should be checked if it is below the ultimate resistance. Equation H-17 presents that the shear stress is 0.004, which is far below the design shear strength of 2.56, according to Table B-8 and the above-mentioned k_{mod} and γ_m.

$$\tau[MPa] = \frac{V[N]}{h[mm] * t[mm]} = \frac{2.94E3}{5000 * 140} = 0.004\ MPa \quad \text{(H.17)}$$

Longitudinal diaphragm action

Figure 10-5 shows that the longitudinal diaphragms have an area of 16.26 meters x 50 meters. Due to the twice smaller width of the ramp grid, the contribution of this grid to the total longitudinal diaphragm action is negligible. So, three diaphragms are left, meaning each diaphragm gets a third of the load.

Equations H.18 to H.20 present the bending moment, tension force, compression force and shear force per diaphragm. Figure H-23 gives a visualization of these loads.

$$M_{max}[kNm] = \frac{1}{8} * \frac{q_{tot,long}\left[\frac{kN}{m}\right]}{3} * l^2[m^2] = \frac{1}{8} * \frac{3.58}{3} * 50^2 = 372.92\ kNm \quad \text{(H.18)}$$

$$F_c[kN] = F_t[kN] = \frac{M_{max}[kNm]}{b\ [m]} = \frac{372.92}{16.26} = 22.93\ kN \quad \text{(H.19)}$$

$$V[kN] = \frac{1}{2} * \frac{q_{tot,long}\left[\frac{kN}{m}\right]}{3} * l[m] = \frac{1}{2} * \frac{3.58}{3} * 50 = 29.83\ kN \quad \text{(H.20)}$$

To check the CLT panel's resistance, the bending and shear stress will be compared with the ultimate resistance of a C24 CLT panel.
Equations H.21 and H.22 give the bending and shear stress below the indicated ultimate design resistances of 9.28 MPa in parallel tension and 2.56 MPa in shear, as calculated from Table B-8. The floor can resist the longitudinal diaphragm loads.

$$\sigma_t[MPa] = \frac{M[Nmm]}{\frac{1}{6} * b[mm] * h^2[mm^2]} = \frac{372.92E6}{\frac{1}{6} * 140 * 16260^2} = 0.06\ MPa \quad \text{(H.21)}$$

$$\tau[MPa] = \frac{V[N]}{h[mm] * t[mm]} = \frac{29.83E3}{16260 * 140} = 0.01\ MPa \quad \text{(H.22)}$$

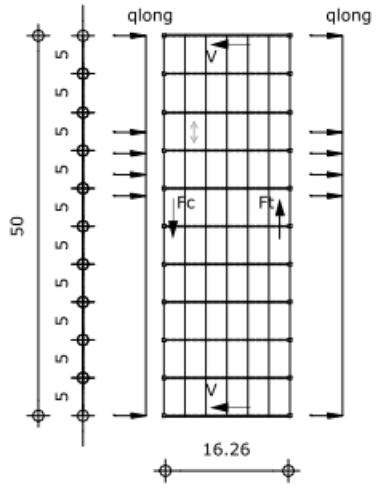

Figure H-23: Longitudinal diaphragm in m

Necessary for dimensioning the connections in the floor systems, Figures H-24 and H-25 show the loads to be taken up by these connections.

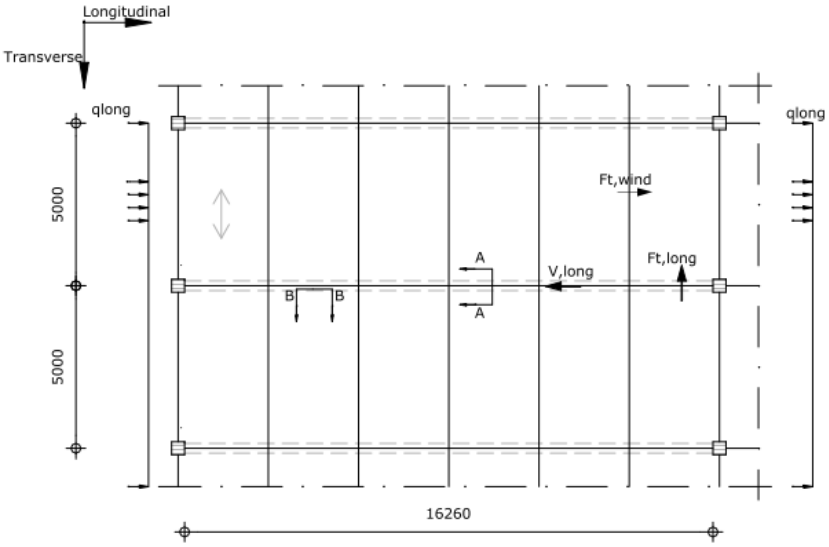

Figure H-24: Floor system forces longitudinal diaphragm action in mm

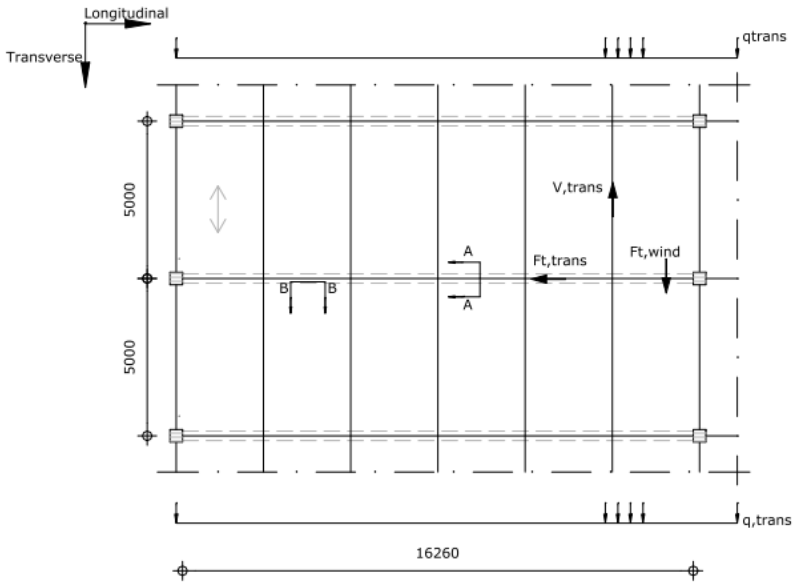

Figure H-25: Floor system forces transverse diaphragm action in mm

H.3.4: Calculations floor-to-floor connection

A floor-to-floor connection like Figure H-26 is most suitable to apply for the following reasons:

- The installation direction is vertical due to the horizontal block by the columns. This statement indicates a conflict with a vertical carpentry joint that also should resist a vertical load.
- A bolt can take up tension instead of a dowel, so the tension wind force can be resisted.
- There are only horizontal loads plus no protruding bolt parts on the top surface possible, so a vertical-orientated bolt is unnecessary and unwanted. Meaning the applied horizontal bolt orientation is favourable.
- Applying a fastening recess on top means no manual activities above head level. This aspect is important for feasibility and safety because there is no need for equipment like scaffolding. Next, safety is higher because there are no manual actions above head level, so there is less risk of falling objects, and the manual actions are easier to perform. In addition, there is no fall risk from scaffolding, for example.

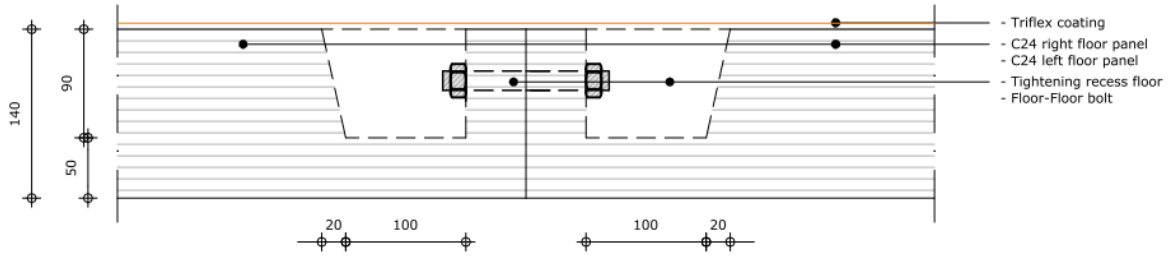

Figure H-26: Cross-section A-A of Figure 10-7 preliminary floor-to-floor connection design in mm

Figure H-26 shows that the floor-to-floor connection is a single-shear plane timber-to-timber connection. That means the failure modes A to F of equation 8.6 in Eurocode 1995 should be investigated for the loads in shear (NEN-EN 1995-1-1+C1+A1, 2011). The axial resistance $F_{ax,rk}$ is the minimum value of $3 * f_{c,90,k}[MPa] * A_{ring}[mm^2]$ & $f_{uk}[MPa] * A_{netto}[mm^2]$.

Three loads are present in this connection, as indicated in sub-paragraph 10.2.4 and shown in Figures H-21 and H-25. Those loads are the shear force from the transverse diaphragm action, the tension force from the wind suction line load, and the concentrated wheel load. For each of the loads, the governing bolt diameter will be determined.

Appendix B.2 presents the required timber material properties, and Appendix B.1 presents the material and safety factors. A steel grade S235 is applied in these design calculations.

<u>Shear force transverse diaphragm</u>

Figure H-27 shows the connection with this load indicated. Equation H.15 calculates that the maximum value of this load is 2.94 kN. From Table H-14, one bolt of M10 is sufficient, with a depth of 50 mm on both sides.

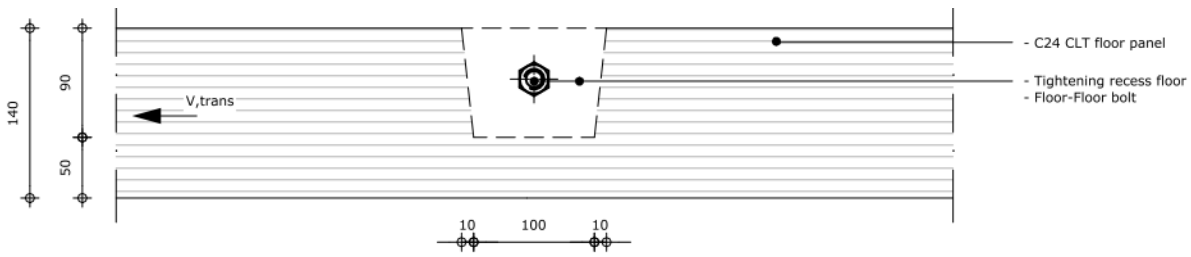

Figure H-27: Cross-section B-B of Figure 10-7 floor-to-floor connection with shear force transverse diaphragm in mm

Table H-14: Bolt resistance shear force transverse diaphragm

Floor-floor connection transverse shear force		
d	10	mm
t_1	50	mm
t_2	50	mm
$f_{h,1,k}$	31.0	MPa
$f_{h,2,k}$	31.0	MPa
$M_{y,Rk}$	42995.57	Nmm
$F_{ax,Rk}$	8576.55	N
$F_{v,Rk,min}$ (Failure mode F)	6473.18	N
n	1	
k_{mod}	0.8	
γ_m	1.3	
$F_{v,Rd}$	3983.49	N
$F_{v,ed}$	2940	N
UC	0.74	

Tension force wind load

Appendix H.3.3 states that the wind suction line load is 1.27 kN/m. The length of each CLT panel is five meters, so it faces a tension load of 6.35 kN. The load is visualized in Figure H-28.
Table H-15 presents that one M16 bolt can resist this axial force.

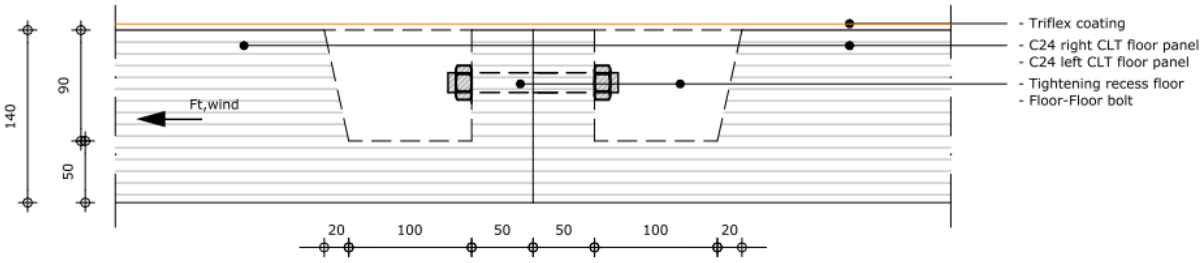

Figure H-28: Cross-section A-A of Figure 10-7 floor-to-floor connection with tension wind force in mm

Table H-15: Bolt resistance tension wind load

Floor-floor connection tension wind load		
d	16	mm
$F_{ax,Rk}$	22218.91	N
k_{mod}	0.8	
γ_m	1.3	
$F_{ax,Rd}$	13673	N
$F_{t,ed}$	6350	N
UC	0.46	

Due to the tightening opening, the axial force creates a small bending moment, as shown in Figure H-29. This bending moment results in a stress of 4.08 MPa. Comparing it with the resistance of a C24 panel of Table B-8 concludes that this stress is below the ultimate resistance.

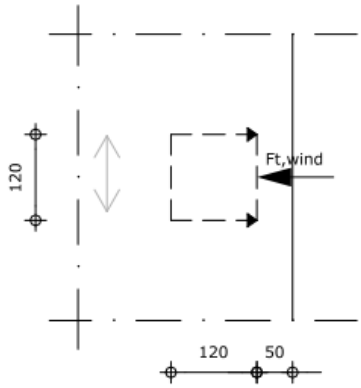

Figure H-29: Bending moment around recess floor in mm

Concentraded wheel load

Figure 5-2 shows the wheel load configuration. Combining this load with the safety factor of Appendix B.1 gives a total surface load of 0.75 MPa.
This load is below the design value of the perpendicular compression of a C24 panel.
In Figure H-30, the load on the floor-to-floor connection is visualized.

However, the opening for tightening the bolt cannot be filled with a PIR isolation material (*IKO Enertherm ALU*, 2020). This material has a compression strength of 0.175 MPa. Meaning it cannot resist the wheel load, see Figure H-30. So, a possible C24 timber block is favourable over a PIR block.

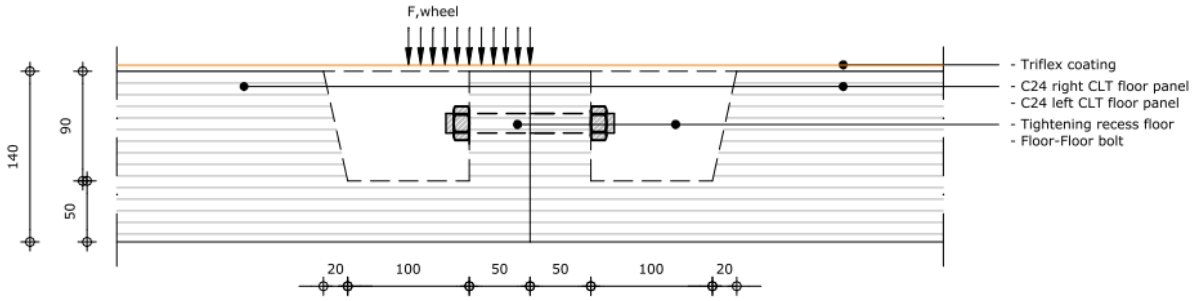

Figure H-30: Cross-section A-A of Figure 10-7 floor-to-floor connection with wheel load in mm

However, the most severe configuration is applying the 10 kN point load (paragraph 5.2) of category F car park load at one panel edge. Table H-16 presents that an S355 M16 bolt with a depth of 100 mm gives a sufficient unity check of 0.94.

Table H-16: Bolt resistance concentrated wheel load

Floor-floor connection concentrated wheel load		
d	16	mm
t_1	100	mm
t_2	100	mm
$f_{h,1,k}$	28.93	MPa
$f_{h,2,k}$	28.93	MPa
$M_{y,Rk}$	206729.94	Nmm
$F_{ax,Rk}$	22218.91	N
$F_{v,Rk,min}$ (Failure mode F)	17297.79	N
n	1	
k_{mod}	0.8	
γ_m	1.3	
$F_{v,Rd}$	10644.79	N
$F_{v,ed}$	10000	N
UC	0.94	

Table H-17 and Figures H-31 to H-36 present the re-mountability of this connection, in which the re-mounting process is vice versa of the demounting process. So, cutting and sanding becomes placing new coating material with the addition of a catalysator to create an initial bond strength between the old and new coating zone. Removing the filling block becomes placing the filling block.
Below, each step in a complete re-mounting process is described.

Table H-17: Procedure demounting and re-mounting floor-to-floor connection

Demounting	Re-mounting
1. Sanding the floor until the membrane layer over an area of 20 cm around the seam or combined with the recess area 2. Cut the seam and recess perimeter 3. Remove the filling material of the recess	4. Install the filling material 5. Place the new coating at the seam and recess perimeter cut with a catalysator 6. Refill the coating sanding area with a new coating plus catalysator

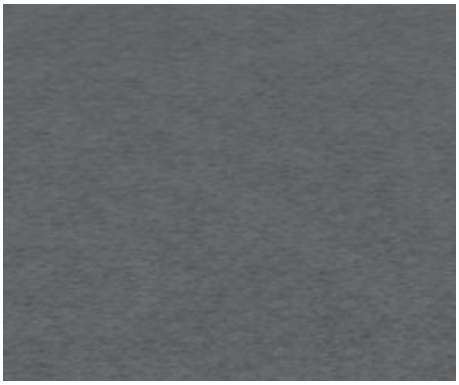

Figure H-31: Initial situation seam and floor-to-floor connection

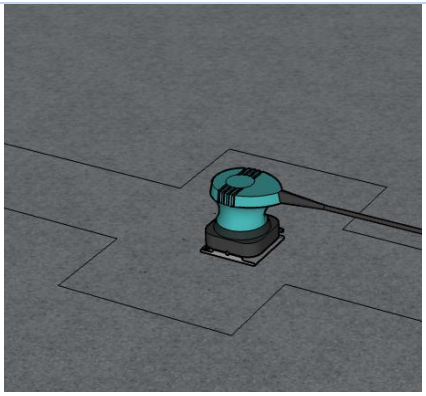

Figure H-32: Sanding area zone (step 1)

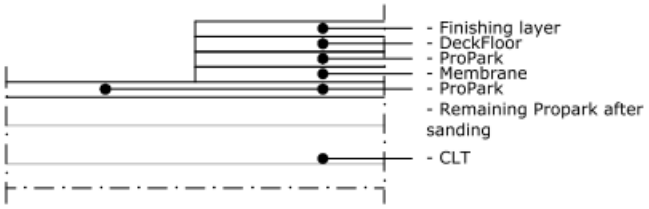

Figure H-33: Layup Triflex coating (*Triflex ProPark Systeem, Variant 1*, n.d.)

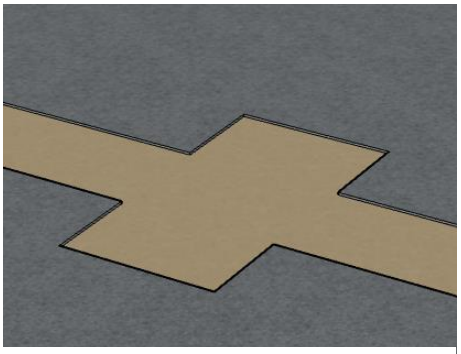

Figure H-34: Seam and connection top surface after sanding

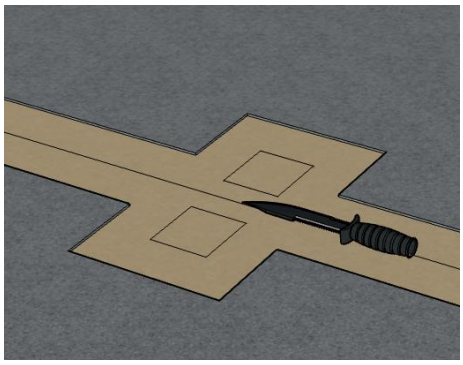

Figure H-35: Cutting seam and recess perimeter (step 2)

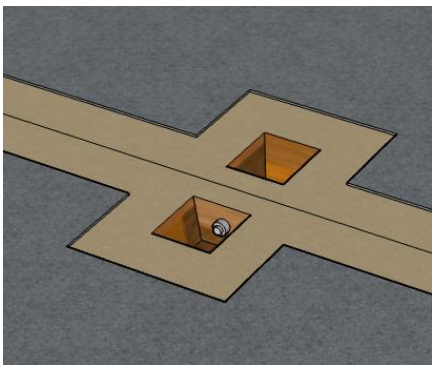

Figure H-36: Remove filling material of the recess (step 3)

H.3.5: Calculations floor-to-beam connection

The floor-to-beam connection has approximately the same layout as the floor-to-floor connection due to the mentioned benefits in H.3.4. Except for the bolt orientation. Therefore, the same shear force failure modes are applicable.

Four forces are present in this connection, as shown in Figures H-37 to H-38. These forces are the tension force from the longitudinal and transverse diaphragm action, the shear force from the longitudinal diaphragm action, and the tensile force from wind suction in the transverse wind direction.

The longitudinal shear and transverse tensile forces act in the same direction, as shown in Figures H-37 and H-38. Those forces cannot act simultaneously. From equations H.14 and H.20, the longitudinal shear force governs.

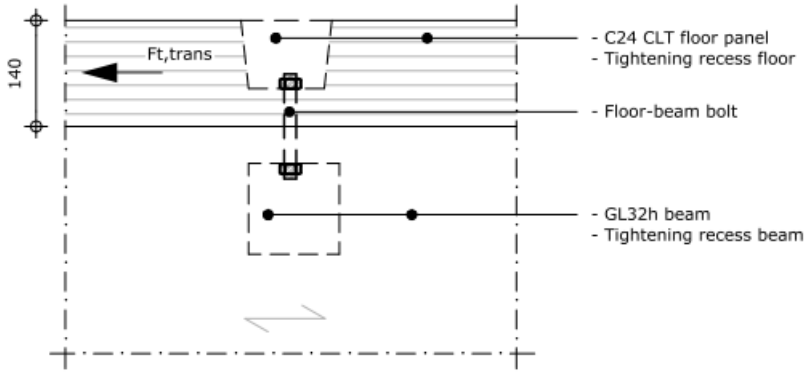

Figure H-37: Cross-section D-D of Figure 10-7 floor-to-beam connection transverse diaphragm tension in mm

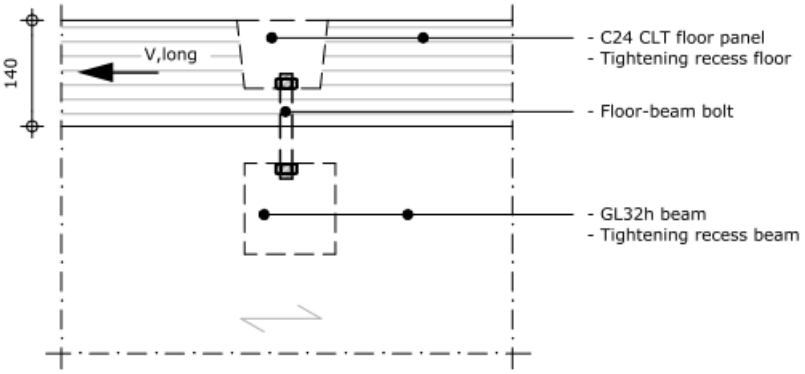

Figure H-38: Cross-section D-D of Figure 10-7 floor-to-beam connection longitudinal diaphragm shear force in mm

Also, the tensile wind suction and longitudinal tensile forces act in the same direction, as visualized in Figures H-39 and H-40. Again, they cannot act simultaneously due to the difference in the origin of wind force.
The tensile wind suction force is 20.33 kN using the calculated suction line load in Appendix H.2. Equation H.19 states that the longitudinal diaphragm tensile force is 22.93 kN, so the governing one. Figures H-39 and H-40 show that those tension forces will be taken up by shear.

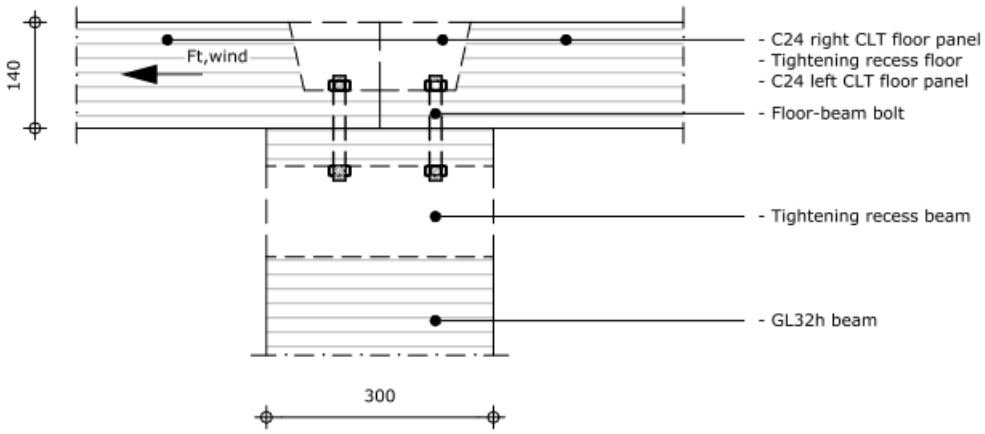

Figure H-39: Cross-section C-C of Figure 10-7 floor-to-beam connection wind force in mm

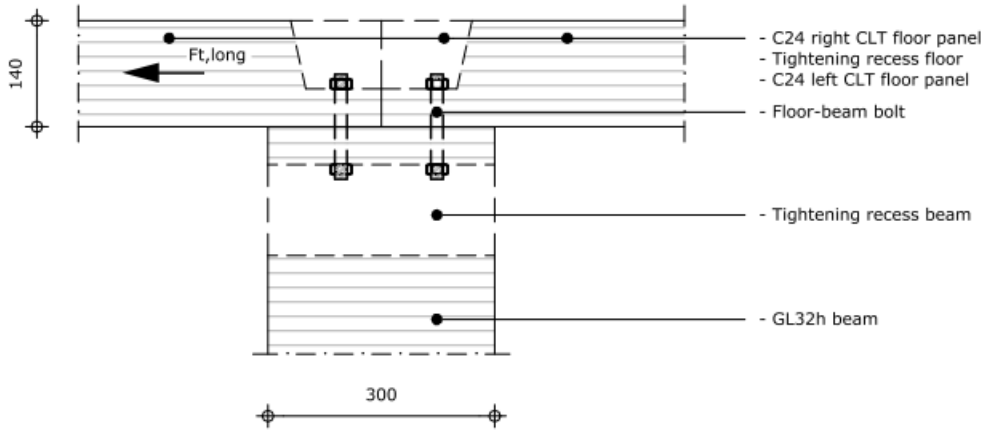

Figure H-40: Cross-section C-C of Figure 10-7 floor-to-beam connection longitudinal diaphragm tension in mm

As Figure 10-12 visualizes, there are 12 bolts per beam. All bolts can take up the longitudinal shear force, but the longitudinal tensile force is only possible by the floor panels in tension. Therefore, the required bolts for this force will be determined first.

Table H-18 presents that four M16 bolts are required to take up this tension force by shear.

Table H-18: Bolt resistance longitudinal diaphragm tension

Floor-beam connection longitudinal tension		
d	16	mm
t_1	50	mm
t_2	50	mm
$f_{h,1,k}$	28.93	MPa
$f_{h,2,k}$	33.75	MPa
$M_{y,Rk}$	145827.02	Nmm
$F_{ax,Rk}$	22218.91	N
$F_{v,Rk,min}$ (Failure mode C)	11764.94	N
n	4	
k_{mod}	0.8	
γ_m	1.3	
$F_{v,Rd}$	28959.85	N
$F_{v,ed}$	22930	N
UC	0.79	

The remaining eight bolts should be able to take up the longitudinal shear force. As Table H-19 indicates, applying eight M16 bolts results in a unity check of 0.52. So, in total, twelve M16 bolts can take up all the present forces. Applying M10 bolts results in a unity check of 0.90 for the same layout.

Table H-19: Bolt resistance longitudinal diaphragm shear force

Floor-beam connection longitudinal shear		
d	16	mm
t_1	50	mm
t_2	50	mm
$f_{h,1,k}$	28.93	MPa
$f_{h,2,k}$	33.75	MPa
$M_{y,Rk}$	145827.02	Nmm
$F_{ax,Rk}$	22218.91	N
$F_{v,Rk,min}$ (Failure mode C)	11764.94	N
n	8	
k_{mod}	0.8	
γ_m	1.3	
$F_{v,Rd}$	57919.70	N
$F_{v,ed}$	29830	N
UC	0.52	

Next to the horizontal shear forces, the vertical upward wind load creates a tension force in the bolts. This force per bolt is 4.2 kN, based on the vertical wind load of Table 10-2 and a CLT panel of 5 meters x 3 meters.
Table H-15 shows that an M16 bolt can easily take up this load because the unity check is 0.3. Combined with the longitudinal shear resistance of Table H-19, it gives an acceptable unity check of 0.42 plus 0.3 is 0.72. However, the combined unity check will be above 1 for the longitudinal tension resistance. So, M20 bolts should be applied to give an acceptable unity check of 0.94.

H.4: Calculations final design column with corresponding connections

All design calculations corresponding to the final design of the column and connections will be given in this paragraph.

The used k_{mod} value in the calculations is 0.8, based on Appendix B.2. Next, the values of γ_m are also given in Appendix B.2.

H.4.1: Calculations column dimensioning

Below, the assumptions of the column design are given.

- The centre and edge columns should have the same final cross-section to ensure a possible car park expansion, and the centre column can also face an asymmetric load.
- Cross-sectional reduction for higher segments, shown in Figure 10-19, is only possible in the direction perpendicular to the beam. Otherwise, multiple beam lengths are necessary, and the façade will be under a slope.
- A hinged column-to-foundation connection is assumed to avoid a bending moment in the foundation. This assumption results in a smaller possible foundation, so a lower cost.
- Due to a diaphragm on each floor, the buckling length equals the height of each floor level.
- A hinge is assumed at the column-to-column connection, 1.2 meters above the column-to-beam connection. It results in a simplified column-to-column connection and has no large impact on the maximum bending moment in the column.

Equation H.23 calculates the value for the force F_{beam} based on the resulting ultimate limit state line loads ($q_{tot,ULS}$) of the beam given in E-23.

$$F_{beam}[kN] = q_{tot,ULS}[kN/m] * \frac{1}{2} * \ l[m] = 23.41 * 8.13 = 190.32\ kN \tag{H.23}$$

Sub-paragraph 10.3.2 indicates that a compression force and bending moment is present in the column. Therefore, the ultimate limit state checks of equations H.23 and H.24 should be applied.

$$\sigma_{c,0,d}[MPa] \leq f_{c,0,d}[MPa] \tag{H.24}$$

$$\frac{\sigma_{c,0,d}[MPa]}{k_{c,y} * f_{c,0,d}[MPa]} + \frac{\sigma_{m,y,d}[MPa]}{f_{m,y,d}[MPa]} \leq 1 \tag{H.25}$$

To determine the factor $K_{c,y}$, equations H.25 to H.38 should be used. The parameter β_c is 0.1 for glued laminated timber (NEN-EN 1995-1-2+C2, 2011). The indicated buckling length in sub-paragraph 10.3.2 corresponds to parameter l_{eff}.

$$k_{c,y} = \frac{1}{k_y + \sqrt{k_y^2 - \lambda_{rel,y}^2}} \tag{H.26}$$

$$k_y = 0.5 * (1 + \beta_c * (\lambda_{rel,y} - 0.3) + \lambda_{rel,y}^2) \tag{H.27}$$

$$\lambda_{rel,y} = \frac{\lambda_y}{\pi} * \sqrt{\frac{f_{c,0k}[MPa]}{E_{0,05}[MPa]}} \tag{H.28}$$

$$\lambda_y = \frac{l_{eff}[mm]}{i_y[mm]} \tag{H.29}$$

Table H-20 presents the compression force in each segment for an edge column and Table H-21 for a centre column by using the force of equation H.23. In an edge column, there is always a bending moment in the column present. However, the loading can be on both sides by a centre column, so there is symmetry in eccentricity. This means both bending moments make a zero resulting bending moment in the column.

Table H-20: Loads on edge column

	Load [kN]
Segment 1	4 * F_{beam}: 761.28 kN
Segment 2	3 * F_{beam}: 570.96 kN
Segment 3	2 * F_{beam}: 380.64 kN
Segment 4	1 * F_{beam}: 190.32 kN

Table H-21: Loads on centre column

	Load [kN]
Segment 1	8 * F_{beam}: 1522.56 kN
Segment 2	6 * F_{beam}: 1141.92 kN
Segment 3	4 * F_{beam}: 761.28 kN
Segment 4	2 * F_{beam}: 380.64 kN

The bending moment is created by the force in the beam, equation H.23, multiplied by the eccentricity. The bending moment line is not constant over the height, so the maximum bending moment value changes per segment.
This eccentricity calculation is shown in equation H.30 based on Figure 10-18. The tolerance means the distance between the end plate and the end of the beam. A value of 20 mm is assumed because BNPC uses this tolerance based on its experience installing a prefab-to-prefab connection.

$$e[mm] = \frac{l_{corbel}[mm]}{2} + t_{tol}[mm] + \frac{h_{col[mm]}}{2} \quad \text{(H.30)}$$

Tables H-22 and H-23 show that the edge column configuration governs where half of the compression force and a bending moment are present. So, the other segments are also designed based on the edge column configuration in Tables H-24 to H-26.

Table H-22: Unity check centre column segment 1

GL32h 300x300 mm					
Compression			Stability		
N_{ed}	1.52E6	N	l_{eff}	3420	mm
$f_{c,0,d}$	20.48	MPa	K_{cy}	0.94	mm
$\sigma_{c,0,d}$	16.92	MPa	$\sigma_{c,0,d}$	16.92	MPa
UC	0.83		$f_{c,0,d}$	20.48	MPa
			M_{ed}	0	Nmm
			$\sigma_{m,d}$	0	MPa
			$f_{m,d}$	20.48	MPa
			UC	0.88	

Table H-23: Unity check edge column segment 1

GL32h 300x300 mm					
Compression			Comp. + bending		
N_{ed}	7.61E5	N	l_{eff}	3420	mm
$f_{c,0,d}$	20.48	MPa	K_{cy}	0.94	mm
$\sigma_{c,0,d}$	8.46	MPa	$\sigma_{c,0,d}$	8.46	MPa
UC	0.41		$f_{c,0,d}$	20.48	MPa
			M_{ed}	4.44E7	Nmm
			$\sigma_{m,d}$	9.86	MPa
			$f_{m,d}$	20.48	MPa
			UC	0.92	

Table H-24: Unity check edge column segment 2

GL32h 300x300 mm					
Compression			Stability		
N_{ed}	5.71E5	N	l_{eff}	3420	mm
$f_{c,0,d}$	20.48	MPa	K_{cy}	0.94	mm
$\sigma_{c,0,d}$	6.34	MPa	$\sigma_{c,0,d}$	6.34	MPa
UC	0.31		$f_{c,0,d}$	20.48	MPa
			M_{ed}	5.64E7	Nmm
			$\sigma_{m,d}$	12.53	MPa
			$f_{m,d}$	20.48	MPa
			UC	0.94	

Table H-25: Unity check edge column segment 3

GL32h 230x300 mm					
Compression			Comp. + bending		
N_{ed}	3.81E5	N	l_{eff}	3420	mm
$f_{c,0,d}$	20.48	MPa	K_{cy}	0.87	mm
$\sigma_{c,0,d}$	5.52	MPa	$\sigma_{c,0,d}$	5.52	MPa
UC	0.27		$f_{c,0,d}$	20.48	MPa
			M_{ed}	4.06E7	Nmm
			$\sigma_{m,d}$	11.77	MPa
			$f_{m,d}$	20.48	MPa
			UC	0.88	

Table H-26: Unity check edge column segment 4

GL32h 300x300 mm					
Compression			Comp. + bending		
N_{ed}	1.90E5	N	l_{eff}	3420	mm
$f_{c,0,d}$	20.48	MPa	K_{cy}	0.94	mm
$\sigma_{c,0,d}$	2.11	MPa	$\sigma_{c,0,d}$	2.11	MPa
UC	0.10		$f_{c,0,d}$	20.48	MPa
			M_{ed}	7.52E7	Nmm
			$\sigma_{m,d}$	16.71	MPa
			$f_{m,d}$	20.48	MPa
			UC	0.93	

The same calculation steps are applied for a strength class GL24h, resulting in the required cross-section per segment of Table H-27.

Table H-27: Required cross-sectional areas C24 edge column

Floor segment	Cross-section [mm]
1	340x340
2	340x340
3	250x340
4	340x340

Another important aspect is fire because the ultimate limit state governs the column design, as shown in the calculations above.
Table B-16 presents a notional charring rate (β_n) of 0.7 mm/min for softwood with a density higher than 290 kg/m^3, which is the case of GL32h and GL24h. In addition, the governing situation is four-sided fire exposure.
Equation H.31 presents the thickness reduction per side for 90 minutes of fire resistance, as stated in paragraph 5.3, based on the parameters mentioned in Appendix B.2.
The total charring depth is 63 mm per side plus a heat-affected zone of 7 mm, so 140 mm per cross-sectional direction.

$$d_{ef}[mm] = d_{char}[mm] + k_0[-] * d_0[mm] = 90 * 0.7 + 1 * 7 = 70\ mm \quad \text{(H.31)}$$

Tables H-28 to H-31 present the minimum required cross-sections for the columns in the fire situation using the adjusted load and strength according to equations B-9 to B-15 of Appendix B.2.

Table H-28: Unity check fire edge column segment 1

Fire GL32h 210x210 mm					
Compression			Comp. + bending		
N_{ed}	4.56E5	N	l_{eff}	3420	mm
$f_{c,0,d,fi}$	36.80	MPa	K_{cy}	0.82	mm
$\sigma_{c,0,d}$	10.33	MPa	$\sigma_{c,0,d}$	10.33	MPa
UC	0.28		$f_{c,0,d,fi}$	36.80	MPa
			M_{ed}	2.82E7	Nmm
			$\sigma_{m,d}$	18.29	MPa
			$f_{m,d,fi}$	36.8	MPa
			UC	0.84	

Table H-29: Unity check fire edge column segment 2

Fire GL32h 210x210 mm					
Compression			Comp. + bending		
N_{ed}	3.42E5	N	l_{eff}	3420	mm
$f_{c,0,d,fi}$	36.80	MPa	K_{cy}	0.82	mm
$\sigma_{c,0,d}$	7.75	MPa	$\sigma_{c,0,d}$	7.75	MPa
UC	0.21		$f_{c,0,d,fi}$	36.80	MPa
			M_{ed}	3.59E7	Nmm
			$\sigma_{m,d}$	23.45	MPa
			$f_{m,d,fi}$	36.8	MPa
			UC	0.89	

Table H-30: Unity check fire edge column segment 3

Fire GL32h 170x210 mm					
Compression			Comp. + bending		
N_{ed}	2.28E5	N	l_{eff}	3420	mm
$f_{c,0,d,fi}$	36.80	MPa	K_{cy}	0.64	mm
$\sigma_{c,0,d}$	6.38	MPa	$\sigma_{c,0,d}$	6.38	MPa
UC	0.17		$f_{c,0,d,fi}$	36.80	MPa
			M_{ed}	2.58E7	Nmm
			$\sigma_{m,d}$	20.67	MPa
			$f_{m,d,fi}$	36.80	MPa
			UC	0.83	

Table H-31: Unity check fire edge column segment 4

Fire GL32h 220x220 mm					
Compression			Comp. + bending		
N_{ed}	1.14E5	N	l_{eff}	3420	mm
$f_{c,0,d,fi}$	36.80	MPa	K_{cy}	0.85	mm
$\sigma_{c,0,d}$	2.35	MPa	$\sigma_{c,0,d}$	2.35	MPa
UC	0.06		$f_{c,0,d,fi}$	36.80	MPa
			M_{ed}	4.84E7	Nmm
			$\sigma_{m,d}$	27.28	MPa
			$f_{m,d,fi}$	26.80	MPa
			UC	0.82	

The resulting cross-sections for a GL24h column in a fire situation are given in Table H-32.

Table H-32: Required cross-sectional areas C24 edge column

Floor segment	Cross-section [mm]
1	230x230
2	240x240
3	180x240
4	240x240

Table H-33 presents the resulting cross-sections per segment for a strength class GL32h and Table H-34 for a strength class GL24h. The governing final cross-section is segment 4 for both strength classes, meaning the upper segment.

Table H-33: Resulting cross-section column segments GL32h

Floor segment	Preliminary cross-section [mm]	Minimum cross-section fire [mm]	Final cross-section [mm]
1	300x300	210x210	350x350
2	300x300	210x210	350x350
3	230x300	170x210	310x350
4	300x300	220x220	360x360

Table H-34: Resulting cross-section column segments GL24h

Floor segment	Preliminary cross-section [mm]	Minimum cross-section fire [mm]	Final cross-section [mm]
1	340x340	230x230	370x370
2	340x340	240x240	380x380
3	250x340	180x240	320x380
4	340x340	240x240	380x380

H.4.2: Calculations review final beam design

Compared to the calculations done in Appendix H.3.2, the beam width can be adjusted to 360 mm instead of 300 mm.

Tablse H-35 and H-36 show that this results in a minimally required beam height of 1040 mm for a GL32h beam and 1090 mm for a GL24h beam.

Table H-35: Final beam design GL32h

Glulam beam 360x1040								
Loads			Bending stress			Global deflection		
$q_{g,floor}$	5.42	kN/m	M_{ed}	783.43	kNm	$u_{inst,g}$	13.78	mm
$q_{g,beam}$	1.83	kN/m	$\sigma_{m,y,d}$	12.07	MPa	$u_{inst,q}$	13.30	mm
$q_{g,tot}$	7.25	kN/m	$f_{m,d}$	19.38	MPa	$u_{fin,g}$	24.80	mm
$q_{q,f}$	10	kN/m	UC	0.62		$u_{fin,q}$	19.68	mm
$q_{tot,SLS}$	14.25	kN/m				$u_{fin,tot}$	44.48	mm
$q_{tot,ULS}$	23.71	kN/m				u_{lim}	48.78	mm
						UC	0.91	

Table H-36: Final beam design GL24h

Glulam beam 360x1090								
Loads			Bending stress			Global deflection		
$q_{g,floor}$	5.42	kN/m	M_{ed}	779.92	kNm	$u_{inst,g}$	13.87	mm
$q_{g,beam}$	1.75	kN/m	$\sigma_{m,y,d}$	10.94	MPa	$u_{inst,q}$	13.55	mm
$q_{g,tot}$	7.27	kN/m	$f_{m,d}$	14.47	MPa	$u_{fin,g}$	24.97	mm
$q_{q,f}$	10	kN/m	UC	0.76		$u_{fin,q}$	20.06	mm
$q_{tot,SLS}$	14.17	kN/m				$u_{fin,tot}$	45.03	mm
$q_{tot,ULS}$	23.60	kN/m				u_{lim}	48.78	mm
						UC	0.92	

In the case of Fire, these beam heights are also sufficient due to the governing serviceability limit state instead of the ultimate limit state. This check is done in Tables H-37 and H-38 by applying the same principles as in Appendix F.1 for the preliminary design because the loads are equal.

Table H-37: Fire resistance check final beam design GL32h

Fire Glulam beam 360x1040→220x970					
Loads			Bending stress		
$q_{g,floor}$	5.42	kN/m	M_{ed}	445.02	kNm
$q_{g,beam}$	1.05	kN/m	$\sigma_{m,y,d}$	12.90	MPa
$q_{g,tot}$	6.47	kN/m	$f_{m,d}$	22.45	MPa
$q_{q,f}$	10	kN/m	UC	0.57	
$q_{tot,fire}$	13.47	kN/m			

Table H-38: Fire resistance check final beam design GL24h

Fire Glulam beam 360x1080→220x1010					
Loads			Bending stress		
$q_{g,floor}$	5.42	kN/m	M_{ed}	443.14	kNm
$q_{g,beam}$	0.99	kN/m	$\sigma_{m,y,d}$	11.85	MPa
$q_{g,tot}$	6.41	kN/m	$f_{m,d}$	16.77	MPa
$q_{q,f}$	10	kN/m	UC	0.71	
$q_{tot,fire}$	13.41	kN/m			

The required taper height increment for the GL32h beam is 125.78 mm based on equation H.32 below. This value is rounded up to 130 mm.

$$\Delta h[mm] = 1\% * \frac{1}{2} * l[mm] + u_{fin,tot}[mm] = 0.01 * \frac{1}{2} * 16260 + 44.48 = 125.78\, mm \quad \text{(H.32)}$$

H.4.3: Calculations column-to-beam connection

The prevention of horizontal movement of the beam is satisfied by applying an elevated edge of the corbel. This elevated edge will face a bending moment and shear force due to the horizontal wind loads during execution and a small horizontal execution load.

Equation H.33 presents that the horizontal wind load (based on Table H-6) on the elevated edge is 12.34 kN, assuming the horizontal execution load is 2.66 kN and the small execution load gives a total horizontal load of 15 kN.

$$F_{h,edge}[kN] = \left(\frac{1}{2}\right) * \left(F_{h,comp}\left[\frac{kN}{m}\right] * b[m] * l[m] + F_{h,suc}\left[\frac{kN}{m}\right] * b[m] * l[m]\right)$$
$$= 0.5 * (0.9 * 1.04 * 16.26 + 0.56 * 1.04 * 16.26) = 12.34\, kN \quad \text{(H.33)}$$

Applying the bending moment and shear resistance of a GL32h timber element results in the minimum required cross-section of 300x120x60 mm, as calculated in Table H-39.
For determining the shear resistance, factor k_{cr} is 0.67 (NEN-EN 1995-1-1+C1+A1, 2011).

Table H-39: Corbel elevated edge design

Bending resisance			Shear resistance		
b	120	mm	b	120	mm
h	300	mm	h	300	mm
t	60	mm	t	60	mm
F_{ed}	15000	N	k_{cr}	0.67	
e	70	mm	h_{eff}	201	mm
M_{ed}	1050000	Nmm	V_{ed}	15000	N
$\sigma_{m,d}$	5.83	MPa	τ_{ed}	1.87	MPa
$f_{m,d}$	20.48	MPa	f_{vd}	2.24	MPa
UC	0.28		UC	0.83	

Like the floor-to-floor and floor-to-beam connection, a tapered edge will be applied to ensure the beam is positioned accurately between the two elevated edges. The thickness increase of the bottom side of the edge is assumed to be 10 mm, resulting in a total thickness of 70 mm at the bottom.

Equation H-34 shows the way to determine the minimum required corbel length. Based on Figure H-41, the required length is 420 mm using the increased corbel width of 360 mm and the elevated edge design. The force (F) on this area is 192.76 kN, calculated by multiplying the ULS load on the beam of Table H-35 and half of the beam length.
Using Table B-7 and the safety factors gives a perpendicular compression strength ($f_{c,90,d}$) of 1.6 MPa for GL32h timber.

$$A_{req}[mm^2] = \frac{F[N]}{f_{c,90,d}[MPa]} \quad \text{(H.34)}$$

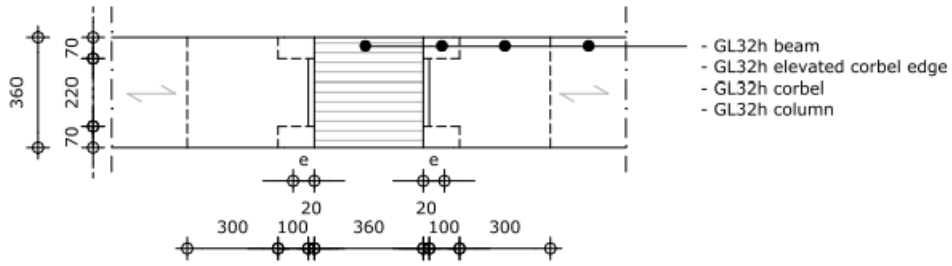

Figure H-41: Corbel area dimensions in mm

Using the above corbel area results in a bending moment in the corbel of 42.41 kNm. This value is calculated in equation H.35 by multiplying the force F with the eccentricity of half of the corbel length plus the indicated tolerance of 20 mm. Because the resulting force (F) acts in the centre of the contact area, so without the tolerance of 20 mm.

$$M_{ed}[kNm] = F_{beam}[kN] * (\frac{l_{corbel}}{2}[m] + e_{tol}[m]) = 192.76 * (200 + 20) = 42.41\ kNm \quad \text{(H.35)}$$

The bending and shear resistance should be checked to determine the minimum required corbel height. It will be assumed that the corbel is made of GL32h, like the beam and column.

Based on Table H-40, it can be assumed that the minimum required height of the corbel is 600 mm for the governing shear resistance check.

Table H-40: Corbel height calculations

Shear resistance			Bending resistance		
h	600	mm	h	600	mm
V_{ed}	192.76	kN	M_{ed}	42.41	kNm
k_{cr}	0.67		$\sigma_{m,y,d}$	1.96	MPa
b_{ef}	241.2	mm	$f_{m,d}$	20.48	MPa
τ_{ed}	2,00	MPa	UC	0.10	
$f_{v,d}$	2.24	MPa			
UC	0.89				

Next to the corbel height check, the remaining beam height above the corbel should also be checked on its resistance.
Equations H.36 and H.37 present the formulas necessary to check the beam resistance using a value of 6.5 for parameter k_n (NEN-EN 1995-1-1+C1+A1, 2011).

$$\tau_{ed}[MPa] = 1{,}5 * \frac{V[N]}{b[mm] * h_{ef}[mm]} \leq k_v * f_{v,d}[MPa] \quad \text{(H.36)}$$

$$k_v = min \begin{cases} 1 \\ \frac{k_n(1+\frac{1.1i^{1.5}}{\sqrt{h}})}{\sqrt{h}*(\sqrt{\alpha(1-\alpha)}+0.8*\frac{x}{h}\sqrt{\frac{1}{\alpha}-\alpha^2})} \end{cases} \quad \text{(H.37)}$$

Applying the dimensions of Figure H-41 and Table H-40 gives an insufficient unity check of 2.91, given in Table H-41. So, the height should increase to 750 mm with a slope of 6 degrees in the beam to get a sufficient unity check of 0.93, as calculated in Table H-42.

Reinforcement in the zone around the beam recess can help increase the shear resistance, as done in the cut-back support for a CLT rib panel (Structural Design Manual CLT Rib Panels, 2022). Further research should investigate the optimization in recess height and minimum required slope.

Table H-41: First beam height check

Shear resistance		
h	1040	mm
h_{ef}	440	mm
V_{ed}	192.76	kN
b	360	mm
τ_{ed}	1.83	MPa
k_n	6.5	
x	200	mm
α	0.42	
i	0	
k_v	0.28	
$f_{v,d}$	0.63	MPa
UC	2.91	

Table H-42: Second beam height check

Shear resistance		
h	1040	mm
h_{ef}	750	mm
V_{ed}	192.76	kN
b	360	mm
τ_{ed}	1.07	MPa
k_n	6.5	
x	200	mm
α	0.72	
i	6	
k_v	0.51	
$f_{v,d}$	1.15	MPa
UC	0.93	

Due to the enlarged beam height above the corbel, the elevated corbel edge will also increase to be higher than the centre line. Assuming a height of 400 mm satisfies this statement. Table H-43 presents that the increased height results in a possible reduction in thickness. Compared to the calculated 60 mm in Table H-39, a thickness of 45 mm is minimally required for a 400 mm height. This adjusted thickness results in a small increase in corbel area, meaning the unity check of equation H.34 drops slightly.

Table H-43: Adjusted corbel elevated edge design

Bending resisance			Shear resistance		
b	120	mm	b	120	mm
h	400	mm	h	400	mm
t	45	mm	t	45	mm
F_{ed}	15000	N	k_{cr}	0.67	
e	70	mm	h_{eff}	268	mm
M_{ed}	1050000	Nmm	V_{ed}	15000	N
$\sigma_{m,d}$	7.78	MPa	τ_{ed}	1.87	MPa
$f_{m,d}$	20.48	MPa	f_{vd}	2.24	MPa
UC	0.38		UC	0.83	

Next, the corbel's shear force and bending moment should be translated to the column. Sub-paragraph 10.3.4 states that the shear force will be translated to the column as a compression force by making a recess in the column. A bolted connection should take up the tensile force from the bending moment in the column.

Table H-44 shows that a recess of 80 mm gives a sufficient compression resistance verification using a GL32h strength class for the corbel and column. This recess depth is also applied in the reference project of Malmö (Appendx A.3).
This results in a stress of 0.4 MPa in the column part below the recess, satisfying the 1.6 MPa perpendicular compression strength.

Table H-44: Column recess calculations

F_{ed}	192.76	kN
l	360	mm
b	80	mm
$\sigma_{c,0,d}$	6.69	MPa
$f_{c,0,d}$	20.48	MPa
UC	0.33	

The bolts should resist the bending moment of 42.41 kNm calculated in equation H.35 for both sides. Table H-45 presents that three rows of three M24 bolts at a height of 230 mm, 330 mm, and 430 mm of the bottom rotation point give a sufficient unity check of 0.93.

Table H-45: Corbel bolt tensile resistance

Corbel bolt tensile resistance		
d	24	mm
$F_{ax,Rk}$	50.30	kN
$F_{ax,Rd}$	30.96	kN
n	3	
e	430	mm
$M_{rd,430}$	39.94	kNm
e	330	mm
$M_{rd,330}$	30.65	kNm
e	230	mm
$M_{rd,230}$	21.36	kNm
$M_{rd,tot}$	91.95	kNm
M_{ed}	84.82	kN
UC	0.92	

Figure H-42 shows the bolt layout, satisfying the minimum distances according to Eurocode (NEN-EN 1995-1-1+C1+A1, 2011).

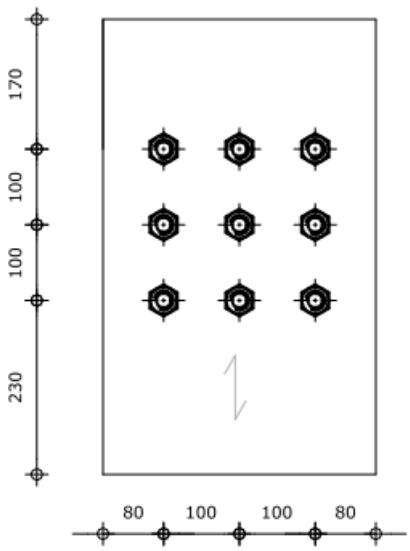

Figure H-42: Bolt layout corbel in mm

H.4.4: Calculations review drainage recess design

Table H-42 shows that the beam height of 750 mm is minimally necessary to get a sufficient shear resistance in the beam.

Reducing the height by 150 mm due to the drainage recess opening, as mentioned in paragraph 9.3, the resistance height of 600 mm is insufficient.
So, the recess should move to the centre of the beam to be not above the corbel, meaning it faces no reduction in shear strength due to the corbel recess in the beam.

The corbel has a length of 420 mm, as mentioned in H.4.2. So, assuming the centre of the 150 mm wide recess (paragraph 9.3) is positioned at 575 mm from the beam end. Table H-46 shows that the shear resistance is sufficient. That means the gutter should move 200 mm to the centre of the beam.

Table H-46: Shear resistance check beam at drainage opening

Shear resistance		
b	360	mm
h	617	mm
k_{cr}	0.67	
b_{eff}	241	mm
V_{ed}	181000	N
τ_{ed}	1.82	MPa
f_{vd}	2.24	MPa
UC	0.81	

H.4.5: Calculations column-to-column connection

Figure 10-19 shows that the first connection from the foundation is 1.2 meters above floor level 1. The resulting bending moment per level on the column is 77.1 kNm, using the equation H.30 and the load of 192.76 kN per level. The connection between segment 3 and segment 4 is governing because it faces the highest shear force of 30.96 kN, which is the only force the steel connection should translate.

Two M16 bolts at a distance of 100 mm are sufficient, as shown in Table H-47, for assuming a steel plate thickness of 10 mm.

Table H-47: Bolt tensile resistance column-to-column

Column-column connection		
d	16	mm
t_1	175	mm
$f_{h,k}$	33.75	MPa
$M_{y,Rk}$	206729.94	Nmm
$F_{ax,Rk}$	22218.91	N
$F_{v,Rk,min}$ (Failure mode H)	51380.48	N
n	2	
a_1	100	
n_{ef}	1.55	
$F_{v,Rd}$	49131.04	N
$F_{v,ed}$	30960	N
UC	0.63	

The steel end plate should have a minimum area of 238x238 mm. This area is based on the governing axial load of 1156.56 kN for connection segments 1 and 2 facing the largest compression force. This force is calculated using Table H-20 and the updated beam load of Table H-35. The design compression strength in grain direction from Table B-7 is 20.48 MPa.

Assume an end plate area of 280x280 mm, creating an edge opening of 40 mm wide per edge according to the total column area of 360x360 mm.

The eccentric loading creates a bending moment in the end plate, as shown in Figure H-43 for the investigated upper part of the end plate in grey. From Table H-48, it can be concluded that the minimum thickness is 50 mm for the S355 steel class.

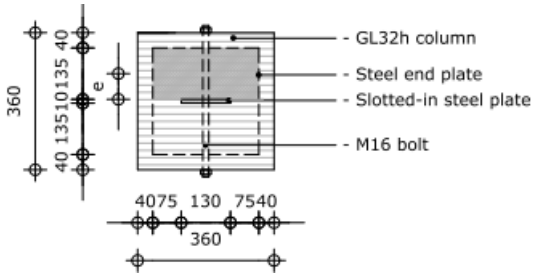

Figure H-43: Eccentricity end plate in mm

Table H-48: End plate thickness design

Bending resisance			Shear resistance		
b	280	mm	b	280	mm
t	50	mm	t	50	mm
F_{ed}	578280	N	V_{ed}	578280	N
e	67.5	mm	τ_{ed}	61.96	MPa
M_{ed}	39030000	Nmm	f_y	355	MPa
$M_{c,rd}$	41416667	MPa	UC	0.30	
UC	0.94				

H.5: Calculations secondary details

In this paragraph, the design calculations of the secondary details are provided.

H.5.1: Calculations bracing system

The bracing diameter can be determined based on the horizontal diaphragm loads determined in Appendix H.3.3.

Transverse vertical stability system

A cable can only take up tension. So, the maximum tension force is 244.43 kN in one of the governing cables depending on the wind direction, as indicated in Figure 10-34. This force is calculated by applying the total shear load per floor level based on equation H.20.

A steel grade of S355 is assumed. The National Annex of Eurcode 3 indicates γ_{m0} is 1 (NEN-EN 1993-1-1+C2+A1, 2016). Equation H.38 provides the resistance in axial tension. The minimum required diameter of the cable is 31 mm.

$$N_{t,rd}[N] = \frac{A[mm^2]*f_y[MPa]}{\gamma_{m0}} = \frac{\frac{1}{4}*\pi*31^2*355}{1} = 267943\ N > 244430\ N \quad \text{(H.38)}$$

In a fire situation, the load is only 20 per cent based on Appendix B.1 and equation B.12 of Appendix B.2. So, the load in a fire situation is 48886 N instead of 244430 N. Based on Table 3.1 of Eurcode 1993-1-2 (NEN-EN 1993-1-2+C2, 2011), if the steel temperature stays below 700 °C, the bracing resistance is sufficient.

H.5.2: Calculation connection bracing to load-bearing system

As mentioned in 10.4.1, only the transverse bracing system is inside the scope of this research.

Transverse bracing system

Below, the reasoning behind the chosen type of connection is given.

As mentioned in 10.4.1, only the transverse bracing system's connection with the column is inside the scope of this research. Using a slotted-in steel plate results in a simple transfer of the tensile through the column. By a bolt connection between the bracing system and the slotted-in steel plate, the tensile force goes from cable to plate to the cable again. A second slotted-in steel plate will be applied to connect the secondary beam to the primary slotted-in steel plate. Because the beam is placed vertically by a crane, the primary steel plate should go exactly through a secondary beam recess. This results in a very detailed and time-consuming erection process.

Eccentricities in the bracing system are avoided to prevent unwanted bending moments. Therefore, due to the large height of the beam, the steel plate should be positioned below the floor. This means the "Willems Anker" should pass the floor panels. This design is not a problem because the bracings are not positioned in a parking lot or driveway, as shown in Figure 10-1. Only an opening in the end floor panel's edge should ensure the anchor can go through the beam. And subsequently, this recess should be made watertight by a Triflex coating.

In the secondary beam, only a compression force is present, with a value of 77 kN. A 90x90 mm C24 beam is minimally required.

The design process starts with the determination of the loads.
The tensile force in the cable is 244.43 kN for cable 1, indicated in Figure H-44 and 191.38 kN for cable 2 in Figure H-44. So, the governing shear force on the column-bracing connection is 244.43 kN.

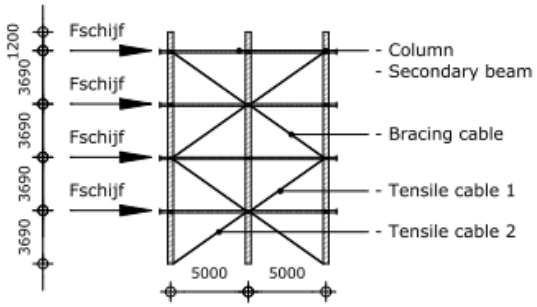

Figure H-44: Transverse bracing system with indicated tensile cables in mm

Sub-paragraph 10.4.2 states that a slotted-in steel plate will be applied in the column. Table H-49 shows that four S355 M27 bolts, in a pattern of two rows of two bolts, can minimally take up the shear force using an internal distance of 300 mm. See Figure H-45 for the bolt layout.

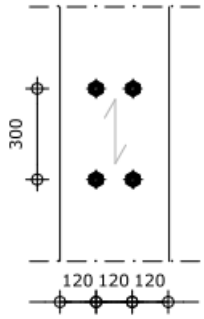

Figure H-45: Bolt layout M27 column-primary slotted-in plate in mm

Table H-49: Connection verification primary slotted-in steel plate to column

Column to primary steel plate connection shear		
d	27	mm
t_1	180	mm
$f_{h,1,k}$	29.33	MPa
$M_{y,Rk}$	805818.47	Nmm
$F_{ax,Rk}$	63752.73	N
$F_{v,Rk,min}$ (Failure mode h)	124174.07	N
n	2 (2 rows)	
a_1	300	
n_{ef}	3.59	
k_{mod}	0.8	
γ_m	1.3	
$F_{v,Rd}$	274213.01	N
$F_{v,ed}$	244430	N
UC	0.89	

Table H-50 provides the check of the column at the recess location. The resulting column width is 296 mm. The cross-section can resist the loads because the governing unity check in this table is below 1. Based on the results in Appendix H.4.1, the governing column segment 4 is checked in Table H-50.

Table H-50: Column resistance check at recess

GL32h 360x296 mm					
Compression			Comp. + bending		
N_{ed}	1.90E5	N	l_{eff}	3690	mm
$f_{c,0,d}$	20.48	MPa	K_{cy}	0.96	mm
$\sigma_{c,0,d}$	1.76	MPa	$\sigma_{c,0,d}$	1.76	MPa
UC	0.09		$f_{c,0,d}$	20.48	MPa
			M_{ed}	7.04E7	Nmm
			$\sigma_{m,d}$	13.04	MPa
			$f_{m,d}$	20.48	MPa
			UC	0.73	

Next, the connection between the cable and the end plate should be designed. The cable is designed as a “Willems Anker”, as determined in sub-paragraph 10.4.1. This results in only one bolt can be used between the steel plate and the “Willems Anker”. One M33 bolt is minimally necessary to take up the governing tensile cable force of 244.43 kN in cable 1 of Figure H-44, as calculated in Table H-51. The resistance is based on a steel-to-steel connection’s shear and bearing strength (NEN-EN 1993-1-8+C2, 2011). This calculation assumes a bolt class of 10.9 and a thickness of 10 mm.

Table H-51: Connection verification primary slotted-in steel plate with “Willems Anker”

Primary steel plate to Willems Anker connection shear		
d	33	mm
t	20	mm
f_u	510	MPa
f_{ub}	1000	MPa
A_s	694	mm^2
α_v	0.5	N
$\gamma_{m,2}$	1.25	
F_{vrd}	277600	N
$F_{b,rd}$	336600	N
n	1	
$F_{rd,min}$	277600	N
$F_{v,ed}$	244430	N
UC	0.88	

The maximum compression force is in the secondary beam of floor level 1, which faces a compression force of 77 kN. Applying a C24 beam gives a minimum required cross-section of 90x90 mm, using the characteristic compression strength given in Table B-8 and the given safety factors k_{mod} of 0.8 and γ_m of 1.3. Table H-52 shows this calculation.

Table H-52: Secondary beam design calculation

C24 parallel compression strength		
b	90	mm
h	90	mm
F_{ed}	77000	N
$\sigma_{c,0,d}$	9.50	MPa
$f_{c,0,k}$	21	MPa
$f_{c,0,d}$	12.9	MPa
UC	0.74	

Table H-53 shows that three M20 bolts are minimally required to connect the secondary slotted-in plate to the secondary beam, combined with a thickness increase of 50 mm to 140 mm for sufficient resistance. Next, the height of the secondary beam should increase to 120 mm to satisfy the edge distance requirement.

Table H-53: Connection verification secondary beam to secondary slotted-in steel plate

Secondary beam – primary steel plate connection shear		
d	20	mm
t_1	70	mm
$f_{h,1,k}$	27.55	MPa
$M_{y,Rk}$	369291.59	Nmm
$F_{ax,Rk}$	34848.12	N
$F_{v,Rk,min}$ (Failure mode g)	50331.49	N
n	1 (2 rows)	
n_{ef}	2	
k_{mod}	0.8	
γ_m	1.3	
$F_{v,Rd}$	92919.66	N
$F_{v,ed}$	77000	N
UC	0.83	

A bolt should connect this secondary slotted-in steel plate to the primary slotted-in steel plate. From Table H-54, one M20 bolt is sufficient to take up the shear force of 77000 kN, assuming a steel plate thickness of 10 mm.

Table H-54: Connection verification primary slotted-in to secondary slotted-in steel plate

Secondary steel plate to primary steel plate connection shear		
d	20	mm
t	10	mm
f_u	510	MPa
f_{ub}	1000	MPa
A_s	245	mm^2
α_v	0.5	N
$\gamma_{m,2}$	1.25	
F_{vrd}	98000	N
$F_{b,rd}$	144000	N
n	1	
$F_{rd,min}$	98000	N
$F_{v,ed}$	77000	N
UC	0.78	

Finally, the thicknesses of the steel plates should be determined. The tensile resistance of the steel plate should be checked using the net cross-section next to the bolt hole (NEN-EN 1993-1- 1+C2+A1, 2016).
This results in a minimum thickness of 2.95 mm, applying steel class S355 and the bolt hole (d_0) of 36 mm. Furthermore, the width of the steel plate at the bolt hole position is 360 mm, based on Figure 10-36.
A common thickness of 10 mm will be assumed for the primary slotted-in steel plate.

The secondary slotted-in steel plate is loaded in compression, resulting in a minimum required thickness of 1.8 mm for an S355 steel plate (NEN-EN 1993-1- 1+C2+A1, 2016). Again, a 10 mm thickness will be assumed.

Like the steel fire assessment in H.5.1, a steel temperature above 700 degrees will result in an insufficient strength of the bracing system.

H.6: Mounting sequence visualization

Paragraph 10.5 presents the mounting and demounting sequence summarized in Figure 10-44. Figures H-46 to H-57 below give a visualization of the mounting sequence. The demounting sequence means following the steps from back to front. So, the start of the demounting process is the situation in Figure H-57. This sequence is shown in Figures H-58 to H-69.

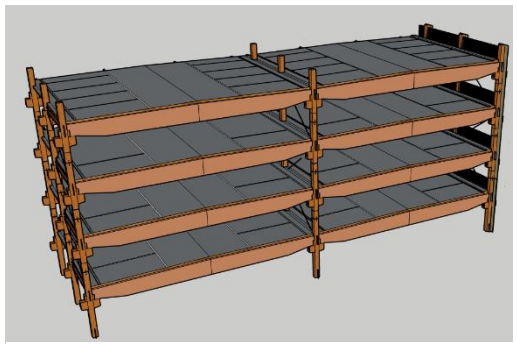

Figure H-46: Starting point mounting sequence

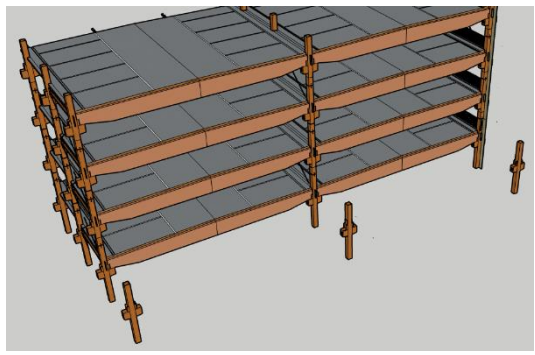

Figure H-47: Construct columns level 1

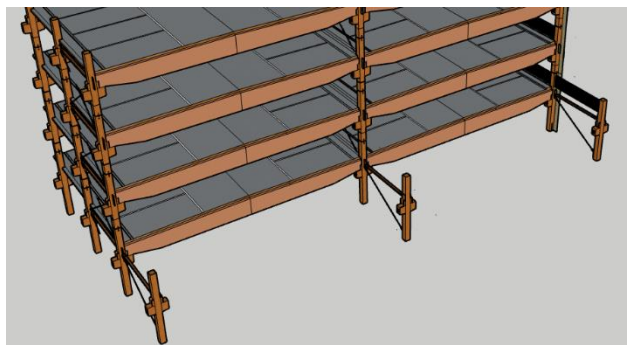

Figure H-48: Construct transverse bracing system level 1

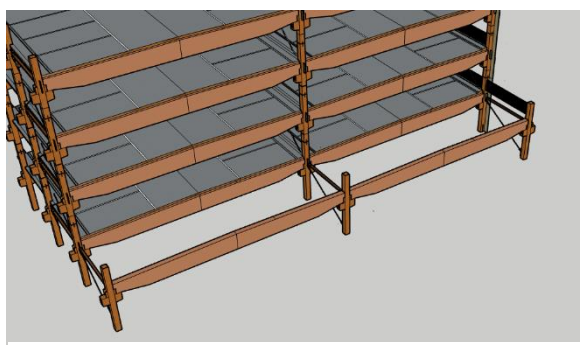

Figure H-49: Construct beams level 1

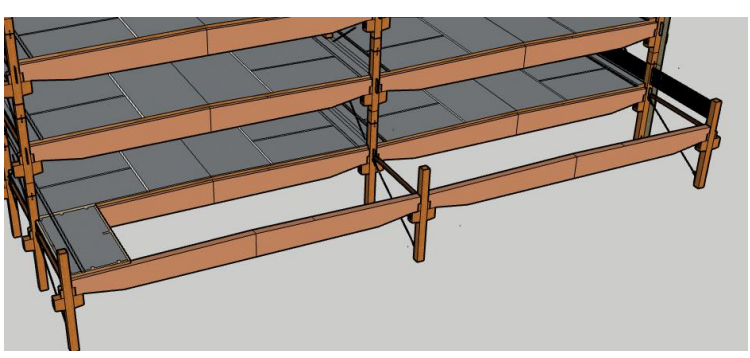

Figure H-50: Construct first CLT panel from stable centre

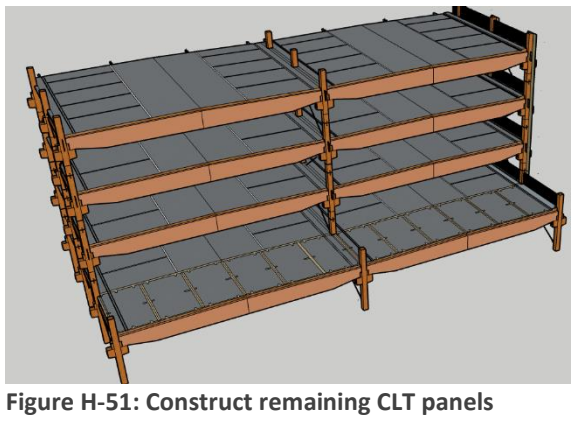

Figure H-51: Construct remaining CLT panels

Figure H-52: Apply Triflex coating on the seams

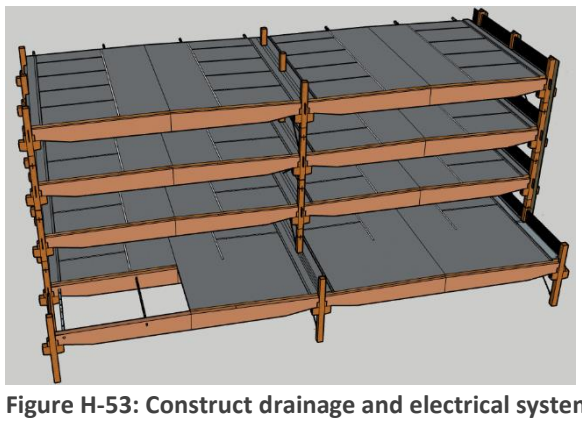

Figure H-53: Construct drainage and electrical system installation

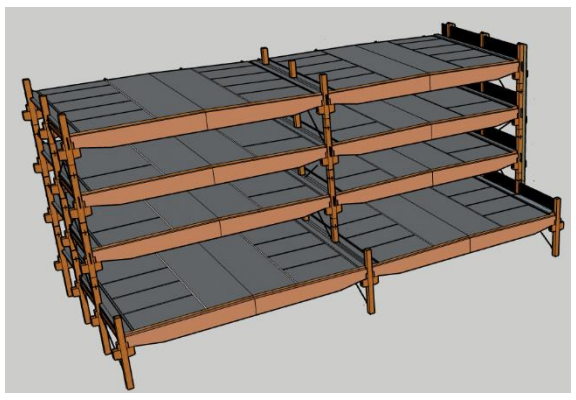

Figure H-54: Apply markings

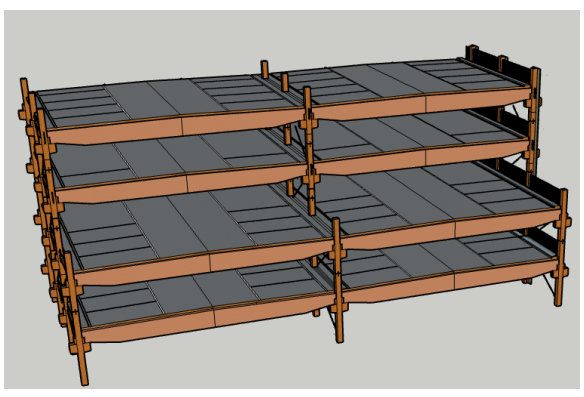

Figure H-55: Construct second level by doing previous steps

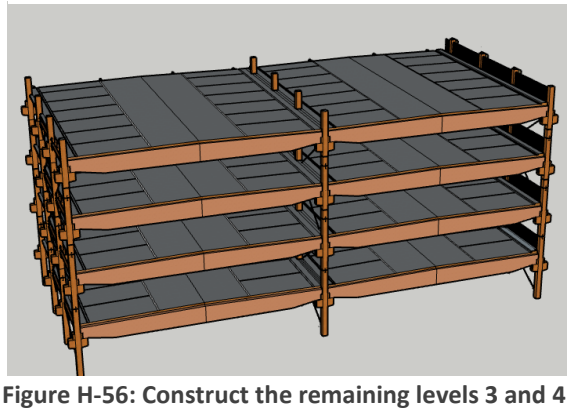

Figure H-56: Construct the remaining levels 3 and 4

Figure H-57: Apply wood protection panel

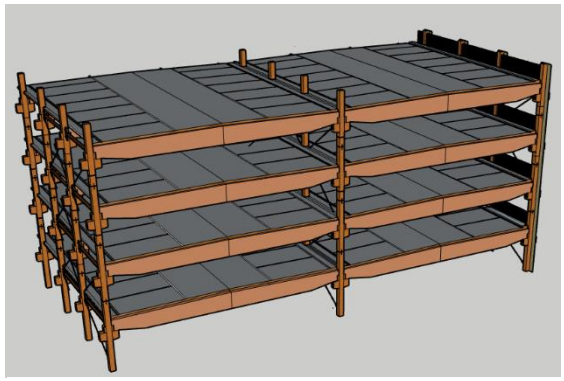

Figure H-58: Starting point demounting sequence

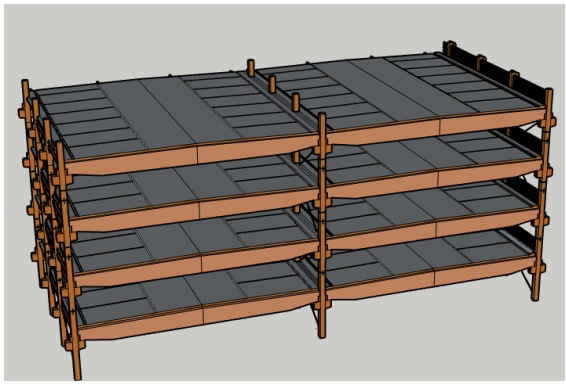

Figure H-59: Demounted wood protection panel

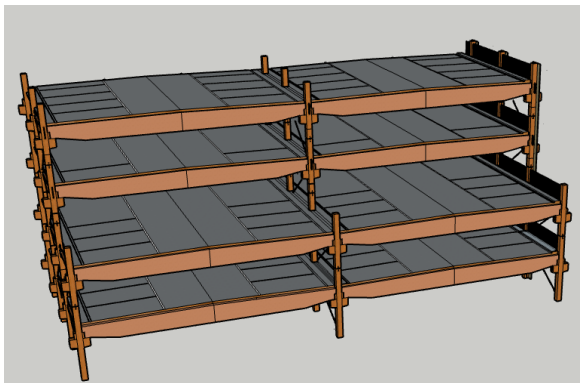

Figure H-60: Demounted levels 3 and 4

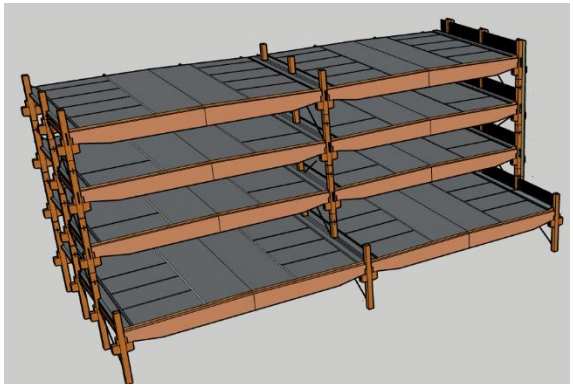

Figure H-61: Demounted level 2

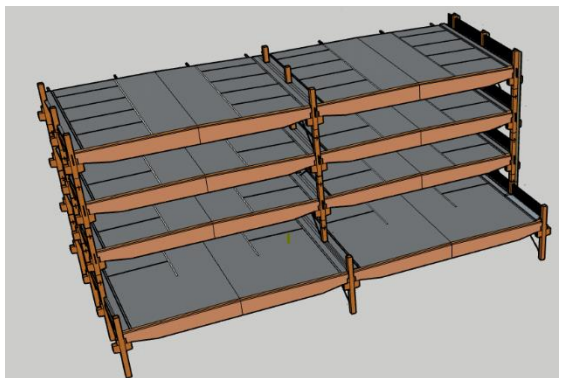

Figure H-62: Removed markings level 1

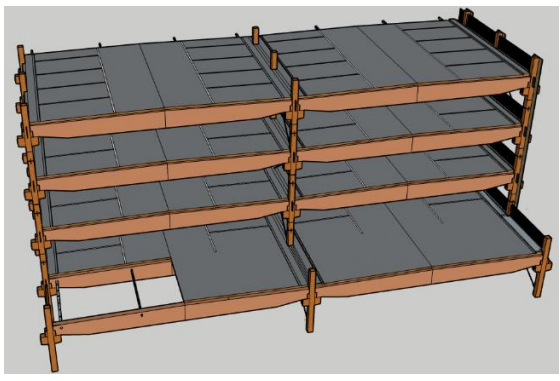

Figure H-63: Demounting drainage and electrical installations level 1

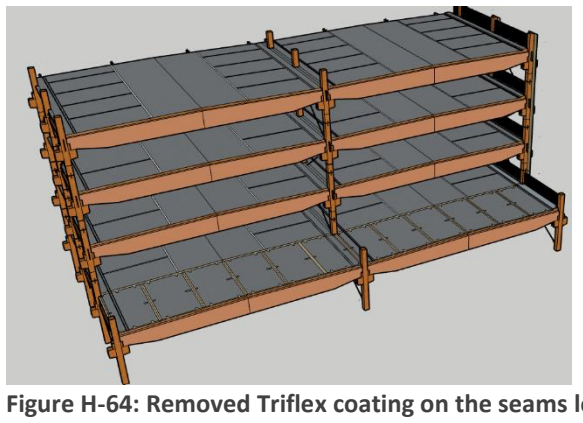

Figure H-64: Removed Triflex coating on the seams level 1

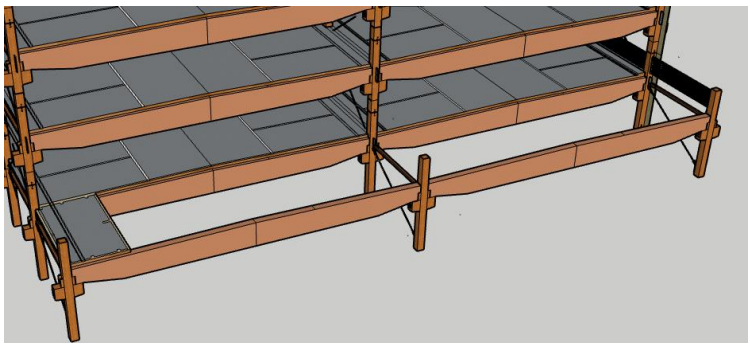

Figure H-65: Demounted CLT panels towards stable centre level 1

Figure H-66: Demounted last CLT panel level 1

Figure H-67: Demounted beams level 1

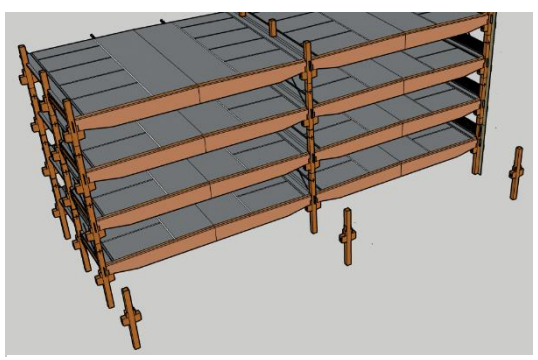

Figure H-68: Demounted transverse bracing system level 1

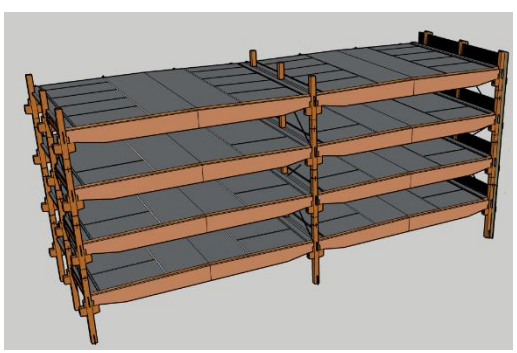

Figure H-69: Demounted columns level 1

I: Concluding visualizations final design

Figures I-1, I-5 and I-9 present the top view of the investigated module, as mentioned in the problem statement.
These top views indicate the cross-sections and details presented below them. All figures together show the final design of the timber re-mountable car park.
Afterwards, the details of the final design are also visualized in 3D.

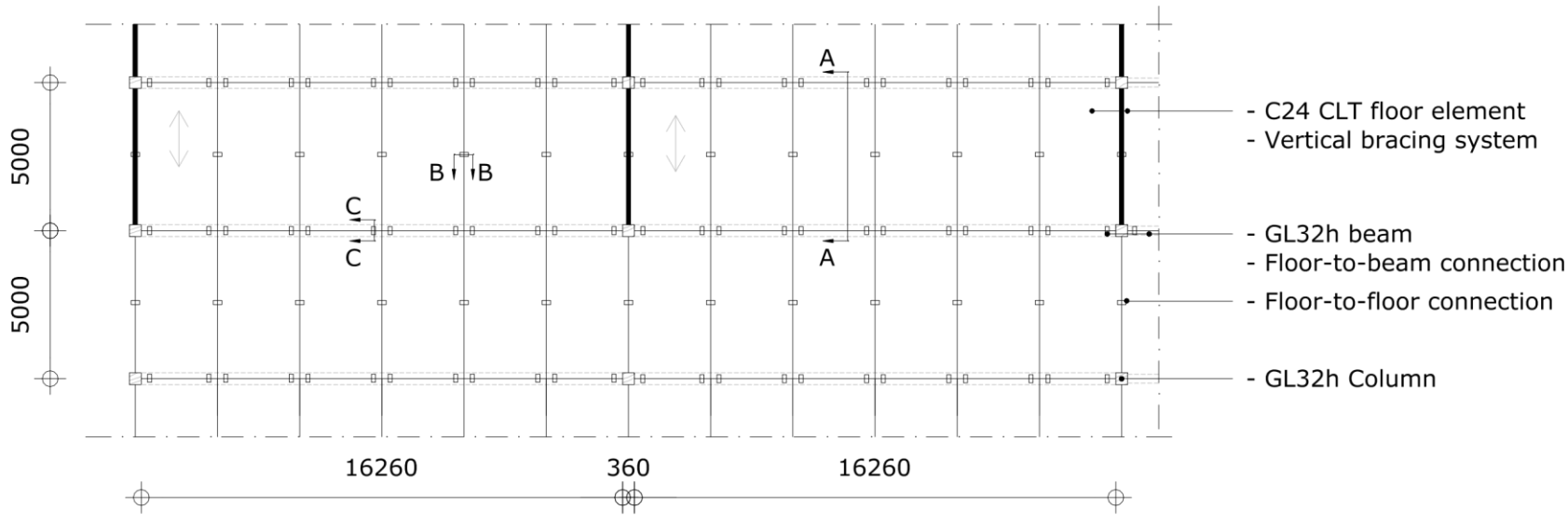

Figure I-1: Top view investigated car park module in mm with cross-section floor systems

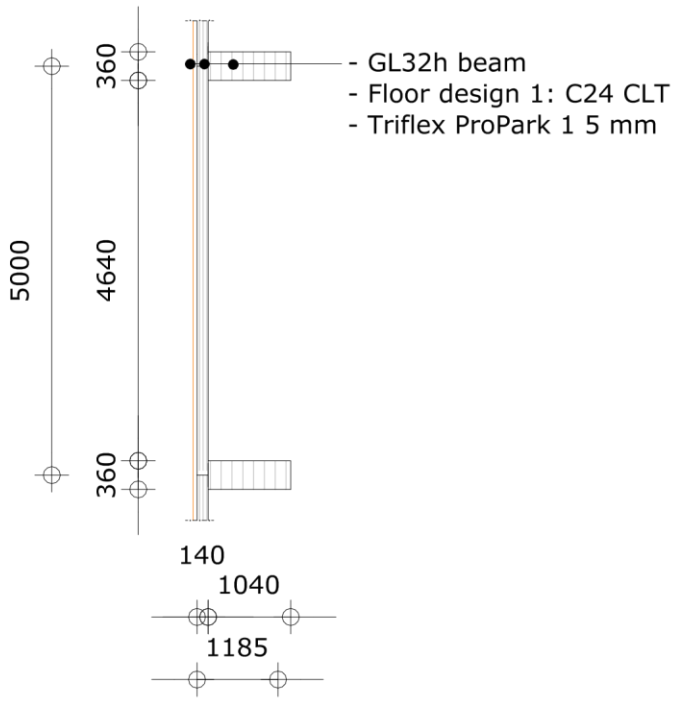

Figure I-2: Cross-section A-A in mm

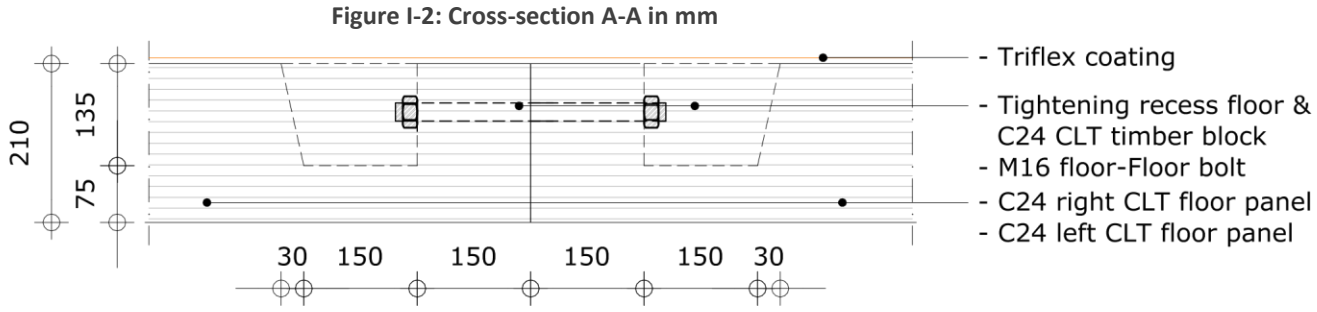

Figure I-3: Cross-section B-B mm

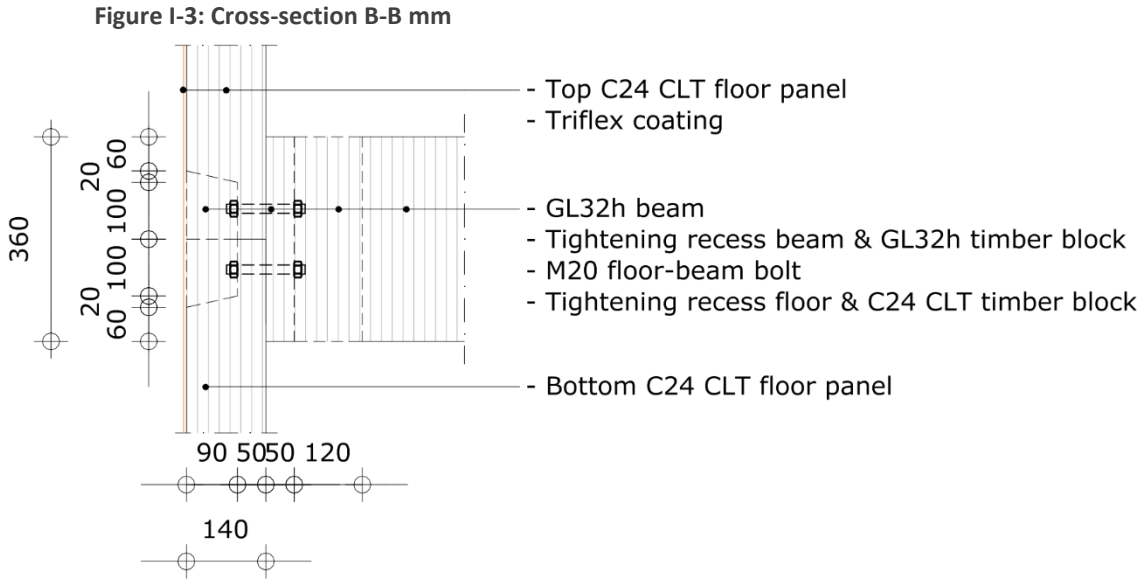

Figure I-4: Cross-section C-C in mm

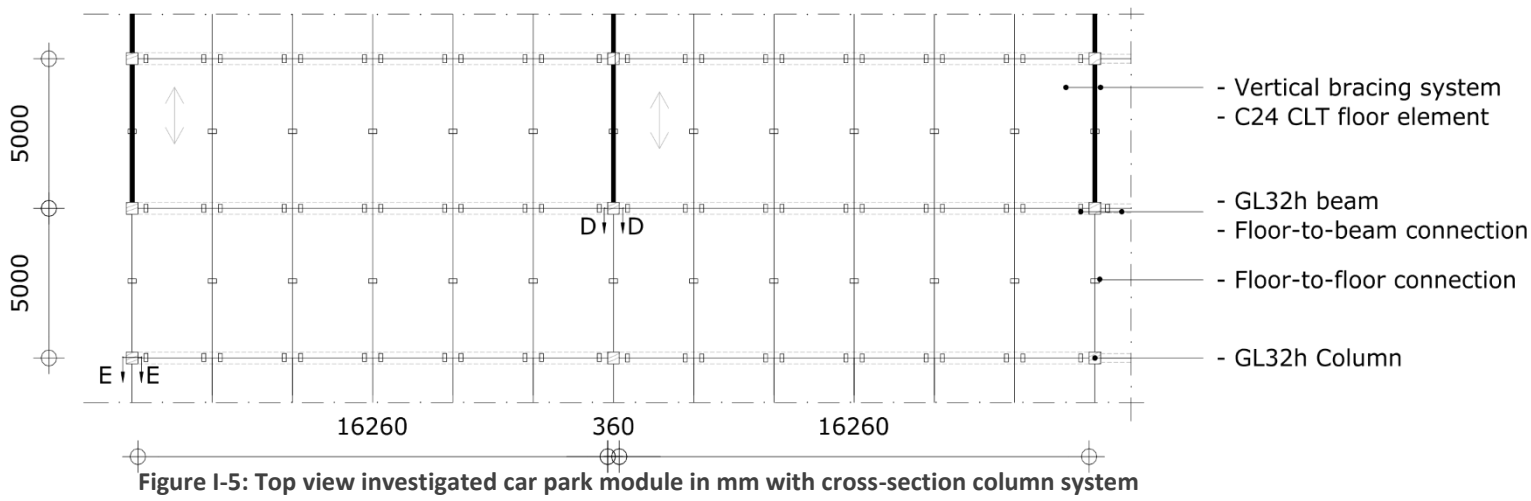

Figure I-5: Top view investigated car park module in mm with cross-section column system

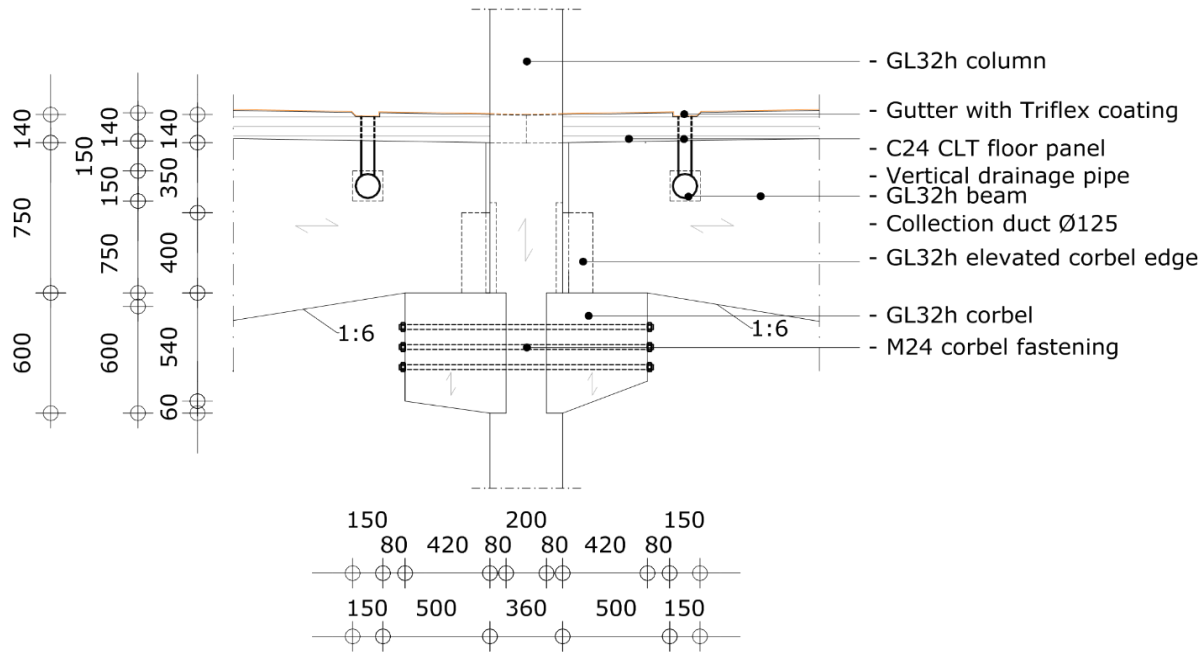

Figure I-6: Cross-section D-D in mm

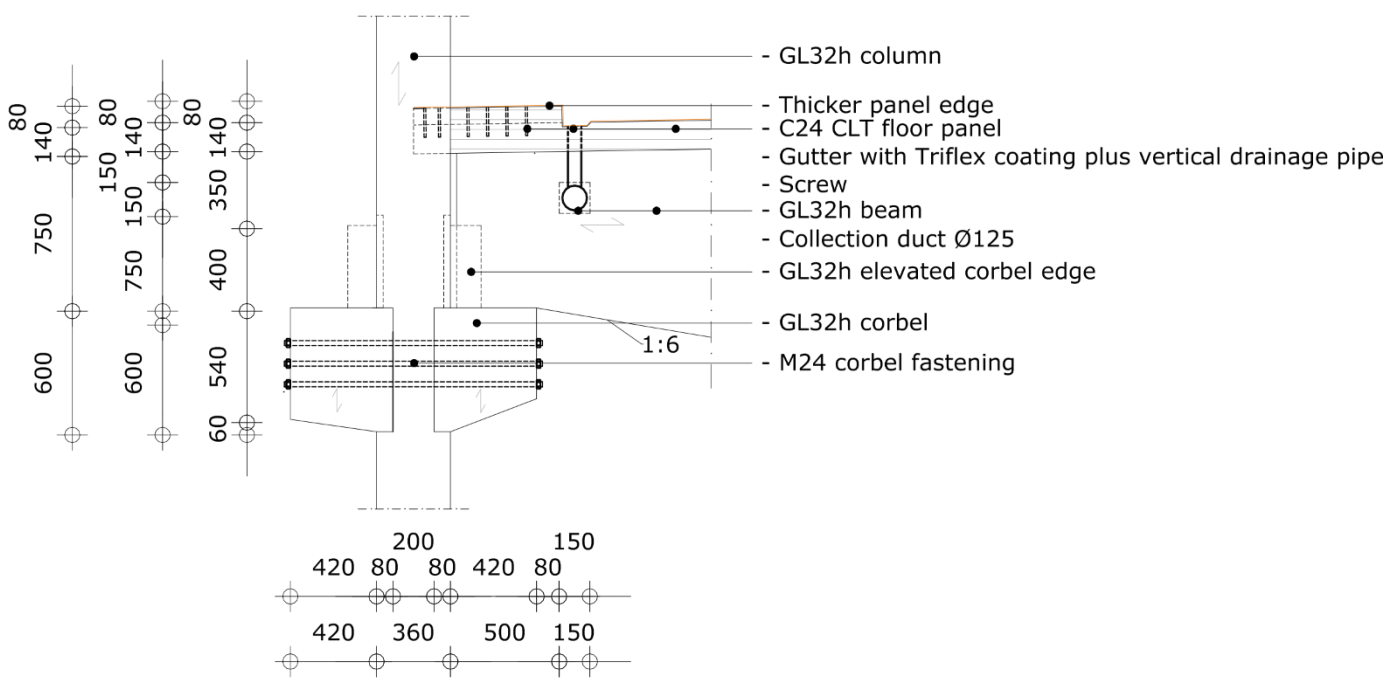

Figure I-7: Cross-section E1-E1 in mm

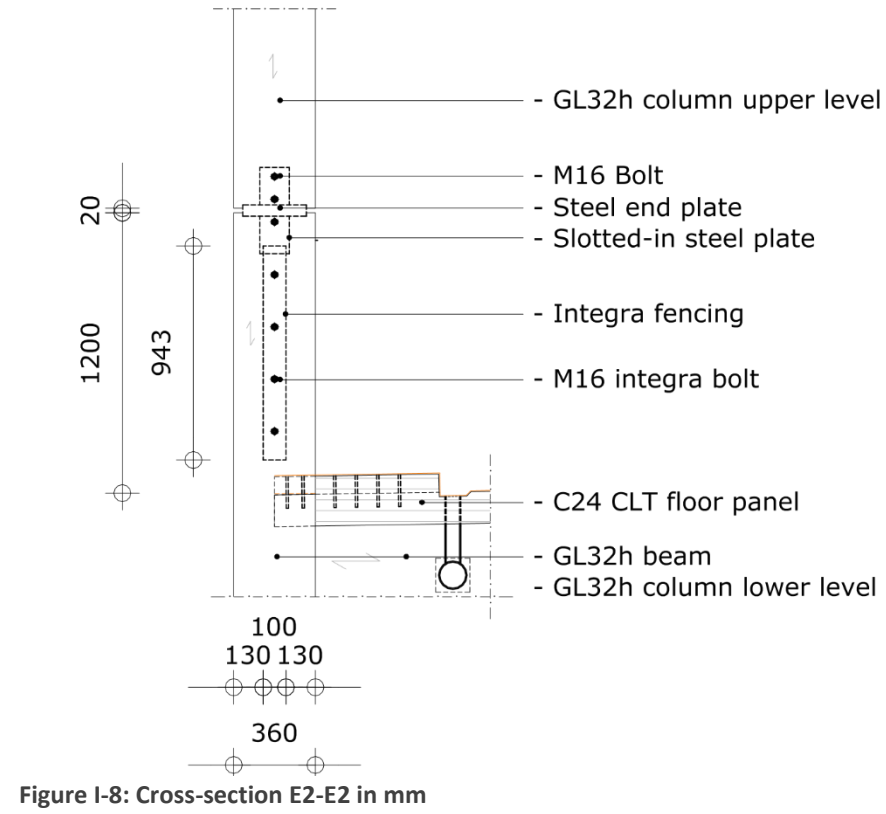

Figure I-8: Cross-section E2-E2 in mm

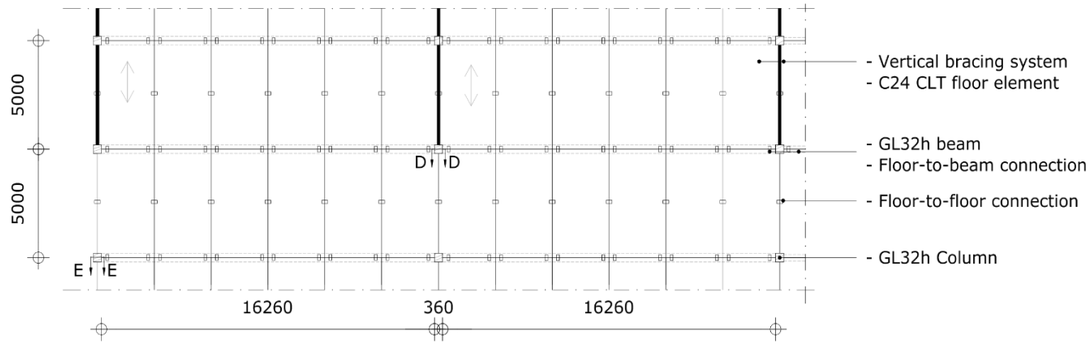

Figure I-9: Top view investigated car park module in mm with cross-section transvserse bracing system

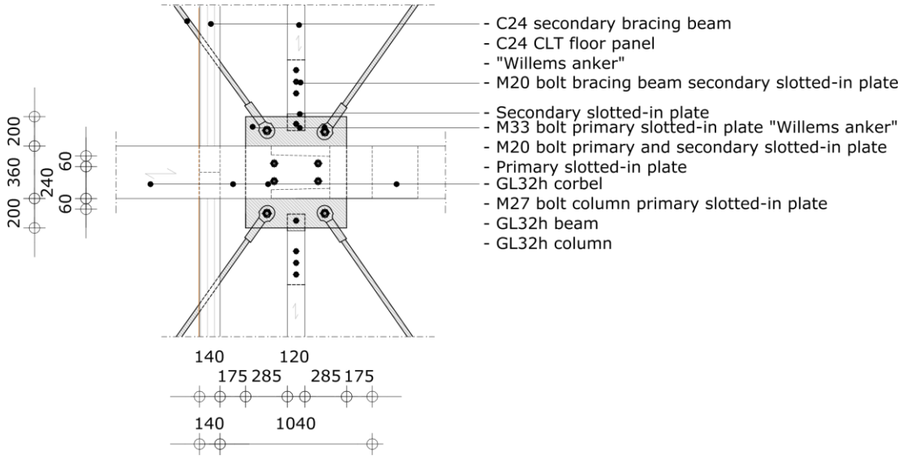

Figure I-10: Cross-section F-F in mm

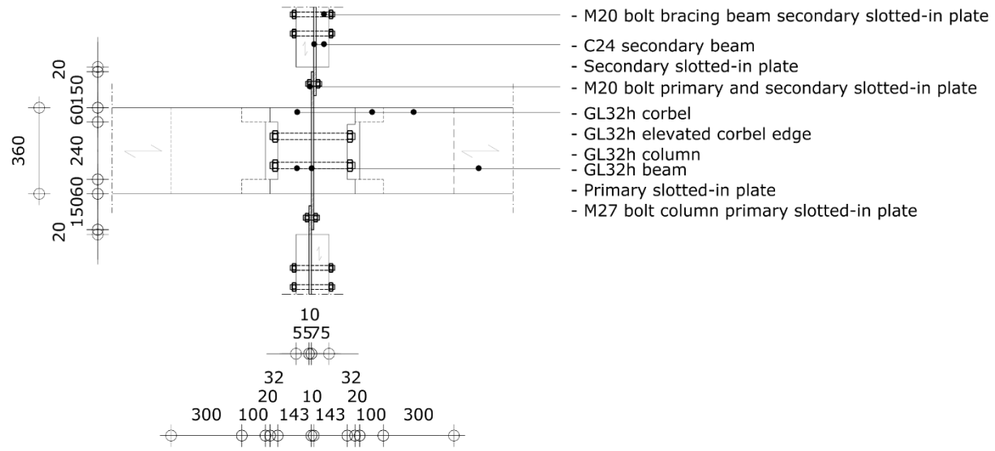

Figure I-11: Detail G in mm

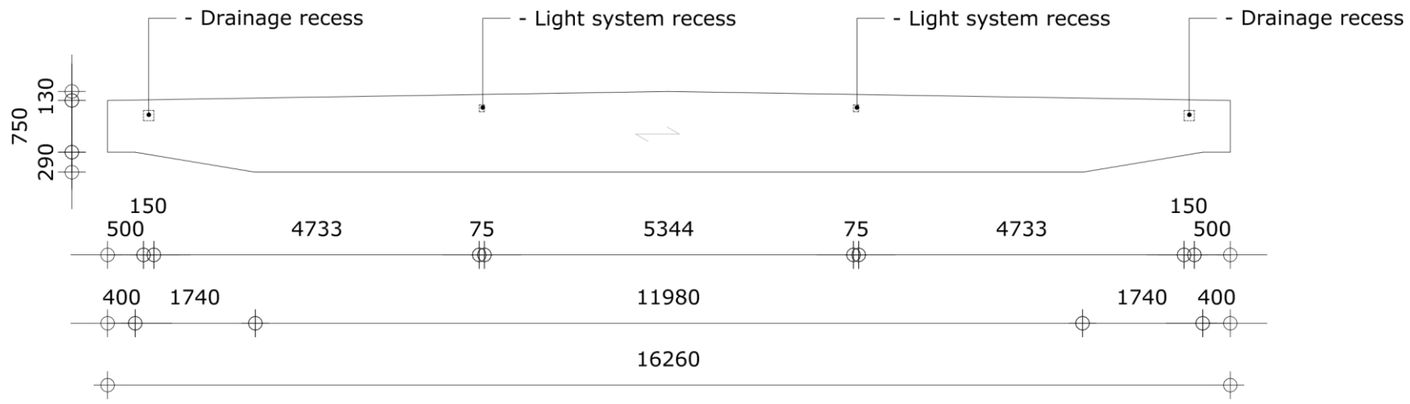

Figure I-12: Beam recesses for installations in mm

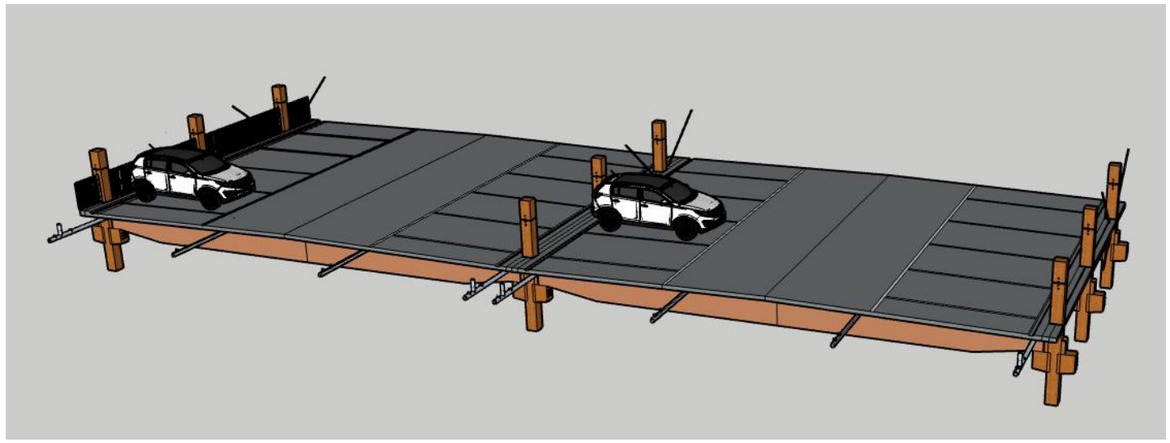

Figure I-13: 3D view investigated four grid module

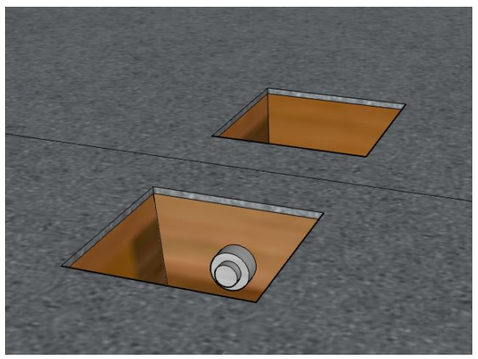

Figure I-14: 3D top view floor-to-floor connection

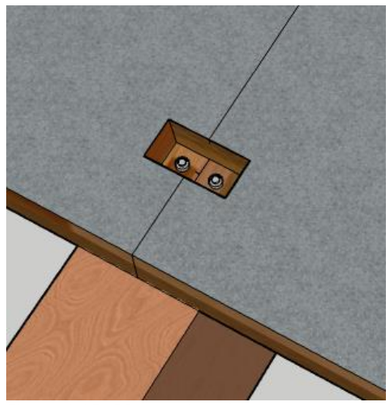

Figure I-15: 3D top view floor-to-beam connection

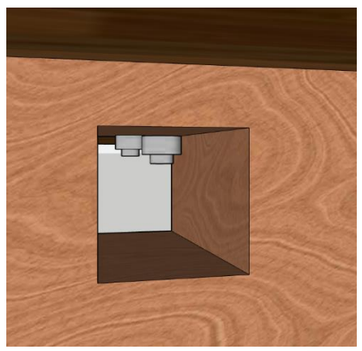

Figure I-16: 3D view recess beam floor-to-beam connection

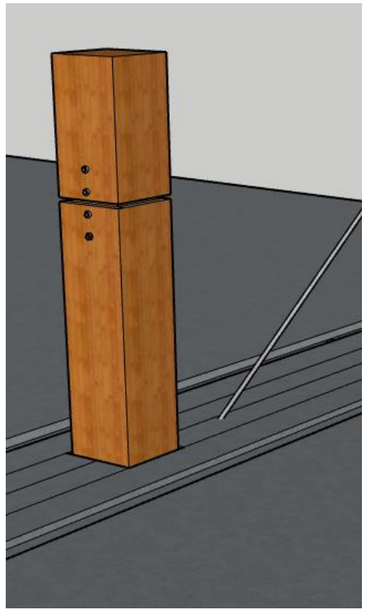

Figure I-17: 3D view centre column

Figure I-18: 3D view edge column

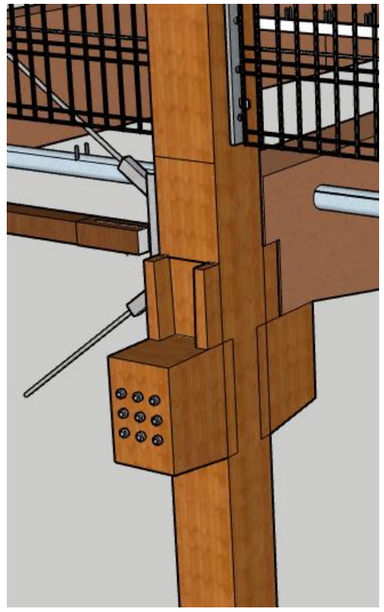

Figure I-19: 3D view column-to-beam connection

Figure I-20: 3D view edge column without floor system

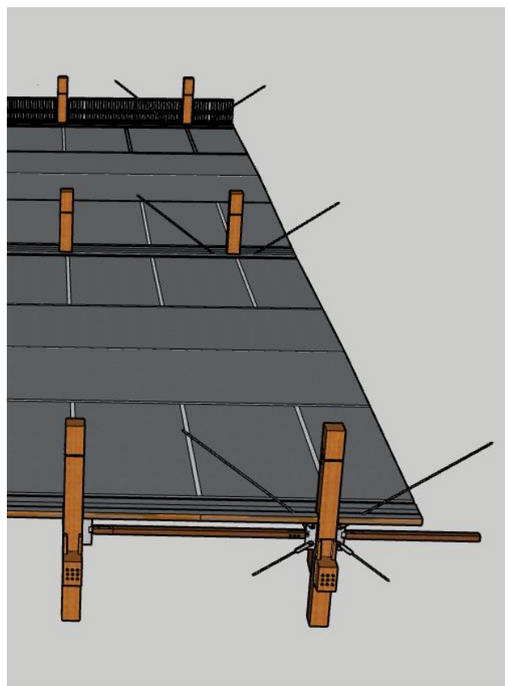

Figure I-21: 3D view vertical bracing system

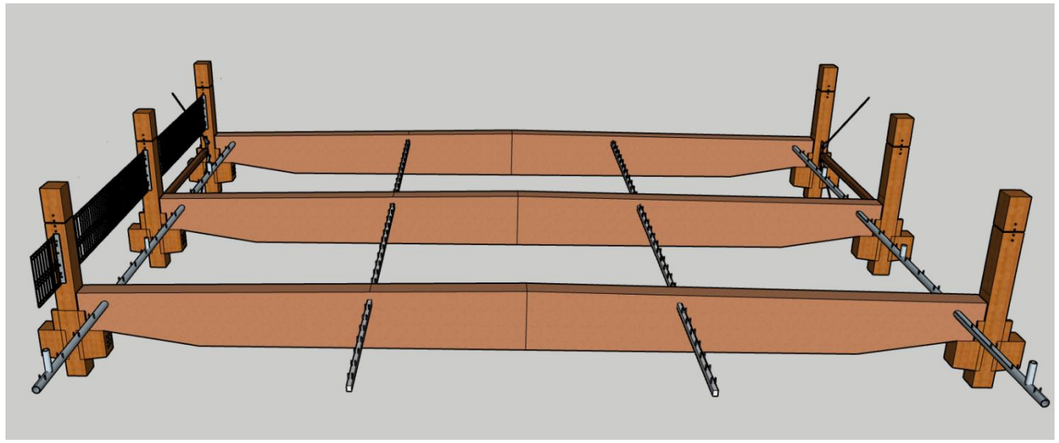

Figure I-22: 3D view drainage and electrical ducts